GEOLOGIJA

2024 | št.: **67/2**









GeoZS
Geološki zavod Slovenije

ISSN
Tiskana izdaja / Print edition: 0016-7789
Spletna izdaja / Online edition: 1854-620X

GEOLOGIJA

67/2 – 2024

GeoZS
Geološki zavod Slovenije

GEOLOGIJA	2024	67/2	187-368	Ljubljana

GEOLOGIJA
ISSN 0016-7789

Izdajatelj: Geološki zavod Slovenije, zanj direktor **dr. Miloš Bavec**
Publisher: Geological Survey of Slovenia, represented by Director **dr. Miloš Bavec**
Financirata Javna agencija za raziskovalno in inovacijsko dejavnost Republike Slovenije in Geološki zavod Slovenije
Financed by the Slovenian Research and Innovation Agency and the Geological Survey of Slovenia

Naslov uredništva / Editorial Office: GEOLOGIJA Geološki zavod Slovenije / Geological Survey of Slovenia
Dimičeva ulica 14, SI-1000 Ljubljana, Slovenija
Tel.: +386 (01) 2809-700, Fax: +386 (01) 2809-753, e-mail: urednik@geologija-revija.si
URL: https://www.geologija-revija.si/

GEOLOGIJA izhaja dvakrat letno. / GEOLOGIJA is published two times a year.
GEOLOGIJA je na voljo tudi preko medknjižnične izmenjave publikacij. /
GEOLOGIJA is available also on exchange basis.

Izjava o etičnosti
Izdajatelji revije Geologija se zavedamo dejstva, da so se z naglim naraščanjem števila objav v svetovni znanstveni literaturi razmahnili tudi poskusi plagiatorstva, zlorab in prevar. Menimo, da je naša naloga, da se po svojih močeh borimo proti tem pojavom, zato v celoti sledimo etičnim smernicam in standardom, ki jih je razvil odbor COPE (Committee for Publication Ethics).

Publication Ethics Statement
As the publisher of Geologija, we are aware of the fact that with growing number of published titles also the problem of plagiarism, fraud and misconduct is becoming more severe in scientific publishing. We have, therefore, committed to support ethical publication and have fully endorsed the guidelines and standards developed by COPE (Committee on Publication Ethics).

Baze, v katerih je Geologija indeksirana / Indexation bases of Geologija: Scopus, Directory of Open Access Journals, GeoRef, Zoological Record, Geoscience e- Journals, EBSCOhost

Cena / Price

Posamezni izvod / Single Issue	Letna naročnina / Annual Subscription
Posameznik / Individual: 15 €	Posameznik / Individual: 25 €
Institucija / Institutional: 25 €	Institucija / Institutional: 40 €

Tisk / Printed by: TISKARNA JANUŠ d.o.o.

Slika na naslovnici: Slike so nastale tekom izobraževalno-ustvarjalnih delavnic slikanja z naravnimi barvami. (Čeru, članek v tej številki)

Cover page: The paintings were created during events of the educational-creative workshops on painting with natural colours. (Čeru, paper in this issue)

VSEBINA – CONTENTS

Članki - Articles

Poročila in ostalo - Reports and More

Nekrolog - In memorium

GEOLOGIJA 67/2, 193-215, Ljubljana 2024

https://doi.org/10.5474/geologija.2024.009

A review of the Neogene formations and beds in Slovenia, Western Central Paratethys

Pregled neogenskih formacij in plasti v Sloveniji, zahodna Centralna Paratetida

Kristina IVANČIČ[1]*, Miloš BARTOL[1], Miha MARINŠEK[1], Polona KRALJ[1], Eva MENCIN GALE[1], Jure ATANACKOV[1] & Aleksander HORVAT[2]

[1]Geološki zavod Slovenije, Dimičeva ulica 14, SI-1000 Ljubljana, Slovenija; *corresponding author: kristina.ivancic@geo-zs.si
[2]ZRC SAZU, Paleontološki inštitut Ivana Rakovca, Novi trg 2, SI-1000 Ljubljana, Slovenija

Prejeto / Received 8. 1. 2024; Sprejeto / Accepted 11. 6. 2024; Objavljeno na spletu / Published online 16. 12. 2024

Key words: Neogene, Miocene, Pannonian Basin System, Central Paratethys, Eastern Slovenia, Formations
Ključne besede: Neogen, Miocen, Panonski bazen, Centralna Paratetida, Vzhodna Slovenija, formacije

Abstract

Neogene sedimentary successions are found in eastern and northeastern Slovenia. Their formation was closely related to the evolution of the western part of the Pannonian Basin System and the Central Paratethys; it was influenced by global transgressive and regressive cycles as well as by global, regional and local tectonics. Several formations and beds were defined within the Neogene sedimentary successions which can be found in three separate areas. The first one includes the formations north of two major fault systems, the Periadriatic Fault System and the Mid-Hungarian Zone, which were associated with the Mura-Zala and the Styrian Basins, respectively. Successions south of these major faults are not formally connected to any of the major basins and developed in two distinct parts: a strip between Tunjice and Kozjansko to the north and the Krško area to the south. From the Egerian to the early Badenian, different areas exhibit different types of sedimentation, whereas from the middle Badenian onwards, sedimentation in different zones is partly comparable, depending on the type of depositional environment. Egerian and Eggenburgian sediments are only found south of the above-mentioned major fault zones, whereas Karpatian sedimentation only occurred north of them. Sediments in both areas are characterized by alternation of shallow marine, brackish and terrestrial sedimentation. In contrast, sedimentary environment in the Badenian evolved from a terrestrial, mainly fluvial environment with alluvial fans, through a transitional stage (delta and lagoon) to a shallow and deep marine environment. The Sarmatian sequences reflect a brackish environment with decreasing salinity and continue into extensive Pannonian delta systems that gradually fill the basins from west to east. The formations that correspond to the Pannonian in the Mura-Zala Basin can be correlated with the formations in the Krško area. The Pliocene is characterized by terrestrial sedimentation with the formation of rivers and lakes in the newly established intramontane basins.

Izvleček

Neogenska sedimentna zaporedja so prisotna v severovzhodnem in vzhodnem delu Slovenije. Njihov nastanek je vezan na razvoj zahodnega dela Panonskega bazena in Centralne Paratetide ter posledično na globalno, regionalno in lokalno tektonsko aktivnost ter globalne transgresijsko-regresijske cikle. Sedimentna zaporedja so opredeljena v več formacijah in plasteh, ki so se razvijala na treh večjih ločenih območjih. Prvo je severno od Periadriatskega preloma in Srednje-madžarske prelomne cone, kjer je bila sedimentacija vezana na Mursko-Zalski in Štajerski bazen. Neogenska zaporedja južno od omenjene prelomne cone so se razvijala na dveh ločenih območjih, v pasu od Tunjic do Kozjanskega ter na območju Krškega in niso del nobenih večjih bazenov. Od egerija do spodnjega badenija se sedimentna zaporedja med različnimi območji izrazito razlikujejo, medtem ko je sedimentacija od srednjega badenija dalje na različnih območjih delno primerljiva. Egerijski in eggenburgijski sedimetni so prisotni le južno od prelome cone, ottnangijske in karpatijske sedimente pa najdemo le severno od nje. V obeh primerih je sedimentacija potekala v plitvomorskem in brakičnem okolju ter na kopnem. Bolj enoten je bil razvoj od badenija dalje, ko je transgresija povzročila poplavitev celotnega ozemlja, kar je omogočilo razvoj podobnega sedimentacijskega okolja v različnih območjih. Sprva kopensko, predvsem rečno okolje z aluvialnimi vršaji se je nadaljevalo v prehodno okolje z deltami in lagunami, ki ga je hitro poplavilo morje Centralna Paratetida. Sarmatijska zaporedja odražajo brakično okolje z zmanjšano slanostjo, ki so počasi prehajala v obsežne sisteme panonskih delt. Te so postopoma zapolnjevala porečja od zahoda proti vzhodu, kar je omogočilo korelacijo formacije v Mursko-Zalskem bazenu in na območju Krškega. V pliocenu je značilna kopenska sedimentacija z nastankom rek in jezer v novo nastalih intramontanih bazenih.

Introduction

The Miocene rocks and sediments, deposited in the Pannonian Basin System (PBS) are found in the eastern and north-eastern parts of Slovenia. They are often present in distinct locations that stretch in an E-W or NW-SE direction. In the Miocene, sedimentation took place in three separate depositional units. In the north-eastern part, north of the Periadriatic Fault System (PFS) and Mid-Hungarian Zone (MHZ), south of it and in the Krško area. Sedimentation north of the PFS and MHZ was subjected to the development of two larger basins, the Mura-Zala and Styrian Basins (Fig. 1). The Mura-Zala Basin represented one of the deepest depressions of the PBS (Fodor et al., 2002), covering most of north and northeast Slovenia in the Miocene (Drobne et al., 2008) (Fig. 1). The Styrian Basin was formed northwest of the Mura-Zala Basin - the boundary between these two basins in the present-day Slovenia is still not defined. It is described in Austria, where the boundary represents the South Burgenland Swell (Hasenhüttl et al., 2001). Each of these two basins is divided into smaller basins. The westernmost part, the Slovenj Gradec Basin, is connected to the Mura-Zala Basin (Ivančič et al., 2018a), while the northernmost part, the Ribnica-Selnica Trough, was subjected to the sedimentation of the Styrian Basin (Gašparič & Hyžný, 2014). The second sedimentation unit was located south of the PFS

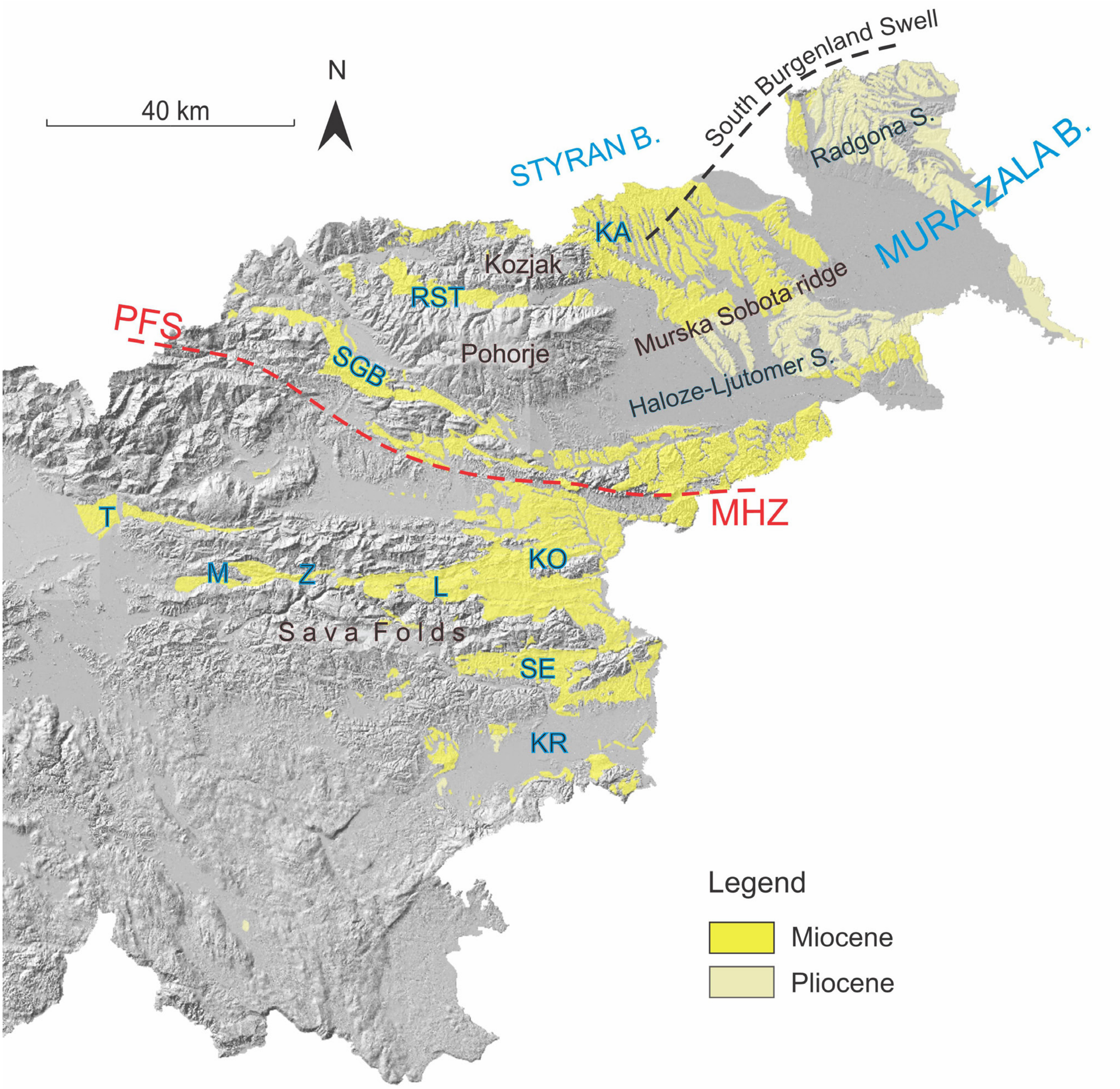

Fig. 1. Distribution of the Miocene and Pliocene rocks in Slovenia. Explanatory notes: B – Basin, KA – Kungota area, KO – Kozjansko area, KR – Krško area, L – Laško area, M – Moravče area, RST – Ribnica Selnica Trough, S – Subbasin, SE – Senovo area, SGB – Slovenj Gradec Basin, T – Tunjice area, Z – Zagorje area (modified after Buser, 2010).

and MHZ. Today, the Miocene rocks are exposed in several parallel running facies belts (structurally forming cores of synclines) between Tunjice in the west through Moravče, Laško and Zagorje to Kozjansko in the east. The third unit is located in the south-east of the Sava Folds and represents the Krško area, which developed independently of the other two (Poljak, 2017a). At various times, the areas were either isolated and experienced unique development or connected and characterized by uniform sedimentation.

Individual sedimentary sequences are combined into groups of strata, members and formations. Some formations are defined in several different regions (e. g., Laško formation, which is known from the area of Tunjice, Laško, Kozjansko and Krško), while other strata and members are associated to a single area (e. g., Radlje beds, which only occur in in the Ribnica-Selnica Trough). Synrift, post-rift and compressional tectonic phases along with eustatic changes have created various terrestrial, shallow- and deep-water sedimentary environments. Each formation represents a particular type of sedimentary fill, characterized by a specific tectonic phase in a particular time interval (Jelen et al., 2006).

This paper presents all the Neogene sedimentary formations described in Slovenia in the transitional zone between the rising Alps and Dinarides on one side and the extensional PBS on the other. Their occurrence is strongly related to local, regional and global tectonic activity. Sedimentary succession has been extensively studied in a wide range of specific areas, but this knowledge has not yet been summarized into an integral picture. This paper aims to improve the general understanding of sedimentary processes taking place during the Neogene.

Structural overview

Northeastern Slovenia lies at the junction of four tectonic units: the PBS, the Southern Alps, the Eastern Alps and the Dinarides. The area is part of the broader collision zone between the African and Eurasian plate, characterized by a triple junction of the European Plate, the Adriatic Microplate and the Pannonian Lithosphere (Brückl, 2010). The deep lithospheric structure is not definitively known, with possible southward subduction of the European plate, northward subduction of the Adriatic plate or a combination of both. The area is split into two distinct zones of somewhat different Cenozoic tectonic evolution by the PFS and the MHZ. The PFS, which transitions into the MHZ, with its northernmost edge delineated by the Balaton Fault. The ALCAPA megaunit, composed of Adria-derived allochthons, underwent eastward lateral extrusion during the Neogene (Vrabec & Fodor, 2006; Schmid et al., 2020 and references therein; Fodor et al., 2021 and references therein).

The zone to the north of the PFS-MHZ line, comprising the ALCAPA megaunit is composed of late Early to Late Cretaceous age Eoalpine generally top-to-north thrust and nappe system of Adria-derived allochthons, generally composed of pre-Permian metamorphic rocks, with upward decreasing metamorphic grade, and overlying Permian to Mesozoic successions (Schmid et al., 2020 and references therein). The basement underwent extensive extensional tectonic deformation in the Miocene, as the result of subduction, slab breakoff and rollback in the Carpathians, the consequent crustal thinning and the formation of the Pannonian Basin and the subsequent mantle upwelling and thermal subsidence of the basin. Extensional tectonics in NE Slovenia initiated at 25–23 Ma (Eggerian), peaking at 19–15 Ma (Eggenburgian to Badenian) and ceasing by 12–11 Ma (Late Sarmatian to early Pannonian) (Fodor et al., 2002, 2021). Extension resulted in the crustal thinning driven along low-angle detachment faults and the formation of an asymmetric metamorphic core complex. It comprises the Pohorje and Kozjak domes, in which the metamorphic basement outcrops at the surface. To the east, the Murska Sobota extensional block or ridge moved eastward and subsided along the Pohorje and Kozjak detachments. Further still to the east, the Transdanubian Range moved east and subsided along the Baján detachment (Fodor et al., 2021). To the west of the Pohorje dome, the structure of the much smaller-scale extensional blocks is somewhat uncertain. The Pohorje and Kozjak domes are separated by the Lovrenc and Primož Faults. The (supradetachment) extensional basins formed both along the higher-angle normal faults that sole to the detachments and the detachments themselves, transitioned from terrestrial in the early Neogene (Eggenburgian to Karpatian, 19–17.25 Ma) into near-shore and bathyal in the Middle Miocene (Badenian, 15.97–12.8 Ma) (Fodor et al., 2021). Deformation subsequently migrated eastwards towards the Transdanubian Range in Hungary. In NE Slovenia, the most important basins include the Slovenj Gradec Basin located west of the Pohorje dome, the Ribnica-Selnica Trough, which formed along the Lovrenc and Primož Faults, separating the Pohorje and Kozjak domes, the Radgona Subbasin, which lies to the north of the Murska Sobota ridge, the Ljutomer Subbasin, also known as the Haloze-Ljutomer-

Budafa Subbasin located south of the Murska Sobota ridge, and the Mura-Zala Basin, which lies east of the Murska Sobota ridge (Fodor et al., 2002, 2021). The extensional tectonic regime persisted until the Sarmatian, after which the region underwent thermal subsidence, as evidenced by the deposition of a further, 1–2 km thick post-tectonic succession of sediments (Fodor et al., 2002). Neogene sediment total thickness reaches up to ~3000 m in the Radgona Subbasin, and more than 5000 m in the Ljutomer Subbasin (Gosar, 2005).

In the latest Miocene and in the Pliocene, the region underwent an inversion of the tectonic regime, with extensional structures reactivated as compressional and transpressional, and extensional basins undergoing inversion (Fodor et al., 2002). The inversion only affected the southern part of the area, including the Ljutomer Subbasin, with the reverse Ljutomer and Haloze North and South faults and the dextral strike-slip Donat Fault (Atanackov et al., 2021), and associated large-scale folds, including the Ormož-Selnica Anticline and smaller-scale folds, such as the Petišovci Anticline.

South of the PFS-MHZ line, the basement is composed of the Adria-derived (eastward extension of the) South Alpine unit, which comprises top-to-south thrust and nappe system composed mostly of Late Paleozoic (Carboniferous and Permian) clastics and Mesozoic carbonates. The South Alpine unit itself is thrust to the south over the External Dinarides, with the two units separated by the South Alpine Thrust Front (Placer, 2008; Schmid et al., 2020). The External Dinarides are a late-Eocene to early-Oligocene top-to-the south thrust / fold and thrust system, composed of Adria-derived allochthons, mostly of the Slovenian carbonate platform and later the Dinaridic carbonate platform, to a much lesser extent the Slovenian Basin, overlain in the western part by Eocene to Oligocene flysch (Placer, 2008; Schmid et al., 2020). The easternmost part of SE Slovenia comprises the transitional zone into the Internal Dinarides along the thinned Mesozoic carbonate platform margin and transition into basinal successions and ophiolites of the Internal Dinarides (Placer, 2008). The basement was dissected by extensional tectonics, at least in SE Slovenia and into Croatia where the structure is well known (Krško Basin), beginning in the early Neogene, continuing until the late Neogene (Tomljenović & Csontos, 2001; Poljak, 2017a). Successions of Neogene marine sediments locally exceeds 1000 m, e.g. ~1500 m in the Globoko Basin (Poljak, 2017b). A Middle to Late-Miocene stress field change to a generally N-S compression resulted in the formation of the Sava Folds (Placer, 1998). This is a fold and thrust belt of E-W to ENE-WSW trending large scale folds, in general east of the Ljubljana Basin and the Žužemberk Fault, reaching east into Croatia. An extension of the Sava Folds to the west into the External Dinarides is strongly suspected (Rižnar, 2009). The formation of the Sava Folds may be asynchronous, post-Sarmatian in the north (Placer, 1998) and post middle-Pannonian in the south (Gosar & Janežič, 2006; Poljak, 2017b; Atanackov et al., 2018). The folds are confirmed active in the south-southeastern part of the Sava Folds (Poljak, 2017a; Atanackov et al., 2018).

Basins North of the Periadriatic Fault System and Mid-Hungarian Zone

Two different series of Neogene sediments have developed in Slovenia. The first to the north, and the second to the south of the PFS and MHZ. In the north, the sedimentary environment is mainly subjected to the development of the Styrian and Mura-Zala Basins. These areas have been influenced by the ongoing tectonic activity in the northern depositional areas. In the southern region, the sedimentary record is variable and does not conform to the large basin framework observed in the north. Neogene tectonic activity influenced the sediments, which are now found in isolated areas (Fig. 1) that were deposited separately from the southern part until the Badenian, when both parts were flooded by the Central Paratethys.

Formations and beds, Associated with the Styrian Basin

The specific area in Slovenia that was subjected to sedimentation in the Styrian Basin has not yet been defined. Furthermore, it is not defined where the border between the Styrian and Mura-Zala Basin is. It is defined by the South Burgenland Swell, but its continuation into the Slovenian area is not clear (Fodor et al., 2002). Fossil remains in the **Ribnica-Selnica Trough** indicate a similarity with the type of sedimentation in the Styrian Basin during the Karpatian transgression (Gašparič & Hyžný, 2014), where conglomerate layers alternate with sandstones and siltstones (Pavšič & Horvat, 2009). The main uncertainty is in the designation of the **Kungota area,** which is, to some extent, the border area between the Steirischer Schlier (Kreuzkrumpel Formation) of the Styrian Basin and the Haloze Formation of the Mura-Zala Basin (Hohenegger et al., 2009; Maros et al., 2012). On the one hand, sedimentation in the Kungota area resembles sedimentation to the

Wagna section (Rijavec, 1965), and the tectonic structures of the Kungota area suggest a connection to the Styrian Basin (Kralj et al., 2009). On the other hand, the sediments in the Kungota area indicate similarities to sedimentation in the Mura-Zala Basin (Fodor et al., 2002; Jelen et al., 2006; Fodor et al., 2011; Maros et al., 2012). This suggest that these two basins might be connected during the Karpatian transgression. However, detailed sedimentological and palaeontological analyses are still missing.

Radlje beds

The oldest Miocene sediments on the northern side of the PFS and the MHZ can be found in northern Slovenia, by the Austrian border, near Radlje ob Dravi (Fig. 2). The strata consist of conglomerate and sandstones, whose Eggenburgian age is questionable (Mioč & Žnidarčič, 1977). The conglomerate and gravel are full of metamorphic rocks fragments, indicating proximity to the hinterland and fluvial sedimentation (Mioč & Žnidarčič, 1977). This corresponds to the Radl Beds of the Eibiswald Formation, whose Ottnangian deposits are interpreted as alluvial fans and proximal delta facies (Stingl, 1994). However, as the Radlje beds have not been explored in the past or in the recent, their evolution and connection with the surrounding basins is not yet defined.

Formations and Beds, Associated with the Mura-Zala Basin

In the Mura-Zala Basin, the Neogene sedimentation began in the Karpatian and continued to the Pliocene. The sedimentation was strongly influenced by tectonic activity and started in the Early

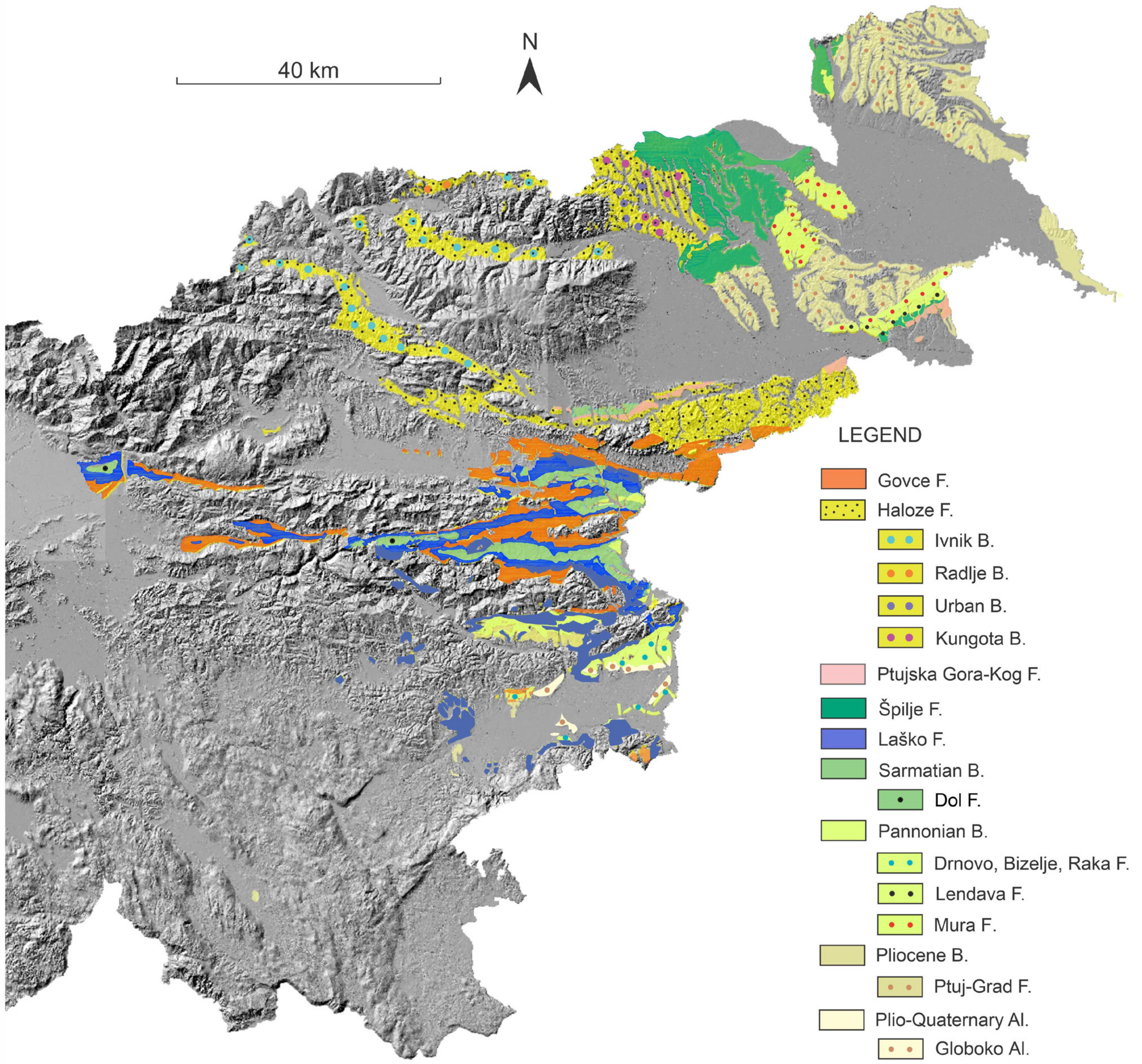

Fig. 2. Distribution of the Miocene formations in Slovenia. Explanatory notes: F – Formation, B – Bed, Al – Alloformation (modified after Buser, 2010).

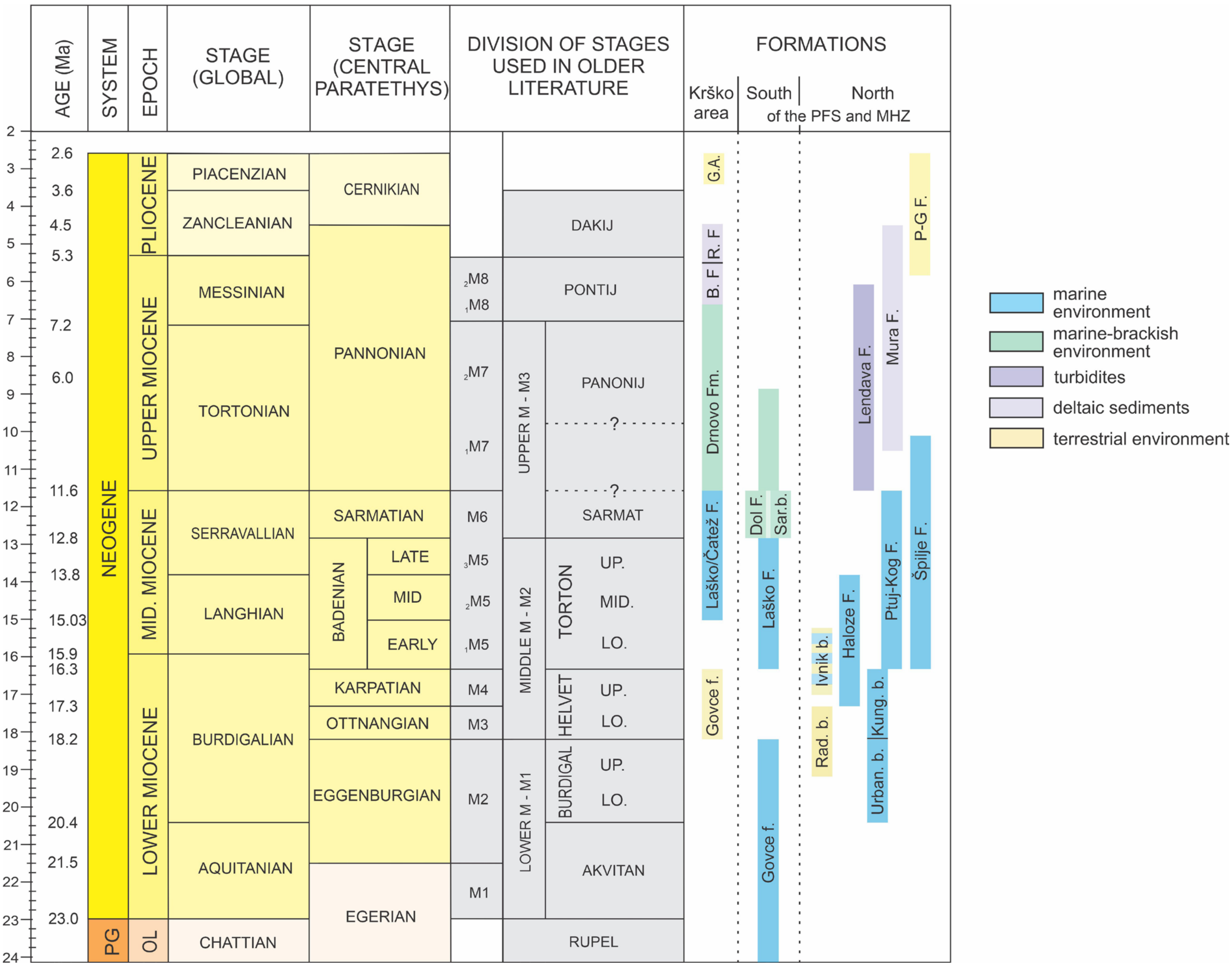

Fig. 3. Correlation of formations described in the paper with the stratigraphic time scale in the Central Paratethys (modified after Rögl et al., 2007 and Hohenegger et al., 2014). Explanatory notes: B.F. – Bizeljsko Formation, R.F – Raka Formation, G.A. – Globoko Alloformation, P-G F. – Ptuj-Grad Formation, Rad. B. – Radlje beds, Sar. b. - Sarmatian beds.

Miocene extension, which led to the thinning of the crust and the formation of half-grabens (Jelen et al., 2006). The filling of the half-grabens was associated with different tectonic phases (post-rift, syn-rift); therefore, several formations were defined, namely the Haloze, Ptujska gora - Kog, Špilje, Lendava, Mura and Ptuj-Grad Formations. Besides those, informal names of beds in particular areas are used in older literature, namely the Ivnik, Urban and Kungota beds (Jelen et al., 2006), which today are attributed to the Haloze Formation.

The Haloze Formation (Karpatian – early Badenian)

Description: Initial sedimentation in the Mura-Zala Basin covered the pre-Cenozoic basement. Alternation of conglomerates, sandstones, muddy breccia with fossils such as oyster shells indicate first infilling of the grabens in the Karpatian (Fodor et al., 2011). In the Slovenj Gradec Basin, initial Karpatian sedimentation starts with the basal conglomerate and muddy breccia and continues with alternating layers of conglomerate, sandstone, siltstone and marlstone of terrestrial character (Ivančič et al., 2018b). Sedimentation continued with the deposition of finer-grained sediments of the Central Paratethys. Nannoplankton assemblages point to functioning connection of Central Paratethys with the Mediterranean Sea (Ivančič et al., 2018a). The Haloze Formation is divided into several members: Plešivec-Urban, Stoperce-Kungota, and Neraplje-Cirknica (Jelen & Rifelj, 2011) as well as into specific beds: Ivnik, Haloze and Urban, which are described in greater detail below. The thickness of sediments is over 1300 m (Fodor et al., 2011) and are located north of the PFS (Fig. 1). The formation extends from the Karpatian to the lower Badenian.

Sedimentation: The Haloze Formation represent the infilling of the half-grabens formed in the first syn-rift phase of the PBS formation (Maros et al., 2012). Regression-transgression cycles alternated twice in the Central Paratethys at this time (Kováč et al., 2018), and strongly affected the PBS, especially the marginal parts (Pavelić & Kovačić, 2018; Ivančič et al., 2018b). Marine transgression caused sedimentation in the shallow marine, near-coast environment, with the deposition of sands, marls and lithothamnium nodules integrated with conglomerate (Maros et al., 2012). Gradually, a deepening of the sea and open-marine sedimentation is indicated by the deposition of sandstones, siltstones and marlstone (Maros et al., 2012). Volcanic activity in the surrounding area resulted in the deposition of tuff layers, called the **Ranca tuff layer** in the Kungota area (Fodor et al., 2011; Maros et al., 2012).

Correlation: Regression stage between the Karpatian/Badenian boundary is not yet defined in the Haloze Formation (Fodor et al., 2011). In the Wagna and Katzengraben sections, distinguished angular discordance can be observed, namely the Styrian Unconformity (Hohenegger et al., 2009). The regression stage between the Karpatian/Badenian boundary is defined by coarse-grained high-energy fluvial sediments (Jelen & Rifelj, 2003, 2005; Jelen et al., 2006; Fodor et al., 2011). The beginning of the early Badenian transgression is characterized by the formation of transitional environment (e.g., lagoonal, deltaic; Ivančič et al., 2018b). The formation represents lateral variation of the Tekeres Formation in Hungary (Fodor et al., 2011).

The Ivnik beds

Description: Initial sedimentation of the Ivnik beds represents basal conglomerates of Karpatian age, which indicate the first infilling of the basin. Regression stage between the Karpatian/Badenian boundary is defined in the Slovenj Gradec Basin, where it is characterized by swamps with thick layers of coal (Ivančič et al., 2018a). Sedimentation continues with deposition of conglomerate, which is gradually replaced by sandstones and, further on, marly siltstones (Ivančič et al., 2018a). Sediments are defined in the Slovenj Gradec Basin and Ribnica-Selnica Trough (Fig. 2). In both areas, sedimentation took place form the Karpatian to the end of early Badenian. The thickness of the Ivnik layers is over 1200 m (Ivančič et al., 2018a).

Sedimentation: Detailed sedimentological, geochemical and paleontological analyses indicate three regression-transgression periods between the Karpatian and the end of the early Badenian (Ivančič et al., 2018a). The three depositional sequences can be correlated to the global third order sequence cycles (TB 2.2, TB 2.3, TB 2.4; cf. Haq et al., 1988; Hardenbol et al., 1998). All three transgressions point to an active marine connection with the Mediterranean Sea. The first Badenian transgression is well defined in the sedimentary successions with lowstand and highstand system tract defined and sedimentation described in detail in Ivančič et al. (2018a).

Correlation: Sedimentation of the Ivnik beds in the Slovenj Gradec Basin and Ribnica-Selnica Trough have specific differences in their sedimentary input. While the sediments in the Slovenj Gradec Basin originated from the south-west, west and subordinately form the south (Ivančič et al., 2018b), the main input into the Ribnica-Selnica Trough originated from the Pohorje Mountains (Mioč, 1978). According to the above, the two basins were probably separated by a barrier in the Karpatian and early Badenian in the form of the partly uplifted Pohorje tectonic block (Trajanova, 2013; Ivančič et al., 2018a), but detailed investigations are still missing. The Ivnik beds in the Slovenj Gradec Basin shows similarities in depositional environment and represent time equivalent with the Haloze Formation (Ivančič et al., 2018a), while in the Ribnica-Selnica Trough with the Styrian Basin (Gašparič & Hyžný, 2014).

The Urban beds

Description: The Burdigalian age (Fig. 3) of the Urban layers is well supported in Rijavec (1965). They are divided into two parts: lower and upper Urban beds. The sediments discordantly cover the Paleozoic basement. In the lower part, breccia (with tonalite and gneiss blocks) is overlain by mica, sandy marlstone, mica carbonate sandstone, and marlstone. Rare conglomerate occurs. Microfossil remains such as foraminifera, ostracod and echinoderms indicate a marine environment. The upper part of the Urban beds consists of conglomerate, sandy marlstone, sand, sandstone and tuff. Microfauna in both parts is similar. The thickness of the Urban beds is over 500 m (Rijavec, 1965). They occur near the Urban hill, NW of Maribor (Fig. 2).

Sedimentation: Sediments were deposited in open-marine environment and indicate similarities to the beds in the Styrian basin (Rijavec, 1965). According to the latest research (Jelen & Rifelj, 2011; Fodor et al., 2011, Maros et al., 2012), the Urban beds are Karpatian in age and belong to the Plešivec-Urban Member of the Haloze Formation.

The Kungota beds

Description: The Kungota beds are well described in Rijavec (1965). They occur in the Kungota area (Fig. 1) and overlie the Urban beds. The lower part of the Kungota beds is composed of conglomerate, sandstone, and marl with clay interlayers. On top of the marlstone, a tuff layer occurs. Microfossils including foraminifera, ostracods and echinoderms indicate Helvetian age (Fig. 3). The fauna differs from that in the Urban beds. The upper part of the Kungota beds is similar to the lower ones but does not contain any tuff layers. The thickness of the Kungota beds is over 400 m (Rijavec, 1965).

Sedimentation: Sedimentation took place in shallow marine environment (Rijavec, 1965). According to research (Jelen & Rifelj, 2011; Fodor et al., 2011; Maros et al., 2012) the Kungota beds are part of the Stoperce-Kungota Member of the Haloze Formation, which also includes the Ranca tuff bed.

The Ptujska Gora – Kog Formation (early Badenian – Sarmatian)

Description: The sedimentary succession of the Ptujska Gora – Kog Formation is composed of conglomerate, gravel, breccia, sandstone, sand, sandy silt, silty marl, marlstone, clayey marl, limestone and dolomite with insertion of coal layers (Jelen & Rifelj, 2011; Maros et al., 2012). It comprises sediments form early Badenian to Sarmatian and can be found in a thin belt southwest northeast of Haloze (Fig. 2).

Sedimentation: Ptujska-Gora Kog Formation is an informal lithostratigraphic unit, which is not commonly used in the literature. Sediments were deposited in various sedimentation environment from shallow marine, nearshore, brackish to fluvial environment (Maros et al., 2012). They represent the filling of the basin in the post-rift and first compressional phase in the PBS (Maros et al., 2012).

The Špilje Formation (early Badenian – early Pannonian)

Description: The Špilje Formation consist mainly of muddy and sandy sediments. In the Kungota area, the beginning of sedimentation is characterized by an unconformity (Rijavec, 1965), where the sediments discordantly overlay Karpatian sediments. The sedimentary succession starts with the basal conglomerates, which represent the first deposits in the basin and are overlain by sandstone, sand, marl, litothamnium limestone and marl (Žnidarčič & Mioč, 1989; Fodor et al., 2011). The thickness of the Špilje Formation is up to 1600 m (Fodor et al., 2011). The sandy beds in the area of Lenart were investigated in two discrete levels which were biostratigraphically assigned to the early-late Badenian (Bartol, 2009). Late Badenian lithothamnium limestones occur in a strip between the Pesnica and Drava Faults and north of the Pesnica Fault as rhodolithic conglomerates and individual rhodoids (Bartol, 2009). They consist of red algae and abundant bryozoans, corals, gastropods, bivalves, sea urchins and other reef-dwelling organisms.

Sedimentation: The sediments were deposited in the basin, formed during the syn- and post-rift phases of the PBS from the early Badenian to the early Pannonian (Jelen & Rifelj, 2005; Bavec et al., 2005; Jelen et al., 2006). Sedimentation took place in shallow and deep marine environment enabling the formation of sandy turbidites (Fodor et al., 2011).

The connection to the transgressive-regressive periods was defined in the vicinity of Lenart, where sediments were correlated with the sea-level lowstand between eustatic cycles TB2.3 and TB2.4 (after Haq et al., 1988). A change from a deeper water depositional system to the sandy-turbiditic regime suggests the formation of restricted sub-basins, as does the contemporaneous reduction in the number of planktonic foraminifera (Fodor et al., 2002). The overlying middle Badenian marls contain diverse nannofossil assemblages (Bartol, 2009) and several horizons enriched in pteropods (Mikuž et al., 2012a), which is consistent with a fully marine environment and functioning marine connections with the surrounding areas.

The sandy and marly beds in the Mura-Zala Basin dated to the boundary of nannofossil biozones NN5 and NN6 (Bartol & Pavšič, 2005; Bartol, 2009) were deposited during the sea-level lowstand at the transition between 3rd order cycles TB 2.4 and TB 2.5. The late Badenian nannofossil assemblages are diverse and enriched in genera that indicate warm water, suggesting a pelagic sedimentary environment and a functioning connection with the Mediterranean (Bartol, 2009; Bartol et al., 2014). Warm hemipelagic environment and connection to Mediterranean in early Badenian indicate also discoasters and pteropods (Bartol & Pavšič, 2005; Mikuž et al., 2012b).

Correlation: Recent research (Jelen & Rifelj, 2011; Fodor et al., 2011) describes the Špilje Formation as one of the formations in the Mura-Zala Basin. The sediments are found in the area between Lenart and Špilje (Fig. 2). Based on the micro- and macrofauna and the lithological similarities with the sediments of the Vienna Basin, the sedimentary succession of the Špilje Formation has been correlated with the sediments of the Vienna Basin (Rijavec, 1965; Kuščer, 1967). Rhodoids represent a littoral reef facies deposited in shallower parts of the basin (Šikić et al., 1979).

The Lendava Formation (Pannonian)

Description: In most cases, the Lendava Formation overlays the Špilje Formation, however in some localities, it overlays the pre-Tertiary beds. The formation consists of up to a few meters thick stack of layers of basal conglomerates at the bottom, the sequence continues with large amounts of sands and sandstones, which represent turbiditic sequences, and in the upper part of the formation, sandy muddy and silty marl and marlstone, clay and marly clay prevail (Jelen & Rifelj, 2011; Fodor et al., 2011). The thickness of sandy turbidites reaches up to 1000 m (Fodor et al., 2011). Sediments of the Lendava Formation are outcroping in small areas north and west of Ormož (Fig. 2).

Sedimentation: The Lendava Formation was defined based on seismic profiles and includes Pannonian sediments, which represent diachronous deposits of a large delta system. They include prograding delta and shelf-slope deposits (fine-grained sediments), and also sandy turbidites between the delta fronts and the deep basin (Jelen & Rifelj, 2003; Bavec et al., 2005; Fodor et al., 2011; Maros et al., 2012). The Lendava Formation is followed by delta front sediments of Mura Formation (Jelen et al., 2006).

Correlation: In general, in Hungary, the lateral equivalents are: Algyo Formation, Ujfalu Formation and Zagyva Formation (Fodor et al., 2011; Maros et al., 2012), while in Austria, they are: the Schichten von Loipersdorf in Unterlamm, Stegersbacher Schichten, Jennersdorfer Schichten, Taborer Schotter in Süsswasser-Kalk (Gross, 2003; Gross et al., 2008).

The Mura Formation (Pannonian)

Description: The Pannonian clastic sediments of the Mura Formation consist of poorly lithified interlaminated or massive silt, clayey silt, sandy silt and marl. In the overlying upward coarsening Pontian succession interlaminated and interbedded sand and silt become more abundant, and locally, gravelly sand and sandy gravel, and coal seams occur (Fodor et al., 2011; Maros et al., 2012).

Sedimentation: The Mura Formation was defined based on seismic profiles. It contains pro-delta and transitional pro-delta to delta front sediments, representing a diachronous continuation of the deltaic sequence from the Lendava Formation (Jelen et al., 2006) (Fig. 4). In the uppermost section coal seams and organic matter occur and indicate the presence of swamps and the transition of environment into delta plain. The delta front deposits form an interconnected sand body that extends in a subsurface area of 22.128 km^2 and yields economically important amount of thermal water (Mioč & Ogorelec, 1991; Kralj, 2001b; Nádor et al., 2012; Šram et al., 2015).

Post-rift subsidence and the ongoing compressional phase (Huismans et al., 2001) of the southwest Pannonian Basin System during upper Pannonian (ex. Pontian) resulted in the retreat of the Lake Pannon toward the east. Fluvial systems draining from the west toward the east and southeast formed diverse deltaic environments along the coastline, and eventually infilled the body of standing water (Kralj, 1995; Jelen et al., 2006; Fodor et al., 2011; Maros et al., 2012; Kováč et al., 2017). The Mura Formation consists of sediments deposited in pro-delta, pro-delta to delta front, delta front and delta plain environment. Jelen and Rifelj (2011) have subdivided the Mura Formation into the Presika-Petišovci Member and the Cogetinci-Kuzma Member. Both members have rather similar lithology and thickness amounting up to 1200 m (Pleničar, 1970; Mioč & Ogorelec, 1991; Kralj, 1995, 2001a; Nádor et al., 2012; Šram et al., 2015).

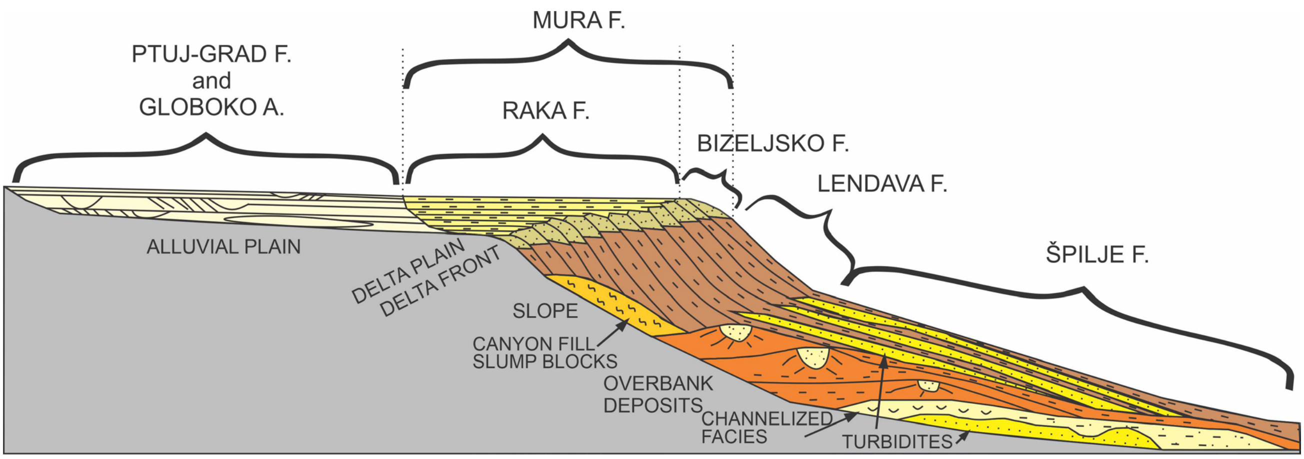

Fig. 4. Distribution of several formations of the Mura-Zala Basin and in the Krško area in relation to the sedimentation environment (modified after Neal et al., 1993). Explanatory marks: F – Formation, A – Alloformation.

The Ptuj-Grad Formation (Pliocene)

Description: The beginning of the Ptuj-Grad Formation is characterized by coal deposits on the alluvial plain (Fig. 4). Generally, the formation consists of alternation of sand, silt, clay marl, lignite and gravel sediments and include numerous gravel bodies of Late Miocene to Pliocene (Maros et al., 2012). Meandering accretions are mainly composed of gravelly sand or sandy gravel, and flood plain deposits of gravelly-silty sand and sand interbedded with silty and clayey fine-grained sediments. The formation includes also extrusive basalt, lava flows, basalt- pyroclastics and subvolcanic basaltic rocks (Maros et al., 2012). In the vicinity of the settlement of Grad, alkali basaltic autoclastic, volcaniclastic and mixed fluvial-volcaniclastic deposits outcrop as erosional remnants of maar, tuff ring and tuff cone. Further to the east of Goričko, the Pliocene deposits are overlain by Early Quaternary gravel, sandy gravel and sand with minor intercalations of fine-grained sediments (Pleničar, 1970; Kralj, 1995).

Sedimentation: As the upper Pannonian deltaic sedimentation prograded toward the east, the Pliocene environment in north-eastern Slovenia changed to terrestrial and dominated by braided and meandering river systems (Kralj, 1995, 2001a). A system of alluvial fans developed, and further to the east, it evolved into a system of braided and meandering rivers.

The formation of the Ptuj Member is still poorly understood, although it has been assumed to be related to the meandering system of the Drava-Drau paleo flow draining into the Ptuj-Lutomer Depression. Rare occurrences of coal indicate the existence of peat swamps (Žnidarčič & Mioč, 1989).

Depositional environment and sedimentary successions of the Grad Member are more complex and closely related to the subsidence of the Styrian Basin and Mura-Zala Basin, and in particular, the Radgona-Radkersburg Depression. The Grad member is assumed to have developed as a result of the drainage systems of Mura-Mur, Zala and Krka-Kerka paleo-streams. Several measured imbrications indicate nearly west-to-east flow directions (Kralj, 1995).

Correlation: Alkali basaltic volcanism is about 3 Ma old and closely related to the Pliocene occurrences in the Styrian Basin and Little Hungarian Plain (Winkler, 1926; 1927; Poulditis, 1981; Kralj, 1995, 2001a; 2010; Martin & Németh; 2004). The early fluvial sedimentation occurred along the South-Burgenland Swell infilling the Radgona-Radkersburg Depression as well.

Formations and beds south of the Periadriatic Fault System and Mid-Hungarian Zone and in Krško area

South of the PFS and MHZ, sedimentation from the Egerian to the Pliocene took place in two separate depositional units. The first extends from Tunjice in the west to Kozjansko in the east, and the second is in the Krško area. Today the sediments are preserved in several isolated areas, which were connected during the Egerian, Eggenburgian and Badenian as part of the Central Paratethys. While the sedimentary successions in the Early Miocene and Badenian were united by the transgression of the Central Paratethys, the Sarmatian and Pannonian sediments are not associated with any specific formation. In the Krško area in particular, several new formations have been defined within the Pannonian, which are shown in the newly published Geological map of the Krško area and described in the Explanatory notes (Poljak, 2017a, b).

The Govce formation (late Egerian, Eggenburgian)

Description: In the area of Zagorje the sequence starts with basal conglomerates and gravel with keratophyre pebbles and Lepidocyclina limestone (Kuščer, 1967). Basal beds are covered by blueish marly clay interchanging in the overlying beds with sand and sandstone that dominate the upper part of the sequence. Sand beds also include keratophyre and carbonate gravel. Locally the sedimentary sequence continues with sandy limestone and occasionally contains *Lepidociclyna*. It is overlain by litothamnian limestone of Lower Miocene age. The upper part of the sequence contains thin coal layers in sand beds (Kuščer, 1967). Formation development varies laterally. In the Tunjice Hills, a 380 m sequence starts with the Govce clay containing sand and sandstone, continues as interchanging marlstone and claystone beds covered by conglomerate and ends with sand and sandstone (Vrabec, Mi., 2000). In the Krško area, the succession starts with silicate-carbonate pebbles and continues with several tens of meters of silicate-carbonate gravel and sand, sandstone, marl, marlstone, tuff and coal (Verbič, 1995; Dozet et al., 1998; Poljak, 2017a). In the area of Kozjansko, the Govce formation comprises a 500–600 m thick sequence of predominantly carbonate conglomerates and sand, sandstone, marl, marlstone, tuff and coal (Aničić et al., 2002). In the surroundings of the Maclje Mountain, the Govce beds contain well lithified green glauconitic Maclje sandstone of Eggenburgian age (Aničić et al., 2002). Marlstone in the Kozjansko area contain numerous calcitic nannoplankton of early and late Egerian, and the upper part could be attributed to the Eggenburgian (Pavšič & Aničić, 1998, 2000). The Govce formation comprises the oldest Miocene deposits in Slovenia. The formation includes poorly lithified sediments of Oligocene and Lower Miocene (Egerian and Eggenburgian) age (Buser, 1978, 1979; Aničić & Juriša, 1985a, 1985b). It has been determined in Tunjice (Premru, 1980; Vrabec, Mi. 2000), Moravče, Sava folds (Hamrla, 1954; Kuščer, 1967), Krško (Poljak, 2017a), Kozjansko (Pavšić & Aničić, 1998; Aničić et al., 2002) and Žetale (Jelen & Rifelj, 2011). The Govce beds lie discordantly on Pre-Cenozoic basement (Kuščer, 1967; Vrabec, Mi., 2000; Poljak, 2017a) or on Paleogene clastic sediments known as the Sivica and Pletovar formation, as well as on Oligocene volcanic rocks (Buser, 1978, 1979; Aničič et al., 2002). According to the correlation with surroundings basins, the sediments of the Govce formation in Krško area are presumably Ottnangian age (Poljak, 2017a).

Sedimentation: Lower Miocene age has been assigned based on foraminifera (Kuščer, 1967). The lower portion of the Govce formation was deposited in littoral environment while the upper part developed in brackish system. However, an abundance of pentalites in Kozjanko area indicate a decrease in salinity in the upper Egerian (Pavšič & Aničić, 1999). In Krško area, the formation is determined based on resemblance to the Govce beds in the Sava Folds, sediments were deposited in fluvial, swamp and lacustrine environment (Poljak, 2017a).

The Laško formation (Badenian)

Description: Sediments of the Laško formation discordantly overlapped the Govce formation in the Krško Basin (Poljak, 2017a) and in the Laško area (Kuščer, 1967). The formation is divided into two parts: Laško marl, and lithothamnium limestone (Buser, 1978; Aničić et al., 2002; Bavec et al., 2005). In the Tunjice area, the Laško formation consists of conglomerates present in the beginning of succession, and alternation of course to fine grained sandstones and siltsotnes (Vrabec, Mi. et al., 2014; Rojnik, 2015). In the Zagorje area, the succession starts with the basal conglomerate, composed of pebbles of eroded Govce beds, and continues with sandstone (with quartz and keratophyre grains), sandy and marly limestone and marl. The top of the succession is characterized by lithothamnium limestone of varying thickness defined as biosparite with rare grains of quartz with foraminifera, lithothamnium, bryozoan, and echinoderms (Strgar, 2003). The abundance of the biogenic component in the sediments is described in the Kozjansko area as well (Aničić et al., 2002). It occurs locally in two levels: below and above the Laško marl (Munda, 1951). Sediments are described as Badenian and in Krško area as Sarmatian age as well (Poljak, 2017a), and are outcropping in wider area from Tunjice, Laško, Zagorje, Kozjansko, Senovo and Krško (Fig. 1).

The Laško marl is rich in bivalve and gastropod macrofossils. Lithothamnium limestone and Laško marl gradually alternate into Sarmatian clay in the area between Hrastnik and Laško (Munda, 1951; Kuščer, 1967) and in the Krško Basin (there is no strict boundary; Poljak, 2017a).

Sedimentation: Sedimentation took place in shallow marine, nearshore, and shoreface environment in the Middle Miocene. A prominent gastropod species *Pereiraeia gervaisi* was found in several localities near Šentjernej reflecting warm shallow water marine environment (Mikuž, 1999). Warm and humid paleoenvironmental conditions are also defined in Tunjice area (Ivančič et al., 2024). Most specimens were dated biostratigraphically to the upper part of the middle Badenian (Bartol et al., 2014), some accompanying nannofossil assemblages were enriched with *Braarudosphaera bigelowii*, which is able to tolerate freshwater influences (Bartol et al., 2008). This could reflect a sea-level lowstand at the boundary of 3rd order cycles TB 2.4 and TB 2.5. Late Badenian foraminiferal assemblages suggest a complex sedimentary environment with outer shelf to bathyal water depths in the Planina Syncline and shallow, nutrient rich and cool water in the Kozjansko area (Oblak Brown, 2006).

Correlation: The formation is described by various authors, south of the PFS and MHZ (Munda, 1951; Hamrla, 1954; Kuščer, 1967; Aničić et al., 2002; Strgar, 2003; Poljak, 2017a). The lithothamnium limestone of Laško formation is macroscopically similar to the lithothamnium limestone of Govce formation (Kuščer, 1967). Stratigraphic equivalent of the Laško marl represents *Šentjur micritic limestone* in the Celje area and Motnik Syncline. It contains remains of pelagic foraminifers and does not contain fragments of lithothamnium algae (Buser, 1979; Aničić et al., 2002).

The Dol formation / Sarmatian beds (Sarmatian)

Description: The Sarmatian sequence generally consists of conglomerate, gravel, sandstone and clayey layers in the lower part and continues with sandy and clayey marl, calcarenite, sandstone, sand and quartz sandstone. In the upper part, mica sand with interlayers of clayey marl prevail (Kuščer, 1967; Žnidarčič & Mioč, 1989; Aničić, 1990; Aničić et al., 2002). The calcareous sandstone is dominated by the remains of lithothamnium and other reef organisms (Buser, 1979; Premru, 1983). The Dol formation is described in the Tunjice and Zagorje areas (Placer, 1998, 1999; Vrabec, Mi. et al., 2014), while in the Kozjansko and Laško area, Sarmatian sediments are not formalized into a specific lithostratigraphic unit. In the Zagorje Syncline, these layers represent the deepest part of the depression. In the Tunjice area, the formation consists of clay, which represents the boundary between the Badenian and the Sarmatian sediments, covered by sand and calcarenite with the gastropods *Cerithium*. The thickness of the Sarmatian succession is up to 400 m (Pavšič & Horvat, 2009). In the Krško Basin, Sarmatian beds overlay Badenian layers in places, but occasionally Sarmatian strata are absent and Pannonian marlstones lie directly on Badenian beds. For this reason, the Sarmatian beds, when present in the Krško Basin, are included into the Laško formation (Poljak, 2017a; Poljak et al., 2016).

Sedimentation: The Sarmatian sediments were deposited in a brackish environment (Rijavec, 1965; Žnidarčič & Mioč, 1989, Aničić et al., 2002). Extensive micropaleontological analyses of foraminifera (Oblak Brown, 2006), ostracods and nanoplankton (Marinšek et al., 2022) were carried out in the Kozjansko area. Based on the ostracod analysis, it was interpreted that the predominant environment was marine to brackish. The ostracod assemblage indicates a lower to middle Sarmatian age. Silicoflagellates in the Tunjice area indicate a marine environment with low inflow and shallowing of the basin. The later is confirmed with a decrease of plankton as well as an increase of epilitic and epiphytic forms (Horvat, 2004). Seashore fossils suggest a good connection of the Central Paratethys with the Indopacific in the early Sarmatian (Pavšič & Horvat, 2009).

Correlation: According to the macro- and microfauna and the lithological profiles in the Špilje area, the Sarmatian Beds are similar to the strata in the Vienna Basin (Rijavec, 1965; Kuščer, 1967).

The Čatež Formation (Badenian, Sarmatian)

Description: The lower part of the succession contains breccias and conglomerates with carbonate matrix and dolomite pebbles, deposited on the pre-Neogene basement. Conglomerate include dolomite, carbonate, chert and marl pebbles. The succession continues with lithothamnium limestone (rudstone), characteristic of shallow marine environments. The Čatež Formation is determined in the north slope of the Gorjanci hills and is divided into the limestone Badenian part and the clastic Sarmatian part (Rižnar et al., 2002).

Sedimentation: The rudstone interchanges with white litothamnium limestone (bindstone) typical of low energy deeper marine environment. It is overlain by somehow deeper water (up to 100 m depth) calcarenite (packstone). The Sarmatian beds are represented by alternation of marlstones, marls and gravel with calcarenite layers, indicating tectonically controlled sedimentation. Foraminiferal assemblages indicate a brackish environment (Rižnar et al., 2002).

The Drnovo Formation (Pannonian)

Description: The formation overlays Sarmatian beds or lies transgressively on Badenian beds or on pre-Cenozoic basement. It consists of Pannonian (including ex. Pontian) marls. The basal part is composed of thin bedded carbonate siltstones, they are followed by poorly lithified sediments (dolomite-calcite silts to siltstones). Towards the upper part, the clay and quartz minerals predominate. (Poljak, 2017a). The Drnovo Formation is defined in the Krško Basin and is generally found in the southern part of the Orlica Mountains and the Krško Hills. Sediments are usually deposited on Laško marls or Litothamnian limestones, but in some specific cases it can be found on Mesozoic limestones (Poljak, 2017a). The thickness of the Pannonian part of the formation is up to 300 m, and the ex. Pontian part up to 200 m. The age of the formation was defined on the basis of gastropods, molluscs and ostracods (Poljak, 2017a).

Sedimentation: Sediments cover the marine-brackish sediments of the Sarmatian or pre-neogene basement and are deposited in freshwater and lake environment (Poljak, 2017a).

Correlation: In the Croatian Zagorje, west of the Krško area, the deposits consist of alternations of sand, silt, marl, and clay of upper Pannonian age, where a turbiditic environment was present (Pikija, 1982).

The Bizeljsko Formation (upper Pannonian)

Description: Sediments of the Bizeljsko Formation are deposited concordantly on sediments of the Drnovo Formation. It consists of an alternation of marl and sand with rare intermediate layers or lenses of gravel. The mineral composition of the formation is identical to that of the Drnovo Formation, and it mostly consists of quartz (Lapajne, 1975). In some upper layers, little pockets of unlithified and well rounded gravel can be found.

They are composed of magmatic and metamorphic rocks originated from the Eastern Alps (Trajanova, 2006). The upper Pannonian age is determined by the ostracod microfauna. The thickness of the beds is up to 800 m (Poljak, 2017a).

Sedimentation: Sedimentation took place in a deltaic environment, containing sediments from the delta front (Fig. 4). Ostracod assemblages indicate a brackish environment with varying energy levels ranging from high and low (Marinšek et al, 2023). Individual sandy layers show evidence of synsedimentary slumps with the presence of rip-up clasts (Poljak, 2017a).

The Raka Formation (upper Pannonian)

Description: The formation consists of almost pure (up to 99 %) quartz sand and only occasionally are some marl lenses are present. In places, thin and irregular beds of oxidized clay sediments can be found. The uppermost Pannonian age of the sediments was determined based on mollusks and ostracods microfauna. The maximum thickness is 500 m. Within the Raka Formation, The Globoko Member occurs, composed of gravel, sand, silt, and clay with coal (Poljak, 2017a).

Sedimentation: Sedimentation took place in a deltaic environment and include delta plain sediments (Fig. 4).

Pliocene - Quaternary Alloformations

Description: The terrestrial sediments of the "Plio-Quaternary" unit comprising gravely, sandy, and muddy sediments are often pedogenized (Šikić et al., 1979; Verbič et al., 2000; Poljak, 2017a). The gravelly part is characterized as non-carbonate and carbonate gravel of Sava and Savinja River provenance (Verbič, 2004; Mencin Gale, 2021) preserved in several terraces (Poljak, 2017a; Mencin Gale et al., 2019a, 2019b, 2024). The thickness of the unit in the Krško Basin (Globoko claypit) is estimated at 30 m (Poljak, 2017a) and in Velenje Basin at 205 m (Brezigar et al., 1985). In the area of Krško Basin, the unit is formally described as the **Globoko Alloformation**. The first attempts at estimating the age of the unit were based on the geological knowledge of the adjacent regions and stratigraphical position and yielded a Pliocene-Lower Pleistocene age (Pleničar & Ramovš, 1954; Šikić et al., 1979). This was later revised to 1–2 Ma based on morphostratigraphy (Kuščer, 1993; Verbič, 2004). The first attempt of absolute dating of the Globoko Alloformation at the Globoko claypit locality employed optically stimulated luminescence (OSL), which yielded a minimum age of 306 000 years ± 2σ (Bavec, 2000), however, the capability of the dating method and sediment properties do not render reliable results (Bavec & Poljak, 2013). Further attempts included dating using terrestrial cosmogenic nuclide (TCN) on the Libna Hill which yielded a minimum of 1.8 Ma (Cline & Cline, 2013; Cline et al., 2016). The latest results of TCN dating at several locations in the basin indicate the Globoko Alloformation spans the time interval from the latest Pliocene to Middle Pleistocene (Cline et al., 2018, personal communication). The latest studies of the "Plio-Quaternary" unit were performed not only in Krško Basin (Mencin Gale, 2021) but also in Slovenj Gradec, Nazarje (Mencin Gale et al., 2019b), Celje, Drava-Ptuj (Mencin Gale et al., 2019b) and Velenje Basin (Mencin Gale et al., 2024). These studies encompass geomorphological, sedimentological, provenance analysis, and in the case of the Velenje Basin also the chronological analysis of the "Plio-Quaternary" unit and represent one step closer to formalizing the newly called Plio-Early Pleistocene unit. Sediments of this unit are characterized by several different facies including matrix and clast supported gravel, massive and cross-bedded fine- to coarse-grained sands and massive fines (silt and clay), in parts containing dropstones.

The Plio-Early Pleistocene unit is followed by the Quaternary sediments encompassing Middle-Late Pleistocene and Holocene deposits. These deposits generally exhibit a less weathered character, higher carbonate content and better preserved morphology (Mencin Gale et al., 2019a, 2019b, 2024; Mencin Gale, 2021).

Sedimentation: The Plio-Early Pleistocene deposits are characterized as a terrestrial succession of fluvial deposits preserved in terrace staircases (Verbič, 2002, 2004; Poljak, 2017a; Mencin Gale et al., 2019a, 2019b, 2024; Mencin Gale, 2021) or buried in the central part of the basins (e.g. Krško Basin; Poljak, 2017a). Generally, sediments from the Plio-Early Pleistocene were deposited in fluvial or alluvial/colluvial fan settings. Interpretation of sedimentary environment is limited due to the poor quality of outcrops and can be only deduced in a few localities. In the Krško Basin, a braided river system was interpreted, characterized by typical features like channel lag, overbank, or abandoned channel deposits (Mencin Gale, 2021). Shorter sections from the Drava-Ptuj Basin might also indicate a braided river system based on their lithofacies assemblages (Mencin Gale et al., 2019b). In the Velenje Basin, the sections suggest a wandering (intermediate category between the braided and meandering river systems) and meandering river system (Mencin Gale et al., 2024) and also lacustrine and swamp sedimentation (Brezigar et al., 1985).

In the Krško Basin, two formal nomenclatures of the Quaternary alloformations and allomembers are currently available. Verbič (2004) discriminates between three Pleistocene (**Dobrava, Brežice** and **Drnovo Alloformations**) and four Holocene terraces (uniform Vrbina Allomember; part of the Drnovo Alloformation). Poljak (2017) on the other hand describes **Brezina, Sotla, Krka, Sava** and **Dobrava Alloformations**, each further divided into several allomembers. The age constraints of Quaternary units using optically stimulated luminescence, infrared stimulated luminescence, ^{14}C, U/Th, and terrestrial cosmogenic nuclides are summarized by Mencin Gale (2021). The age of the unit in the Velenje Basin was constrained by isochron-burial dating using cosmogenic ^{26}Al and ^{10}Be which yielded an age 2.7 ± 0.3 Ma (Mencin Gale et al., 2024), which is in excellent agreement with the biostratigraphic data (Rakovec, 1968, Debeljak, 2017; Drobne et al., 2017).

Correlation: In general, the comparison of the Plio-Early Pleistocene unit between Slovenj Gradec, Nazarje, Velenje, Celje, Drava-Ptuj, and Krško Basins exhibits differents extent of the deposits.

In the Velenje and Slovenj Gradec Basins Plio-Early Pleistocene unit strongly prevail over younger Middle-Late Pleistocene surfaces, distinguishing them from the Nazarje, Celje, and Drava-Ptuj intramontane basins nearby. This could be due to specific tectonic changes, meaning that Pliocene-Quaternary fluvial sequence can serve as an important marker of tectonic processes (Mencin Gale et al., 2024).

In the Krško Basin, correlation with cross-border area is suggested by fossil material. No fossil material was found in the "Plio-Quaternary" unit of the Krško Basin. However, the "Plio-Quaternary" unit was also mapped in the near-border area in northwest Croatia (Zagreb region), where some fossil material was found in Majdačko selo consisting of unionids and melanopsids of Pliocene age (Šikić et al., 1979). This indicates that the »Plio-Quaternary« sediments represent the lateral equivalent of upper *Viviparus* beds (Šimunić & Avanić, 1985). It is, however, possible that the fauna was re-worked as the age determination is in contradiction with stratigraphic Bistra unit (Zagreb area), which indicates Pleistocene age (Bakrač & Koch, 1999, Grizelj et al., 2017).

Discussion

Marine connection of individual areas

There are prominent differences in the Central Paratethys transgression and regression stages between the individual basins north and south of the PAF and the MHZ. In the southern basins, Neogene sedimentation started in the Egerian and continued to Eggenburgian, where the Govce formation is described. In the northern basins, the Eggerian and Eggenburgian sediments are not defined, and this transgression has not reached the Krško area either. However, the Govce formation is described in the Krško area as well, but sediments were deposited in Ottnangian in terrestrial environment, based on similarities with sediments in the Medvednica Mountains (Čorić et al., 2009; Poljak, 2017a). The fact that the transgression in the Egerian and Eggenburgian did not reach the area north of the PFS and the MHZ as well as south of the central Sava folds (Fig. 5) suggests that the transgression was of lesser extent, or the local tectonic uplift (or delayed subsidence) of individual blocks prevented the northward and southward spreading of the Central Paratethys.

Prominent paleogeographic changes led to variable sedimentation in the late Early Miocene. Ottnangian sedimentation took place only in the Krško area, where Ottnangian/Karpatian alluvial, lacustrine and even marine sediments have been described (Verbič, 1995; Dozet et al., 1998; Rižnar, 2005; Poljak, 2017a). Karpatian transgression influenced sedimentation in the basins north of the PFS and the MHZ (Fig. 5) and caused the first marine transgression in the Early Miocene. The nanoplankton assemblages in the Slovenj Gradec Basin and the decapod crustacean fauna in the Ribnica Selnica Through indicate a marine connection with the Mediterranean Sea in the Karpatian (Gašparič & Hyžný, 2014; Ivančič et al., 2018a). In the areas south of the PFS and the MHZ, the Ottnangian and Karpatian sediments are not defined.

While Karpatian marine sedimentation continued in the Badenian in the Mura-Zala Basin (Maros, 2012), the early Badenian transgression correlated with TB 2.3 (Haq et al., 1988) is defined only in the Slovenj Gradec Basin (Ivančič et al., 2018a). Nanoplankton assemblages point to the connection with the Mediterranean Sea (Ivančič et al., 2018a). The extent of the transgression towards the west is not yet defined (Fig. 5). South of the PFS and MHZ, the early Badenian transgression has been proven in the Kozjansko area (Aničić et al., 2002) and presumable in the Tunjice and Moravče area.

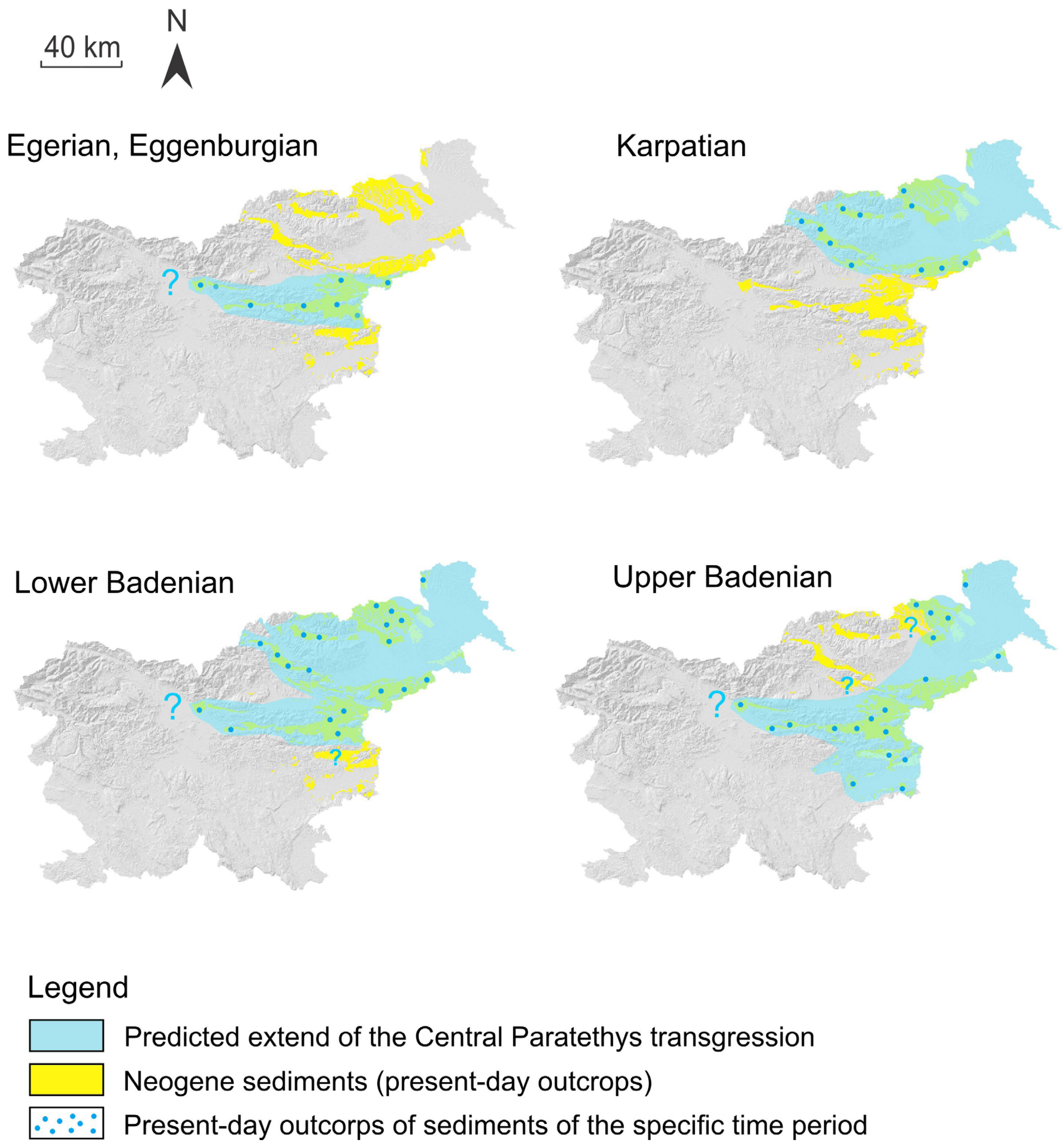

Fig. 5. Transgressions of the Central Paratethys in the Slovenian area, through the Early and Middle Miocene stages: blue colour indicates presumed extension of the Central Paratethyan transgression, yellow colours indicate distribution of actual outcrops of Neogene sediments.

At the end of the early Badenian, widespread palaeogegographic changes led to a cassation of Miocene sedimentation in the Ribnica Selnica Through, the Slovenj Gradec Basin and Kungota area due to the exhumation of the Pohorje Tectonic Block (Trajanova, 2013). The subsequent transgression of the Central Paratethys in the late Badenian caused the flooding of the areas north and south of the PFS and MHZ, as well as the Krško area (Fig. 5). Marine sedimentation continued in the Sarmatian, but the gradual filling of the basin and the cassation and closure of the marine connection to the open sea caused first brackish and later deltaic and terrestrial sedimentation in the Pannonian with the deposition of fine-grained sediments, white intercalations of coarse-grained sediments and coal.

Different names of lithological units

The difficulty in comparing beds and formations in various areas sometimes lies in the different naming of the individual lithological units. More precise investigations have rarely been carried out, so usually only the descriptive field name of the unit has been established, which is sometimes inaccurate. With coarse-grained sediments, this problem is not so pressing, as the names of the units can be determined fairly accurately in the field. The problem arises when fine-grained sediments or different types of limestone and calcarenites are present. For example, the term lithothamnium limestone is commonly used in the literature, but sometimes the name is not appropriate because of the involvement of different fossils. In several places, the terms lithotamnium limestone, calcarenite or algal limestone are used. Rarely, lithothamnium limestone is defined more precisely (bindstone, rudstone) (Rižnar et al., 2002). The difficulties in defining lithothamnium limestone have been emphasised by various authors (Fuchs, 1894; Mikuž et al., 2014; Poljak, 2017a). Within the Badenian there are several layers of lithotamnium limestones, which are not precisely dated. It is possible that the lithothamnium limestone belongs to different 3rd order sequence cycles, but without detailed sedimentological, stratigraphical and especially paleontological analyses, it is impossible to distinguish between them. Similar uncertainty with the commonly used term Laško marl (Laški lapor), which is present in more than one undefined horizon (bellow and over lithothamnium limestone). Moreover, the name Laško marl is commonly used for thicker sequences of silty sediments.

Correlation of different fauna between separate basins

Palaeontological studies are occasionally well documented in individual areas, but they have rarely been compared with neighboring basins. The exception is a small part of Kozjansko area, which contains Pannonian sediments and has been the subject of a few studies (Stevanović & Škerlj, 1989, Aničić et al., 2002, Marinšek et al., 2022). The ostracod and mollusk fauna of the Kozjansko area can easily be correlated to the Bizeljsko Formation in the Krško area. In both areas an abundant ostracod assemblage, which assigned to the upper Pannonian (ex.“Pontian”) stage, can be found. The assemblage includes some characteristic species like *Bakunella anae, Bakunella dorsarcuata, Hemicytheria Croatica* and *Camptocypria acranasuta and* can be correlated with the Croatian Mt. Medvednica and the Styrian Basin (Sokač, 1972; Gross, 2008). Correlations with the fauna in the Mura-Zala basin are still missing.

Formalising the “Plio-Quaternary” unit

The informal “Plio-Quaternary” unit has been a matter of debate for what is now a long while. This unit represents the onset of the youngest terrestrial sedimentation, marked by successions of clastic sediments abundant in central, southern and eastern Slovenia. Rare adequate exposures and subsurface data, strong weathering and degraded geomorphological characteristics have prevented research on the composition, provenance, genesis and age of the “Plio-Quaternary” fluvial terrace sequences in Slovenia, resulting in scarce relevant data in the past (Pleničar & Ramovš, 1954; Brezigar et al., 1985, 1987; Markič & Rokavec, 2002; Bavec et al., 2003; Verbič, 2004; Bavec & Poljak, 2013; Poljak, 2017a). The lack of knowledge concerning these units constitutes a scientific gap in the stratigraphy of the region, which limits our understanding of the Quaternary evolution of the entire pan-Alpine region.

The latest studies of the “Plio-Quaternary” unit in Slovenj Gradec, Nazarje, Velenje, Celje, Drava-Ptuj and Krško Basins followed multi-methodological approach (Mencin Gale et al., 2019a, 2019b; Mencin Gale, 2021) and provided the basic ground for formalizing the alloformations. However, except in Velenje and Krško Basin, no numerical age dating is available, which is the main aim of the future studies and the main condition for formalizing the sequence.

Conclusions

The Neogene period is characterized by significant paleoenvironmental, structural, paleogeographical and climatic changes. During this period, different depositional environments evolved which resulted in the deposition of several formations. Their composition reflects sea level fluctuations, which influenced not only the sedimentation processes, but also the connection of the Central Paratethys with the Mediterranean Sea and the open ocean. Such connections were established through the so-called Trans Tethyan (Slovenian) Corridor during the Karpatian and Badenian transgressions. While formations in the Mura-Zala Basin (Haloze, Špilje, Lendava, Ptuj-Grad, Ptuj-Kog, Mura) were defined primarily on the basis of seismic profiles, the formations in other parts were defined on the basis of biostratigraphic correlations. The oldest sediments are described south of the PFS as the Govce formation, which includes largely silty marl deposits of Egerian and Eggenburgian age that were deposited in a shallow marine to brackish environment. Ottnangian and Karpatian sediments are only present north of the PFS and the MHZ. Ottnangian sediments, known as the Radlje layers, consist mainly of conglomeratic successions, deposited in fluvial environments. The Haloze Formation consists of fine- to coarse-grained sediments of Karpatian age deposited in terrestrial, transitional and shallow marine environments. According to new data, it comprises the Urban, Kungota and Ivnik beds. The Badenian transgressions flooded the entire study area. The Špilje and Ptujska Gora – Kog Formation are described in the Mura-Zala Basin, while the Laško and Čatež Formations are defined south of the PFS and MHZ; their successions consist of comparable sediments. Sedimentation begins with conglomerate layers overlain by sand, silt and marl with interbedded limestone layers. Sarmatian sediments are deposited concordantly on Badenian. South of the PFS and the MHZ, the Dol formation is described, comprises conglomeratic, sandy, silty and marly layers, deposited in marine and brackish environment. During the Pannonian, the Lendava, Mura and Ptuj-Grad formations were deposited in the Mura-Zala Basin. The sediments were initially deposited in a turbiditic and later in a deltaic environment where deposition of clayey, silty and sandy sediments prevail. South of the PFS and the MHZ, Pannonian sediments are present in the Kozjansko and Krško area. While sediments are not described in any formation in the Kozjansko area, the Drnovo, Bizeljsko and Raka Formations are defined in the Krško area. In this area, the sandy and silty sediments were initially deposited in a brackish environment which evolved towards a deltaic setting. Pliocene and Quaternary formations are only well defined in the Krško area, with the Globoko Alloformation consisting of non-carbonate gravel, sandy and silty layers.

Many uncertainties remain obscuring the overall structure of the studied part of the PBS and its sedimentary evolution during the Neogene due to lack of research. This review provides some guidelines for further research with the aim of expanding our knowledge of:

- the precise age of individual formations,
- stratigraphic, paleontological, and sedimentological correlations between different formations,
- temporal and spatial description of the Trans-Tethyan Trench corridor,
- standardization of different names/descriptions of similar lithological units,
- formalization of the Plio-Quaternary units.

Acknowledgments

The authors gratefully acknowledge financial support from the Slovenian Research and Innovation Agency - Research Core Funding No. P1-0025 “Mineral Resources”, No. P1-0011 »Regional Geology« and No. P1-0419 »Dynamic Earth«.

Reference

Aničić, B. 1990: Geological setting of the Orlica mountain. Geologija, 33/1: 233–287. https://doi.org/10.5474/geologija.1990.005

Aničić, B. & Juriša, K. 1985a: Osnovna geološka karta SFRJ 1:100 000. List Rogatec. Zvezni geološki zavod, Beograd.

Aničić, B. & Juriša, K. 1985b: Osnovna geološka karta SFRJ 1:100 000. Tolmač lista Rogatec. Zvezni geološki zavod, Beograd: 76 p.

Aničić, B., Ogorelec, B., Kralj, P. & Mišič, M. 2002: Lithology of Tertiary beds in Kozjansko, Eastern Slovenia. Geologija, 45/1: 213–246. https://doi.org/10.5474/geologija.2002.017

Atanackov, J., Jamšek Rupnik, P., Rižnar, I., Bavec, M., Petronio, L., Cline, K., M., Cline, M., Logan & Quittmeyer, R. 2018: High-resolution seismic reflection surveys in the Krško basin. In: Novak, M. & Rman, N. (eds.): 5. slovenski geološki kongres: Zbornik povzetkov, Velenje, 3–5. oktober 2018. Ljubljana, Geološki zavod Slovenije: 25 p.

Atanackov. J, Jamšek Rupnik, P., Jež, J., Celarc, B., Novak, M., Milanič, B., Markelj, A., Bavec, M. & Kastelic, V. 2021: Database of Active Faults in Slovenia: Compiling a New Active Fault Database at the Junction Between the Alps, the Dinarides and the Pannonian Basin Tectonic Domains. Front. Earth Sci. 9: 604388. https://doi.org/10.3389/feart.2021.604388

Bakrač, K. & Koch, G. 1999: A palynological contribution to the Quaternary deposits in the wider ares of Zagreb (Croatia). Acta Palaeobotanica Supplementum, 2: 467–469.

Bartol, M. 2009: Middle Miocene Calcareous Nannoplankton of NE Slovenia (Western Central Paratethys), Založba ZRC, Ljubljana: 136 p.

Bartol, M. & Pavšič, J. 2005: Badenian Discoasters from the Section in Lenart (Northeast Slovenia, Central Paratethys). Geologija, 48/2: 211–23. https://doi.org/10.5474/geologija.2005.018.

Bartol, M., Pavšič, J., Dobnikar, M. & Bernasconi, S.M. 2008: Unusual Braarudosphaera bigelowii and Micrantholithus vesper enrichment in the Early Miocene sediments from the Slovenian Corridor, a seaway linking the Central Paratethys and the Mediterranean. Palaeogeography, palaeoclimatology, palaeoecology, 267/1: 77–88. https://doi.org/10.1016/j.palaeo.2008.06.005

Bartol, M., Mikuž, V. & Horvat, A. 2014: Palaeontological Evidence of Communication between the Central Paratethys and the Mediterranean in the Late Badenian/Early Serravalian. Palaeogeography, Palaeoclimatology, Palaeoecology, 394: 144–57. https://doi.org/10.1016/j.palaeo.2013.12.009

Bavec, M. 2000: Poročilo o določanju starosti kvartarnih sedimentov v Krški kotlini z metodo termoluminescence (TL) in optično stimulirane luminescence (OSL) - unpublished report. Ljubljana, Geološki zavod Slovenije.

Bavec, M. & Poljak, M. 2013: Plio-Quaternary sediments in Krško Basin, Knjiga sažetaka: 3. znastveni skup Geologija kvartara u Hrvatskoj s međunarodnim sudjelovanjem, povodom 130 godina rođenja akademika Marijana Salopeka i u spomen znastvenici Maji Paunović na 10. obljetnicu smrti, Zagreb 21.–23.3.2013. Zagreb, Hrvatska akademija znanosti i umjetnosti, Zavod za paleontologiju i geologiju kvartara: 65–67.

Bavec, M., Novak, M., Poljak, M. & Skaberne, D. 2003: Peleoseismic investigations on Krško basin. Geological Survey of Slovenia, Ljubljana: 19 p.

Bavec, M., Budkovič, T., Brenčič, M., Jelen, M., Kumelj, Š., Lapanje, A., Marinko, M., Markič, M., Mišič, M., Ogorelec, B., Placer, L., Poljak, M., Prestor, J., Rajver, D., Ribičič, M., Skaberne, D., Trajanova, M. & Urbanc, J. 2005: Overview of geological data for deep repository for radioactive waste in argillaceous formations in Slovenia. Geološki zavod Slovenije, Ljubljana: 124 p.

Brezigar, A., Kosi, G., Vrhovšek, D. & Velkovrh, F. 1985: Paleontološke raziskave pliokvartarne skladovnice velenjske udorine. Geologija, 28/1: 93–119.

Brezigar, A., Ogorelec, B., Rijavec, L. & Mioč, P. 1987: Geološka zgradba predpliocenske podlage Velenjske udorine in okolice. Geologija, 30/1: 31–65.

Brückl, E., Behm, M., Decker, K., Grad, A., Guterch, A., Keller, G.R. & Thybo, H. 2010: Crustal structure and active tectonics in the Eastern Alps. Tectonics, 29/2. https://doi.org/10.1029/2009TC002491

Buser, S. 1978: Osnovna geološka karta SFRJ 1:100 000. List Celje. Zvezni geološki zavod, Beograd.

Buser, S. 1979: Osnovna geološka karta SFRJ 1:100 000. Tolmač lista Celje. Zvezni geološki zavod, Beograd: 72 p.

Buser, S. 2010: Geological Map of Slovenia 1:250.000 1:250.000. Geological Survey of Slovenia.

Cline, M.L. & Cline, K.M. 2013: Characterization of the Libna fault and tectonic framework of the Krško Basin, Slovenia. Final report. Pitsburgh, Paul C. Rizzo Associates, Inc.: 78 p.

Cline, M. L., Cline, K., M., Jamšek Rupnik, P., Atanackov, J., Bavec, M. & Lowick, S.E. 2016: Tectonic geomorphology and geochronology supporting a probablistic seismic hazard analysis in the Krško Basin, Slovenia: implications for a critical infrastructure. In: McCalpin, J. &Gruetzner, C. (eds.): 7th International INQUA Meeting on Paleoseismology, Active Tectonics and Archeoseismology (PATA Days). Crestone, Colorado, USA, Crestone: 63–66.

Cline, M., L., Atanackov, J., Bavec, M., Cine, K., M., Rižnar, I., Jamšek Rupnik, P., Lowick, S.E., Rittenour, T. & Quittmeyer, R. 2018: Recent updates to the geochronological constraints in the Krško basin and surrounding region. In: Novak, M. & Rman, N. (eds.): 5. slovenski geološki kongres: Zbornik povzetkov, Velenje, 3.–5. oktober 2018. Ljubljana, Geološki zavod Slovenije: 36 p.

Ćorić, S., Pavelić, D., Rögl, F., Mandic, O. & Vrabac, S. 2009: Revised Middle Miocene datum for initial marine flooding of North Croatian Basins (Pannonian Basin System, Central Paratethys). Geologica Croatica, 62: 31–43. https://doi.org/10.4154/GC.2009.03

Debeljak, I. 2017: Fosilni trobčarji iz Šaleške doline. Zbornik Šaleški razgledi (2016-2017): 35–50.

Dozet, S., Rijavec, J., Aničić, B., Škerlj, Ž. & Stojanovič, B. 1998: Neogene beds of the Krško-Brežice plain and its borderland (southeastern Slovenia). RMZ – Materials and Geoenvironment, 45/3-4: 375–404.

Drobne, K., Ogorelec, B., Pavšič, J. & Pavlovec, R. 2008: Palaeogene and Neogene. Slovenian Tethys basins. In: McCann, T. (ed.): The geology of Central Europe. London: The Geological Society, 1093-1098.

Drobne, K., Mikuž, V. & Pavšič, J. 2017: Tapir - edinstveni pliocenski sesalec iz Šaleške doline. In: Grmovšek, S., Hudales, J. & Ravnikar, T. (eds.): Zbirka Šaleški razgledi, 15: 67–74.

Fodor, L., Jelen, B., Márton, E., Rifelj, H., Kraijic, M., Kevrić, R., Marton, P., Koroknai, B. & Baldi-Beke, M. 2002: Miocene to Quaternary deformation, stratigraphy and paleogeography in Northeastern Slovenia and Southwestern Hungary. Geologija, 45/1: 103–114. https://doi.org/10.5474/geologija.2002.009.

Fodor, L., Uhrin, A., Palotás, K., Selmeczi, I., Nádor, A., Tóth-Makk, Scharek, P., Rižnar, I. & Trajanova, M. 2011: Geološki konceptualni model v okviru projetka T-JAM. Ljublajana, Budimpešta.

Fodor, L., Balázs, A., Csillag, G., Dunkl, I., Héja, G, Jelen, B., Kelemen, P., Kövér, S., Németh, A., Nyíri, D., Selmeczi, I., Trajanova, M., Vrabec, M. & Vrabec, Mi. 2021: Crustal exhumation and depocenter migration from the Alpine orogenic margin towards the Pannonian extensional back-arc basin controlled by inheritance. Global and Planetary Change, 201: 103475. https://doi.org/10.1016/j.gloplacha.2021.103475

Fuchs, Th. 1894: Tertiaerfossilien aus den kohlenfuhrenden Miocaenablagerungen der Umgebung von Krapina und Radoboj ünd tiber die Stellung der sogenannten »Aquitanischen Stufe«. Mitt. Jb. ung. geol. Anst., X., Budapest.

Gašparič, R. & Hyžný, M. 2014: An early Miocene deep-water Decapod Crustacean Faunule from the slovenian part of the Styrian Basin and its palaeoenvironmental and palaeobiogeographical significance. Papers in Palaeontology, 1/2: 141–166. https://doi.org/10.1002/spp2.1006

Gosar, A. 2005: Seismic reflection investigations for gas storage in aquifers (Mura Depression, NE Slovenia). Geologica Carpathica, 56/3: 285–294.

Gosar, A. & Janežič, B. 2006: Structural maps of seismic horizons in the Krško basin = strukturne karte seizmičnih horizontov v Krški kotlini. RMZ - Materials and geoenvironment: periodical for mining, metallurgy and geology, 53/3: 339–352.

Grizelj, A., Bakrač, K., Horvat, M., Avanić, R. & Hećimović, I. 2017: Occurrence of vivianite in alluvial Quaternary sediments in the area of Sesvete (Zagreb, Croatia). Geologia Croatica, 70/1: 41–52. https://doi.org/10.4154/gc.2017.01

Gross, M. 2003: Beitrag zur Lithostratigraphie des Oststeirischen Beckens (Neogen/Pannonium; Österreich). In: Piller, W.E. (ed.): Stratigraphia Austriaca. Österr. Akad. Wiss., Schriftenr. Erdwiss. Komm. 16: 11–62.

Gross, M., Minati, K., Danielopol, D. & Piller, W. 2008: Environmental changes and diversification of Cyprideis in the Late Miocene of the Styrian Basin (Lake Pannon, Austria). Palaeobio. Palaeoenv., 88: 161–181. https://doi.org/10.1007/BF03043987

Hamrla, M. 1954: Geološke razmere ob severnem robu laške sinklinale vzhodno od Savinje. Geologija, 2: 118–144.

Haq, B.U., Hardenbol, J. & Vail, P.R. 1988: Mesozoic and Cenozoic chronostratigraphy 753 and eustatic cycles. In: Wilgus, C.K., Hastings, B.S., Posamentier, H., van Wagoner, J., Ross, C.A. & Kendall, C.G.St.C. (eds.): Sea-level changes: An integrated approach. SEPM Spec. Publ., 42: 71–108.

Hardenbol, J., Thierry, J., Farley, M.B., Jacquin, T., de Graciansky, P.C. & Vail, P.R. 1998: Mesozoic and Cenozoic sequence chronostratigraphic framework of European Basins. In: de Graciansky, P.C., Hardenbol, J., Jacquin, T. & Vail, P.R.: (eds.): Mesozoic and Cenozoic sequence stratigraphy of European Basins. SEPM Spec. Publ., 60: 3–13.

Hasenhüttl, C., Kraljič, M., Sachsenhofer, R.F., Jelen, B. & Rieger, R. 2001: Source rocks and hydrocarbon generation in Slovenia (Mura Depression, Pannonian Basin). Marine and Petroleum Geology, 18: 115–132.

Hohenegger, J., Rögl, F., Ćorić, S., Pervesler, P., Lirer, F., Roetzel, R., Scholger, R. & Stingl, K. 2009: The Styrian Basin: A key to the Middle Miocene (Badenian/Langhian) Central Paratethys transgressions. Austrian Journal of Earth Sciences, 102: 102–132.

Hohenegger, J., Ćorić, S. & Wagreich, M. 2014: Timing of the Middle Miocene Badenian Stage of the Central Paratethys. Geologica Carpathica, 65/1: 55–66. https://doi.org/10.2478/geoca-2014-0004

Horvat, A. 2004: Srednjemiocenske kremenične alge Slovenije: Paleontologija, stratigrafija, paleoekologija, paleobiogeografija. ZRC SAZU, Ljubljana: 255 p.

Huismans, R.S., Podladchikov, Y.Y. & Cloeting, S. 2001: Transition from passive to active rifting: Relative importance of astenospheric doming and passive extension of the litosphere. Journal of geophysical research, 106/11: 271–291.

Ivančič, K., Trajanova, M., Ćorić, S., Rožič, B. & Šmuc, A. 2018a: Miocene Paleogeography and Biostratigraphy of the Slovenj Gradec Basin: A Marine Corridor between the Mediterranean and Central Paratethys. Geologica Carpathica, 69/6: 528–44. https://doi.org/10.1515/geoca-2018-0031

Ivančič, K., Trajanova, M., Skaberne, D. & Šmuc, A. 2018b: Provenance of the Miocene Slovenj Gradec Basin Sedimentary Fill, Western Central Paratethys. Sedimentary Geology, 375: 256–67. https://doi.org/10.1016/j.sedgeo.2017.11.002.

Ivančič, K., Brajkovič, R. & Vrabec, Mi. 2024: Geochemical and Mineralogical Approaches in Unraveling Paleoweathering, Provenance, and Tectonic Setting of the Clastic Sedimentary Succession (Western Central Paratethys). Appl. Sci. 14: 537. https://doi.org/10.3390/app14020537

Jelen, B. & Rifelj, H. 2003: The Karpatian in Slovenia. In: Brzobohaty, R., Cicha, I., Kovač, M. & Rogl, F. (eds.): The Karpatian. A Lower Miocene Stage of the Central Paratethys. Masaryk Universiy, Brno: 133–139.

Jelen, B. & Rifelj, H. 2005: Inner geodynamic control on the Late Paleogene and Neogoene stratigraphy in Slovenia. In: Patterns and Processes in the Neogene of the Mediterranean Region. 12th Congress R.C.M.N.S. Vienna.

Jelen, B. & Rifelj, H. 2011: Karta neogenske tektonske strukture podlage Mursko-Zalskega bazena. 1: 250.000, Ljubljana, Geološki zavod Slovenije.

Jelen, B., Rifelj, H., Bavec, M. & Rajver, D. 2006: Opredelitev dosedanjega konceptualnega geološkega modela "Murske depresije" Geološki zavod Slovenije: 28 p.

Kováč, M., Hudáčková, N., Halásová, E., Kováčová, M., Holcová, K., Oszczypko-Clowes, M., Báldi, K., Less, G., Nagymarosy, A., Ruman, A., Klučiar, T. & Jamrich, M. 2017: The Central Paratethys palaeoceanography: a water circulation model based on microfossil proxies, climate, and changes of depositional environment. AGEOS, 9/2: 75–114.

Kováč, M., Halásová, E., Hudáčková, N., Holcová, K., Hyžný, M., Jamrich, M. & Ruman, A. 2018: Towards better correlation of the Central Paratethys regional time scale with the standard geological time scale of the Miocene Epoch. Geologica Carpathica, 69/3: 283–300.

Kralj, P. 1995: Lithofacies of the Pliocene Volcaniclastic and fluvial complex of Grad, north-eastern Slovenia. Ph.D. University of Zagreb, Faculty of mining, geology and petroleum engineering, Zagreb.

Kralj, P. 2001a: Pliocene clastic sediments in Western Goričko, Northeastern Slovenia. Geologija, 44/1: 73–79. https://doi.org/10.5474/geologija.2001.004

Kralj, P. 2001b: Das Thermalwasser-System des Mur-Beckens in Nordost-Slowenien. Mitteilungen zur Ingenieurgeologie und Hydrogeologie 81, RWTH Aachen.

Kralj, P. 2010: Eruptive and sedimentary evolution of the Pliocene Grad Volcanic Field, North-east Slovenia. Journal of Volcanology and Geothermal Research, 201: 272–284. https://doi.org/10.1016/j.volgeores.2010.09.004

Kralj P., Eichinger L. & Kralj, P. 2009: The Benedikt hydrothermal system (north-eastern Slovenia). Environvilonmental Geology, 58: 1653–1661. https://doi.org/10.1007/s00254-008-1631-3

Kresevič, A. 2016: Sedimentologija in tektonska struktura srednjemiocenskih plasti v Tunjiškem gričevju. Diplomsko delo. Univerza v Ljubljani, Naravoslovnotehniška fakulteta: 92 p.

Kuščer, D. 1967: Zagorski terciar. Geologija, 10: 5–85.

Kuščer, D. 1993: Neotektonika Krške kotline. Predhodno poročilo. Ljubljana: Geološki zavod Slovenije: 28 p.

Lapajne, J. 1975: Geofizikalne raziskave na območju Čateških Toplic = Geophysical Exploration of the Čatež Thermal Springs Area. Geologija, 18/1: 315–324.

Marinšek, M., Hajek-Tadesse, V., Kolar-Jurkovšek, T. & Gale, L. 2022: Ostrakodi Kozjanskega - preliminarni rezultati. Rman, N., Bračič Železnik, B. & Žvab Rožič, P. (ur.): Zbornik povzetkov, 6. Slovenski geološki kongres / Vedeti (ne)vidno – vloga geologije v naši družbi, 3.-5. oktober 2022 Rogaška Slatina. Slovensko geološko društvo, str. 62.

Marinšek, M., Hajek-Tadesse, V., Poljak., M., Kolar-Jurkovšek, T. & Gale, L. 2023: Upper Miocene ostracods form the Krško Basin, SE Slovenia. Geologia Croatica, 76/2: 57–72. https://doi.org/10.4154/gc.2023.07

Markič, M. & Rokavec, D. 2002: Geološka zgradba, nekovinske mineralne surovine in lignit okolice Globokega (Krška kotlina). Rudarsko metalurški zbornik, 49/2: 229–266.

Maros, G., Jelen, B., Lapanje, A., Rifelj, H., Rižnar, I. & Trajanova, M. 2012: Summary report of the geological models, TRANSENERGY project. Ljubljana: Geološki zavod Slovenije; Bratislava: Štátny geologický ústav Dionýza Štúra; Budapest: Magyar Földtani és Geofizikai Intézet. Wien: Geologische Bundesanstalt: 189 p.

Martin, U. & Nemeth, K. 2004: Mio/Pliocene phreatomagmatic volcanism in the Western Pannonian Basin. Geol. Hungarica, 26: 1–191 Budapest.

Mencin Gale, E. 2021: Pliocene to Quaternary sedimentary evolution of intramountain basins at the junction pf Alps, Dinarides and Pannonian Basin. Doktorska disertacija. Univerza v Ljubljani, Naravoslovnotehniška fakulteta, Ljubljana: 187 p.

Mencin Gale, E., Jamšek Rupnik, P., Trajanova, M., Bavec, M., Anselmetti S., F. & Šmuc, A. 2019a: Morphostratigraphy and provenance of Plio-Pleistocene terraces in the south-eastern Alpine foreland: the Mislinja and Upper Savinja valleys, northern Slovenia. Journal of quaternary science, 9/ 2: 1–17. https://doi.org/10.1002/jqs.3156

Mencin Gale, E., Jamšek Rupnik, P., Trajanova, M., Gale, L., Bavec, M., S. Anselmetti, F. & Šmuc,

A. 2019 b: Provenance and morphostratigraphy of the Pliocene- Quaternary sediments in the Celje and Drava-Ptuj Basins (eastern Slovenia). Geologija, 62/2: 189–218.

Mencin Gale., E., Jamšek Rupnik, P., Akçar, N., Christl, M., Vockenhuber, C., Anselmetti, F.S. & Šmuc, A. 2024: The onset of Pliocene - Early Pleistocene fluvial aggradation in the Southeastern Alpine Foreland (Velenje Basin, Slovenia) and its paleoenvironmental implications. Journal of Quaternary Science. 1–19. https://doi.org/10.1002/jqs.3623

Mikuž, V. 1999: Pereiraea gervaisi (Vezian) from Miocene beds south of Šentjernej in Lower Carniola, Slovenia. Geologija, 42/1: 123–140.

Mikuž, V., Bartol, M. & Ulaga, Š. 2012a: The Brachiopod Lingula from the Middle Miocene – Badenian Beds of Slovenia. Geologija 55/2: 271–74. https://doi.org/10.5474/geologija.2012.017

Mikuž, V., Gašparič, R., Bartol, M., Horvat, A. & Pavšič, J. 2012b: Miocenski pteropodi s Poličkega Vrha v Slovenskih goricah = Miocene pteropods from Polički Vrh in Slovenske gorice, northeast Slovenia. Geologija, 55/1: 67–75. https://doi.org/10.5474/geologija.2012.005

Mikuž, V., Bartol, M. & Ulaga, Š. 2014: Ribje vretence iz miocenskih plasti v okolici Govc. Geologija, 57/1: 27–32. https://doi.org/10.5474/geologija.2014.003

Mioč, P. 1978: Osnovna geološka karta SFRJ 1:100 000. Tolmač lista Slovenj Gradec. Zvezni geološki zavod, Beograd: 74 p.

Mioč, P. & Žnidarčič, M. 1977: Osnovna geološka karta SFRJ. 1:100 000. List Slovenj Gradec. Zvezni geološki zavod, Beograd.

Mioč, P. & Ogorelec, B. 1991: Raziskave nafte in plina v Sloveniji: geološke raziskave: poročilo za leto 1991. Zv. 1, Murska depresija. Ljubljana: Geološki zavod Ljubljana, Inštitut za geologijo, geotehniko in geofiziko: 111 p.

Munda, M. 1951: Geološko kartiranje med Hrastnikom in Laškim. Geologija, 1: 37–89.

Nádor, A., Lapajne, A., Tóth, G., Rman, N., Sőcs, T., Prestor, J., Uhrin, A., Rajver, D., Fodor, L., Muráti, J. & Székely, E. 2012: Transboundary geothermal resources of the Mura-Zala basin: a need for joint thermal aquifer management of Slovenia and Hungary. Geologija, 55/2: 209–224. https://doi.org/10.5474/geologija.2012.013

Neal, J., Risch, D. & Vail, P. 1993: Sequence stratigraphy–A global theory for local success. Oilfield Rev., 2: 51–62.

Oblak Brown, K. 2006: Foraminiferna taksonomija, biostratigrafija in paleoekologija badenija v Planinski sinklinali (vzhodna Slovenija, Centralna Paratetida. Doktorska disertacija. Ljubljana, Univerza v Ljubljani, Naravoslovnotehniška fakulteta: 310 p.

Pavelić, D. & Kovačić, M. 2018: Sedimentology and Stratigraphy of the Neogene Rift-Type North Croatian Basin (Pannonian Basin System, Croatia). Marine and Petroleum Geology, 91: 455–469. https://doi.org/10.1016/j.marpetgeo.2018.01.026.

Pavšič, J. & Aničić, B. 1998: Nanoplanktonska stratigrafija oligocenskih in miocenskih plasti na Plohovem bregu pri Podčetrtku (Vzhodna Slovenija) = Nannoplankton stratigraphy of Oligocene and Miocene strata on Plohov breg near Podčetrtek (Eastern Slovenia). Razprave, 39: 55–79.

Pavšič, J. & Aničić, B. 1999: S pentaliti bogate spodnjemiocenske plasti v profilu Plohov Breg pri Podčetrtku (Kozjansko, Vzhodna Slovenija) = Lower Miocene Beds Rich in Pentalites in the Plohov Breg profile at Podčetrtek (Kozjansko, Eastern Slovenia). Razprave, 40: 57–65.

Pavšič, J. & Aničić, B. 2000: Lower miocene Braarudosphaera - and Micrantholithus - rich layers of eastern Slovenia. Journal of Nannoplankton Research, 22/2: 130–131.

Pavšič, J. & Horvat, A. 2009: Eocen, oligocen in miocen v osrednji in vzhodni Sloveniji. In: Pleničar, M., Ogorelec, B. & Novak, M. (eds.): The Geology of Slovenia. Geological survey of Slovenia, Ljubljana, 373–426.

Pikija, M. 1982: Turbiditne karakteristike dijela gornjopanonskih sedimenata u području Mihovljan-Labor (sjeverozapadna Hrvatska). Geol. vjesn., 35: 59–63.

Placer, L. 1998: Contribution to the macrotectonic subdivision of the border region between Southern Alps and External Dinarides. Geologija, 41/1: 223–255. https://doi.org/10.5474/geologija.1998.013

Placer, L. 1999: Structural meaning of the Sava folds. Geologija, 41/1: 191–221. https://doi.org/10.5474/geologija.1998.012

Placer, L. 2008: Principles of the tectonic subdivision of Slovenia = Osnove tektonske razčlenitve Slovenije. Geologija, 51/2: 205–217. https://doi.org/10.5474/geologija.2008.021

Pleničar, M. 1970: Osnovna geološka karta SFRJ 1:100 000. List Goričko. Zvezni Geološki zavod, Beograd.

Pleničar, M. & Ramovš, A. 1954: Geološko kartiranje severovzhodno od Brežic. Geologija, 2: 242–253.

Poljak, M. 2017a: Geološka karta vzhodnega dela Krške kotline 1:25.000. Tolmač. Geološki zavod Slovenije, Ljubljana: 108.

Poljak, M. 2017b: Geološka karta vzhodnega dela Krške kotline 1:25.000. Geološki zavod Slovenije, Ljubljana.

Poljak, M., Mikuž, V., Trajanova, M., Hajek-Tadesse, V., Miknić, M., Jurkovšek, B. & Šoster, A. 2016: Badenijske in sarmatijske plasti v gradbeni jami za hidroelektrarno Brežice. Geologija, 29/2: 129–153. https://doi.org/10.5474/geologija.2016.008

Poulditis, Ch. 1981: Petrologie und Geochimie basaltischer Gesteine des steirischen Vulkanbogens in der Steiermark und im Burgenland. Diss. Univ. Wien, Wien: 146 p.

Premru, U. 1983: Osnovna geološka karta SFRJ 1:100 000. List Ljubljana. Zvezni geološki zavod, Beograd.

Premru, U. 1983: Osnovna geološka karta SFRJ 1: 100 000. Tolmač lista Ljubljana Zvezni geološki zavod Beograd: 75 p.

Rojnik, A. 2015: Sedimentološke in petrološke značilnosti klastičnih kamnin Laške formacije v profilu Doblič. Diplomsko delo. Univerza v Ljubljani, Naravoslovnotehniška fakulteta, Ljubljana: 46 p.

Rakovec, I. 1968: O mastodontih iz Šaleške doline. Razprave, XI/IV: 301–350.

Rijavec, J. 1965: Mikrofavna terciarnih plasti in njih stratigrafija severno od Maribora. Disertacija. Geološki zavod, Ljubljana: 119 p.

Rižnar, I. 2005: Geološka zgradba mejnega področja med Zunanjimi in Notranjimi Dinaridi vzhodne Slovenije. Doktorska disertacija, Prirodoslovno-matematički fakultet, Sveučilište u Zagrebu, Zagreb: 146 p.

Rižnar, I. 2009: Gube med Ljubljanskim barjem in Južnimi Alpami. Geološki zbornik, 20: 136–138.

Rižnar, I., Miletić, D., Verbič, T. & Horvat, A. 2002: Srednjemiocenske kamnine severnega pobočja Gorjancev med Čatežem in Kostanjevico. Geologija, 45/2: 531–536. https://doi.org/10.5474/geologija.2002.060

Rögl, F., Ćorić, S., Hohenegger, J., Pervesler, P., Roetzel, R., Scholger, R., Spezzaferri, S. & Stingl, K. 2007: Cyclostratigraphy and transgressions at the Early/Middle Miocene (Karpatian/Badenian) boundary in the Austrian Neogene basins (Central Paratethys). Scripta Facultatis Scientiarum Naturalium Universitatis Masarykianae Brunensis, Geol., 36: 7–12.

Schmid, S., Fügenschuh, B., Kounov, A., Matenco, L., Nievergelt, P., Oberhänsli, R., Pleuger, J., Schefer, S., Schuster, R., Tomljenović, B., Ustaszewski, K. & van Hinsbergen, D. 2020: Tectonic units of the Alpine collision zone between Eastern Alps and western Turkey. Gondwana Research, 78: 308–374. https://doi.org/10.1016/j.gr.2019.07.005

Sokač, A. 1972: Pannonian and Pontian ostracode fauna of Medvednica. Pal. Jugoslav., 11: 1–140.

Stevanović, P. & Škerlj, Ž. 1989: The Pontian sediments of Slovenia. In: Malez, M. & Stevanović, P. (eds.): Chronostratigraphie und Neostratotypen, Pliozan, Pontien, bd. VIII. – Jugosl. Akad. D. Wissen. Und Kunste: 153–179.

Stingl, K. 1994: Depositional environment and sedimentary facies of the basinal sedi- ments in the Eibiswalder Bucht (Radl Formation and Lower Eibiswald Beds), Miocene Western Styrian Basin, Austria. Geologische Rundschau, 83: 811–821.

Strgar, I. 2003: Geološke raziskave nahajališč litotamnijskega apnenca na območju med Breznim in Savinjo. Geologija, 46/2: 313–328. https://doi.org/10.5474/geologija.2003.027

Šikić, K., Basch, O. & Šimunić, A. 1979: Osnovna geološka karta SFRJ 1:100 000. Tolmač lista Zagreb. Zvezni geološki zavod, Beograd: 81 p.

Šimunić, A. & Avanić, R. 1985: Korelacija geoloških odnosa in području Medvednice NW djela Savske potoline in djela Vukomeričkih gorica. Zagreb, Geološki zavod, Odur za geologiju i paleontologiju.

Šram, D., Rman, N., Rižnar, I. & Lapajne, A. 2015: The three-dimensional regional geological model of the Mura-Zala Basin, northeastern Slovenia. Geologija, 58/2: 139–154. https://doi.org/10.5474/geologija.2015.011

Tomljenović, B. & Csontos, L. 2001: Neogene–Quaternary structures in the border zone between Alps, Dinarides and Pannonian Basin (Hrvatsko zagorje and Karlovac Basins, Croatia). International Journal of Earth Sciences, 90: 560–578.

Trajanova, M. 2006: Granulometrijska in litološka sestava vzorcev proda iz lokacije Vrbina (Sv. Urh in Libna). Geološki zavod Slovenije, Ljubljana: 9 p.

Trajanova, M. 2013: Starost pohorskega magmatizma; nov pogled na nastanek Pohorskega tektonskega bloka = Age of the Pohorje mountains magmatism; mew view on the origin of the Pohorje tectonic block. Doktorska disertacija. Uiverza v Ljubljani, Naravoslonotehniška fakulteta, Ljubljana: 183 p.

Verbič, T. 1995: Kvartarni sedimenti v vzhodnem delu Krške kotline. Poročilo, Arhiv URSJV, Ljubljana: 248 p.

Verbič, T. 2002: Lito- in alostratigrafija kvartarnih sedimentov ter neotektonska aktivnost v vzhodnem delu Krške kotline. 1. slovenski geološki kongres, Črna na Koroškem, 9.–11. oktober. Ljubljana, Geološki zavod Slovenije: 98–99.

Verbič, T. 2004: Stratigrafija kvartarja in neotektonika vzhodnega dela Krške kotline. 1. del: Stratigrafija. Razprave, 45/3: 171–225.

Verbič, T., Rižnar, I., Poljak, M., Demšar, M. & Toman, M. 2000: Quaternary sediments of the Krško Basin. 2. hrvatski geološki kongres, Cavtat-Dubrovnik 17.–20.5.2022. Zbornik radova, Zagreb: 451-457.

Vrabec, M. & Fodor, L. 2006: Late Cenozoic tectonics of Slovenia: structural styles at the Northeastern corner of the Adriatic microplate. In: Pinter, N., Gyula, G., Weber, J., Stein, S. & Medak, D. (eds.): The Adria microplate: GPS geodesy, tectonics and hazards. NATO Science Series IV, Earth and Environmental Sciences, 61: 151–168. https://doi.org/10.1007/1-4020-4235-3_10

Vrabec, Mi. 2000: Govški Peščenjak v Profilu Doblič. Diplomsko Delo. Univerza v Ljubljani, Naravoslovnotehniška fakulteta, Ljubljana: 100 p.

Vrabec, Mi., Brajkovič, R. & Skaberne, D. 2014: Sedimentološke značilnosti terciarnih kamnin Tunjiškega gričevja. In: Rožič, B., Verbovšek, T. & Vrabec, Mi. (eds.): Zbornik povzetkov, 4. slovenski geološki kongres, Ankaran, 8.–10. 10. 2014. Oddelek za geologijo v sodelovanju s Slovenskim geološkim društvom. Naravoslovnotehniška fakulteta, Ljubljana: 75–76.

Winkler, A. 1926: Geologische Spezialkarte der Republik Österreich, Blatt Gleichenberg. Geologische Bundesanstalt, Wien.

Winkler, A. 1927: Erlauterungen zur geologischen Spezialkarte der Republik Österreich, Blatt Gleichenberg. Geologische Bundesanstalt, Wien: 164 p.

Žnidarčič, M. & Mioč, P. 1989: Osnovna geološka karta SFRJ 1:100 000. Tolmač listov Maribor in Leibnitz. Zvezni geološki zavod, Beograd: 60 p.

GEOLOGIJA 67/2, 217-236, Ljubljana 2024
https://doi.org/10.5474/geologija.2024.010

Late Cretaceous turbidite systems of southern Belgrade outskirts: Constraints on the Santonian convergence onset, evidence from the Sava Suture Zone (Guberevac-Babe, northern Šumadija, Serbia)

Zgornjekredni turbiditi južnega obrobja Beograda: Podrobna opredelitev začetka santonijske konvergence, dokazi iz Savske šivne cone (Guberevac-Babe, severna Šumadija, Srbija)

Darko SPAHIĆ[1]*, Dragan SIMIĆ[1], Miljan BARJAKTAROVIĆ[3] & Lidja KUREŠEVIĆ[2]

[1]Geological Survey of Serbia, Rovinjska 12, 11000 Belgrade, Serbia; *corresponding author: darkogeo2002@hotmail.com
[2]IMS Institute, Bulevar vojvode Mišića 43, 11000 Belgrade, Serbia
[3]University of Vienna, Department of Geology, Jozef-Holaubek Platz 2, 1090 Vienna, Austria

Prejeto / Received 28. 6. 2023; Sprejeto / Accepted 4. 6. 2024; Objavljeno na spletu / Published online 16. 12. 2024

Key words: Sava Suture Zone, Upper Cretaceous turbidites, folding and thrust faulting, Guberevac-Babe-Ropočevo, suture reactivation
Ključne besede: Savska šivna cona, zgornjekredni turbiditi, gubanje in narivanje, Guberevac-Babe-Ropočevo, reaktivacija stika

Abstract

As ancient depositional systems associated with active continental margins, turbidites may provide crucial information on orogenic evolution. This paper offers new stratigraphic and structural data on one of the late Alpine turbidite systems of the Late Cretaceous age (Guberevac-Babe-Ropočevo area; Serbia). The two opposite yet juxtaposed tectonic systems were initially deposited within the Sava Suture Zone and East Vardar Zone, whereby the former experienced Upper Cretaceous contractional- and extensional-type deformations. The new biostratigraphic dating constrains the age of mapped compressional structures, which indicates their Santonian age. This deformed segment of the newly dated Santonian clastic-carbonate turbidite sequence near the Guberevac site exposes new important compressional structures. The folds, reverse faults, and tectonic stylolites are allocated several kilometers from the primary deformation (Bela Reka thrust fault), positioned within the crustal footwall of the overriding East Vardar Zone.

The complexity of the geological processes in the Guberevac-Babe-Ropočevo area is further revealed by the previously mapped layering of Upper Cretaceous strata, exposed within the wider investigated area. Our combined field study provides a new statistical analysis of structural elements such as faults, folds, and bedding planes, adding to the depth of the understanding of the Sava Suture Zone. The observed contractional structures, mesoscopic folds, thrust faults, two-generation cleavage planes, as well as the produced statistical structures, are mostly imprinted into the out-of-deformation front or within the mixed clastic-carbonate turbidites of the Sava Suture Zone (Guberevac-Babe area). The composite study shows that the investigated footwall segment, represented by the deformed Sava Suture Zone turbidites, underwent tectonic shortening during Santonian (convergence onset). After the main crustal thickening event ceased, the Guberevac-Babe-Ropočevo suture segment was reactivated several times (post-orogenic extension). The investigated segment of the Neotethyan Vardar paleosuture experienced a total of four deformation stages spanning Late Cretaceous to Miocene times. These include the Late Oligocene reactivation and emplacement of the Glavčina-Parlozi Late Oligocene subvolcanic body and the slightly younger Stenička bara Miocene igneous system.

Izvleček

Turbiditi, kot sedimentacijski sistemi, vezani na aktivne robove celin, so turbiditi nosilci pomembnih podatkov o orogenem razvoju območja. V tem članku so predstavljeni novi stratigrafski in strukturni podatki o enem od alpskih turbiditnih sistemov iz časa pozne krede (območje Guberevac-Babe-Ropočevo; Srbija). Znotraj Savske šivne cone in Vzhodne Vardarske cone sta bili odloženi dve sinorogeni zaporedji, pri čemer je bilo prvo podvrženo poznokrednim kompresijskim in ekstenzijskim deformacijam. Glede na nove biostratigrafske podatke je do nastanka kompresijskih struktur prišlo v santoniju. V deformiranem delu santonijskega klastično-karbonatnega turbiditnega zaporedja v bližini Guberevaca so vidne nove pomembne kompresijske strukture. Gube, reverzni prelomi in tektonski stiloliti so vidni nekaj kilometrov stran od primarne deformacije (nariv Bela Reka), v talnini narinjene Vzhodne Vardarske cone.

O kompleksnosti geoloških procesov na območju Guberevac-Babe-Ropočevo pričajo tudi plasti zgornjekrednih kamnin, ki so bile predhodno kartirane na širšem območju. V sklopu naše terenske študije smo izvedli statistično analizo strukturnih elementov, kot so prelomi, gube in plasti, kar prispeva k boljšemu razumevanju Savske šivne cone. Opazovane kompresijske strukture, kot so mezoskopske gube, narivi in klivažne ravnine dveh generacij, kot tudi pridobljeni statistični podatki o strukturah, se večinoma pojavljajo v prednarivnem čelu ali znotraj mešanih klastično-karbonatnih turbiditov Savske šivne cone (območje Guberevac-Babe). Celotna študija kaže, da je bil preiskovani segment talnine, ki ga predstavljajo deformirani turbiditi Savske šivne cone, izpostavljen tektonskemu krčenju v santoniju (začetek konvergence). Po koncu glavnega dogodka debeljenja skorje je bil šivni segment Guberevac-Babe-Ropočevo večkrat reaktiviran (postorogena ekstenzija). Preučevani segment neotetidine vardarske paleosuture je med pozno kredo in miocenom skupaj doživel štiri faze deformacij. Te vključujejo pozno-oligocensko reaktivacijo ter umestitev pozno-oligocenskega subvulkanskega telesa Glavčina-Parlozi in nekoliko mlajšega, miocenskega magmatskega sistema Stenička bara.

Introduction and problem statement

One of the most intriguing issues in the reconstruction of the complex geodynamic evolution of the Jurassic and/or Cretaceous “northwestern branch” of the peri-Neotethyan oceanic realm (Dimitrijević, 2001) is related to the evolution of collisional Sava Suture Zone (SSZ; Schmid et al., 2008, 2020; Spahić & Gaudenyi, 2022; Fig. 1). In the literature, SSZ is also known as the “Sava Vardar Zone” of Pamić (2002), “Sava Zone” of Schmid et al., (2008), or “Central Vardar Zone” of Dimitrijević (1997) and Toljić et al., (2019). Nevertheless, much prior definition of the Vardar Zone by Dimitrijević (1997) or Pamić’s (2002), “Sava Vardar Zone”, given in the paper published in 1973 by Anđelković SSZ is indicated. This early paper shows that the complex geology of the Belgrade area contains the magmatism that is of Cretaceous age. Investigated scarcely developed magmatic episode is younger or of Upper Cretaceous age, emplaced much later than it was previously mapped and designated (Jurassic; see Spahić, 2022, for a review). A 1000 km long composite tectonic zone either belongs to a “relic Neotethyan ocean” (e.g., Karamata et al., 2000; Schmid et al., 2008; Ustaszewski et al., 2009, 2010) or represents a former post-Neotethyan Cretaceous marine (strike-slip; Grubić, 2002; Pamić et al., 2002; Handy et al., 2015; Köpping et al., 2019) corridor intervening Dinarides and European margin (Spahić & Gaudenyi, 2022).

The Late Cretaceous post-Neotethyan-type deep marine corridor exposes bimodal-type magmatic, metamorphic, and turbidite complexes, inclusive of the segment positioned near the city of Belgrade (Anđelković, 1973; Toljić et al., 2018; Spahić & Gaudenyi, 2022; Fig. 1). The investigated SSZ segment is an exhumed crustal fragment represented by a fault bounded km-scale block, which is connecting the tectonic units derived from the (i) Eurasian (Europe) and (ii) mixed Gondwana/Adria/Dinarides. The convergent assembly includes Vardar Zone oceanic and continental plates (Fig. 2a,b). The mapped segment of the SSZ exposes the two almost identical Upper Cretaceous turbidite sequences that originate from two different Late Cretaceous–Paleogene tectonic-paleogeographic realms: (i) foredeep suture-trench associated with the aforementioned narrowing marine corridor (K_2-SZ at Fig. 2b), and (ii) overriding foreland basin turbidites of the East Vardar Zone (K_2-EV at Fig. 2b; Schmid et al., 2020; Toljić et al., 2018, Spahić & Gaudenyi, 2022).

Before the latest Cretaceous–Paleogene continent-continent collision and the precursory production of two turbidite systems, the origin of modern-day SSZ (“Piemont-Liguria, Vahic, Inacovce-Kriscevo, Szolnok, Sava unit” at Fig. 1) can be interpreted following the two different lithospheric-scale mechanisms or plate tectonic scenarios. The first option poses the orthogonal subduction model, elaborated by a „closing“ Neotethys Vardar ocean, also referred to as the ”Sava Ocean” (Schmid et al., 2008). The second proposes the model of a renewed strike-slip oblique subduction having occurred along the Cretaceous corridor intervening Adria and Europe (Spahić & Gaudenyi, 2022). In the study area, these imprints are well-hidden by the two different Upper Cretaceous turbidite sequences. Near city of Belgrade, turbidites have just recently been separated into the two tectonic domains divided by the NNW-SSE striking west-vergent Bela Reka reverse fault (Toljić et al., 2018; Fig. 2b). The Bela Reka thrust fault separates the Western Vardar Zone including Sava Suture Zone (Adria-derived units), from the Eastern Vardar turbidite-ophiolitic units of European affinity (Schmid et al., 2008, 2020; Boev et al., 2018; Toljić et al., 2018; Fig. 1). With regards to the two contemporaneous turbidite sequences, these exhibit different levels of deformation, and are very challenging for clear field recognition (Anđelković, 1973; Toljić et al., 2018; Fig. 2b). As study will show, the investigated near Belgrade suture segment further exposes some previously

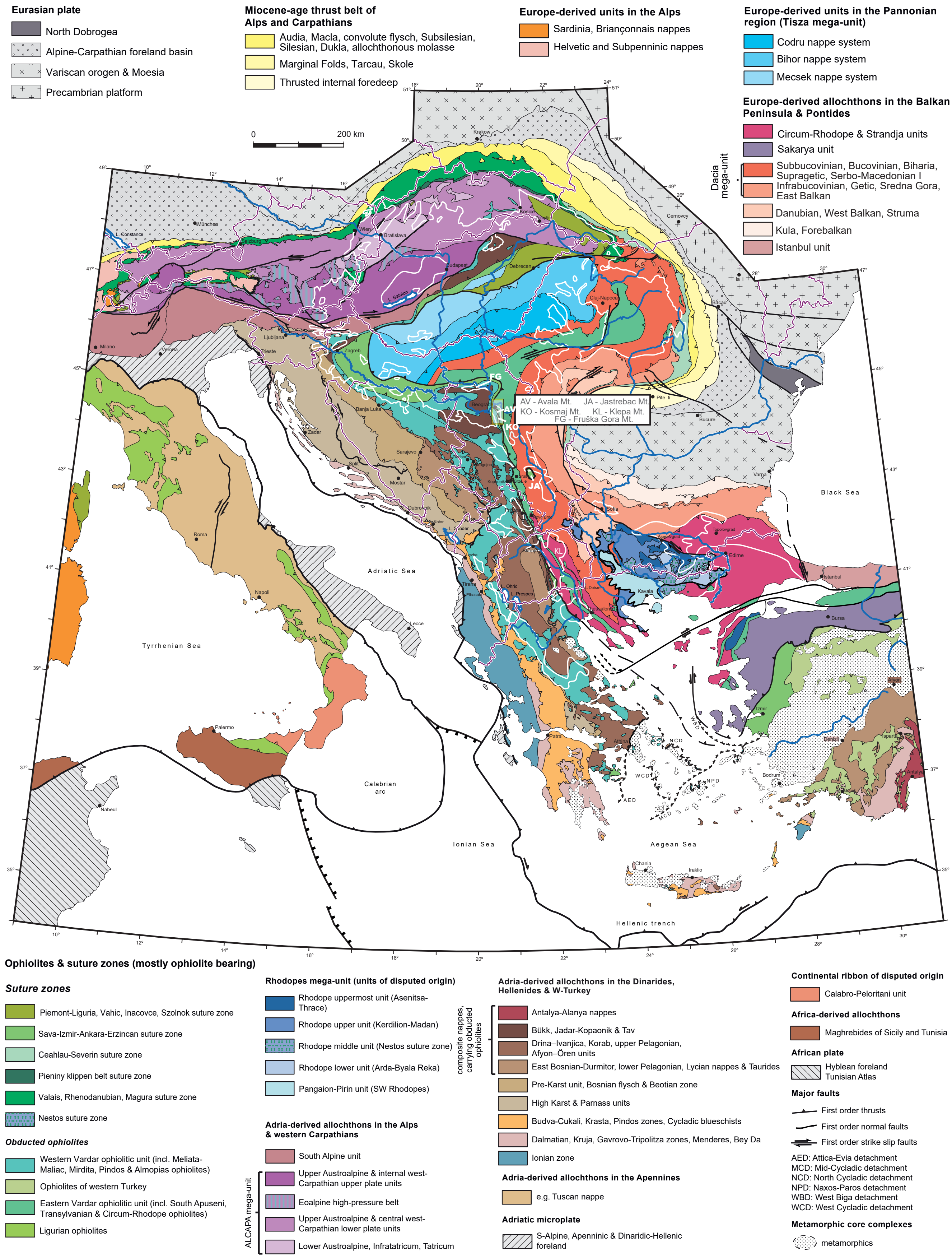

Fig. 1. The position of the investigated segment of the Sava Suture Zone, central Balkan Peninsula, Central Serbia, including the surrounding Alpine (modified after Schmid et al., 2008, 2020).

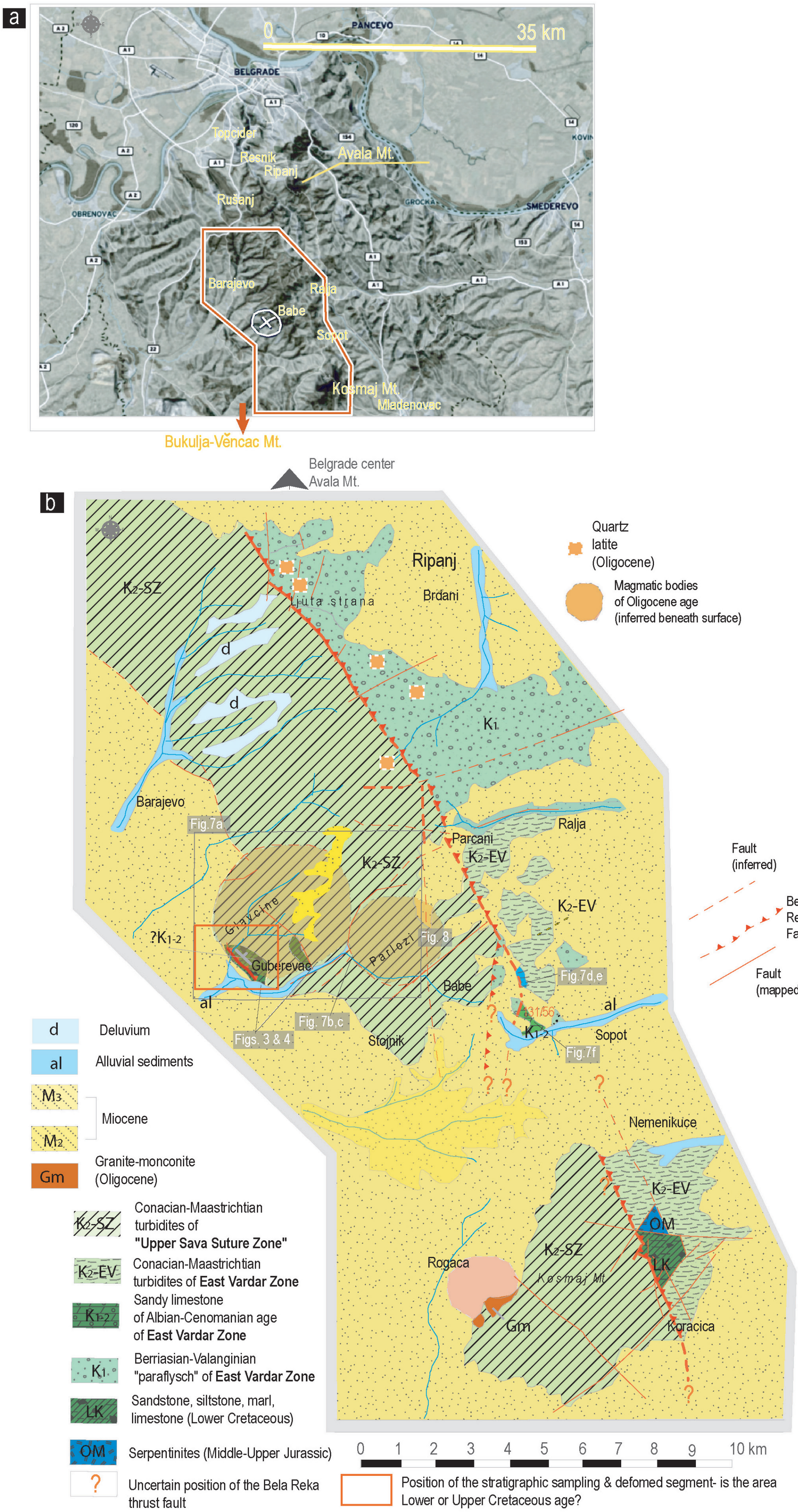

Fig. 2. a. The relief map of the wider southern Belgrade area, including the position of the figure 2b and key locations; b. Simplified geological sketch map of the Ripanj-Ropočevo-Kosmaj Mt. segment (significantly modified after inset of Radulović, 1987). The geological sketch-map includes the collected field mapping data, including the position Bela Reka fault proposed by Toljić et al. (2018).

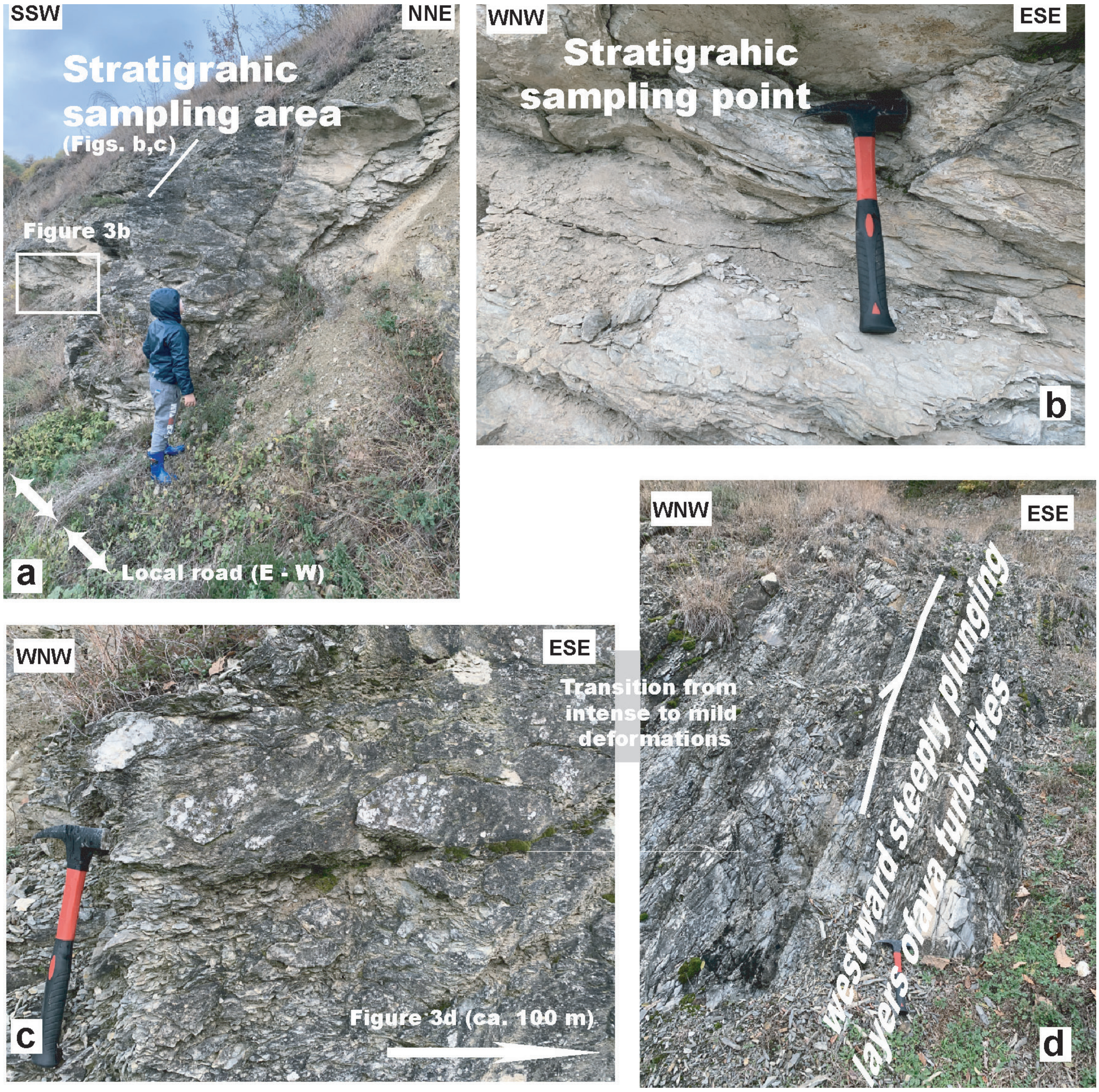

Fig. 3. a. The photos taken near Guberevac village, exposing the intensive folding (photo taken by D. Spahić). b. Intensely deformed rock, sampling area. c. The peculiar outlook of the outcropping deformed rock of questionable age: is the rock of latest Jurassic age or Late Cretaceous? d. Ca. 100 m towards the east (by road) Sava Suture Zone turbidites have regular layered form steeply plunging towards the west (likely induced by the Glavčina ring structure).

non-mapped compressional-type structures that are important for deciphering the exact convergence onset. The investigated tectonic relations (Fig. 2b) are additionally discussing the observed two-staged post-collisional extension-related tectonic episodes (Late Oligocene and Miocene times, e.g., Radulović, 1987; Vasković, 1987; Márton et al., 2022).

The primary purpose of this study is to provide a new stratigraphic and structural contribution to the ongoing debate revolving around the exact onset of the Neotethys Vardar-related late Alpine convergence. The convergence connects the (Adria) Dinarides and the former southern Eurasian margin (Robertson et al., 2008; Schmid et al., 2008). The field mapping and data collection is based upon the W–E-directed transect (Guberevac-Babe area). The measurements cover the exposed and deformed (former) Neotethyan lower plate. The lower plate is represented by a turbidite set that belongs to the SSZ(K_2-SZ) (Figs. 2a, b, red rectangle, and Figs. 3, 4, 5). In addition, the field mapping results shows that the investigated Guberevac-Babe area exposes a few inconsistencies relevant to final (Neo)Tethyan termination and late Alpine collision. The first is the exact age of the K_2-SZ / "Upper SSZ" sequence or Sava Suture Zone at the Guberevac-Babe area, which has been interpreted either as of the Jurassic age (sandy limestone; Radulović, 1987; Fig. 2b, 3a,b,c,d) or as the Lower Cretaceous flysch (Filipović et al., 1973; Fig. 6a). The inconsistency is further spiced by a recent sketch map of Toljić et al. (2018), which shows that a Miocene veneer overlies the highly deformed Guberevac-Babe turbidites. Aiming to solve these inconsistencies, the following regional geological study provides essential new stratigraphic data on the age of the newly discovered deformed Guberevac-Babe lower plate, i.e., its youngest SSZ turbidite sequence (K_2-SZ; Fig. 2b). The importance and the tectonic activity of this Sava Suture Zone segment is additionally indicated by imprints related to the post-orogenic Oligocene and Miocene magmatic stages.

Regional geology

Crosscutting the central part of the Balkan Peninsula along the W-E-trending Sava River, in the form of isolated outcrops (Hungary, Croatia, Bosnia & Herzegovina; Pamić et al., 2000, 2002; Pamić, 2002; Hrvatović, 2006; Grubić et al., 2009, 2010; Ustaszewski et al., 2009, 2010; Milošević, 2017; Maffione & van Hinsbergen, 2018; Farics et al., 2019; Gerčar et al., 2022), the Sava Suture Zone is passing near the Jadar block (e.g., Gerzina, 2010; Spahić & Gaudenyi, 2020). It further strikes across the Pannonian Basin and the Fruška Gora Mt. (Stojadinović et al., 2013, 2022; Dunčić et al., 2017; Toljić et al., 2019; Fig. 1), whereby this suture complex crops out in the immediate surrounding of the city of Belgrade, Serbia (southern city outskirts; Fig. 1, 2a,b; Toljić et al., 2018, 2021; Sokol et al., 2019; Márton et al., 2022; Spahić, 2022; Fig. 1, 2,b). The investigated Upper Cretaceous-Paleogene turbidites are striking across Central Serbia (Jastrebac Mt., Marović et al*.,* 2007a; Petrović et al., 2015; Erak et al., 2016), crossing into North Macedonia (Klepa Mt., Prelević et al., 2017; Köpping et al., 2019; Spahić et al., 2019), Greece and Turkey (Axios-Vardar Zone transferring into the İzmir-Ankara-Sava suture; e.g., van Hinsbergen & Schmid, 2012; Fig. 1). The investigated Upper Cretaceous complex *s.l.* (Fig. 6a), including the displaced mafic-type Jurassic magmatic sequences of the reactivated NeoTethyan suture, constitutes a regional bedrock system accommodated mostly underneath the broader area of Belgrade and its surroundings (e.g., Anđelković, 1973; Marinović & Rundić, 2020).

The wider Belgrade Alpine tectonic amalgamation comprises: (i) older Neotethyan magmatic-sedimentary complex or Jurassic ophiolites belonging to the Western and East Vardar Zones, including the associated ophiolitic mélange of the Jurassic age (Dimitrijević et al., 2003; Schmid et al., 2008; Bragin et al., 2011, 2019; Toljić et al., 2018, 2021; Marinović & Rundić, 2020; Spahić, 2022; Fig. 1). The older crustal elements of the Middle Jurassic age are tectonically emplaced on top of the younger Late Jurassic, or middle Oxfordian to a late Tithonian interval. Deep wells show depths of over 1500 m in the Pančevo area, which is positioned across the Danube River (Marinović & Rundić, 2020; Fig. 2a). Unconformably placed on top of the East Vardar Jurassic oceanic formations, the Tithonian limestones and the Lower Cretaceous "Paraflysch" were deposited (Anđelković, 1973; Dimitrijević & Dimitrijević, 2009; Toljić et al., 2018; Marinović & Rundić, 2020; Spahić et al., 2023).

In the overlying position on top of the Tithonian-Lower Cretaceous Vardar Zone s.s. (both Western- and East Vardar Zone) are unconformable clastic sequences represented by the two similar turbidite units of the Upper Cretaceous age. Two turbidite belts have almost identical color and are of similar composition (Toljić et al., 2018; K2-SZ *vs.* K2-EV; Fig. 2). In their lower basal sections, the turbidites may contain different remnants of scarce bimodal basic and acidic magmatic signals (e.g., Anđelković, 1973; Karamata et al., 1997, 2005; Sokol et al., 2020). A recent study subdivided Sava Suture Zone into a lower-positioned slightly older SSZ segment containing the bimodal magmatics which is referred to as the "Lower SSZ" (Fig. 1, yellow rectangles), while the Upper Cretaceous turbidites are referred to as the "Upper SSZ" (turbidites that outcrop to the west of Bela Reka fault line; Fig. 2, K_2-SZ; Spahić & Gaudenyi, 2022). To the east of the Bela reka fault are East Vardar Upper Cretaceous turbidies (Fig. 2b).

However, surface mapping of the two flysch-type units of the Upper Cretaceous age permits a poor distinguishing of the tectonic boundary separating the latter turbidites (Fig. 2b; also in Radulović, 1987). The Bela reka thrust faults disconnecting the two turbidite systems inferred during field work. To subdivide turbidites we use the following surface-subsurface markers: (i) the presence of Jurassic-Lower Cretaceous markers belonging to the footwall of both turbidite systems, inclusive the (ii) underlying NNW-SSE striking deep subsurface geophysical lineaments (Vukašinović, 1973a,b; Spahić et al., 2023). Constraints include (iii) the visualized localized aeromagnetic anomalies that are allowing insight into the near-surface configuration, in particular into the hidden magmatic areas (Vukašinović, 1973a,b; Spahić et al., 2023).

With regards to the recurring magmatism that is localized along the strike of this regional-scale tectonic interface, the investigated Ripanj-Ropočevo-Kosmaj Mt. area belongs to a belt striking from the Avala Mt. at the north, over Rudnik Mt. (Kostić, 2021) further towards south including

Željin and Kopaonik Mts. (Figs. 1, 2a). The Guberevac-Babe-Ropočevo area exposes Cretaceous rocks with some evidence of Cretaceous magmatism to the north in Ripanj (Sokol et al., 2020; Fig. 6, Fig. 7a-f). The postdating subvolcanic magmatic activity in the Oligocene induced the formation of Glavčina and Parlozi volcano-tectonic ring structures having a diameter of 2.5–3 km (Radulović, 1987; Fig. 2b, 7a-c). The emplacement of Oligocene magmatics resulted in a number of round-shaped morphological features (Fig. 2b). The intrusion further induced a steep inclination of roofing turbidite layers (e.g., layers that are outcropping near Guberevac, vicinity of Glavčina intrusive feature; Fig. 3d, 7b). Another intrusion along the tectonic lineament is very near Kosmaj Mt. (Oligocene monzogranite, K-Ar on two whole rock samples yielded 30-29 Ma; Lovrić, 1982/83 in Vasković, 1987; Fig. 2a,b). The roofing turbiditic sequence contains predominantly quartz, mica-type minerals, feldspars, and fragments of these Tertiary igneous rocks (Radulović, 1987). In summary, the following regional geological study aims to define the intermittent Late Cretaceous–Miocene lithospheric-scale activities along the proposed tectonic boundary, bondary, that disconnects the investigated two Upper. Cretaceous–Paleogene turbidite systems.

Methods

Taking into consideration the controversial age relations of the stacked turbidite complexes (Anđelković, 1953; Radulović, 1987; Toljić et al., 2018), in particular, deformation age, we conducted the biostratigraphical and structural investigations of the exposed highly deformed mainly folded and thrust turbidite deposits of the SSZ (Figs. 4, 5). The data was collected by mapping the W – E transect connecting the Guberevac area with the Ropočevo quarry site (Fig. 2b).

Biostratigraphic methods

Several thin sections were produced from the pelagic highly-deformed rocks collected in the Guberevac area (Figs. 2, 3). These thin sections were investigated by the optical microscope to determine the presence of microfossils by applying magnifications of 2.5× and 10× (Fig. 5). Sampled turbidite could be defined as a calciturbiditic bed. Thin sections show that planktonic foraminifera are the main constituent of all analyzed microfossil assemblages.

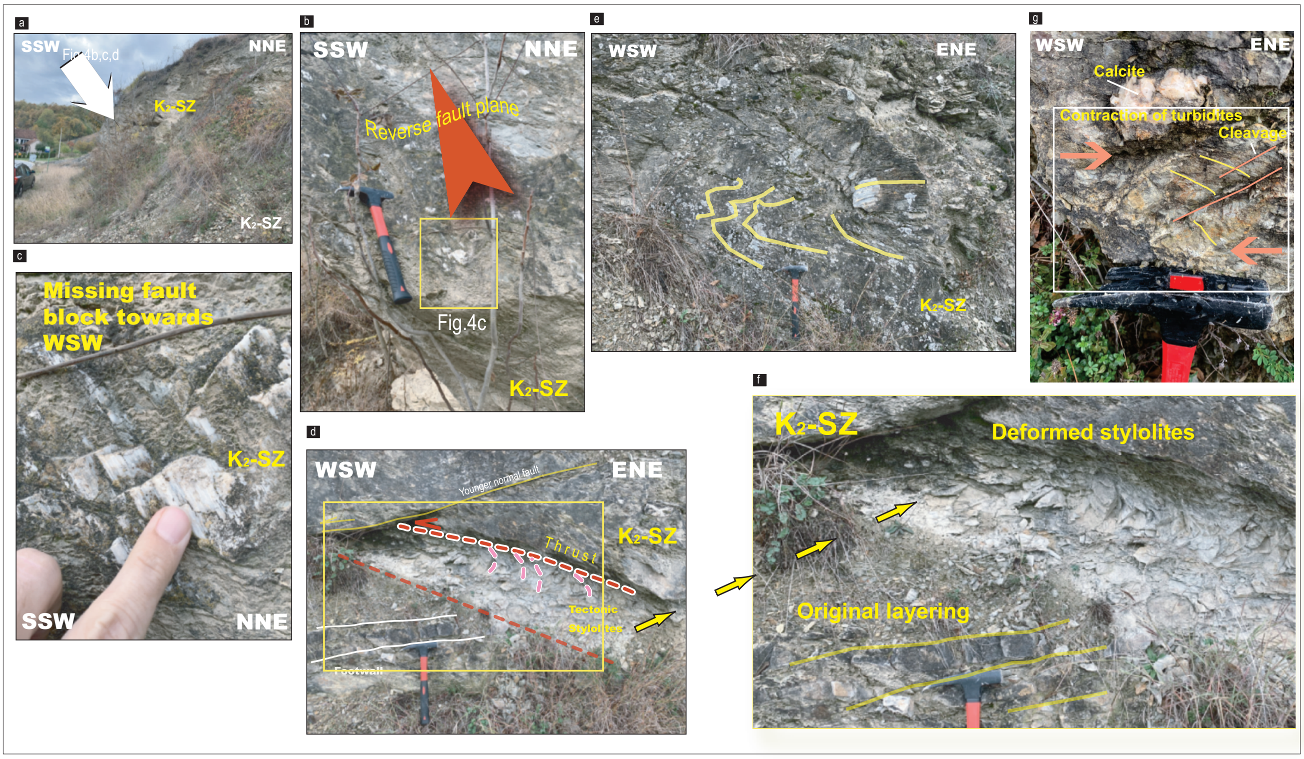

Fig. 4. a. The same outcrops near Guberevac village exposing highly deformed, previously unmapped deformations. b, c. The reverse fault, its hanging wall. Slickensides indicate reverse upwards-directed movement. d. The tectonic stylolite's confirming reverse kinematics, and proximity of thrust fault. e. Intensely folded isocline folds in the peculiar Sava Suture sediments. The fold hinge plunges towards NNE. f. Detail view of tectonic stylolite. g. Evidence of contraction and cleavage formation.

Structural analysis

Preliminary field mapping of the critical outcrops yielded the presence of atypically complex folded turbidite sequences that, according to scarce available literature data, can be either of the latest Jurassic (Radulović, 1987) or the Upper Cretaceous age (Filipović et al., 1973). Observed deformations have not been mapped to date. To address these issues, we have applied the methods of lithostratigraphic and structural field mapping of the key outcrops, including the analysis of bedding data measured in a wider investigated area. The structural data (dip-direction/dip angle) are extracted from the Basic Geological Map of Yugoslavia on a scale of 1:100,000, sheets Obrenovac and Smederevo (Filipović et al., 1973; Pavlović et al., 1979; Fig. 6a, b, c). We additionally measured other field kinematic indicators, such as slickensides, striations, tectonic stylolites, and cleavage, to determine the displacement directions (Fig. 4a-g).

Results

From the Guberevac area towards the Bela Reka fault, the mapped Upper Cretaceous turbidites turbidites are changing gradually changing (no sharp contact) into the heterogeneous sequence with dominant marlstone-type deposits (Anđelković, 1953; Fig. 7e-yellow-colored rocks, 8a, d). Such a change marks the transition from a shallower marine environment towards a deeper environment to the west of the Babe village. No sharp lithological change or tectonically displaced contact between the two turbidite belts is visible in the investigated area. There are no regional metamorphic changes, except in a few locations wherein small portions of Late Cretaceous turbidites are metamorphosed. According to the literature data, these spots were affected by the post-dating subvolcanic activity exposed at Stenička Bara, Babe village (Radulović, 1987; Fig. 7a, b, c, 8b).

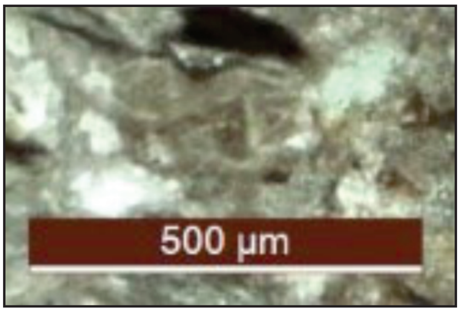

a. *Contusotruncana* cf. *C. fornicata* Plummer

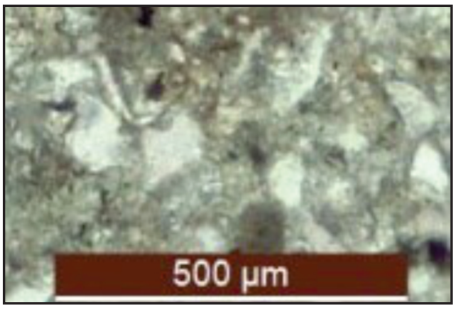

b. *Dicarinella* cf. *D. concavata* Brotzen

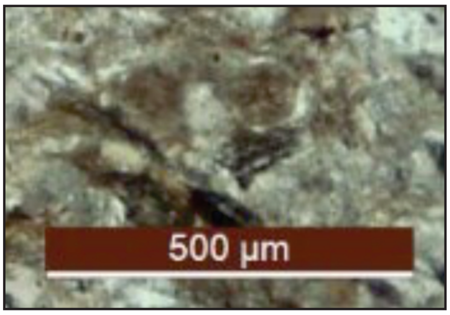

c. *Dicarinella* sp.

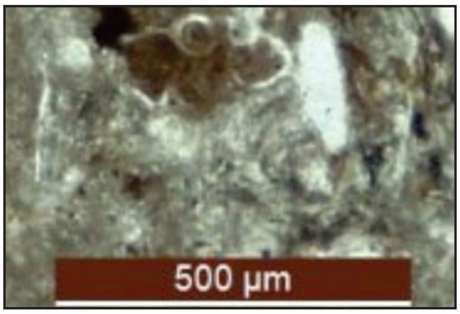

d. *Globotruncana hilli* Pessagno

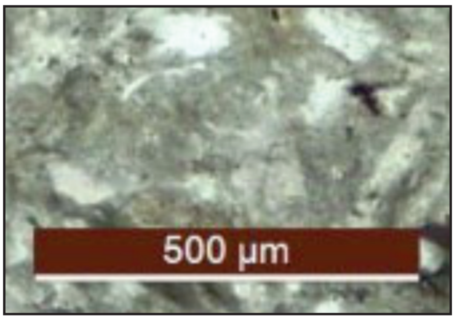

e. *Globotruncana hilli* Pessagno

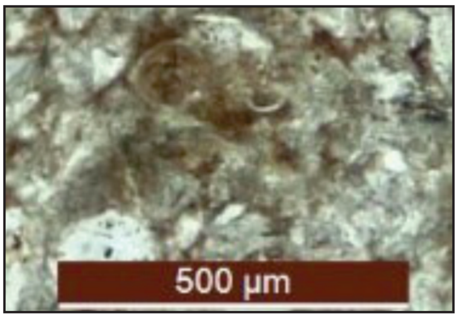

f. *Hedbergella* sp.

Fig. 5. Microfauna from the selected samples is define and is scarce, and some of them are deformed Foraminifera species from the deformed Guberevac turbidites: *Contusotruncana* cf. *C. fornicata* Plummer, *Dicarinella* cf. D. *concavata* Brotzen, *Dicarinella* sp., *Globotruncana hilli* Pessagno, *Hedbergella* sp.

Stratigraphic update: Cretaceous stratigraphic investigation regarding the age of Sava Suture Zone turbidites

As mentioned earlier, Toljić et al. (2018) proposed the distinction between the turbidite deposits: (i) in the hanging wall East Vardar Coniacian-Maastrichtian (lowermost Paleogene) turbidites *vs.* (ii) overriding Campanian (lowermost Paleogene) SSZ turbidites (divided by the Bela Reka fault; Fig. 2b). This study on the Upper Cretaceous turbidite sequences yielded (ii) the new stratigraphic data, whereby sequence positioned to the east of Bela Reka fault represents a subsystem of the Coniacian-Maastrichtian (-lowermost Paleogene) turbidites. The latter flysch belongs to the Upper Cretaceous foreland system of the East Vardar Zone/former south European foreland (separated by the Bela Rela fault; Toljić et al., 2018; see Spahić et al., 2023, for tectonic inheritance) (Fig. 2b). At the same time, the here presented new fossil content collected from the deformed SSZ(K_2-SZ) turbidites indicated that the observed structures are of the Santonian (late Santonian) age "likely of syn-contractional origin".

The new micropaleontological data of the rocks at the Guberevac locality has demonstrated the presence of identifiable pelagic foraminifera and some foraminifera species that cannot be determined. Microfauna is scarce and difficult to determine, mainly because samples were collected from highly deformed rocks. The presence of foraminifera species indicates deeper, calmer, and cooler water with an average salinity (pelagic, open sea environment). The following species were identified: *Contusotruncana* cf. *C. fornicata* Plummer, *Dicarinella* cf. *D. concavata* Brotzen, *Dicarinella* sp., *Globotruncana hilli* Pessagno, *Hedbergella* sp. (Fig. 5). The new biostratigraphic assembly pinpoints the exact Santonian age of the highly deformed Guberevac turbidites (lower plate), thus being the key information for dating of the observed structural elements embedded therein. This Santonian turbidite sequence should connect with the tuffs and andesite embedded into a thick succession of Santonian marlstones (according to Toljić et al., 2018). However, during this field mapping campaign, we observed no such Upper Cretaceous magmatic equivalents across the investigated area.

Structural analysis

Analysis of bedding planes

Field mapping of faults and folds, including the statistical analysis of the previously mapped turbidite layers (Fig. 6a) taken from the Basic Geological Map of Yugoslavia on a scale of 1:100,000 yielded the two distinctive directions among mapped deformations, E-W and NE-SW (Fig. 6b). The S_1 and S_2 diagrams (Fig. 6b) are depicting the bedding data from the sheets Obrenovac and Smederevo, respectively (Fig. 6a). The Basic Geological Map has no distinction of the Sava Suture Zone and East Vardar Zone turbidites. Thus, the measured dip direction/dip angle of the strata represents the bulk Upper Cretaceous measurements (Filipović et al., 1973; Pavlović et al., 1979; Fig. 6a). Nevertheless, to obtain the best results, we separated the Upper Cretaceous sediments into the SSZ and the East Vardar Zone (S_2) (Fig. 2b). The S_1 and S_2 diagrams are representing the manually subdivided trends of the same deformation age deducted from the bulk data (Fig. 6a-c). The S_1 has a bedding trend with dip directions orientation to the NE and SW, exposing the two π belts with the maximum of 047/68 and 214/77. The majority of the measurements have a SW-directed dipping of strata (Fig. 6b). From these statistical poles (maxima), we have extracted the two statistically calculated fold limbs (represented by the traces). The limb one has a dip direction/dip angle of 227/22, whereas the limb two has 030/13. The statistical axial plane has a dip direction/dip angle of 040/86, whereas the statically calculated b-axis/fold axis has a trend/plunge of 310/03 (aligned with the Alpine trend in the area; see Đoković 1985, for the explanation of the folding and associated b-axis/fold axis trends). The S_2 diagram has the statistical bedding with the principal dip directions of E-W, clustering the two π belts or a statistical maximum of the poles that have the maxima of 089/62 and 270/62 (with the majority of the measurements dipping towards the west). From these π belts/pole data, we have further extracted the two statistically calculated fold limbs, which are entirely in line with the observed cluster of field data: dip-direction/dip of the bedding, spatial position of west-divergent fault planes, including the important fold axes. Other rather subordinate maxima likely represent the clustering of the structural elements adjacent to the brittle faults (strata are allocated and shifted by the subsequent post-Cretaceous fault activity). Limb one has a dip direction/dip angle of 270/27, and limb two has measurements of 091/28. The statistical axial plane has a dip direction/dip angle of 270/89, whereas the b-axis/fold axis has a trend/plunge angle of 180/01. The two trends are exposed in Figs. 6b, c, showing that the Upper Cretaceous *s.l.* bedding (Fig. 6a) can be subdivided into the two principal shortening trends – NE-SW and E-W-directed (Fig. 6b).

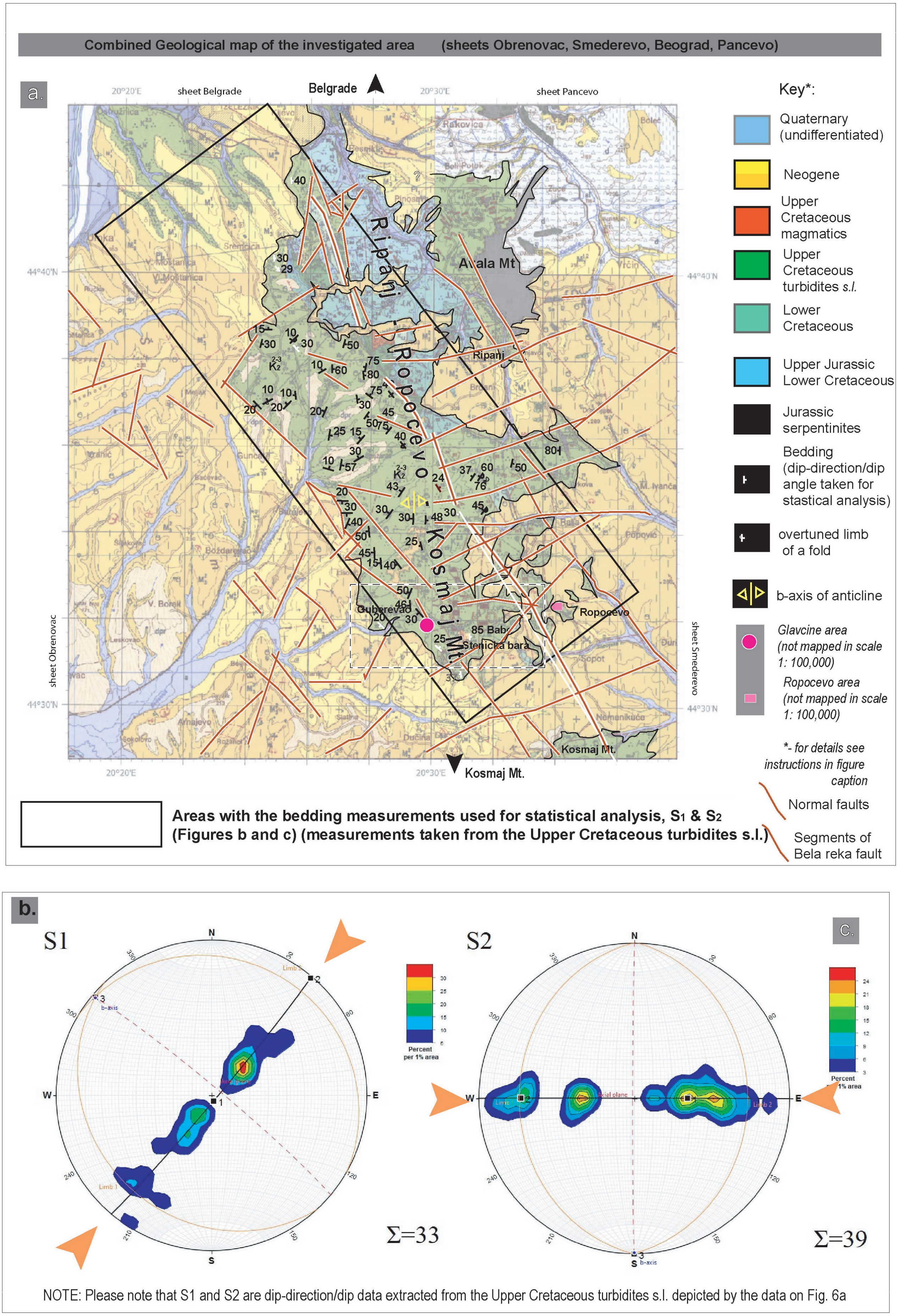

Fig. 6. a. Combined geological map of the investigated area. b. S_1 and S_2 diagrams present bedding data from segments of sheets Obrenovac and Smederevo. See text for details.

Results of key-area structural analysis

Observing compressional field kinematic indicators, such as slickensides, striations, tectonic stylolites, and cleavage, allowed us to determine the displacement directions (Fig. 4a-g). The outcrops expose a reverse fault plane, exposing its footwall domain and missing hangingwall. The plane is dipping towards the ENE with a dip of 55-60 and the azimuth of ca. 80, whereby the slickensides corroborate reverse upwards-directed movement towards the WSW (Fig. 4b, c, d). Intensely folded isocline folds in the peculiar Sava Suture sediments (Fig. 4e) are located slightly east of the slickensides (Fig. 4f). The fold hinge plunges towards NNE. In addition, the Guberevac outcrop exposes compressional cleavages observed earlier (Sajić, 1987).

Farther to the east (Fig.6a), away from the Guberevac site, between the Babe and Ropočevo areas (Fig. 2b, 3c, d, 7a-d), measurements show a significant change from the highly deformed into steeply inclined thin layered sequence (Fig. 3d). The latter sequence is represented by steeply inclined turbiditic layers that are disturbed by the emplacement of the Glavčine granitoid body. As mentioned, the measurements show steeper dip angles (Radulović, 1987). At the Babe village, the marlstones have sharp yet largely diluvium-covered contact with the older Albian limestone of the East Vardar Zone. This lithostratigraphic change presumably marks the covered thrust-type contact (as per Toljić et al., 2018; also in Spahić & Gaudenyi, 2022; Fig. 2b, 7e). Despite the widespread Quaternary cover, the subsurface lineament or Bela Reka fault is also inferred by the presence of the Albian sequence of the overriding East Vardar Zone (just a few meters from the presumed fault; Fig. 2b, 7d-f). The nearby "Ropočevo breccia" and the Albian sandy limestone sequence/calcareous-arenitic units are lithostratigraphic members of the "paraflysch" sequences (latest Tithonian-earliest Berriasian, Albian-Cenomanian; Dimitrijević & Dimitrijević, 2009; Spahić et al., 2023). The "paraflysch" is the clastic-carbonates sequence of Lower Cretaceous deposited on the reacivated and subsided European foreland (Dimitrijević & Dimitrijević, 2009; Spahić et al., 2023).

Discussion: Late Cretaceous convergence onset, post-collisional magmatic reactivation, and suture kinematics

In the wider Belgrade area Guberevac-Babe -Glavčine-Ropočevo area (Figs. 2a,b, 7, 8), the exact age of the onset of the regional lithospheric-scale contraction has not been previously constrained by field deformations. Nevertheless, a few recent reports proposed a similar Cretaceous onset of the convergence-related compressional deformations related to Apulia/Adria/Dinarides collision with the former south European foreland (Schmid et al., 2008; Toljić et al., 2018, Marton et al., 2022). Reports mainly highlight a tectonic connection of flysch deposits, describing the investigated Upper Cretaceous sequence as syn-contractional turbidites (Pamić, 2002).

Constraints on the Upper Cretaceous (Paleogene) regional compressional event (Cleavage patterns, folding and reverse faults)

The collected field data and constraints on deformation stages (Fig. 9), coupled together with previous papers published from the studied area, point to the presence of two cleavage trends: first, older NE-dipping cleavage (Sajić, 1987) overprinted by cleavage trending depicted during fieldwork (developed within west-vergent folds; Fig. 4e). The older stage fits with the precursory latest Jurassic mild collision (Spahić et al., 2023, 2024), frequently interpreted as an obduction-related event (hereinafter **Stage#0**; Maleš et al., 2023; Fig. 9). This pre-Cretaceous Tethyan convergent configuration is characterized by an intra-oceanic magmatic response of the latest Jurassic age (documented within the central East Vardar Zone; Resimić-Šarić et al., 2005; Šarić et al., 2009). Thus, we interpret this older cleavage pattern as a remnant of an earlier compressional stage related to the latest Jurassic closure of Neotethys (see also Spahić et al., 2023).

The second cleavage pattern fits into the N-S- (in Cretaceous reference) or today, E-W-directed shortening and development of folds (hereinafter **Stage#2;** Fig. 9). This second or younger N-S cleavage trend (Fig. 4g) and the observed folds are consistent with the investigated Late Cretaceous compressional event (**Stage#1**). **Stage#1** represents the onset of late Alpine Upper Cretaceous contraction, locally indicated by the observed folds (Fig. 4e). The observed folds have a west-northwest-vergence being of syn-contractional origin (b-axis or fold axis 12/9). Such combined fold–cleavage patterns may suggest the presence of a progressive Upper Cretaceous deformation (Stage 1 and Stage 2; Fig. 4g). According to the collected stratigraphic and structural data, it appears that the investigated late Mesozoic deformation was initiated already during the (late) Santonian.

During **Stage#3** (Fig. 9), the ongoing late Cretaceous shortening and collision produced the observed thrust faults (note that the thrust faults and folds are in a confined place; Fig. 4). The presence of reverse faults attests to the continuity of the Upper Cretaceous shortening (also indicated by the curved geometry of tectonic stylolites; Fig. 4d, f). The progressive thrusting contributed to a further narrowing the remaining marine Upper Cretaceous corridor (deep sea). Eventually, the Upper Cretaceous - Paleogene shortening reached the (micro)continent-continent collision stage. The investigated reverse fault planes measured within the "Upper SSZ" are cropping at a distance from the area of the Bela Reka fault (Guberevac section; Fig. 2b, 4). Such a distance from the main deformation front could suggest the presence of the oblique motion of the two crustal domains documented to the south in North Macedonia (Köpping et al., 2019; see later in the text).

Stage#4 exhibit evidence of the Stage 4 exhibit evidence of much younger regional extension (Fig. 9). The statistical results extracted from the Cretaceous layers show that the observed Late Cretaceous compressional trends (bedding; Fig. 6) are affected by the emplacement of the younger magmatic bodies or doming (e.g., the layering in the vicinity of the Glavčine ring structure; Radulović, 1987; Figs. 6a, 7a). In addition, the younger extensional-type brittle faults have the strike values dissipating towards the north (10-20°) and NNW (ca. 310°) (Fig. 6a). The statistical fault strike data are consistent with the younger extensional episodes (see Marović et al., 2007b; Marinović & Rundić, 2020, for details). Such a configuration suggests the latest Oligocene-Miocene extensional interference followed by the fault reactivation. In addition,

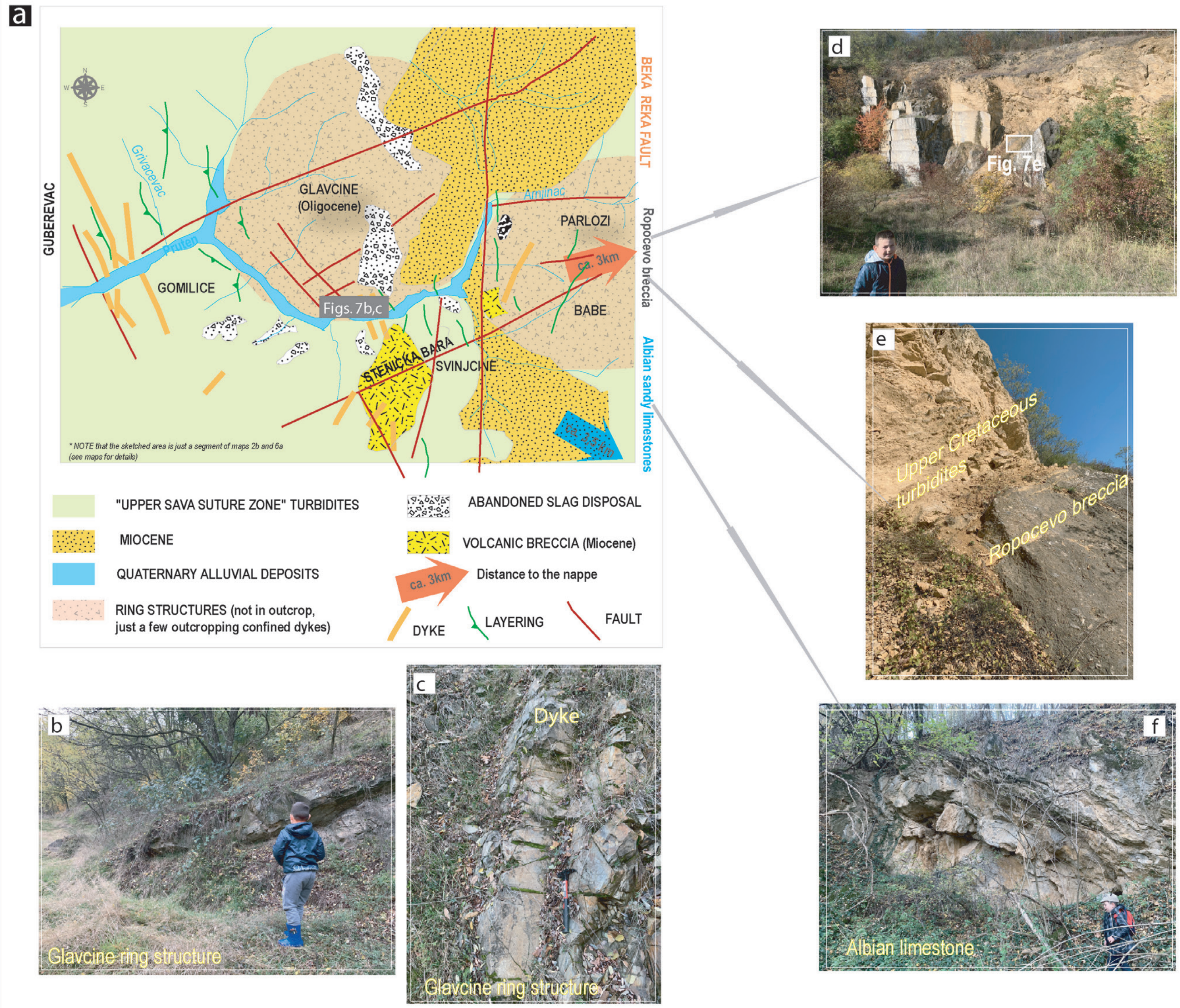

Fig. 7. a. Geological sketch-map of the Babe ore-baring Glavčine-Parlozi structure (inset from Radulović, 1987, modified). b, c. The emplacement of the magmatic body explains the post-depositional tilting near across Glavčine-Parlozi area. The entire area is abundant with the ancient Roman-time abandoned slag deposits, spread all over the mapped ring structures (Spahić et al., 2007; Tančić et al., 2009). d, e. Ropočevo abandoned quarry, East Vardar Zone turbidite segment as carrier of complex brecciated body (Fig. 2b; see Kurešević et al., 2022, Spahić et al., submitted, for details). f. Albian sandstones (also in Pavlović et al., 1979), according to Toljić et al. (2018) it is of East Vardar inheritance (see Fig. 2b).

literature data show that the investigated area experienced a two-staged post-collisional magmatic interference during the Tertiary (e.g., Pamić et al., 2002; Cvetković et al., 2004; Palinkaš et al., 2008).

Tertiary magmatic stages, evidence of extensional (post-orogenic) suture reactivation

Distribution of the Oligocene-Miocene magmatic entities implies that the late Paleogene igneous activity is clustered along the major NNW-SSE striking deep-crustal subsurface remnant lineament (Guberevac-Babe-Ropočevo segment). This NNE-SSW fault or subsurface geophysical lineament extends further to the south, striking across the Rudnik- Topola area and further in North Macedonia (Vukašinović, 1973b; Kostić, 2021; Toljić et al., 2021; Fig. 1, 2a). The emplacement of the subvolcanic bodies was also guided by the local faults, likely reactivated strike-slip fault near the Babe area (Spahić & Gaudenyi, 2022; Fig. 7a, red bold lines). Such a position could indicate the location of the overprinted former restraining band (compression) and releasing band (extension).

The post-collisional extension-type reactivation and the emplacement of magmatic bodies occurred mainly in both the SSZ- and East Vardar turbidites (Fig. 9). However, within the investigated area, its former overriding plate (Albian sandstone, “Ropočevo breccia” of the East Vardar Zone) carries no magmatic entities except for the kersantite body in the Ripanj area (Sokol et al., 2020). The former descending plate and SSZ turbidites are accommodation places of both (i) the Oligocene subvolcanic Glavčine-Parlozi ring structure (Fig. 8a,b) and (ii) the second Miocene igneous body exposed at the Stenička bara (Fig. 7a,b,c). The exposed pyroclastic rocks outline the youngest Miocene volcanic episode (25.12-23.27 Ma; Vasković, 1987). The presence of a suture-related

Fig. 8. The outcrops showing the “Upper Sava Zone” turbidite sequence at the top of Parlozi ring structure. b. “Pyroclastic bomb” found in the Parlozi area (also in Radulović, 1987), c. Thermally affected turbidites in the area of the principal Babe fault indicate proximity of the magmatic levels, d. Typical marlstone of the area.

post-collisional subvolcanic magmatic body could further be inferred by the occurrence of the rarely exposed eruptive igneous breccias (Fig. 8b). There, the underlying Glavčine-Parlozi magmatic body has thermally and chemically affected the surrounding cap-rocks, altering the investigated turbidites at their base (silification and turmalinization observed in the Babe village; Zrnić et al., 1998; Fig. 8c). The subsurface conditions are characterized with high temperature and lower pressure, typical for a subvolcanic level or shallow crust depths (Radulović, 1987; Zrnić et al., 1998; Logar et al., 1998). The sulfidic mineralizations are associated with quartz-latite, riolite, and explosive igneous breccias (Zrnić et al., 1998). Such an assembly indicated a protracted magma-related near-suture activity (Radulović, 1987).

The Guberevac-Glavčine-Stenička bara igneous sub-province is additionally depicted by the subsurface aeromagnetic anomaly (Vukašinović, 1973b). The subsurface data delineate the geometry of the emplaced entities beneath the ring structures (Fig. 2b, 7a). According to the geophysical record, the subsurface igneous bodies have a NNW-SSE direction or towards the Avala Mt. and slightly southward, towards the nearby Kosmaj Mt. (Fig. 2b). The maximum values of ΔT intensity reaching 1000-1200 nT are positioned precisely at the aforementioned ring structures, the Babe-Glavčine and Kosmaj Mt., including the anomaly beneath the Venčane igneous area north of Bukulja and Rudnik Mts. (Vukašinović, 1973b; Fig. 1, 2a). Further to the south, the SSZ can be traced by this Oligocene magmatic reactivation (e.g., at Rudnik Mt., Kostić, 2021; Kostić et al., 2021; Fig. 1).

Orthogonal vs. oblique underplating?

Recent papers dealing with the investigated Belgrade area mainly explain the orthogonal subduction (relative to stable Europe), resulting initially in a fore-arc extension of its upper plate (Toljić et al., 2018, 2021). Accordingly, the presumed fore-arc extension provided the conditions further allowing the extrusion of bimodal magmas of the Upper Cretaceous age (e.g., Grubić et al., 2009; Ustaszewski et al., 2010; Cvetković et al., 2014, 2016; Sokol et al., 2019). However, a few earlier (Dimitrijević & Dimitrijević, 1975; Dimitrijević, 1997) and some more recent observations have indicated that this area or the area of NeoTethys Vardar Ocean underwent a multistage oblique lithospheric-scale collision starting in the latest Jurassic (Fig. 9). According to this scenario, after the oceanic closure occurred in the latest Jurassic, the narrowing of the remaining deep-sea Cretaceous strike-slip corridor stepped into the final stage of the continent-continent collision (see Farangitakis et al., 2020, for the kinematic modeling Köpping et al., 2019; Spahić & Gaudenyi, 2022).

The principal difference between these two (Upper) Cretaceous tectonic models is the lower plate configuration. Instead of the proposed orthogonal subduction, the oblique dextral underplating beneath the European plate occurred in the following two stages: (i) initially causing the Late Jurassic NeoTethyan Vardar closure and obduction; (ii) the terminal Late Cretaceous - Paleogene (micro-continent) collision (Dimitrijević & Dimitrijević, 1975; Grubić, 2002; Willingshofer et al., 1999; Pamić et al., 2002; Šarić et al., 2009; Bonev & Stampfli, 2008, 2011; Marroni et al., 2014; Köpping et al., 2019; Spahić & Gaudenyi, 2022; Spahić et al., 2023).

The Cretaceous lower plate remobilization of Jurassic oceanic crust contributed to the production of Cretaceous pull-apart basins and associated bimodal magmatism (Köpping et al., 2019; Spahić & Gaudenyi, 2022; Fig. 1, yellow-black rectangles). Once developed, pull-apart transtensional releasing bend segments allowed the deposition of turbidities and intrusion of the Upper Cretaceous (Coniacian) bimodal magmatism. This hypothesis of releasing and restraining bends could be verified by this study, which provides new constraints on a distant position of the Guberevac folds (restraining bend positioned away from the Bela Reka fault; Fig. 2). Such a strike-slip faulting mechanism is frequently associated with evidence of crustal “telescoping”. Telescoping allows the tectonic exposure of different crustal levels, further involving the exhumation of deeper lithosphere sections (Cao & Neubauer, 2015). The bimodal magmatic signal is documented across the entire Sava Suture Zone (former deep sea marine corridor; Fig. 1). These bimodal magmatic imprints can be found exclusively within the localized near-suture (thinned) lithospheric fragments (see different locations and their Upper Cretaceous magmatic imprints within the Sava Suture Zone: Ustaszewski et al., 2009; Cvetković et al., 2014; Prelević et al., 2017; Balen et al., 2020; Sokol et al., 2020; Toljić et al., 2021; Fig. 1). Accordingly, this Upper Cretaceous magmatism could serve as a marker of pull-apart mini-basins associated with strike-slip movements (releasing bend that was reactivated in Oligocene and Miocene, see earlier in text). Thus, the investigated Ripanj -Babe - Guberevac area could be described as a configurational crossover between the overprinted restraining and releasing bends segments of the strike-slip Sava Suture Zone. Nevertheless, the complexity of the wider investigated area requires further study.

Conclusions

The study shows that the onset of the Late Alpine collision was during the (late) Santonian. A principal difference between the two almost identical, tectonically superimposed turbidites of the Upper Cretaceous age, can be attributed to observed different levels of the exposed compressional-type deformations. The "Upper Sava Suture Zone" positioned to the left of the Bela Reka fault experienced more intense compressive deformation, resulting in structural elements like folds, thrust faults, and tectonic stylolites. These structures are consistent with their foredeep-related depositional system, typical for turbidites. Second or the East Vardar Zone flysch (overriding plate) has no prominent Upper Cretaceous deformation observed across the investigated area. Thus, the entire Sava Suture Zone sector near Belgrade needs further study.

Based on field mapping and previously published geophysical and structural data (Filipović et al., 1973; Pavlović et al., 1979), the imprints of four tectono-deformational phases were interpreted since the end of the Jurassic. The interpretation yielded four tectono-deformational phases since the end of the shortening. The Santonian shortening marks the here-depicted onset of the contractional deformation. The Upper Cretaceous shortening led to the folding and progressive Upper Cretaceous–Paleogene contraction and thrust faulting. Progressive deformation led to the development of brittle structures, represented by the prominent reverse faults (Guberevac area). After the crustal thickening ceased in the early Paleogene, the area was reactivated by the Oligocene igneous intrusion (Glavčine-Parlozi) and Miocene volcanic episode (Stenička bara). Other main conclusions are:

The Guberevac-Babe SSZ sector holds evidence of the two-staged contractional events: the latest Jurassic closure of Neotethys Vardar ocean (Stage#0, not investigated in this study) and intense Santonian to post-Santonian tectonic events marking the late Alpine progressive compressional

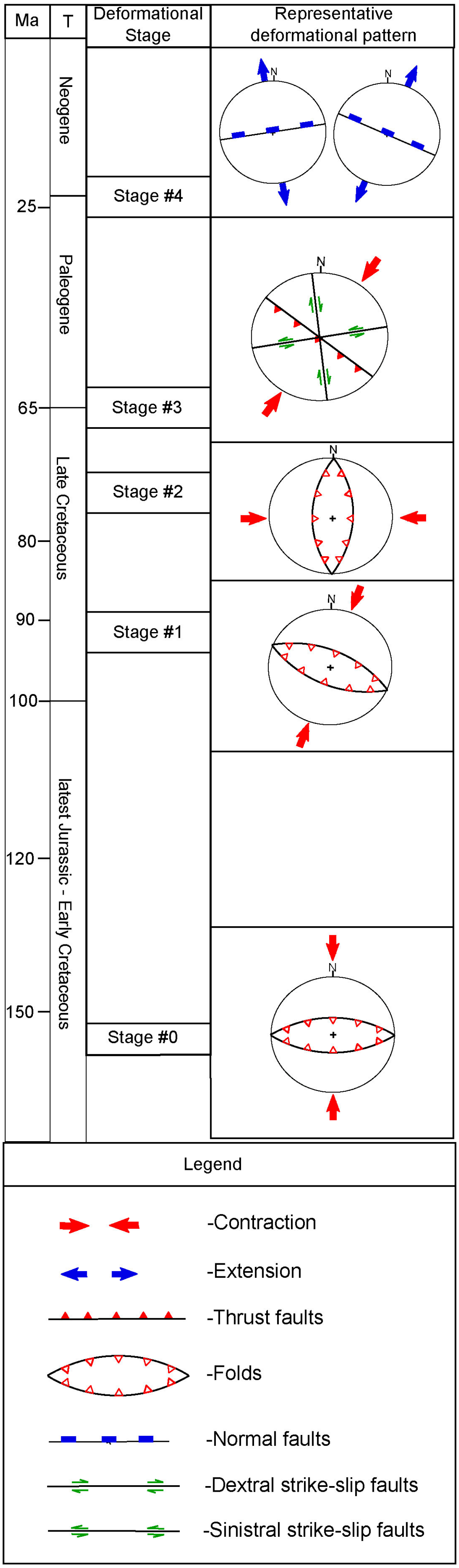

Fig. 9. Deformation stages extracted from the study: Stage#0: latest Jurassic – Early Cretaceous compression; **Stage#1**: initial folding at the beginning of Upper Cretaceous with NNE-SSW tensors; **Stage#2:** folding at the end of Upper Cretaceous with E- W tensors; **Stage#3:** collision (transpression); **Stage#4:** post-orogenic extension and magmatic emplacement.

stage (Stages#1,2,3). This new insight resolves the previous conflicting lithostratigraphical interpretations by confirming the presence of the Santonian SSZ turbidites in Guberevac.

The intense initial post-Santonian (plastic) folding, including the observed vergence, suggests the presence of (late) Santonian syn-contractional deposition and progressive development of cleavage (Stages#1 and 2);

The observed thrust faults in the Guberevac area are marking the post-Santonian onset of the Adria-Europe collision (Stage#3). The reverse faults in the Guberevac-Babe SSZ segment are tectonically shifted several kilometers away from the main Bela Reka thrust interface;

The exhumed Guberevac-Babe-Kosmaj Mt. paleosuture segment has been interrupted by a few post-orogenic extensional episodes characterized by intense igneous activity (Stage#4): (i) initially during late Paleogene/Oligocene time by the emplacement of the subvolcanic Glavčine ore body, and (ii) during the Miocene, accounting for the widespread regional extension and the emplacement of the Stenička bara volcanic system. The study further shows that these suture-related intrusions may or may not penetrate the overlaying Upper Cretaceous turbidites in regional terms.

References

Anđelković, M.Ž. 1953: Contribution à la connaissance géologique et paléontologique des environs du village Babe et du village Guberevac (Kosmaj). Geološki anali Balkanskoga poluostrva, 21: 29–54.

Anđelković, M.Ž. 1973: Geology of the Mesozoic in the vicinity of Belgrade. Geološki anali Balkanskoga poluostrva, 38 (Géologie): 1–142.

Anđelković, M.Ž. 1975: Gornja kreda – okolina Beograda = Upper Cretaceous, wider Belgrade area. In: Petković, K. (ed.): Geologija Srbije, ii-2, Stratigrafija, mezozoik = Geology of Serbia, ii-2, Mesozoic: 280-300. Zavod za regionalnu geologiju i paleontologiju, RGF, Univerzitet u Beogradu, Belgrade.

Boev, B., Cvetković, V., Prelević, D., Šarić, K. & Boev, I. 2018: East Vardar ophiolites revisited: A brief synthesis of geology and geochemical data. Contributions, Section of Natural, Mathematical and Biotechnical Sciences MASA, 39/1: 51–68.

Bonev, N. & Stampfli, G. 2008: Petrology, geochemistry, and geodynamic implications of Jurassic island arc magmatism as revealed by mafic volcanic rocks in the Mesozoic low-grade sequence, eastern Rhodope, Bulgaria. Lithos, 100/1–4: 210–233. https://doi.org/10.1016/j.lithos.2007.06.019

Bonev, N. & Stampfli, G. 2011: Alpine tectonic evolution of a Jurassic subduction-accretionary complex: Deformation, kinematics and $^{40}Ar/^{39}Ar$ age constraints on the Mesozoic low-grade schists of the Circum-Rhodope Belt in the eastern Rhodope-Thrace region, Bulgaria-Greece. Journal of Geodynamics, 52/2: 143–167. https://doi.org/10.1016/j.jog.2010.12.006

Bragin, N., Bragina, L., Gerzina-Spajić, N., Đerić, N. & Schmid, S.M. 2019: New radiolarian data from the Jurassic ophiolitic mélange of Avala Mountain (Serbia, Belgrade Region). Swiss Journal of Geosciences, 112: 235–249. https://doi.org/10.1007/s00015-018-0313-8

Bragin, N.Y., Bragina, L.G., Đerić, N. & Toljić, M. 2011: Triassic and Jurassic radiolarians from sedimentary blocks of ophiolite mélange in the Avala Gora area (Belgrade surroundings, Serbia). Stratigraphy and Geological Correlation, 19: 631–640. https://doi.org/10.1134/S0869593811050030

Cao, S. & Neubauer, F. 2015: How Orogen-scale Exhumed Strike-slip Faults Initiate. In AGU Fall Meeting Abstracts, MR33C-2690. How Orogen-scale Exhumed Strike-slip Faults Initiate - NASA/ADS (harvard.edu)

Cvetković, V., Prelević, D., Downes, H., Jovanović, M., Vaselli, O. & Pécskay, Z. 2004: Origin and geodynamic significance of Tertiary postcollisional basaltic magmatism in Serbia (central Balkan Peninsula). Lithos, 73/3–4: 161–186. https://doi.org/10.1016/j.lithos.2003.12.004

Dimitrijević, M. D. 2001: Dinarides and the Vardar Zone: a short review of the geology. Dinarides and the Vardar Zone: a short review of the geology. Acta Vulcanologica, 13/1–2: 1–13.

Dimitrijević, D.M. & Dimitrijević, N.M. 1975: Ofiolitski melanž Dinarida i Vardarske Zone: Geneza i geotektonsko znacenje = Ophiolite melange of the Dinarides and the Vardar Zone: Genesis and its geotectonic importance. II godišnji znanstveni skup, Znanstveni savjet za naftu JAZU, Sekcija za primjenu geologije, geofizike I geokemije, ser. A, 5: Zagreb19753946 (in Serbo-Croatian).

Dimitrijević M.N. & Dimitrijević, M.D. 2009: The Lower Cretaceous paraflysch of the Vardar Zone: composition and fabric. Geološki anali Balkanskoga poluostrva, 70: 9–21.

Dimitrijević, M.N., Dimitrijević, M.D., Karamata, S., Sudar, M., Gerzina, N., Kovács, S., Dosztály, l., Gulászi, Z., Less, G. & Pelikán, P. 2003: Olistostrome/mélanges - an overview of the problems and preliminary comparison of such formations in Yugoslavia and NE Hungary. Slovak Geological Magazine, 9/1: 3–21.

Dunčić, M., Dulić, I., Popov, O., Bogićević, G. & Vranjković, A. 2017: The Campanian- Maastrichtian foraminiferal biostratigraphy of the basement sediments from the southern Pannonian Basin (Vojvodina, northern Serbia): implications for the continuation of the Eastern Vardar and Sava zones. Geologica Carpathica, 68/2: 130–146. https://doi.org/10.1515/geoca-2017-0011

Erak, D., Matenco, L., Toljić, M., Stojadinović, U., Andriessen, P.A.M., Wilingshofer, E. & Ducea, M.N. 2016: From nappe stacking to extensional detachments at the contact between the Carpathians and Dinarides – The Jastrebac Mountains of Central Serbia. Tectonophysics, 710–711: 162–183. https://doi.org/10.1016/j.tecto.2016.12.022

Farangitakis, G. P., McCaffrey, K. J., Willingshofer, E., Kalnins, L. M., van Hunen, J., Persaud, P. & Sokoutis, D. 2020: The structural evolution of pull-apart basins in response to relative plate rotations; A physical analog modeling case study from the Northern Gulf of California. In EGU General Assembly Conference Abstracts (p. 5378).

Farics, É., Dunkl, I., Józsa, S., Haas, J. & Kovács, J. 2019: Traces of the Late Eocene–Early Oligocene volcanic activity in the Buda Hills (Transdanubian Range, Hungary): link to the volcanism along the Periadriatic–Mid-Hungarian–Sava-Vardar zone. In Geophysical Research Abstracts, 21: 1.

Filipović, I., Gagić, N., Rodin, V. & Avramović, V. 1973: Osnovna geološka karta SFRJ 1: 100 000. List Obrenovac L 34-138 = Explanatory notes for the Basic geologic map of Yugoslavia 1:100000. Sheet Obrenovac L 34-1113 - in Serbian; English and Russian Summaries. Federal geologic survey, Belgrade.

Gerčar, D., Zupančič, N., Waśkowska, A., Pavšič, J. & Rožič, B. 2022: Upper Campanian Bentonite Layers in the Scaglia-type Limestone of the Northern Dinarides (SE Slovenia), Cretaceous Research, 134: 105158. https://doi.org/10.1016/j.cretres.2022.105158

Gerzina, N. 2010: Structural Characteristics and Tectogenesis of Zvornik Suture zone. Faculty of Mining and Geology, Belgrade University, Belgrade: 142 p.

Grubić, A. 2002: Transpressive Periadriatic suture in Serbia and SE Europe. Geologica Carpathica - Special Issue, 53: 141–142.

Grubić, A., Radoičić, R., Knežević, M. & Cvijić, R. 2009: Occurrence of Upper Cretaceous pelagic carbonates within ophiolite-related pillow basalts in the Mt. Kozara area of the Vardar zone western belt, northern Bosnia. Lithos, 108: 126–130. https://doi.org/10.1016/j.lithos.2008.10.020

Grubić, A., Ercegovac, M., Cvijić, R. & Milošević, A. 2010: The age of the ophiolite mélange and turbidites in the North-Bosnian zone. Bulletin de Academie Serbe des Sciences et des Arts 140 (Classe des Sciences Mathematiques et Naturelles, Sciences Naturelles), 46: 41–56.

Handy, M. R., Ustaszewski, K. & Kissling, E. 2015: Reconstructing the Alps–Carpathians–Dinarides as a key to understanding switches in subduction polarity, slab gaps, and surface motion. International Journal of Earth Sciences, 104: 1–26.

Hrvatović, H. 2006. Geological guidebook through Bosnia and Herzegovina. Geological Survey of Federation Bosnia and Herzegovina, Sarajevo: 164 p.

Ivković, A., Vuković, A., Nikolić, J., Kovačević, D., Palavestrić, Lj., Petrović, V., Jovanović, Lj., Trifunović, R. & Sibinović, Lj. 1966: Osnovna geološka karta SFRJ 1:100 000. List Pančevo L34-114 = Basic Geologic Map of SFRY at scale 1:100 000. Sheet Pančevo L34-1114 - in Serbian; English and Russian Summaries. Federal Geological survey, Belgrade.

Karamata, S., Knežević, V., Cvetković, V., Srećković, D. & Marčenko, T. 1997: Upper Cretaceous andesitic volcanism in the surrounding of Belgrade. Romanian Journal of Mineral Deposits, 78: 73–78.

Karamata, S., Sladić-Trifunović M., Cvetković V., Milovanović D., Šarić K., Olujić J. & Vujnović L. 2005: The western belt of the Vardar zone with special emphasis to the ophiolites of Podkozarje - the youngest ophiolitic rocks of the Balkan Peninsula. Bulletin de l'Académie Serbe des sciences et des arts (Classe des sciences mathématiques et naturelles, Sciences naturelles), 130/43: 85–96.

Köpping, J., Peternell, M., Prelević, D. & Rutte, D. 2019: Cretaceous tectonic evolution of the Sava-Klepa Massif, Republic of North Macedonia - Results from calcite twin based automated paleostress analysis. Tectonophysics, 758: 44–54. https://doi.org/10.1016/j.tecto.2019.03.010

Kostić, B., Srećković-Batoćanin, D., Filipov, P., Tančić, P. & Sokol, K. 2021: Anisotropic grossular-andradite garnets: Evidence of two stage skarn evolution from Rudnik, Central Serbia. Geologica Carpathica, 72/1: 17–25. https://doi.org/10.31577/GeolCarp.72.1.2

Kostić, B. 2021: Contact metamorphism of upper cretaceous sedimentary rocks of Rudnik. Faculty of Mining and Geology. University of Belgrade, Belgrade: 124 p.

Kurešević, L., Septfontaine, M., Vušović, O. & Delić-Nikolić, I. 2022: Contribution to geology and genetic pathway of the Ropočevo breccia – an "orphan" olistolithic body within the Upper Cretaceous flysch near Sopot (central Serbia). Geologica Macedonica, 36/1: 5–18. https://doi.org/1.46763/GEOL22361005k

Logar, M., Zrnić, B. & Sajić, D. 1998: The geostatistical model of galena, sphalerite and chalcopyrite weathering in the polymetalic deposit Babe, Kosmaj mountain (Serbia, Yugoslavia). Geološki anali Balkanskoga poluostrva, 62: 287–304.

Maffione, M. & van Hinsbergen, D.J.J. 2018: Reconstructing plate boundaries in the Jurassic NeoTethys from the East and West Vardar Ophiolites (Greece and Serbia). Tectonics, 37/3: 858–887. https://doi.org/10.1002/2017TC004790

Maleš, D., Cvetkov, V., Vasiljević, I. & Cvetković, V. 2015: A new geophysical model of the Serbian part of the East Vardar ophiolite: implications for its geodynamic evolution. Journal of Geodynamics, 90: 1–13. https://doi.org/10.1016/j.jog.2015.07.003

Marinović, Đ. & Rundić, L. 2020: Depth geological relations of the wider area of Belgrade – based on the wells and geophysical data. Geološki anali Balkanskoga poluostrva, 81/2: 1–32.

Marković, B., Veselinović, M., Obradović, Z., Anđelković, J., Atin, B. & Kostadinov, D., 1984: Osnovna geološka karta SFRJ 1:100 000. List Beograd L34-113 = Basic Geologic Map of SFRY at scale 1:100 000. Sheet Belgrade L34-1113 - in Serbian; English and Russian Summaries. Federal Geological survey, Belgrade.

Marović, M., Toljić, M., Rundić, Lj, & Milivojević, J. 2007a: Neoalpine Tectonics of Serbia. Serbian Geological Society, Belgrade: 87 p.

Marović, M., Đoković, I., Toljić, M., Milivojević, J. & Spahić, D. 2007b: Paleogene–Early Miocene deformations of Bukulja–Venčac crystalline (Vardar Zone, Serbia). Geološki anali Balkanskoga poluostrva, 68: 9–20.

Marroni, M., Frassi, C., Göncüoğlu, M. C., Di Vincenzo, G., Pandolfi, L. U. C. A., Rebay, G. & Ottria, G. 2014: Late Jurassic amphibolite-facies metamorphism in the Intra-Pontide Suture Zone (Turkey): an eastward extension of the Vardar Ocean from the Balkans into Anatolia? Journal of the Geological Society, 171/5: 605–608.

Márton, E., Toljić, M. & Cvetkov, V. 2022: Late and post-collisional tectonic evolution of the Adria-Europe suture in the Vardar Zone. Journal of Geodynamics, 149: 101880. https://doi.org/10.1016/j.jog.2021.101880

Milošević, A. 2017: Formation of Orahova gneiss and quartz/sericite schistes in the north of mountain Prosara. Herald, 21: 91–106. https://doi.org/10.7251/HER2117091M

Palinkaš, L.A., Šoštarić, S.B. & Palinkaš, S.S. 2008: Metallogeny of the northwestern and central Dinarides and southern Tisia. Ore geology reviews, 34/3: 501–520.

Pamić, J. 2002: The Sava-Vardar Zone of the Dinarides and Hellenides versus the Vardar Ocean. Eclogae Geologicae Helvetiae, 95/1: 99–113.

Pamić, J., Belak, M., Bullen, T.D., Lanphere, M.A. & McKee, E.H. 2000: Geochemistry and geodynamics of a Late Cretaceous bimodal volcanic association from the southern part of the Pannonian Basin in Slavonija (North Croatia). Mineralogy and Petrology, 68: 217–296. https://doi.org/10.1007/s007100050013

Pamić, J., Balen, D. & Herak, M. 2002: Origin and geodynamic evolution of Late Paleogene magmatic associations along the Periadriatic-Sava-Vardar magmatic belt. Geodinamica Acta, 15/4: 209–231. https://doi.org/10.1016/S0985-3111(02)01089-6

Pavlović, Z., Marković, B., Atin, B., Dolić, D., Gagić, N., Marković, O., Dimitrijević, M.N. & Vuković, Z. 1979: Osnovna geološka karta SFRJ 1:100 000. List Smederevo L34-126 = Basic Geologic Map of SFRY at scale 1:100 000. Sheet Smederevo L34-12 - in Serbian; English and Russian Summaries. Federal Geological survey, Belgrade.

Prelević, D., Wehrheim, S., Reutter, M., Romer, R.L., Boev, B., Božović, M., van den Bogaard, P., Cvetković, V. & Schmid, S.M. 2017: The Late Cretaceous Klepa basalts in Macedonia (FYROM) Constraints on the final stage of Tethys closure in the Balkans. Terra Nova, 29/3: 145–153. https://doi.org/10.1111/ter.12264

Radulović, P. 1987: The polymetalic Pb-Zn deposit Babe (Kosmaj). Proceedings of Geoinstitute, 20: 116–126.

Resimić-Šarić, K., Cvetković, V. & Balogh, K. 2005: Radiometric K/Ar data as evidence of the geodynamic evolution of the Ždraljica ophiolitic complex, central Serbia. Geološki anali Balkanskoga poluostrva, 66/1: 73–79. https://doi.org/10.2298/GABP0566073R

Robertson, A., Karamata, S. & Šarić, K. 2009: Overview of ophiolites and related units in the Late Palaeozoic–Early Cenozoic magmatic and tectonic development of Tethys in the northern part of the Balkan region. Lithos, 108/1–4: 1–36. https://doi.org/10.1016/j.lithos.2008.09.007

Sajić, D. 1987: A contribution about the knowledge of tectonic framework of Babe deposit. Proceedings of Geoinstitute, 20: 129–141.

Šarić, K., Cvetković, V., Romer, R. L., Christofides, G. & Koroneos, A. 2009: Granitoids associated with East Vardar ophiolites (Serbia, FYR of Macedonia and northern Greece): origin, evolution and geodynamic significance inferred from major and trace element data and Sr–Nd–Pb isotopes. Lithos, 108/1–4: 131–150. https://doi.org/10.1016/j.lithos.2008.06.001

Schmid, M.S., Bernoulli, D., Fügenschuh, B., Matenco, L., Schefer, S., Schuster, R., Tischler, M. & Ustaszewski, K. 2008: The Alps-Carpathians-Dinarides-connection: a correlation of tectonic units. Swiss Journal of Geosciences, 101/1: 139–183. https://doi.org/10.1007/s00015-008-1247-3

Schmid, M.S., Fügenschuh, B., Kounov, A., Matenco, L., Nievergelte, P., Oberhänsli, R., Pleugerg, J., Schefer, S., Schuster, R., Tomljenović, B., Ustaszewski, K. & van Hinsbergend, D.J.J. 2020: Tectonic units of the Alpine collision zone between Eastern Alps and western Turkey. Gondwana Research, 78: 308–374.

Sokol, K., Prelević, D., Romer, R.L., Božović, M., van den Bogaard, P., Stefanova, E., Kostić, B. & Čokulov, N. 2019: Cretaceous ultrapotassic magmatism from the Sava-Vardar Zone of the Balkans. Lithos, 354–355: 105–268.

Spahić, D. 2022: The birth of the Sava Suture Zone: The early geological observations and the context of bimodal magmatism (southern Belgrade outskirts; Anđelković, 1973). Geološki anali Balkanskoga poluostrva, 83/1: 23–37. https://doi.org/10.2298/GABP220404004S

Spahić, D., Barjaktarović, M., Mukherjee, S. & Bojić, Z. 2024: Tithonian limestone as a marker of early contraction of NeoTethyanardar Ocean: structural constraints on the latest Jurassic–earliest Cretaceous "docking" (Dobroljupci, Kuršumlija, Jastrebac Mt., Serbia). Carbonates & Evaporites, 39: 75. https://doi.org/10.1007/s13146-024-00983-0

Spahić, D. & Gaudenyi, T. 2020: The role of the "Zvornik suture" for assessing the number of Neotethyan oceans: Surface-subsurface constraints on the fossil plate margin (Vardar Zone vs. Inner Dinarides). Geološki anali Balkanskoga poluostrva, 81/2: 63–86.

Spahić, D. & Gaudenyi, T. 2022: On the Sava suture zone: Post-Neotethyan oblique subduction and the origin of the Late Cretaceous mini magma pools. Cretaceous Research, 131: 105062. https://doi.org/10.1016/j.cretres.2021.105062

Spahić, D., Gaudenyi, T. & Glavaš-Trbić, B. 2019: A hidden suture of the western Palaeotethys: Regional geological constraints on the late Paleozoic "Veleš Series" (Vardar Zone, North Macedonia). Proceedings of Geologists' Association 130/6: 130136.

Spahić, D., Kurešević, L. & Cvetković, Ž. 2023: The paleokarst origin of the carbonate "Ropočevo breccia" and a closing Neotethys: Regional Geological constraints on the Vardar Zone s.s. (Belgrade area, Central Serbia). Carbonates and Evaporites, 38: 51. https://doi.org/10.1007/s13146-023-00863-z

Stojadinović, U., Đerić, N., Radivojević, D., Krstekanić, N., Radonjić, M. & Džinić, B. 2022: Late Jurassic radiolarites in the sub-ophiolitic mélange of the Fruška Gora (NW Serbia) and their significance for the evolution of the Internal Dinarides. Ofioliti, 47/2: 103–112.

Stojadinović, U., Matenco, L., Andriessen, P.A., Toljić, M. & Foeken, J.P. 2013: The balance between orogenic building and subsequent extension during the Tertiary evolution of the NE Dinarides: Constraints from low-temperature thermochronology. Global and Planetary Change, 103: 19–38.

Toljić, M., Matenco, L., Stojadinović, U., Willingshofer, E. & Ljubović-Obradović, D. 2018: Understanding fossil fore-arc basins: Inferences from the Cretaceous Adria-Europe convergence in the NE Dinarides. Global and Planetary Change, 171: 167–184. https://doi.org/10.1016/j.gloplacha.2018.01.018

Toljić, M., Stojadinović, U. & Krstekanić, N. 2019: Vardar Zone: New insights into the tectono-depositional subdivision. In: Geological Congress of Bosnia and Herzegovina with international participation Laktaši: 60–73.

Toljić, M., Glavaš-Trbić, B., Stojadinović, U., Krstekanić, N. & Srećković-Batoćanin, D. 2021: Geodynamic interpretation of the Late Cretaceous syn-depositional magmatism in central Serbia: Inferences from biostratigraphic and petrographical investigations. Geologica Carpathica, 71/6: 526–538. https://doi.org/10.31577/GeolCarp.71.6.4

Ustaszewski, K., Schmid, S.M., Lugović, B., Schuster, R., Schaltegger, U., Bernoulli, D., Hottinger, L., Kounov, A., Fügenschuh, B. & Schefer, S. 2009: Late Cretaceous intra-oceanic magmatism in the internal Dinarides (northern Bosnia & Herzegovina): Implications for the collision of the Adriatic and European plates. Lithos, 108: 106–125. https://doi.org/10.1016/j.lithos.2008.09.010

Ustaszewski, K., Kounov, A., Schmid, S.M., Schaltegger, U., Krenn, E., Frank, W. & Fügenschuh, B. 2010: Evolution of the Adria-Europe plate boundary in the northern Dinarides: From continent-continent collision to back-arc extension. Tectonics, 29: TC6017.

van Hinsbergen, D.J. & Schmid, S.M. 2012: Map view restoration of Aegean–West Anatolian accretion and extension since the Eocene. Tectonics, 31/5: TC5005. https://doi.org/10.1029/2012TC003132

Vasković, N. 1987: Petrogenetic characteristics on Kosmaj monzogranite. Proceedings of Geoinstitute 20: 91–113.

Vukašinović, S. 1973a: Contribution to the geotectonic distinction of the interboundary space of the Dinaride, Panonide and Serbo-macedonian Mass. Zapisnici Srpskog geološkog društva za 1972. godinu: 1–18.

Vukašinović, S. 1973b: Interpretation of Kosmaj-Barajevo aeromagnetic anomaly. Proceedings of Institute for geological and mining investigation and exploration of nuclear and other raw materials in Belgrade, 8: 48–52.

Zanchetta, S., Montemagni, C., Mascandola, C., Mair, V., Morelli, C. & Zanchi, A. 2023: The Meran-Mauls Fault: Tectonic switching from compression to transpression along a restraining bend of the Periadriatic Fault. Journal of Structural Geology, 172: 104878. https://doi.org/10.1016/j.jsg.2023.104878

Zrnić, B., Cvetković, Lj. & Obradović, Lj. 1998: Mineral parageneses of the ore deposit Babe-Kosmaj. Geološki anali Balkanskoga poluostrva, 62: 267–285.

GEOLOGIJA 67/2, 237-248, Ljubljana 2024

https://doi.org/10.5474/geologija.2024.011

Alternative gold prospecting methods used by artisanal and small scale miners: A review

Alternativne metode iskanja zlata, ki jih uporabljajo obrtniki in rudarji v majhnem obsegu: pregled

Fredrick Martin MANGASINI[1,3*], Michael MSABI[1], Athanas MACHEYEKI[1] & Alex KIRA[2]

[1]Department of Geology, College of Earth Sciences and Engineering, University of Dodoma, Tanzania;
(*) corresponding author: mangatz@yahoo.co.uk, e-mail: mmsabi@yahoo.com, asmacheyeki@yahoo.com
[2]Department of Accounting and Finance, College of Business and Economics, University of Dodoma, Tanzania,
e-mail: alexkira10@gmail.com
[3]State Mining Corporation, P. O. Box 981, Dodoma, Tanzania

Prejeto / Received 4. 4. 2023; Sprejeto / Accepted 21. 5. 2024; Objavljeno na spletu / Published online 16. 12. 2024

Key words: field geology, geological exploration, indicator minerals, mineralization, precious mineral
Ključne besede: terenska geologija, geološke raziskave, indikatorski minerali, mineralizacija, dragoceni mineral

Abstract

Artisanal and Small Scale Mining (ASM) is distinctive to Industrial Mining (IM) upon minimal applications of scientific methods and inadequate funding of its geological exploration activities. Revision of scholarly sources indicate that for ASM, gold prospecting is done using visual features that signify zones of mineralization. Such features comprise soil and lithological indicators, geo-biotic indicators, indicator minerals, pathfinder elements and associate minerals. Others include physical features and mine vestiges. Imminent research on ASM rests upon studying scientific inter-relationships of such techniques and suitable mechanisms of financing activities related to geological exploration, an inordinate barrier to smart productivity of ASM.

Izvleček

Obrtniško rudarjenje in rudarjenje v majhnem obsegu (ASM) se od industrijskega rudarjenja (IM) razlikuje po minimalni uporabi znanstvenih metod in nezadostnem financiranju potrebnih geoloških raziskav. Pregled znanstvenih virov kaže, da se pri ASM iskanje zlata izvaja z uporabo vizualnih značilnosti, ki označujejo območja mineralizacije. Takšne značilnosti obsegajo talne in litološke indikatorje, geobiotske indikatorje, indikatorske minerale, sledilne elemente in povezane minerale. Druge vključujejo fizične značilnosti in ostanke rudarjenja. Bližnje raziskave ASM temeljijo na preučevanju znanstvenih medsebojnih odnosov takšnih tehnik in ustreznih mehanizmov financiranja dejavnosti, povezanih z geološkimi raziskavami, kar je pretirana ovira za pametno produktivnost ASM.

Introduction

Artisanal and Small Scale Mining is distinguished from Industrial Mining owing to its low levels of production, lower degree of mechanization and technological applications (ASM often use picks, chisels, sluices and pans), high degree of labour intensity and little capital investment. Other factors include lack of long-term planning, informality, poor occupational health, safety and environment conditions (Chaparro Ávila, 2003; Hinton et al., 2003; Lahiri-Dutt, 2004; Hinton, 2006; Adler et al., 2013).

Financing of geological exploration operations is yet another key difference between two modes of mining. IM finance exploration through debt, equity or own funding (Myers & Majluf, 1984) whereas ASM own funding is the foremost financing alternative. Nonetheless, ASM are financially constrained, so they do not carry out geological exploration to a stage of reserve and resource classification prior to operating their mines (Hentschel et al., 2003). Limited to using simple prospecting techniques (indicators), they work only to discover availability of the mineralization, and start mining instantaneously.

Indicators, in principle entail visual features that signify areas where mineral commodity, such as gold may be found. Skills and abilities involved to identify such features comprise activity, observation, knowledge, insight, opportunism, lateral thinking and luck (Marjoribanks, 1997). Little has been written about simple prospecting methods applied by ASM in gold exploration. It is very timely to report these methods and provide basic scientific explanations to enable an ever more realistic mineral localization predictions in future.

Apprehension of these techniques by the public is vital based on the fact that they are inexpensive, quick and simple, centered on field experience and minimal professional training, therefore they can be widely applied particularly in low income societies. The methods do not readily follow procedures of traditional geochemical prospecting yet they provide physical evidence of the presence of gold mineralization or alteration (McClenaghan, 2005).

Methodology

This work involved desk review of various documents including books, book chapters, academic journals and articles, conference papers and scientific reports. These documents were filtered using Google search engine on different platforms mainly Google scholar, ResearchGate and ScienceDirect.

The keyword terms for this search were designed to identify any study on gold prospecting related to ASM. Studies related to IM contexts were deliberately not included. The search keyword terms used include: gold exploration, controls of gold mineralization, indicators of gold mineralization, gold prospecting techniques, and geological prospecting methods.

A total of seventy eight (78) references based on different gold prospecting techniques were selected for the review. Amongst are 6 books and 8 book chapters, 3 conference papers, 54 journal articles, and 7 scientific reports. Therefore, this work is confined to secondary sources of information that have provided qualitative data that support different techniques employed by ASM to discover zones of gold mineralization.

Results and discussion

We begin with soils and rocks to discuss how they are applied by ASM to prospect for gold mineralization. Next we show how the biota is expedient for auriferous prospecting, pointing specifically to how some plants bolster sighting of mineralized zones. We also discuss uses of indicator minerals and surface features to point out potentials of gold locations. We conclude with the discussion of how historical features including reports and old infrastructures ease ASM prospecting for gold mineralization.

Soil indicators

Whereas local geology and surface conditions sustain, soils make the simplest way of discovering gold deposits. Soil texture, color and profiles have been extensively used by ASM to identify zones of mineralization.

Insitu weathered soils

Soils in tropical environments evolved from gold bearing greenstones for example, become slowly enriched in gold as the bedrock weathers. In the Tapajós region in the Brazilian Amazon, ASM are reported panning this type of soil to locate and define the size of deposits (Veiga et al., 2006). Quartz fragments and/or flaky grains of hematite (an iron oxide mineral) together with gold particles are checked to determine if the gold particles originate from a vein, or is supergenic. Primary gold is usually angular and dendritic (tree-shape) containing more impurities, such as copper and silver than the recrystallized gold (Sarala, 2015). Large (over 1m) gold bearing quartz veins have been detected using this method.

Lateritic soils

Lateritic soils develop essentially from long term exposure of cratonal rocks to the atmosphere and hydrosphere in equatorial and tropical climates (Colin et al., 1997). If they have for example developed from Archean to lower Proterozoic gold-rich formations, their profiles usually show an increasing gold concentration towards the bed rock. This is due to progressive weathering and leaching (Colin et al., 1997). Therefore, once discovered, they make good indicator of potential gold mineralization.

Rocks and ore bodies oxidized to depths of 30 to 100 meters in Geita, northern Tanzania (Cowley, 2001) exemplify this mode of mineralization. Other reported localities consisting similar form of gold mineralization include the Dondo Mobi gold deposit in Gabon (Colin & Vieillard, 1991), Amani gold deposit in southwest Tanzania (Dunn & von der Heyden, 2021); and Abim district gold deposit in northeastern Uganda (Voormeij, 2021).

Soil color change

Related to that is soil color change. It usually signifies change in elemental content or oxidation states of elements and mineralogy of the soil; and can help to locate zones of gold mineralization (Rigobert et al., 2013). Goethite (α-FeOOH) and Haematite (α-Fe_2O_3), the most widespread Fe oxide and oxyhydroxide minerals in soils, particularly in well-drained tropical soils, greatly influence soil color (Allen & Hajek 1989; Schwertmann, 1988).

These minerals are formed by weathering of primary Fe-bearing minerals, such as pyrite, pyroxene, olivine, augite, hornblende and biotite. Mafic intrusive rocks (for example Dolerite dykes), where these minerals originate, are mostly host of auriferous quartz–carbonate–sulfide veins (Fielding et al., 2018). Therefore, ASM though unfamiliar to chemical relations between gold localization and presence of Fe-rich soils, have been curious in identifying soil color changes considering them as important pointers to sources of gold mineralization.

Soil color change may also be characteristic to lithological contacts (Graham et al., 1994; Wysocki et al., 2005). Formed through deposition, magma intrusion, and /or deformation of rock units, lithological contacts create weak zones through which hydrothermal fluids penetrate and precipitate mineralized veins (Zhu et al., 2011). Therefore, contiguous color changes in soil makes another important indicator to ASM of a probable gold setting. Buhemba and Nyasanero mines in Tanzania (Henckel et al., 2016) are example of places where ASM are mining quartz veins at lithological contacts.

Light colored soils

Furthermore, soils in lighter colors may be due to acidic mineral solutions bleaching lode deposits underground (Kontak & Kerrich, 1995). Both pre and syn-ore alteration, alters the physicochemical properties of the mineralizing fluids and thus promotes gold precipitation (Hastie et al., 2020; Williams-Jones et al., 2009). For example, in the vicinity of an oxidizing sulfide deposit, large quantities of both sulfate and metals go into solution in the ground water, creating extremely acidic condition by the free sulfuric acid resulting from the oxidation of pyrite and marcasite.

As a result, the mobility of elements in these areas will be higher than that in normal areas. Acidic solutions bleach host rocks to commonly exhibit yellow to pale grey coloration (Xu et al., 2017). Youthful soils developed from such bleached (light-colored) parent rocks will usually be lighter (Finkl, 1988). This feature has been used as an important indicator of gold mineralization in the deposits of Geita (Kwelwa et al., 2018) and Nyasirori (Yuan et al., 2019) in Tanzania; and Hira-Buddini in India (Sahoo et al., 2018).

Lithological indicators

Rocks are main hosts to primary gold mineralization. However, a handful rock types have been found to be useful to ASM as indicators for possible gold mineralization settings.

Quartz veins and reefs

On a global scale, ubiquitous orogenic quartz veins and reefs have been a focus of ASM in their prospecting for gold mineralization (Goldfarb, 2001; Vishiti et al., 2019). Being limited on exploration and metallurgical technology, ASM generally have less interest on low grade ores of wall rocks; rather they are focused onto highest-grade portions of the lodes. Logically, owing to their low production capacities, high grade veins seem necessary to ASM for two reasons. First, to minimize metallurgical costs; and secondly to earn more profit. Bismark reefs in the Lake Victoria Goldfield of Tanzania; and quartz veins mining in the Nazca-Ocoña belt in Peru are examples of gold discoveries in quartz veins by ASM (Hester et al., 1995; Alfonso et al., 2019).

Occurrence of gold mineralization in quartz veins can be explained using Bowen's reaction series, which posits that quartz (silica) precipitates last from the magma thus filling fissures and cavities of the host rock (Bowen, 1922). Since gold is chemically inert and does not react with most elements, it precipitates within or along fractures of these veins. This is why quartz veins mostly associate with primary gold mineralization.

Also, although gold is relatively soft (ductile and malleable), both quartz and gold also display relative resistance to physical weathering (Colin et al., 1997; Itamia et al., 2019). Their ability to sustain immediate physical and chemical changes help them to occur together, a fact that prompts ASM to look for quartz veins in their search for gold.

Lamprophyres

Another gold indicating rock is lamprophyre, a porphyritic igneous rock consisting of a fine-grained feldspathic groundmass with phenocrysts chiefly of biotite (McLennan, 1915). Gold enrichment of the lamprophyres is supported by their exceptionally deep origins in presumed Au-rich regions of the earth (>150 km), high F, K, Ba, and Rb and moderate S contents. $H_2O/(H_2O + CO_2)$ ratios and fluidized condition together make them uniquely similar to auriferous ore fluids in their element abundances and possibly in their physical state. These features brand them well suited to transporting gold into the crust (McNeil & Kerrich, 1986; Rock et al., 1989). Golden Pride intrusions in Nzega Greenstone Belt of northern Tanzania are examples of the ASM mined lamprophyres (Kwelwa et al., 2013).

Porphyries

Porphyry, an igneous rock containing conspicuous crystals (phenocrysts) surrounded by a matrix of finer-grained minerals is another rock unit indicator of gold mineralization if it is associated with quartz veinlets. Similar to the lamprophyres, gold in porphyries occurs in a stockwork of quartz veinlets within host rock units and their ores display remarkably consistent grade (Vila et al., 1991). Porphyries are commonly classified based on their main mineral contents. The carrier unit of gold is the Cu-Au porphyry. Amani and Mpanga Hills in southwest Tanzania where Cu-Au mineralization is hosted within impure micaceous marbles are the known ASM worked Cu-Au porphyry deposits (Dunn et al., 2021).

Breccia

Breccia, a rock composed of large angular broken fragments of minerals or rocks cemented together by a fine-grained matrix associated with either in situ deformation of rock, cataclastic deformation in tectonic shear zones, or mass flow deposits such as landslides or rock falls (Gibson et al., 1996), is another rock type considered in the search of gold mineralization. They may be mineralized within clasts and /or networks of epithermal quartz veins and veinlets (Sutarto et al., 2015; Rottier et al., 2018). The well-known breccia deposit mined by ASM is the Mananila deposit in Morogoro, Tanzania. This is the 400 to 450 meters long, and from 60 to 80 meters thick gold mineralized zone with echelon systems of quartz veins and veinlets, steeply dipping bodies of quartz breccia ranging from 1.0 to 1.5 meters thick. It is localized within tectonically sheared zones of Early Precambrian granitic-gneisses (Mykhailov et al., 2020).

Conglomerates

We note that auriferous conglomerates have also been a focus in the search for places of gold mineralization. These are clastic sedimentary rocks made up of rounded gravel and boulder sized clasts cemented or in a matrix support (Migoń, 2020). Generally, they mark periods of deep secular weathering that is favorable for the production of gold placers. Their gold grains may be of detrital origin, but they may also be in crystallized forms indicating hydrothermal emplacement caused by localized remobilization (Taylor and Anderson, 2018). Surface indications of auriferous conglomerates have been found to include manifestation of large amount of pyrite in the rocks, excess quantities of quartz pebbles or sands in streams or soil, large concentration of SO_4 in ground and surface waters due to the oxidation of pyrites, abundant iron staining and occurrence of gossans both residual and transported.

In Tanzania, ASM are mining gold nuggets in the conglomeratic horizons within the braided river channels of the Amani River (Dunn et al., 2019).

Banded iron formations

Incongruent to clastic sediments are the chemically precipitated banded iron formations (BIFs). They are used in localization of gold places because gold in these rocks is found in cross-cutting quartz veins and veinlets, or as fine disseminations associated with pyrite, pyrrhotite and arsenopyrite. Gold-bearing BIFs may also include native gold, magnetite, chalcopyrite, sphalerite, galena and stibnite. BIF make excellent prospecting targets because of their scalability, often being found in clusters. A good example of BIF gold deposit exploited by ASM is the Mwamola gold deposit in northern Tanzania (Yuan et al., 2019).

Geo-biotic indicators

Scientific observations involving plant-soil relations on natural plant communities show that certain species can be used for the detection of elemental enrichments arising from mineralization in the underlying bedrock (Timperley et al., 1972). An urge of using plants in the search of economic deposits is based on either the ability of plants to absorb or to be affected by high concentrations of metals from considerable depths and/or from a mineralized halo surrounding the ore (Cannon, 1960).

Botany provide evidence that plants can be used in geological prospecting in three ways: (a) through mapping distribution of particular species (indicator plants) most affected by the mineral sought, (b) by the physiological and morphological changes in plants growing in mineralized grounds (appearance), and (c) via the differences in chemical composition, that is plant analysis (Hawkes, 1957). Here (i-vi), we use category (a) and present species mostly used by ASM to ascertain the presence of gold mineralization. The discussed species are shown in figure 1.

Ocimum centraliafricanum (Copper plant)

It is a subshrub and grows primarily in the seasonally dry tropical biome. It is a perennial herb found in Africa (especially in Tanzania, the Democratic Republic of Congo, Zambia and Zimbabwe). It is well known for its tolerance of high levels of copper in the soil (Paton et al., 2009). Since Cu sometimes occur with Au, the plant has been looked after by ASM to prospect for gold.

Acacia mellifera (Black thorn)

Known to up-take gold (Taylor, 2009), black thorn is an african shrub that grows to a height of about 9 m having an extensive root system that penetrates through large volumes of soils, allowing its survival in dry areas. It grows better on sandy, clayey or stony-rocky soils but it is tolerant of a wide range of soils, including black cotton soils (vertisols). The black thorn is found in regions with 400-800 mm annual rainfall but it can grow in areas with a minimum of 100 mm rainfall; and along seasonal watercourses or drainage networks (Heuzé & Tran, 2015). For ASM, its ability to occur along watercourses, attracts them to locate Au placers along paleostreams.

Eriogonum caespitosum (Wild Buckwheat)

Occurs in areas highly mineralized with Cu, Pb, Au, Ag and U; the secondary mineral dispersion zones due to mechanical and /or chemical weathering (Smee, 1998). The *Eriogonum caespitosum* genus is tolerant of metals in the dispersion zones and accumulates them, making it a focus to metal prospectors (Cannon et al., 1986).

Monardella odoratissima
(Alpine Mountainbalm or Coyote Mint)

A grayish, aromatic plant with erect, bunched, leafy stems bearing opposite leaves and topped by small, whitish to pale purple or pink flowers in a dense head; grows in sandy soils in Au-Ag, Cu mineralized grounds in the secondary dispersion halos. Like *Eriogonum caespitosum,* it has been used by prospectors to identify areas of gold mineralization (Cannon et al., 1986).

Debarked trees

Unlike specific flora species discussed above, ASM have also been looking for "sign trees" during gold prospecting. These are debarked trees to indicate presence and direction of the gold mineralized veins. Early explorers in Tropical areas (especially along the Proterozoic Ubendian belt in the southwestern Tanzania) prior to the wider applications of the Global Positioning System (GPS), debarked tree trunks to mark gold locations. In Africa, apart from locating gold, debarking was also done for other purposes such as trail making, ground water location and cultural activities (Atindehou et al., 2022).

However, the scars for gold were made in a special way to point to the direction of the mineralization. Depth and width of the mineralized veins are indicated by the length and width of the scars. Where longer and wider scar is made, it means the vein is buried at depth and is thick (over 5 m). Nevertheless, narrow and shallower veins are represented by narrow and short scars. In the Lupa Goldfield, SW Tanzania debarked trunks are currently followed by ASM to identify locations of gold mineralized veins (Bryceson et al., 2012).

Termitaria

Mounds made by termites are fauna-related features useful for mineral exploration. Termites move large amounts of soil material, and thereby bring up anomalous materials from depth to the surface through bioturbation process.

For insitu soils, the moved up material is usually representative of the underlying bed rock. Therefore, termite mound allows observation and/or sampling of geochemical materials from the interior without need for drilling and with much better certainty than surface soil sampling enabling locating of gold anomalous zones (Arhin et al. 2010; Petts et al., 2009).

Indicator minerals

Whereas indicator minerals can indicate the presence of a specific mineral deposit, alteration or rock lithology, their physical and chemical characteristics, including visual distinctiveness, moderate to high density, silt or sand size, and ability to survive weathering and/or clastic transport, allow them to be readily recovered from exploration sample media. In addition, their abundance, grain morphology, and surface textures help prospectors to determine their relative distance from the source (McClenaghan, 2005).

There is overwhelming evidence that indicator minerals: (1) offer an ability to detect haloes much larger than the mineralized target including associated alteration; (2) provide physical evidence of the presence of mineralization or alteration; (3) have the ability to provide information about the source (that traditional geochemical methods cannot), including nature of the ore, alteration, and proximity to source (Brundin & Bergstrom, 1977). Gold grains, pathfinder minerals and black sands help to support this conclusion.

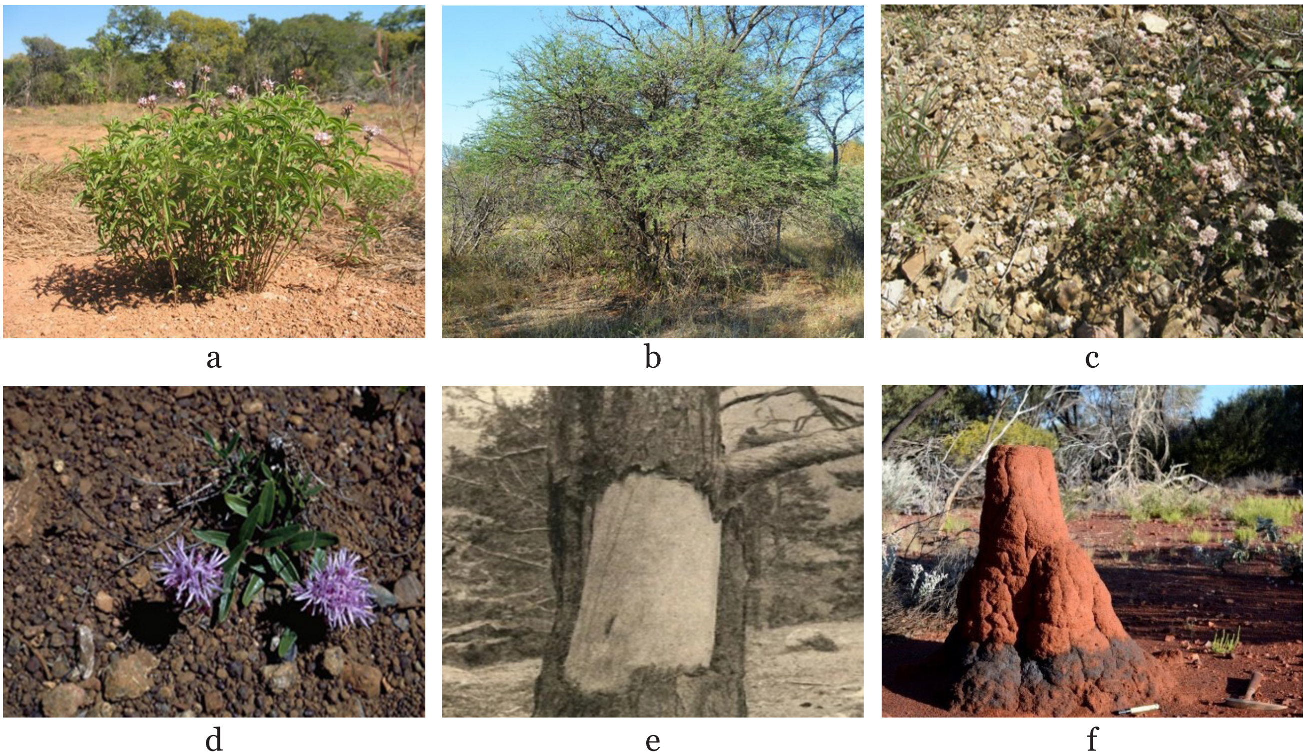

Fig. 1. Geobiotic indicators (a) *Ocimum centraliafricanum* a plant tolerant to high levels of Cu in the soil used to search for Au, (b) *Acacia mellifera* up-taker and tracer of Au, (c) *Eriogonum caespitosum* grows in Cu, Pb, Au, Ag and U dispersion zones, (d) *Monardella odoratissima* grows in sandy rich in Au-Ag, Cu halos, (e) Debarked tree trunk indicate direction, size and depth of mineralized vein (f) Termitaria showing >30 cm of haematitic oxidation at base an indication of Fe enrichment from the underlying bed rock. Rocks rich in Fe-containing minerals are mostly host to Au mineralization.

Gold grains

Gold grain condition including grain abundance, size, shape, flatness and fineness is useful in the determination of availability of gold mineralization and its proximity to the source. Based on gold grain characteristics, mineralogists have rated them as pristine, modified or reshaped (McClenaghan, 2005). They are briefly discussed below and figure 2 indicates their appearance.

(i) Pristine gold grains

They maintain their primary shapes and surface textures; and appear to be undamaged during transport. They often occur as angular wires, rods and delicate leaves being casts of fractures they once in-filled. Two possibilities help to interpret transport history of pristine grains: (1) gold grains were eroded from a bedrock source nearby and transported to the site with little or no surface modification; and (2) gold grains were liberated from rock fragments during in situ weathering of transported sulphide grains containing gold. However, discovery of pristine grains indicate that the sample is less than 500 meters from the source (McClenaghan, 2005; Sarala, 2015).

(ii) Modified gold grains

Comparable to pristine samples, the primary surface textures in modified gold grains are retained. However, all edges and protrusions are damaged because of transportation. They are striated and the protrusions are crumpled, folded and curled; grain moulds and primary surface textures are preserved only on protected faces of grains. Samples that contain elevated concentrations of modified grains are generally proximal to the bedrock source (Kelley et al., 2011). Experience shows that the discovery of modified gold grains indicate that the sample is less than 1,000 meters away from the source.

(iii) Reshaped gold grains

Important aspect of reshaped grains is that all primary surface textures have been destroyed mostly loosing the original grain shapes. They are flattened to rounded as a result of repeated folding of leaves, wires and rods (Marquez-Zavalia et al., 2004). Grain surfaces may be pitted from impact marks from other grains. Although these grains can have a complex transport history, the presence of large numbers of reshaped grains is significant to prospectors. It shows that the grains have been transported more than a kilometer from the source (Averill, 1988). Reshaped gold grains are best indicators of placer deposits.

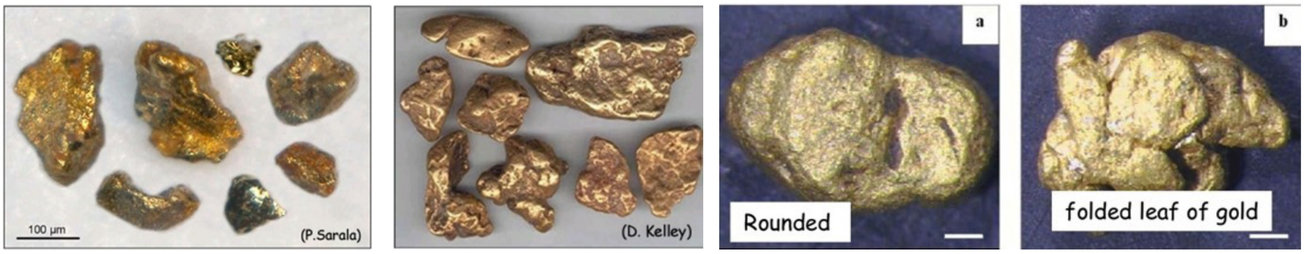

i ii iii

Fig. 2. Gold grains: (i) Pristine gold grains, (ii) Modified gold grains, and (iii) Reshaped gold grains (After Sarala, 2015; Kelley et al., 2011; McClenaghan, 2005).

Pathfinder elements

Owing to their ability to form broader halos and their relative ease of detection by analytical methods, pathfinder elements are relatively easily found. Ag, Cu, Pb, Zn, Co, Ni, As, Sb, Te, Se and Hg are geochemical indicators for gold. However, for ASM only Cu and Ag are the familiar elements, and are therefore used to trace associated gold mineralization. A good example of this discovery by ASM are the mines near Nyakona Hill in the Musoma-Mara greenstone belt in northern Tanzania (Taylor, 2009). Gold was discovered when artisanal miners were working for copper ore

Black sands

The widely accepted explanation for black sand is that it comes from eroded volcanic material such as basalt and other dark-colored rocks and minerals. It is enriched in heavy minerals, including ilmenite ($FeTiO_3$), rutile (TiO_2), zircon ($ZrSiO_4$), monazite (Ce, La, Nd, Th)PO_4 and xenotime (YPO_4), and a mix of other iron-group minerals such as hematite (Fe_2O_3) and magnetite (Fe_3O_4) (Peristeridou et al., 2022). Gold found in black sand comes in the form of small nuggets and flakes that are not attached to any of the minerals. Its abundance, shape and size helps ASM in the search of its source. ASM gold mines in the Mkuvia area along the Mbwemkuru river plateau, southern Tanzania is an example of a mineralization zone where gold is found in significant amounts in black sands (Hathout, 1983).

Associate (Sulphide) minerals

Pyrite, arsenopyrite, pyrrhotite and chalcopyrite (copper sulphide) minerals form the commonest host ore minerals of gold (Yang et al., 2020). Gold may associate with these minerals in a variety of ways. It may occur physically within the minerals in coarse to submicroscopic sizes, chemically as gold compounds and in solid-solutions. Some of the gold may also occur in fractures, along cleavages and at mineral grain boundaries (Schwartz, 1944).

Most of times it is uncommon to see sulphide minerals on the surface in tropical areas because of oxidation. However, Pseudomorphoses of pyrite and rarely pyrrhotite and chalcopyrite are common, which the prospectors focus on while looking for gold mineralization (Taylor, 2011).

Physical indicators

Reports indicate that ASM have been able to discover gold mineralization through prospecting certain geologic features. Simply stated they include extensions of known mineral areas, similar geologic areas nearby and consideration of the correct topography.

Extensions of known mineral areas

Most small scale gold deposits have a linear component. It is fairly common that new deposits can be found along this linear zone of deposition by looking for extensions along the line of deposition (see figure 4). ASM usually use the idea of

i ii iii

Fig. 3. Examples of boxwork textures after sulphides (i) Boxwork texture after chalcopyrite contains orange zones of limonite, green colored mineral is malachite, (ii) Spongy boxwork after coarse grained pyrite, and (iii) Sponge-style gossan with boxwork that has developed directly over a pyrrhotite zone (After Taylor, 2011).

a b

Fig. 4. Linear ASM Gold Deposits (a) A photography displaying a WNW–ESE trending ASM hardrock mining indicated by blue tarps used to cover ASM shafts, (b) Topographical image showing ASM workings along NE-SW trend (After Voormeij, 2021).

extension of known zones of mineralization to discover new gold deposits,

Similar geologic areas nearby

If a certain rock type or geologic environment has been productive for gold in one area, and the same rock type or environment occurs a few kilometers away in the same mountain range, it is likely that mineralization of the first area can be found in the second. It is most likely that mineralization in these areas were caused by same regional geologic event (Kwelwa et al., 2018; Kuehn et al., 1990). This feature has locally been useful to ASM while looking for new gold deposits.

Correct topography

It is well known that most of the placers form in areas with moderate to flat slopes. For example, alluvial placers are formed by the deposition of gold particles at a site where water velocity remains below that required to transport them further. Typical locations for alluvial gold placer deposits are on the inside bends of rivers and creeks; in natural hollows; at the break of slope on a stream; the base of an escarpment, waterfall or other barrier. Stream placers are the most common types of placers prospected and mined by ASM in Tanzania (Shand & Jønsson, 2011; Dunn et al., 2019).

Anthropogenic indicators

These are indicators for places of gold mineralization based on previous human activities. They include old reports and mining remnants.

Old reports

In many places of the world, gold has been mined since ancient times. In Africa, the search for gold in the Sahara for example is reported beginning as early as 4000 BC (Klemm & Klemm, 2013; Miller et al., 2000). In northern Africa specifically, reports indicate that between 1480–1340 BC many important gold mining sites in the eastern Desert of Egypt and in the Nubian Desert were discovered and exploited (Klemm et al., 2001). Information in old reports, such as Olfert Dapper's description of Africa, first published in Amsterdam in 1668 (Habashi, 2009), has helped many explorers to locate places of gold mineralization.

Mining remnants

In addition to old reports are the relics of old mine workings being mostly the development excavations of old mines, especially adits and shafts; as well as preserved fragments of mining surface infrastructure consisting of buildings and machinery. Although these features whenever found are considered archaeological items, hence are protected by heritage laws (Kaźmierczak et al., 2019), to ASM they indicate proximity to areas of potential mineralization.

Conclusions

ASM, although employs simple technology in its operations; and is limited from accessing formal financing for its activities related to gold exploration, has devised some prospecting techniques capable of locating zones of gold mineralization.

The techniques are basically visual features of soil, rocks, biotic resources, mineralogical and elemental indicators as well as physical and human-based indicators. The techniques are inexpensive, quick and simple, centered on field experience and minimal professional training. They can be widely applied by gold prospectors in most regions, particularly in low income societies.

Interestingly, the techniques are supported by scientific explanations related to occurrences of gold mineralization. This implies that, detailed scientific research can be done to deduce theoretical principles behind them.

In addition, the techniques are in essence limited to surface observations, and they cannot be used to explore concealed sub-surface resources that require application of modern technologies and advanced scientific techniques. Therefore, to enable ASM acquire such tools necessary for systematic exploration, a study is being proposed on appropriate funding mechanisms beyond available traditional financing schemes to support ASM exploration activities.

Acknowledgements

Authors are grateful to Prof. J. Ntalikwa and Prof. G. Kombe for their constructive suggestions upon improvements in text clarity. The authors would also like to thank the anonymous reviewers and the editor for their constructive comments, which helped to improve the manuscript.

References

Adler, M. R., Bergquist, B.A., Adler, S.E., Guimarães, J.R.D., Lees, P.S.J., Niquen, W., Velasquez-López, P.C. & Veiga, M.M. 2013: Challenges to measuring, monitoring, and addressing the cumulative impacts of artisanal and small-scale gold mining in Ecuador, Resources Policy, 38/4: 713–722. https://doi.org/10.1016/j.resourpol.2013.03.007

Alfonso, P., Anticoi, H., Yubero, T., Bascompta, M., Henao, L., Garcia-Valles, M., Palacios, S. & Yáñez, J. 2019: The Importance of Mineralogical Knowledge in the Sustainability of Artisanal Gold Mining: A Mid-South Peru Case. Minerals, 9/6: 345. https://doi.org/10.390/min9060345

Allen, B.L. & Hajek, B.F. 1989: Mineral Occurrences in Soil Environments. In: Dixon, J.B. & Weed, S.B. (eds.): Minerals in Soil Environments, 2nd ed, Soil Science Society America, Madison.

Arhin, E. & Nude, P.M. 2010: Use of termitaria in surficial geochemical surveys: Evidence for >125-µm size fractions as the appropriate media for gold exploration in Northern Ghana, Geochemistry: Exploration, Environment, Analysis, 10: 401–406. https://doi.org/10.1144/1467-7873/09-004

Atindehou, M.M.L., Avakoudjo, H.G.G., Idohou, R., Azihou, F.A., Assogbadjo, A.E., Adomou, A.C. & Sinsin, B. 2022: Old Sacred Trees as Memories of the Cultural Landscapes of Southern Benin (West Africa). Land, 11/4: 478. https://doi.org/10.3390/land11040478

Averill, S.A. 1988: Regional variations in the gold content of till in Canada. In: Macdonald, D.R. & Mills, K.A. (eds.): Prospecting in Areas of Glaciated Terrain – 1988. Canadian Institute of Mining and Metallurgy: 271–284.

Bowen, N.L. 1922: The Reaction Principle in Petrogenesis. The Journal of Geology, 30/3: 177–198. https://doi.org/10.1086/622871

Brundin, N.H. & Bergstrom, J. 1977: Regional prospecting for ores based on heavy minerals in glacial till. Journal of Geochemical Exploration, 7: 1–19. https://doi.org/10.1016/0375-6742(77)90071-1

Bryceson, D., Jonsson, J., Kinabo, C. & Shand, M. 2012: Unearthing treasure and trouble: mining as an impetus to urbanisation in Tanzania. Journal of Contemporary African Studies, 30/4: 631–649. https://doi.org/10.1080/02589001.2012.724866

Cannon, H.L. 1960: Botanical Prospecting for Ore Deposits: How plant chemistry is being used to aid the geologist in his search for metals at home and abroad. Science, 132/3427: 591–598. https://doi.org/10.1126/science.132.3427.591

Cannon, H.L., Trimby, S., Harms, T.F. & Mosier, E.L. 1986: Some observations on plant assemblages and elemental content of plants in mineralized areas of the Walker Lake 1°×2° quadrangle, US Dept. of Inter. Geological Survey, California-Nevada.

Chaparro Ávila, E. 2003: Small-scale mining: a new entrepreneurial approach, Comisión Económica para América Latina (CEPAL), United Nations, Santiago, Chile: 82 p.

Colin, F. & Vieillard, P. 1991: Behavior of gold in the lateritic equatorial environment: weathering and surface dispersion of residual gold particles, at Dondo Mobi, Gabon. Applied Geochemistry, 6/3: 279–290. https://doi.org/10.1016/0883-2927(91)90005-A

Colin, F., Sanfo, Z., Faso, Brown, E., Bourlès, D. & Minko, A.E. 1997: Gold: A tracer of the dynamics of tropical laterites. Geology, 25/1: 81–84. https://doi.org/10.1130/0091-7613(1997)025<0081:GATOTD>2.3.CO;2

Cowley, P.N. 2001: The discovery and development of the Geita gold deposits, Northern Tanzania. New Gen Gold Conference 2001, Perth Australia: 123–135.

Dunn, S.C., von der Heyden, B.P., Rozendaal, A. & Taljaard, R. 2019: Secondary gold mineralization in the Amani Placer Gold Deposit, Tanzania. Ore Geology Reviews, 107: 87–107. https://doi.org/10.1016/j.oregeorev.2019.02.011

Dunn, S.C. & von der Heyden, B.P. 2021: Gold remobilization in gossans of the Amani area, southwestern Tanzania. Ore Geology Reviews, 131: 104033. https://doi.org/10.1016/j.oregeorev.2021.104033

Dunn, S.C., von der Heyden, B.P., Steele-MacInnis, M., Kramers, J.D., St. Pierre, B., Erasmus, R. & Harris, C. 2021: Neoproterozoic copper-gold mineralization in the Amani area, southwestern Tanzania. Ore Geology Reviews, 132: 104070. https://doi.org/10.1016/j.oregeorev.2021.104070

Fielding, I.O.H., Johnson, S.P., Zi, J., Sheppard, S. & Rasmussen, B. 2018: Neighboring orogenic gold deposits may be the products of unrelated mineralizing events. Ore Geology Reviews, 95: 593–603. https://doi.org/10.1016/j.oregeorev.2018.03.011

Finkl, C.W. 1988: Soils and weathered materials, field methods and survey. In: General Geology. Encyclopedia of Earth Science. Springer, Boston, MA. https://doi.org/10.1007/0-387-30844-X_107

Gibson, I.L., Milliken, K.L. & Morgan, J.K. 1996: Serpentinite-breccia landslide deposits generated during crustal extension at the Iberia margin. In: Whitmarsh, R.B., Sawyer, D.S., Klaus, A. & Masson, D.G. (eds.): Proceedings of the Ocean Drilling Program, Scientific Results, 149.

Goldfarb, R.J., Groves, D.I. & Gardoll, S. 2001: Orogenic gold and geologic time: A global synthesis. OreGeology Reviews, 18/1-2: 1–75. https://doi.org/10.1016/S0169-1368(01)00016-6

Graham, R.C., Tice, K.R. & Guertal, W.R. 1994: The pedologic nature of weathered rock. In: Whole Regolith Pedology, D. L. Cremeens, R. B. Brown & J. H. Huddleston (eds.): Special Publication, 34: 21–40. https://doi.org/10.2136/sssaspecpub34.c2

Habashi, F. 2009: Gold in the ancient African kingdoms. De Re Metallica, 12: 65–69.

Hastie, E.C.G., Kontak, D.J. & Lafrance, B. 2020: Gold Remobilization: Insights from Gold Deposits in the Archean Swayze Greenstone Belt, Abitibi Sub-province, Canada. Economic Geology, 115: 241–277. https://doi.org/10.5382/econgeo.4709

Hathout, S.A. 1983: Soil atlas of Tanzania. Tanzania Publishing House, Dar es Salaam, Tanzania.

Heuzé, V. & Tran, G. 2015: Black thorn (Acacia mellifera). Feedipedia, a programme by INRAE, CIRAD, AFZ & FAO. https://www.feedipedia.org/node/347 (17.2.2023)

Hawkes, H.E. 1957: Principles of geochemical prospecting, U.S. Geol. Survey Bull. 1000-F: 225–355.

Henckel, J., Poulsen, K.H., Sharp, T. & Spora, P. 2016: Lake Victoria Goldfields. Episodes. 39/2: 135–154. https://doi.org/10.18814/epiiugs/2016/v39i2/95772

Hentschel, T., Hruschka, F. & Priester, M. 2003: Artisanal and Small-Scale Mining: Challenges and Opportunities. Mining, Minerals and Sustainable Development Project, International Institute for Environment and Development, London: 94 p.

Hester, B.W., Barnard, F. & Johnson, A. 1995: Opportunities for Mineral Resource Development: Tanzania. Ministry of Water, Energy and Minerals, United Republic of Tanzania, Knudsen Printing, Denver: 108 p.

Hinton, J.J., Veiga, M.M. & Veiga, A.T.C. 2003: Clean artisanal gold mining: a utopian approach? Journal of Cleaner Production, 11/2: 99–115. https://doi.org/10.1016/S0959-6526(02)00031-8

Hinton, J. 2006: Communities and small scale mining: an integrated review for development planning. Report to the World Bank, Communities and Small-Scale Mining (CASM) Initiative, Washington DC.

Itamiya, H., Sugita, R. & Sugai, T. 2019: Analysis of the surface microtextures and morphologies of beach quartz grains in Japan and implications for provenance research. Progress in Earth and Planetary Science, 6: 43. https://doi.org/10.1186/s40645-019-0287-9

Kaźmierczak, U., Strzałkowski, P. & Lorenc, M.W. 2019: Post-mining Remnants and Revitalization. Geoheritage, 11: 2025–2044. https://doi.org/10.1007/s12371-019-00408-8

Kelley, K.D., Eppinger, R.G., Lang, J., Smith, S.M. & Fey, D.L. 2011: Porphyry Cu indicator minerals in till as an exploration tool: Example from the giant Pebble porphyry Cu-Au-Mo deposit Alaska, USA. Geochemistry: Exploration, Environment, Analysis, 11: 321–334. https://doi.org/10.1144/1467-7873/10-IM-041

Kontak, D.J. & Kerrich, R. 1995: Geological and geochemical studies of a metaturbidite-hosted lode gold deposit; the Beaver Dam deposit, Nova Scotia: II. Isotopic studies. Economic Geology, 90: 885–901. https://doi.org/10.2113/gsecongeo.90.4.885

Klemm, D., Klemm, R. & Murr, A. 2001: Gold of the Pharaohs – 6000 years of gold mining in Egypt

and Nubia. Journal of African Earth Sciences, 33/3–4: 643–659. https://doi.org/10.1016/S0899-5362(01)00094-X
Klemm, R. & Klemm, D. 2013: Gold and Gold Mining in Ancient Egypt and Nubia. Geoarchaeology of the Ancient Gold Mining Sites in the Egyptian and Sudanese Eastern Deserts. Springer, Berlin-Heidelberg: 649 p.
Kuehn, S. Ogola, J. & Sango, P. 1990: Regional setting and nature of gold mineralization in Tanzania and southwest Kenya. Precambrian Research, 46/1–2: 71–82. https://doi.org/10.1016/0301-9268(90)90067-Z
Kwelwa, S., Manya, S. & Vos, I.M.A. 2013: Geochemistry and petrogenesis of intrusions at the Golden Pride gold deposit in the Nzega greenstone belt, Tanzania. Journal of African Earth Sciences, 86: 53–64. https://doi.org/10.1016/j.jafrearsci.2013.06.012
Kwelwa, S.D., Dirks, P.H.G.M., Sanislav, I.V., Blenkinsop, T. & Kolling, S. 2018: Archaean Gold Mineralization in an Extensional Setting: The Structural History of the Kukuluma and Matandani Deposits, Geita Greenstone Belt, Tanzania. Minerals, 8/4: 171. https://doi.org/10.3390/min8040171
Lahiri-Dutt, K. 2004: Informality in mineral resource management in Asia: Raising questions relating to community economies and sustainable development. Natural Resources Forum, 28/2: 123–32. https://doi.org/10.1111/j.1477-8947.2004.00079.x
Marjoribanks, R.W. 1997: Prospecting and the Exploration Process. Geological Methods in Mineral Exploration and Mining, Springer, Dordrecht: https://doi.org/10.1007/978-94-011-5822-0_1.
Marquez-Zavalia, M.F., Southam, G., Craig, J.R. & Galliski, M.A. 2004: Morphological and chemical study of placer gold from the San Luis Range, Argentina. Canadian Mineralogist, 42: 169–182. https://doi.org/10.2113/gscanmin.42.1.169
McClenaghan, M.B. 2005: Indicator mineral methods in mineral exploration. In: Geochemistry: Exploration, Environment, Analysis, 5: 233–245. https://doi.org/10.1144/1467-7873/03-066
McLennan, J.F. 1915: Quartz veins in lamprophyre intrusions: Engineering Mining Journal, 99: 11–13.
McNeil, A.M. & Kerrich, R. 1986: Archean amprophyre dykes and gold mineralization, Matheson, Ontario: The conjunction of LILE enriched mafic magmas, deep crustal structures, and Au concentration: Canadian Journal of Earth Sciences, 23: 324–343.
Migoń, P. 2020: Geomorphology of conglomerate terrains – Global overview, Earth-Science Reviews, 208: 103302. https://doi.org/10.1016/j.earscirev.2020.103302
Miller, D., Desai, N. & Lee-Thorp, J. 2000: Indigenous gold mining in Southern Africa: A review. South African Archeological Society, Goodwin Series, 8: 91–99.
Myers, S.C. & Majluf, N.S. 1984: Corporate Financing and Investment Decisions when Firms Have Information that Investors Do Not Have. Journal of Financial Economics, 13: 187–221. https://doi.org/10.1016/0304-405X(84)90023-0
Mykhailov, V., Andreeva, O. & Omelchuk, O. 2020: Model of the new gold deposit Mananila (Tanzania). Geoinformatics: Theoretical and Applied Aspects 2020, European Association of Geoscientists and Engineers, 11–14 May 2020, Kyiv, Ukraine.
Paton, A.J., Bramley, G., Ryding, O., Polhill, R., Harvey, Y., Iwarsson, M., Willis, F., Phillipson, P., Balkwill, K., Lukhoba, C., Otiend, D. & Harley 2009: Lamiaceae (Labiatae). Flora of Tropical East Africa: 430 p.
Peristeridou, E., Melfos, V., Papadopoulou, L., Kantiranis, N. & Voudouris, P. 2022: Mineralogy and Mineral Chemistry of the REE-Rich Black Sands in Beaches of the Kavala District, Northern Greece. Geosciences, 12: 277. https://doi.org/10.3390/geosciences12070277
Petts, A.E., Hill, S.M. & Worrall, L. 2009: Termite species variations and their importance for termitaria biogeochemistry: towards a robust media approach for mineral exploration. Geochemistry: Exploration, Environment, Analysis, 9/3: 257–266. https://doi.org/10.1144/1467-7873/09-190
Rigobert, T., Jean-Claude, D., Marambaye, D. & Yannick, B. 2013: On the occurrence of gold mineralization in the Pala Neoproterozoic formations, South-Western Chad. Journal of African Earth Sciences, 84: 36–46. https://doi.org/10.1016/j.jafrearsci.2013.03.002
Rock, N.M.S., Groves, D.I., Perring, C.S. & Golding, S.D. 1989: Gold, lamprophyres, and porphyries: What does their association mean? In: Keays, R.R. Ramsay, W.R.H. & Groves, D.I. (eds.): The geology of gold deposits. Economic Geology Monograph: 609–625. https://doi.org/10.5382/Mono.06.47
Rottier, B., Kouzmanov, K., Casanova, V., Bouvier, A., Baumgartner, L. P., Wälle, M. & Fontboté,

L. 2018: Mineralized breccia clasts: a window into hidden porphyry-type mineralization underlying the epithermal polymetallic deposit of Cerro de Pasco (Peru). Miner Deposita, 53: 919–946. https://doi.org/10.1007/s00126-017-0786-9

Sahoo, K.A., Krishnamurthi, R. & Sangurmath, P. 2018: Nature of ore forming fluids, wall rock alteration and P-T conditions of gold mineralization at Hira-Buddini, Hutti-Maski Greenstone Belt, Dharwar Craton, India. Ore Geology Reviews, 99: 195–216 https://doi.org/10.1016/j.oregeorev.2018.06.008

Sarala, P. ed. 2015: Novel technologies for greenfield exploration. Geological Survey of Finland, Special Paper, 57: 11–22

Schwartz, G.M. 1944: The host minerals of native gold, Economic Geology, 39/6: 371–411.

Schwertmann, U. 1988: Occurrence and Formation of Iron Oxides in Various Pedoenvironments. In: Stucki, J.W., Goodman, B.A. & Schwertmann, U. (eds.): Iron in Soils and Clay Minerals. NATO ASI Series, 217. Springer, Dordrecht. https://doi.org/10.1007/978-94-009-4007-9_11

Shand, M. & Jønsson, J.B. 2011: Tanzania gold mines and minerals map. University of Glasgow, UPIMA project.

Smee, B.W. 1998: A new theory to explain the formation of soil geochemical responses over deeply covered gold mineralization in arid environments, Journal of Geochemical Exploration, 61: 149–172. https://doi.org/10.1016/S0375-6742(98)00007-7

Sutarto, S., Idrus, A., Harijoko, A., Setijadji, L.D. & Meyer, F.M. 2015: Veins and hydrothermal breccias of the Randu Kuning porphyry Cu-Au and epithermal au deposits at Selogiri area, central Java Indonesia, Journal of Applied Geology, 7/2: 80–99. https://doi.org/10.22146/jag.26982

Timperley, M.H., Brooks, R.R. & Peterson, P.J. 1972: Trend analysis as an aid to the comparison and interpretation of biogeochemical and geochemical data: Econ. Geol., 67/5: 669–676.

Taylor, M.J. 2009: Report on the Kibara Mineral Exploration Property of Tanzanian Royalty Exploration Corporation in the Bunda District, Mara Region of the United Republic of Tanzania, East Africa, unpublished report.

Taylor, R. 2011: Boxworks and related features. In: Gossans and Leached Cappings: Springer, Berlin, Heidelberg. https://doi.org/10.1007/978-3-642-22051-7_7

Taylor, R.D. & Anderson, E.D. 2018: Quartz-pebble-conglomerate gold deposits, U.S. Geological Survey Scientific Investigations Report 2010–5070–P, 34 p. https://doi.org/10.3133/sir20105070P

Veiga, M.M., Metcalf, S.M., Baker, R.F., Klein, B., Davis, G., Bamber, A., Siegel, S. & Singo, P. 2006: Manual for Training Artisanal and Small-Scale Gold Miners, GEF/UNDP/UNIDO, Vienna, Austria: 144 p.

Vila, T., Sillitoe, R.H., Betzhold, J. & Viteri, E. 1991: The porphyry gold deposit at Marte, northern Chile. Economic Geology, 86/6: 1271–1286. https://doi.org/10.2113/gsecongeo.86.6.1271

Vishiti, A., Etame, J. & Suh, C.E. 2019: Features of gold-bearing quartz veins in an artisanal mining-dominated terrain, Batouri gold district, Eastern region of Cameroon, Episodes, 42/3: 199–212. https://doi.org/10.18814/epiiugs/2019/019016

Voormeij, D. 2021: Gold exploration in tropical landscapes. Fifth Edition. Mynah Exploration Inc.

Williams-Jones, A.E., Bowell, R.J. & Migdisov, A.A. 2009: Gold in Solution. Elements 5/5: 281–287. https://doi.org/10.2113/gselements.5.5.281

Wysocki, D.A., Schoeneberger, P.J. & Lagarry, H.E. 2005: Soil surveys: a window to the subsurface. Geoderma, 126/1–2: 167–180. https://doi.org/10.1016/j.geoderma.2004.11.012

Xu, D., Deng, T., Chi, G., Wang, Z., Zou, F., Zhang, J. & Zou, S. 2017: Gold mineralization in the Jiangnan Orogenic Belt of South China: Geological, geochemical and geochronological characteristics, ore deposit-type and geodynamic setting. Ore Geology Reviews, 88: 565–618. https://doi.org/10.1016/j.oregeorev.2017.02.004

Yang, Y., Chen, J., Liu, W., Zhong, S., Ma, Y., Gao, X. & Chen, M. 2020: The impacts of pyrite/pyrrhotite on aqueous arsenic species in arsenopyrite pressure leaching: An XAS study, Minerals Engineering, 155: 106447. https://doi.org/10.1016/j.mineng.2020.106447

Yuan, Y., Li, S., Peng, J., Si, J., Cheng, H., Sun, J., Wei, J. & Shao, J. 2019: An integrated ore prospecting model for the Nyasirori gold deposit in Tanzania. China Geology, 2/4: 407–421. https://doi.org/10.31035/cg2018127

Zhu, Y., An, F. & Tan, J. 2011: Geochemistry of hydrothermal gold deposits: A review. Geoscience Frontiers, 2/3: 367–374. https://doi.org/10.1016/j.gsf.2011.05.006

GEOLOGIJA 67/2, 249-271, Ljubljana 2024

https://doi.org/10.5474/geologija.2024.012

Geologic structure and origin of the Zadlog karst polje

Geološka zgradba in nastanek kraškega polja Zadlog

Jože ČAR[1] & Ela ŠEGINA[2]*

[1]Beblerjeva 4, SI-5280 Idrija, Slovenija; e-mail: joze.car@siol.net

[2]Geološki zavod Slovenije, Dimičeva ulica 14, SI-1000 Ljubljana, Slovenija; *corresponding author: ela.segina@geo-zs.si

Prejeto / Received 29. 2. 2024; Sprejeto / Accepted 20. 8. 2024; Objavljeno na spletu / Published online 16. 12. 2024

Key words: karst polje, thrust and fault tectonics, dolomite, hydrogeology, Zadlog, Zadloško polje

Ključne besede: kraško polje, narivna in prelomna tektonika, dolomit, hidrogeologija, Zadlog, Zadloško polje

Abstract

In the wider Idrija area in western Slovenia, several large plains formed along the thrusts within the dolomite and at the contact of dolomite and limestone. The purpose of this paper is to present the detailed structural-geological background of one such plain, namely the Zadlog plain, and based on these findings, to provide new starting points for analyzing the genetic conditions of other karst poljes in Notranjska. The Zadloško polje was formed in a wider near-fault crushed zone at the contact of two structural units within the Upper Triassic Norian-Rhaetian dolomite, with the thrust crossing the polje in its central part. The initially lowered area at the thrust represented a morphological basis, and the crushed zones in the dolomite played a hydrological retention role inducing the stagnation of surface water and, as a result, the formation of the karst polje. Younger fault tectonics then established efficient drainage of surface water and the erosion of sediments to the karst underground. Besdies this, slope equilibration leads us to conclude that the karst polje capability of hydrologic retention is recently decreased. The example of Zadloško polje shows that the thrust structures and associated hydrological conditions are the key elements for the formation of karst poljes in the dissected karst surface. Further detailed structural-geological mapping will reveal whether similar structural-geological conditions are the basis for the formation of other karst poljes in the region.

Izvleček

Vzdolž narivov znotraj dolomita in narivov na kontaktu dolomita in apnenca so na Idrijskem v zahodni Sloveniji mestoma nastale večje izravnave. Namen tega prispevka je predstaviti podrobno strukturno-geološko ozadje ene takih izravnav, in sicer Zadloške uravnave in na podlagi teh ugotovitev podati nova izhodišča za prevetritev genetskih razmer tudi drugih kraških polj na Notranjskem. Zadloško polje je tako nastalo v razširjeni obprelomni zdrobljeni coni ob stiku dveh strukturnih enot znotraj zgornjetriasnega norijsko-retijskega dolomita, pri čemer narivnica prečka polje v njegovem osrednjem delu. Začetna obnarivna izravnava je predstavljala morfološko zasnovo, zdrobljeni coni v dolomitu pa sta imeli ključno vodno-zadrževalno vlogo pri zastajanju površinske vode in posledično pri nastanku kraškega polja. Mlajša prelomna tektonika je nato vzpostavila efektivno odvajanje voda in odnašanje sedimentov v kraško podzemlje. Prav tako opazujemo uravnavanje pobočij izravnave, zaradi česar menimo, da je vodno-zadrževalna sposobnost kraškega polja recentno zmanjšana. Primer Zadloškega polja kaže, da so narivna zgradba in z njo povezane hidrološke razmere ključni element za oblikovanje kraškega polja v razčlenjenem kraškem površju. Ali so podobne strukturno-geološke razmere osnova nastanka tudi ostalih kraških polj v regiji, bo razkrilo nadaljnje podrobno strukturno-geološko kartiranje.

Introduction

On the extensive Črni Vrh plateau, northwest of Črni Vrh above Idrija, lies a 2 km long and up to 800 m wide plain, which locals simply call Zadlog but sometimes also Zadloško polje (Fig. 1A, B). On the plain lies the dispersed settlement of Zadlog with many names for the different parts of the pol-je. The Zadlog plain is surrounded by higher eleva-

Uvod

Na obsežni Črnovrški planoti severozahodno od Črnega Vrha nad Idrijo leži 2 km dolga in do 800 m široka izravnava, ki ji domačini rečejo preprosto Zadlog (v Zadlogu), včasih pa tudi Zadloško polje (sl. 1A, B). Na izravnavi leži raztreseno naselje Zadlog, s številnimi imeni posameznih predelov polja. Zadloška izravnava je z tions on all sides and is therefore often referenced as Zadloška kotlina (Zadlog basin) on geographical maps. Leaving aside different geographical definitions, the term Zadloško polje or just Zadlog will be used hereinafter.

On a printed geological map of Idrija at the scale of 1:25000, the structure of the Zadloško polje area and its surroundings appears to be simple and uncomplicated (Mlakar & Čar 2009, Fig. 1). The conditions are logically and, according to the figures, adequately explained. The geological structure of Zadlog seems very simple for the otherwise complex territory of Idrija. However, a quick geological examination of the central part of Zadloško polje revealed that the geological conditions are quite different. This was indeed reason enough for a renewed, more detailed geological survey of Zadlog and its surrounding area. It revealed that Zadloško polje and its surroundings have a more complex structural-geological composition than previously believed, which is hardly recognizable due to the naturally level terrain, continuous farming and extensive land improvement works. There are few discussions of the Zadlog polje: before the results of detailed fieldwork presented in this research and the identification of complex structural-tectonic conditions, Zadlog was on a geological map represented only in his general features. Although the hydrological conditions were generally known, no one had yet considered them in the wider hydrological context. The findings of the new structural-geological mapping presented here can be used to explain the position of the polje within the broader structural situation of the area, the formation of the karst polje, the position and formation of swallets, and to explain general hydrological and morphological features and how it fits into the broader geological structure of the Črni Vrh plateau and wider Idrija region. The formation of the initial plain of the karst polje is in the existing karst literature often associated with tension conditions (Gams 1978, Vrabec, 1994; Gracia et al., 2003; Doğan et al., 2017), while the formation of the karst polje in the context of thrust tectonics has not yet been discussed.

General features of Zadloško polje

The geographical features of Zadloško polje were discussed in 1968 by Habič in his PhD thesis (Habič, 1968). Only some data from his work that is relevant to this discussion is summarised here.

The extensive plain of Zadlog is located on the western edge of the Črni Vrh plateau at an altitude of between 716 and 720 m. To the north and east towards the Idrijca valley, Idrijski Log and

vseh strani obdana z višjim vzpetinami, zato je na geografskih kartah večkrat označena tudi kot Zadloška kotlina. Ne glede na različne geografske opredelitve bomo v nadaljevanju uporabljali poimenovanje Zadloško polje, ali pa samo Zadlog.

Pogled na natisnjeno idrijsko geološko karto v merilu 1 : 25.000 kaže, da ima območje Zadloškega polja z okolico preprosto in enostavno zgradbo (Mlakar & Čar, 2009, sl. 1). Razmere so logično in, glede na podatke, primerno razložene. Za sicer geološko zapleteno idrijsko ozemlje izgleda geološka zgradba Zadloga zelo enostavna. Vendar je že hiter geološki ogled osrednjega dela Zadloškega polja pokazal, da so geološke razmere očitno drugačne. Seveda je bil to zadosten razlog za ponovno, natančnejše geološko kartiranje Zadloga in okolice. Pokazalo se je, da ima Zadloško polje z okolico bolj zapleteno strukturno-geološko zgradbo od predhodno razumljene, ki je zaradi naravne izravnave terena, stalnega kmetovanja in obsežnih melioracijskih del težje prepoznavna. O Zadloški izravnavi obstaja le malo razprav. Pred, v tej raziskavi predstavljenimi rezultati podrobnega terenskega dela in ugotovitvijo zapletenih strukturno-tektonskih razmer, je bil Zadlog na geoloških kartah izrisan samo v svojih splošnih potezah. Hidrološke razmere so bile sicer v splošnem znane, toda nihče jih še ni obravnaval v širšem hidrološkem kontekstu. Na podlagi ugotovitev tukaj predstavljenih rezultatov strukturno-geološkega kartiranja pa se da dobro razložiti lego polja v širši strukturni zgradbi ozemlja, nastanek kraškega polja, lego in nastanek ponikev in pojasniti splošne hidrološke in morfološke značilnosti ter vpetost v širšo geološko strukturo Črnovrške planote in Idrijskega ozemlja. Nastanek začetne uravnave kraškega polja se v obstoječi krasoslovni literaturi pogosto povezuje z nateznimi razmerami (Gams, 1978; Vrabec, 1994; Gracia et al., 2003; Doğan et al., 2017), medtem ko nastanek kraškega polja v okviru narivne tektonike še ni bil obravnavan.

Splošne značilnosti Zadloškega polja

Geografske značilnosti Zadloškega polja je obravnaval Habič v svojem doktoratu leta 1968 (Habič, 1968). Iz njegovega dela povzemamo le nekaj, za naše razpravljanje pomembnih podatkov.

Obsežna zadloška uravnava na zahodnem obrobju Črnovrške planote leži na višini med 716 in 720 m. Na severu in vzhodu proti dolini Idrijce, Idrijskemu Logu in Koševniku je obrobljena z nižjim grebenom s številnimi manjšimi dolinami, ki se iztekajo na eni strani proti Zadlogu, na

Koševnik, it is lined by a lower ridge with numerous smaller valleys leading towards Zadlog on one side and Idrijski Log on the other (Fig. 1A, B). The ridge, which runs only some 40 m above the present-day base of the plain, is interrupted by a number of indistinct peaks rising up to no more than 100 m above the base of Zadloško polje. The lowest points of the ridge are the distinct pass close to the Podtisov Vrh peak at 724 m, where a forest road from the Belca valley leads to Zadlog, and the pass near Kočar (above Ivanšek) (735 m), where the road from Zadlog leads to Idrijski Log and Idrijska Bela. On the southern edge of Zadlog, there are steep and poorly dissected slopes with ca. 1100 m high peaks. The only notch in the slope is the Bukovska Rovna ledge (782 m) extending into a distinctly dry and heavily karstified lowered area towards Mrzli Log and the pass near Šoštar, where the main road leads to Črni Vrh. Here is also the lowest point of the edge of Zadloško polje at an altitude of 718 m. Given the above-mentioned data, Zadlog could indeed be referred to as a shallow basin.

drugi strani pa proti Idrijskemu Logu (sl. 1A, B). Greben, ki poteka le kakih 40 m nad današnjim dnom izravnave, je prekinjen z nekaj neizrazitimi vrhovi, ki se vzpenjajo največ do 100 m nad dnom Zadloškega polja. Najnižji točki grebena sta izrazita prehod pri Podtisovem Vrhu na višini 724 m, kjer je na Zadlog speljana gozdna cesta iz doline Belce, in prelaz pri Kočarju (nad Ivanškom) (735 m), kjer poteka cesta iz Zadloga proti Idrijskemu Logu in Idrijski Beli. Na južnem obrobju Zadloga ležijo strma in slabo razčlenjena pobočja z vrhovi na višini okrog 1100 m. Zarezo v pobočju predstavlja le polica Bukovska Rovna (782 m), ki se podaljša v izrazito suho in močno zakraselo znižanje proti Mrzlemu Logu, ter prehod pri Šoštarju, kjer poteka glavna cesta proti Črnemu Vrhu. Tu je tudi najnižja točka obrobja Zadloškega polja na višini 718 m. Iz zgornjih podatkov izhaja, da ima Zadlog značilnosti plitve kotline.

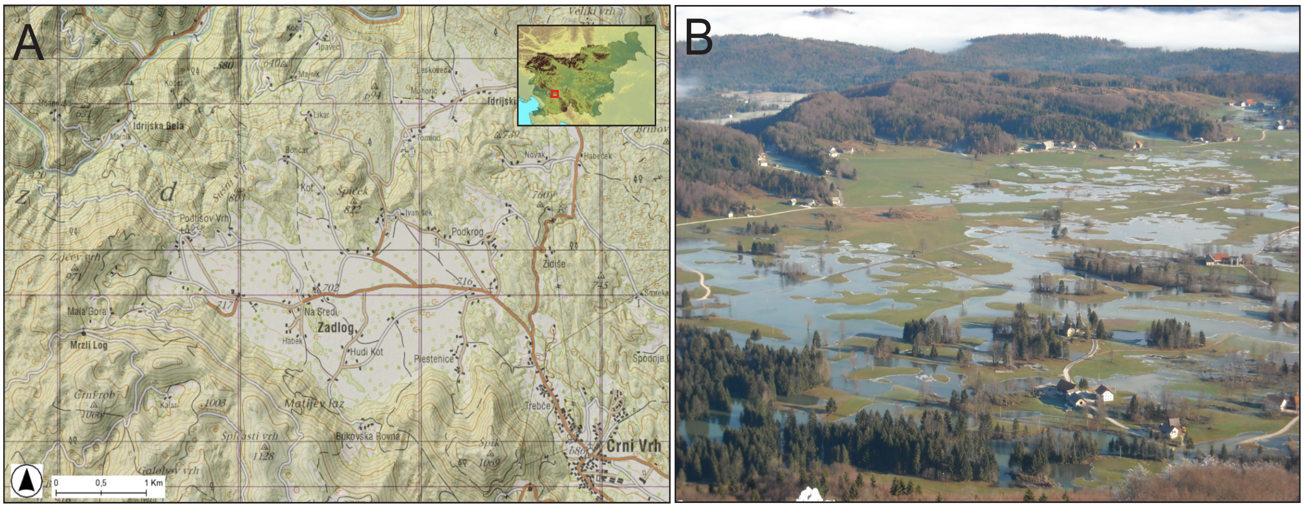

Fig. 1. A – Location and basic topographic features of the Zadloško polje area. B – View on Zadloško polje during floods (18. 12. 2009). Photo: Bojana Zagoda.

Sl. 1. A – Lokacija in osnovne topografske značilnosti območja Zadloškega polja. B – Pogled na Zadloško polje v času poplav (18. 12. 2009). Foto: Bojana Zagoda.

Geographers and geologists alike write about how the Idrijca, the Belca and the Kanomljica once probably flowed together across the Zadloško polje, the Črni Vrh plateau and further along the Hotenjsko podolje valley system towards the Ljubljanica (Savnik, 1959; Melik, 1963; Mlakar, 2002). The flow of the watercourses in Idrija towards the Ljubljanica river was discussed in great detail and supported by geomorphological data by Mlakar (2002). Such an assessment is not supported by any material evidence. Habič (1968) had already determined that on the Zadlog-Črni Vrh plateau and the Hotenjsko podolje area between

O tem, da naj bi nekdaj Idrijca, Belca in Kanomljica združeno tekale čez Zadloško polje, Črnovrško planoto in dalje po Hotenjskem podolju proti Ljubljanici, so pisali tako starejši geografi kot tudi geologi (Savnik, 1959; Melik, 1963; Mlakar, 2002). Še posebej podrobno in podprto z geološkimi in morfološkimi podatki je pretok idrijskih vodotokov proti Ljubljanici obravnaval Mlakar (2002). Materialnih dokazov za tako mnenje ne navaja. Že Habič (1968) je ugotovil, da na Zadloško-Črnovrški planoti in Hotenjskem podolju med Godovičem in Hotedršico ni sledov rečne erozije ali prodov, ki bi vsekakor morali biti

Godovič and Hotedršica there are no traces of fluvial erosion or cobble, which should certainly have been preserved, even if only here and there and in marginal amounts. Zadloško polje is covered by an unevenly thick yellowish dolomitic clayey eluvium with rare, small and irregular millimetre-sized chert clasts showing no signs of transport. The clasts were not studied in detail, however, they represent sparingly soluble residue and certainly originate from the parent rock. The thickness of eluvium is locally increased in some lower parts of the terrain. The internal texture shows that it was transported for only a short distance.

The entire Zadloško polje was artificially levelled (ameliorated) to a considerable extent. To get land for farming, the lower dolomite outcrops were mostly levelled out. At the northern and central parts of Zadloško polje, however, there are still dolomite hummocks rising about 1.5 to some metres from the plain that mainly run northwest to southeast and are aligned with strata of dolomite. They are either bare or covered with shallow turf, shrubbery, individual trees or sparse woods. Nowadays it is impossible to deduce how many dolines and other karst formations have been filled. Given the conditions elsewhere on the dolomitic part of the Črni Vrh plateau (Črni Vrh, Predgriže, Koševnik and Idrijski Log), which has comparable structural composition (Zagoda, 2004), it can be concluded that the Upper Triassic dolomite in Zadlog is also relatively poorly karstified, which is as well supported by geological mapping of the same kind of dolomite in a comparable structural position in Idrijski Log and Predgriže. However, there are some morphologically distinctive sinking areas with ponors on Zadloško polje.

The influence of the Pleistocene glaciation on the morphology of Zadlog has not yet been studied and is currently unknown. Undoubtedly, such cold climatic conditions influenced the faster denudation of dolomites in the hinterland and more intense transport of the weathered material to the karst polje.

Geological structure of Zadloško polje

Earlier data

Existing geological maps (Buser et al., 1967; Mlakar, 1969; Pleničar, 1970; Mlakar & Čar, 2009) suggest that the structure of Zadloško polje and its wider surroundings is very simple. The Postojna sheet from the Basic geological map (Osnovna geološka karta, OGK) and the interpreter to this sheet (Pleničar et al., 1970) show that Zadlog and its wider surroundings are made of thinly to moderately stratified Upper Triassic Norian-Rhaetian

ohranjeni, pa čeprav le tu in tam in v neznatnih sledovih. Zadloško polje sicer prekriva neenakomerno debela dolomitna rumenkasta glinasta preperina z redkimi, majhnimi in nepravilnimi klasti roženca milimetrskih dimenzij, ki ne kažejo znakov premeščanja, saj so povsem nepravilnih oblik. Klastov na tem mestu nismo raziskovali, vendar predstavljajo težje topni ostanek in zagotovo izhajajo iz matične kamnine. Preperina je na nekaterih nižje ležečih predelih lokalno debelejša. Notranja tekstura kaže, da je preložena le na kratko razdaljo.

Celotno Zadloško polje je bilo s posegi v dobršni meri umetno izravnano (meliorirano). Za potrebe kmetovanja so bile izravnane predvsem nižje dolomitne golice. V severnem in osrednjem delu Zadloškega polja pa še vedno štrle iz izravnave od 1,5 do nekaj metrov visoke dolomitne grbine, ki potekajo v glavnem v smeri severozahod – jugovzhod, skladno s slemenitvijo dolomitnih plasti. So gole ali pa pokrite s plitvo rušo, grmovjem, posameznimi drevesi ali redkim gozdom. Koliko je v podlagi zasutih vrtač in drugih kraških oblik ni raziskano. Iz razmer drugod na dolomitnem delu Črnovrške planote (Črni Vrh, Predgriže, Koševnik in Idrijski Log), ki ima primerljivo strukturno zgradbo (Zagoda, 2004), lahko sklepamo, da je zgornjetriasni dolomit tudi v Zadlogu razmeroma slabo zakrasel. To podpira tudi geološko kartiranje enakega dolomita v primerljivi strukturni legi v Idrijskem Logu in Predgrižah. Se pa na Zadloškem polju nahaja nekaj morfološko izrazitih ponikalnih območij.

Vpliv pleistocenske poledenitve na morfologijo Zadloga še ni bil preučen in ga ta hip ne poznamo. Nedvomno pa so hladnejše podnebne razmere vplivale na hitrejšo denudacijo dolomitov v zaledju polja in intenzivnejše površinsko premeščanje preperine na izravnavo.

Geološka zgradba Zadloškega polja

Starejši podatki

Pogled na dosedanje geološke karte (Buser et al., 1967; Mlakar, 1969; Pleničar, 1970; Mlakar & Čar, 2009) pokaže, da naj bi bilo Zadloško polje s širšo okolico zelo preprosto zgrajeno. Glede na OGK list Postojna in tolmača k temu listu (Pleničar et al., 1970) vidimo, da Zadlog s širšo okolico gradi tanko do srednje plastnati zgornjetriasni norijsko-retijski (ti. glavni) dolomit. Dno zadloške uravnave v celoti pokrivajo kvartarni sedimenti – nanosi rek in potokov (Pleničar et al., 1970). Od terciarne tektonike je dolomite (so-called main dolomite). The base of the Zadlog plain is entirely covered by quaternary sediments – river and stream deposits (Pleničar et al., 1970). Regarding tertiary tectonics, only the thrust line between the Lower Cretaceous limestone of the first 'slice' (today: Koševnik nappe slice) and the Upper Triassic dolomite of the second 'slice' (today: Čekovnik thrust slice) running north and east of Zadlog along the plain of Idrijski Log and Koševnik is delineated. No other potential tectonic elements have been identified.

Zadloško polje was not remapped during the production of the new 1:25,000 scale geological map (Mlakar & Čar, 2009). The conditions thus remain nearly identical as when delineated and described by Mlakar on his 1969 geological map, while the new map includes corrections of thrust unit designations. According to Placer's (Placer, 1981, 2008) thrust dissection of western Slovenia and his recent oral proposal, the *Hrušica nappe* lies in the deeper bedrock of the territory of Idrija, and over it follow the *Koševnik, Čekovnik and Kanomlje interjacent slice* (*nappe slice* in this paper), covered by the Lower thrust block of Trnovo nappe, which is nowadays divided into four internal overthrust bodies (Mlakar & Čar, 2009; Čar, 2010; Čar et al., 2021). The entire Zadloško polje and its wider surroundings consist of two thrust packages of Upper Triassic Norian-Rhaetian dolomite. The northern border of Zadloško polje and a large portion of the central part belong to the *Čekovik nappe slice*. The Upper Triassic dolomite has a normal stratigraphic position according to recent findings (Čar, 2010). The southern slopes towards Špičasti vrh (822 m), Mrzli Log and Špik also consist of the Norian–Rhaetian dolomite, but it belongs to the Trnovo nappe overthrust unit, i.e. the Tičnica inner thrust sheet (Čar, 2010). The thrust line between the two units should run along the southern edges of Zadlog, the same way as it is delineated on Mlakar's map (1969). Two fault lines are delineated on the map: the first one runs from Mrzli Log across Bukovska Rovna, intersects Zadloško polje and continues across Kotenjski rob (along the location Kot) into the Belca valley, while the second fault intersects the eastern part of Zadloško polje. It enters the polje in Plestenice and continues past Klančar and across Koševnik into the Idrijca valley. This map dating in 1969 also shows that the base of Zadloško polje is covered by alluvial deposits (Mlakar & Čar, 2009).

Previous geological maps (Pleničar, 1970; Mlakar, 1969; Mlakar & Čar, 2009) did not take into account the hydrological conditions in Zadlog and the remarks on the coverage of the polje floor already observed and written down by Habič

izrisana le narivnica med spodnjekrednim apnencem prve luske (danes: Koševniška krovna luska) in zgornjetriasnim dolomitom druge luske (danes: Čekovniška krovna luska), ki poteka severno in vzhodno od Zadloga po uravnavi Idrijskega Loga in Koševnika. Drugi tektonski elementi niso bili ugotovljeni.

Pri izdelavi nove geološke karte v merilu 1: 25 000 (Mlakar & Čar, 2009). Zadloškega polja nismo na novo kartirali. Razmere zato ostajajo skoraj enake, kot jih je izrisal in opisal Mlakar na svoji geološki karti iz leta 1969, vendar s popravki poimenovanja narivnih enot. Soglasno s Placerjevo narivno razčlenitvijo zahodne Slovenije in njegovim novejšim ustnim predlogom (Placer, 1981, 2008) leži v globlji podlagi Idrijskega ozemlja *Hrušiški pokrov,* nad njim si sledijo *Koševniška, Čekovniška in Kanomeljska krovna luska*, pokriva jih spodnji narivni blok Trnovskega pokrova, ki je danes razdeljen na štiri notranje narivne grude (Mlakar & Čar, 2009; Čar, 2010; Čar et al., 2021). Celotno Zadloško polje in njegovo širšo okolico gradita dva narivna paketa zgornjetriasnega norijsko-retijskega dolomita. Severno obrobje Zadloškega polja in velik delež osrednjega dela pripada *Čekovniški krovni luski*. Zgornjetriasni dolomit ima po novejših ugotovitvah normalno stratigrafsko lego (Čar, 2010). Južna pobočja proti Špičastemu vrhu (822 m), Mrzlemu Logu in Špiku gradi prav tako norijsko-retijski dolomit, le da pripada narivni enoti *Trnovskega pokrova* in sicer *Tičenski notranji narivni grudi* (Čar, 2010). Narivnica med obema enotama naj bi potekala po južnem obrobju Zadloga, enako kot je izrisana na Mlakarjevi karti (1969). Na karti sta izrisani dve prelomni liniji: prva poteka iz Mrzlega Loga čez Bukovsko Rovno, seka Zadloško polje in se nadaljuje čez Kotenjski rob (po lokaciji Kot) v dolino Belce, drugi prelom pa seka vzhodni del Zadloškega polja. Na polje prihaja v Plestenicah in se nadaljuje mimo Klančarja in čez Koševnik v dolino Idrijce. Tudi na tej karti iz leta 1969 je izrisano, da prekrivajo dno Zadloškega polja aluvialni nanosi (Mlakar & Čar, 2009).

Pri izdelavi dosedanjih geoloških kart (Pleničar, 1970; Mlakar 1969; Mlakar & Čar, 2009) niso upoštevane hidrološke razmere v Zadlogu in pripombe o pokritosti dna polja, ki jih je ugotovil in zapisal že Habič (1968). To je bil povod za podrobnejše geološko kartiranje Zadloga z obrobjem v merilu 1 : 5000.

(1968). This prompted a more detailed geological mapping of Zadlog and its edges at a scale of 1:5,000.

Fault tectonics

For an easier interpretation and a better understanding of the thrust and thrust–shear deformations on Zadloško polje and its edges, fault tectonics are discussed first. The fault and thrust fracturing nomenclature below and their variability in horizontal and vertical directions is in line with the one published in the discussion by Čar (2018). The data presented are the result of detailed structural-geological mapping, which was carried out for the purposes of the present research.

In the western part of Zadloško polje, from its edges eastwards follow the *Figar, Podtis and Zadlog faults* (Fig. 2). The faults are dextral strike-slips of varying strength and are oriented northwest–southeast. They are grouped together in the *western Zadlog set of faults*. The *Figar fault* is up to 300 m wide, consists of four narrow crushed zones and strong interjacent broken zones, has a general 80° dip to the southwest and runs over the far western edge of Zadloško polje (Fig. 2). The southwestern part of the fault zone transitions over the steep slope on the southern edges of Zadlog into a wide fissure zone, which is typical of the longitudinal changes in fault zones (Čar, 2018). The northeastern part runs along the foot of the Špičasti vrh and later joins the Zadlog fault. The double *Podtis fault* with an approximately 150 m wide fault zone leads from Belca valley across the Podtisov Vrh saddle. The Podtisov Vrh saddle formed in crushed zones with an 80° dip to the southwest (Fig. 3 A). The fault zone runs across the western part of Zadloško polje and joins the strong Zadlog fault, which runs from the Belca valley to the edge of Zadloško polje at Gozdnik and then progresses across the polje all the way to Bukovska Rovna (Fig. 2). The strong fault zone of the Zadlog fault is up to 200 m wide and progresses towards Mrzli Log and Kanji Dol. Within this zone formed a deepened, morphologically dissected, strongly karstified and lowered zone which leads between Bukovska Rovna and Mrzli Log. The degree of rock fracturing varies along the zone from crushed to widely fractured, and fissured zones of varying strength can be observed in the outer fault zones.

The eastern part of Zadloško polje and its edges are also intersected by a series of faults, grouped together in the *eastern Zadlog set of faults*. Running from west to east: *Plestenice, Klančar, Črni Vrh, Abraht (named after a farm)* and stronger *Pred-*

Prelomna tektonika

Za lažjo razlago in boljše razumevanja narivnih in obnarivnih deformacij na Zadloškem polju in njegovem obrobju obravnavamo najprej prelomno tektoniko. Poimenovanje pretrtosti ob prelomih in narivih ter njihovo spreminjanje v horizontalni in vertikalni smeri je soglasno z nomenklaturo v Čarjevi razpravi (2018). Predstavljeni podatki so rezultat podrobnega strukturno-geološkega kartiranja, ki je bilo izvedeno za namene te raziskave.

V zahodnem delu Zadloškega polja sledijo od njegovega obrobja proti vzhodu *Figarjev, Podtisov in Zadloški prelom* (sl. 2). Prelomi so desno-zmični, različno močni in imajo smer severozahod – jugovzhod. Združujemo jih v *zahodni zadloški prelomni snop*. Na skrajnem zahodnem obrobju Zadloškega polja poteka do 300 m širok, iz štirih ožjih zdrobljenih con in močnih vmesnih porušenih con zgrajen *Figarjev prelom* s splošnim vpadom 80° proti jugozahodu (sl. 2). Jugozahodni del prelomne cone prehaja v strmem pobočju južnega obrobja Zadloga v široko razpoklinsko cono, značilno za vzdolžno spreminjanje prelomnih con (Čar, 2018). Severovzhodni del poteka vzdolž vznožja Špičastega vrha in se v nadaljevanju priključi na *Zadloški prelom*. Čez sedlo Podtisov Vrh poteka iz doline Belce dvojni *Podtisov prelom* z okrog 150 m široko prelomno cono. Sedlo Podtisov Vrh se je oblikovalo v zdrobljenih conah z vpadom 80° proti jugozahodu (sl. 3A). Prelomna cona poteka čez zahodni del Zadloškega polja in se v nadaljevanju priključi na močan Zadloški prelom, ki poteka iz doline Belce do roba Zadloškega polja pri Gozdniku in se nadaljuje čez polje do Bukovske Rovne (sl. 2). Močna prelomna cona Zadloškega preloma je široka do 200 m in se nadaljuje proti Mrzlemu Logu in Kanjemu Dolu. V njej se je oblikovala poglobljena, morfološko razgibana, močno zakrasela in znižana cona, ki poteka med Bukovsko Rovno in Mrzlim Logom. Stopnja pretrtosti kamnin se vzdolž cone spreminja od zdrobljenih do širokih porušenih con, v zunanjih prelomnih conah opazujemo različno močne razpoklinske cone.

Tudi vzhodni del Zadloškega polja in njeno obrobje prav tako seka niz prelomov, združujemo jih v *vzhodni zadloški prelomni snop*. Od zahoda proti vzhodu si sledijo: *Plesteniški, Klančarjev, Črnovrški, Abrahtov* (ime po kmetiji) in močnejši *Predgriški prelom* (sl. 2). Plesteniški prelom je v severnem delu Zadloga usmerjen od severozahoda proti jugovzhodu, v nadaljevanju se približuje močni in široki coni Zadloškega preloma in *griže fault* (Fig. 2). The Plestenice fault runs northwest to southeast in the northern part of Zadlog, and then it approaches the strong and wide Zadlog fault zone and joins it southeast of Mrzli Log outside of this map. Other faults have NNW-SSE direction in the northern part of the geologic map and later turn to NW-SE direction and predominantly appear as relatively wide broken and fissured zones in the dolomite. The fractured zones in both of the examined Zadlog set of faults are densely stacked with only 100 to 300 m distances in-between on average. All faults are dextral strike-slips. The displacements along these faults would need to be determined more precisely, but we estimate that they are relatively small.

se nanjo priključi jugovzhodno od Mrzlega Loga izven okvirja naše karte. Ostali prelomi imajo na severnem delu geološke karte smer SSZ-JJV, nato pa povijejo v smer SZ-JV in se kažejo predvsem kot sorazmerno široke porušene in razpoklinske cone v dolomitu. V obeh obravnavanih prelomnih snopih se pretrte cone nizajo na gosto, med njimi so razdalje v povprečju le od 100 do 300 m. Pri vseh prelomih gre za desne zmike. Kakšni so premiki ob njih, bi bilo potrebno natančnejše ugotoviti, vendar ocenjujemo, da so relativno majhni.

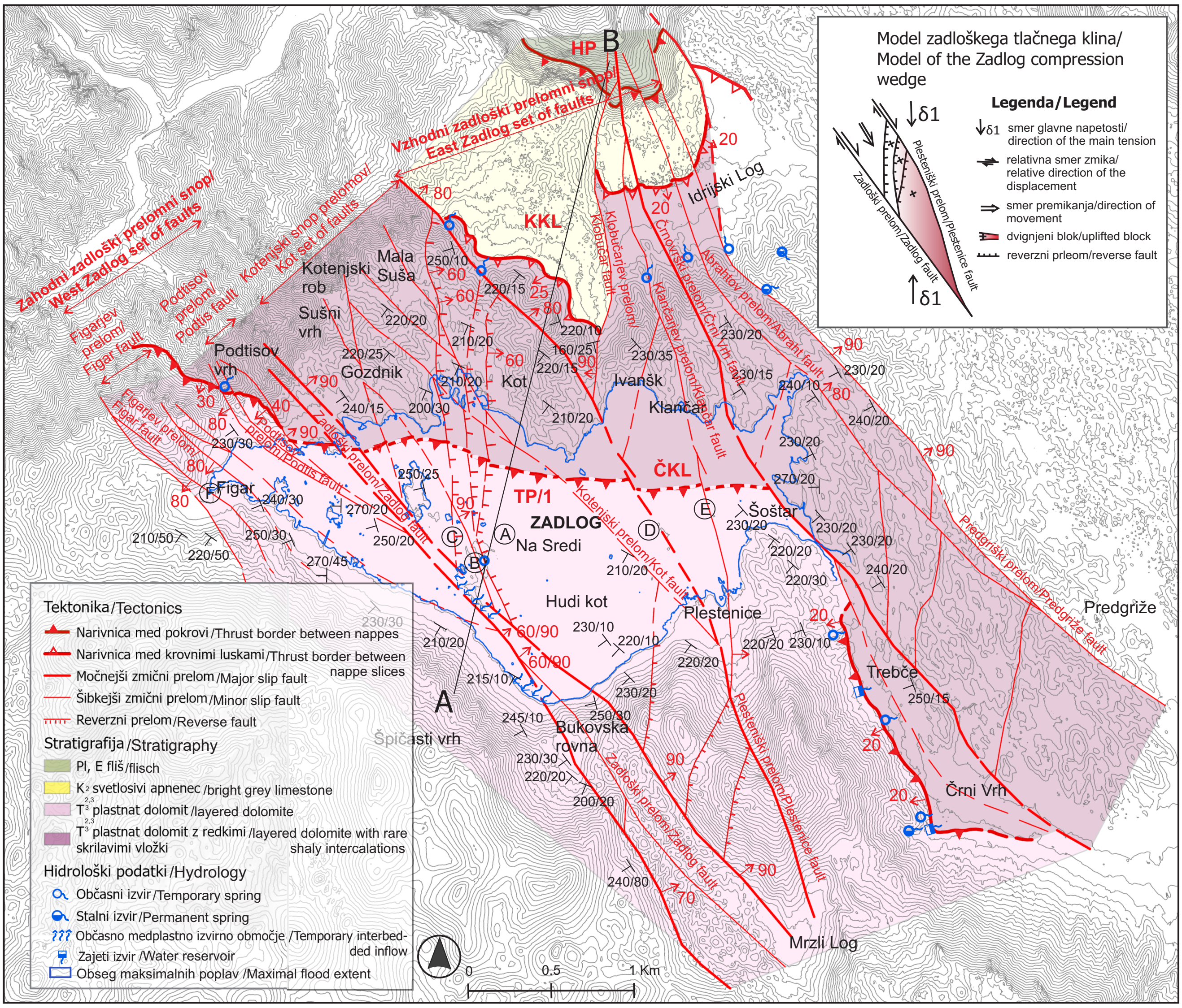

Fig. 2. Structural-geological map of Zadloško polje. The AB profile is shown in Figure 4. HP – Hrušica nappe, TP/1 – Lower thrust block of Trnovo nappe, ČKL – Čekovnik nape slice, KKL – Koševnik nappe slice. Ponor zones: A – Štefkova rupa, B – Ponikva, C – Ponor at Cigale farm, D – Štirnska rupa, E – no name ponor zone, F – Figar ponor zone.

Sl. 2. Strukturno-geološka karta Zadloškega polja. Profil AB je prikazan na sliki 4. HP – Hrušiški pokrov, TP/1 – Spodnji narivni blok Trnovskega pokrova, ČKL – Čekovniška krovna luska, KKL – Koševniška krovna luska. Ponikalna območja: A – Štefkova rupa, B – Ponikva, C – Ponikva pri kmetiji Cigale, D – Štirnska rupa, E – ponikalno območje brez imena, F – Figarjevo ponikalno območje.

The central part of Zadlog, which is loctated between the Zadlog and Plestenice faults, is about 1300 m wide at the northwestern edge of the polje and gradually becomes narrower towards the southeast (Fig. 2). It encompasses Hudi Kot on the southern edges of the polje, the central part of the polje Na Sredi and the levelled extensions between numerous dolomite outcrops towards Sušni vrh, Mala Suša and Kot in the northwest. The faults intersecting the central part of Zadloško polje are genetically distinct. The eastern faults branch off the Plestenice fault in the area of Kot and Mala Suša, and lean on the approximately 300 m long area of the Zadlog fault at the Na Sredi site. This is the 'Kotenjski niz' (after the hamlet of Kot) set of three morphologically less distinct, reverse faults in the north–south direction. According to the geological data, they are the result of secondary pressure conditions between the Plestenice fault on the one hand and the Zadlog fault on the other. Both dextral strike-slip faults are relatively strong and, as already mentioned, converge and merge towards the southeast. A pressure wedge has formed between them where weak and branched reverse faults formed due to intense dextral strike-slips (Zadlog compression wedge model, Fig. 2). They dip about 60° to the east, which is in line with their origin. Along these there are slightly uplifted eastern blocks. The western set consists of several weaker branched out strike-slip faults of Kot with narrow fault zones. On the northwestern edges of Zadloško polje they run in the NW–SE direction, then gently bend in the SSW–SSE direction, intertwine with eastern set of reverse faults zones at location Na Sredi and lean on the Zadlog fault at the same section as the reverse faults. The entwinement at Na Sredi shows that reverse faults are slightly older as they are intersected by strike-slip faults (Fig. 2). Intersections of reverse and strike-slip fault zones are connected to the sinking zones at Na Sredi (Fig. 2).

Thrust tectonics

Reflecting on the hitherto inconsistent designation of the different types of thrust units, as well as the differing graphic tracing of thrust contacts between them on geological maps, a table with the subdivision and designation of individual thrust elements was presented in 2021 (Čar et al., 2021).

The deeper bedrock of the Idrija territory contains Upper Cretaceous limestones and through erosion overlying Palaeocene-Eocene flysch rocks of the Hrušica nappe (HP) (Fig. 4), which are visible at the southern margin of the Strug tectonic window. According to older literature, the above-mentioned thrust unit is believed to be native bedrock of the Idrija territory (Mlakar, 1969, Fig. 5; Placer, 1973, 1981).

Osrednji del Zadloga med Zadloškim in Plesteniškim prelomom je na severozahodnem robu polja širok okrog 1300 m, proti jugovzhodu pa se postopno oži (sl. 2). Zaobjema Hudi Kot na južnem obrobju polja, osrednji del polja Na Sredi in izravnane podaljške med številnimi dolomitnimi izdanki proti Sušnemu vrhu, Mali Suši in Kotu na severozahodu. Prelomi, ki sekajo osrednji del Zadloškega polja, so genetsko različni. Vzhodni se odcepijo od Plesteniškega preloma na območju Kota in Male Suše, in se naslanjajo v okrog 300 m dolgem območju na Zadloški prelom na lokaciji Na Sredi. Gre za *Kotenjski* (po zaselku Kot) *niz* treh morfološko manj izrazitih, reverznih prelomov v smeri sever-jug. Glede na geološke podatke ugotavljamo, da so rezultat sekundarnih tlačnih razmer med Plesteniškim prelomom na eni in Zadloškim na drugi strani. Oba desno zmična preloma sta razmeroma močna in se proti jugovzhodu, kot smo že omenili, približujeta in združita. Med njima je nastal tlačni klin, v katerem so ob intenzivnih desnih zmikih nastali šibki reverzni prelomi (Model zadloškega tlačnega klina, sl. 2). Vpadajo okrog 60° proti vzhodu, kar je v soglasju z njihovim nastankom. Ob njih so vzhodni bloki nekoliko dvignjeni. Zahodnejši snop sestavlja več šibkejših in razvejanih Kotenjskih zmičnih prelomov z ozkimi prelomnimi conami. Na severozahodnem obrobju Zadloškega polja potekajo v smeri SZ-JV, nato povijejo rahlo v smer SSZ-JJV. Na lokaciji Na Sredi se prepletejo s conami vzhodnega reverznega prelomnega snopa in naslanjajo na Zadloški prelom na istem odseku kot reverzni prelomi. Pri prepletanju Na Sredi vidimo, da so reverzni prelomi nekoliko starejši, saj jih zmični prelomi sekajo (sl. 2). Na sekanje omenjenih reverznih in zmičnih prelomnih con so vezana ponikalna območja Na Sredi (sl. 2).

Narivna tektonika

Ob premisleku o doslej neenotnem poimenovanju različnih tipov narivnih enot, kot tudi zaradi različnih grafičnih izrisov narivnih stikov med njimi na geoloških kartah smo leta 2021 podali preglednico razčlenitve in poimenovanje posameznih narivnih elementov (Čar et al., 2021).

V globlji podlagi idrijskega območja ležijo zgornjekredni apnenci in erozijsko na njih paleocensko-eocenske flišne kamnine Hrušiškega pokrova (HP) (sl. 4), ki se na obravnavanem območju pojavijo v južnem obrobju Tektonskega okna Strug. Po starejši literaturi naj bi bila omenjena narivna enota avtohtona podlaga idrijskega območja (Mlakar, 1969, sl. 5; Placer, 1973, In the Idrija area, Lower and Upper Cretaceous limestone of the Koševnik nappe slice (KKL) is thrust onto the rocks of the Hrušica nappe in a normal position and measures 100 to 500 m in thickness (Fig. 4). In view of the geological conditions in the Strug tectonic window and Idrijska Bela, the Koševnik nappe slice underneath Zadloško polje mainly consists of Upper Cretaceous limestone, but may deeper down already continuously transition into Lower Cretaceous limestones with rare intercalations of early diagenetic dolomite. Along the thrust line, soft flysch rocks are often pushed out in such a way that Upper Cretaceous limestones of the Hrušica nappe are directly overlain by Lower or Upper Cretaceous limestones of the Koševnik nappe slice (Fig. 4). The Koševnik nappe slice is covered by Norian-Rhaetian dolomite of the Čekovnik nappe slice (ČKL) in its normal position. The morphologically very distinctive thrust line between the two nappe units runs along the northern preiphery of Idrijski Log (Zagoda, 2004) (Fig. 2) and then crosses Predgriško polje east of Črni Vrh (Mlakar & Čar, 2009). The northern edges and northern part of Zadloško polje consist of Upper Triassic dolomite of the Čekovnik nappe slice. The remaining part of Zadlog as well as its southern and western edges consist of the Trnovo nappe Norian-Rhaetian dolomite (TP/1 – the Trnovo nappe underthrust block). High below the northern edge of Trnovski gozd (not shown in Fig. 2), the Norian-Rhaetian dolomite of the Trnovo nappe is sliced by another thrust plane (Čar, 2010). Over it lies the Norian-Rhaetian dolomite with continuous transitions to Jurassic limestones of the next thrust unit (TP/2 – Trnovo nappe overthrust block, outside Fig. 2).

The Norian-Rhaetian dolomite has a normal position and practically identical dip and strike in the Čekovnik nappe slice as well as in the lower part of the Trnovo nappe (TP/1). The strata dip from 10 to 30° to the southwest. The dolomite is generally medium to thick-bedded (10 to 30 cm), with thinner (10 cm) or thicker strata (up to one metre) only as an exception. The dolomite is light to dark grey, here and there nearly white, and most often laminated or stromatolitic. In some places, thinly coated flat pebble conglomerate can be observed on the top surface. In the Norian-Rhaetian dolomite sequence of the Čekovnik nappe slice, interbedded claystone intercalations and rare strata with fine oncoids occur in the lower part of the sequence in the Belca valley. Thin interbedded intercalations of shaly claystone and dolomitic marlstone occur only above Carnian clastic rocks in the Norian-Rhaetian dolomite in the Idrija area. This indicates that the dolomite of the Čekovnik nappe slice is part of the lower Norian-Rhaetian dolomite sequence. Within the Trnovo nappe, there are no shaly

1981). Na Idrijskem je na kamnine Hrušiškega pokrova narinjen spodnje in zgornjekredni apnenec Koševniške krovne luske (KKL) v normalni legi in debelini od 100 do 500 m (sl. 4). Glede na geološke razmere v Tektonskem oknu Strug in Idrijski Beli gradi Koševniško krovno lusko pod Zadloškim poljem predvsem zgornjekredni apnenec, v globljih delih pa že lahko zvezno prehaja v spodnjekredne apnence z redkimi vložki zgodnjediagenetskega dolomita. Ob narivnici so mehke flišne kamnine pogosto iztisnjene tako, da na zgornjekrednih apnencih Hrušiškega pokrova ležijo neposredno spodnje ali zgornjekredni apnenci Koševniške krovne luske (sl. 4). Koševniško krovno lusko prekriva norijsko-retijski dolomit Čekovniške krovne luske (ČKL) v normalni legi. Morfološko zelo izrazita narivnica med krovnima enotama poteka po severnem obrobju Idrijskega Loga (Zagoda, 2004) (sl. 2), nato pa poteka čez Predgriško polje vzhodno od Črnega Vrha (Mlakar & Čar, 2009). Zgornjetriasni dolomit Čekovniške krovne luske gradi severno obrobje in severni del Zadloškega polja. Preostali del Zadloga in njegovo južno in zahodno obrobje je iz norijsko-retijskega dolomita Trnovskega pokrova (TP/1- spodnji narivni blok Trnovskega pokrova). Visoko pod severnim robom Trnovskega gozda (ni prikazano na karti sl. 2) reže norijsko-retijski dolomit Trnovskega pokrova še ena narivna ploskev (Čar, 2010). Nad njo leži norijsko-retijski dolomit z zveznimi prehodi v jurske apnence naslednje narivne enote (TP/2 - zgornji narivni blok Trnovskega pokrova, izven okvirja sl. 2).

Norijsko-retijski dolomit ima v Čekovniški krovni luski, kot tudi v spodnjem delu Trnovskega pokrova (TP/1) normalno lego in praktično enak vpad. Plasti vpadajo od 10 do 30° proti jugozahodu. Dolomit je v splošnem srednje do debelo (od 10 do 30 cm) plastnat, le izjemoma opazujemo tanjše plasti (10 cm) ali debele do enega metra. Dolomit je svetlo do temno siv, tu in tam skoraj bel, največkrat laminiran ali stromatoliten. Ponekod opazujemo na zgornji površini plasti tanke prevleke nadplimskega konglomerata. V zaporedju norijsko-retijskega dolomita Čekovniške krovne luske se v spodnjem delu plasti v dolini Belce pojavljajo medplastni vložki glinavca in redke plasti z drobnimi onkoidi. Tanki medplastni vložki skrilavega glinavca in dolomitnega laporovca se v norijsko-retijskem dolomitu na Idrijskem pojavljajo le nad karnijskimi klastiti. To kaže, da je dolomit Čekovniške krovne luske del spodnjega zaporedja norijsko-retijskega dolomita. V okviru Trnovskega pokrova v norijsko-retijskem marlstone intercalations in the Norian-Rhaetian dolomite. The same dip of strata and strong lithological similarity between the dolomites of both thrust units were an important reason why the thrust line between the Čekovnik nappe slice and the Trnovo nappe was previously delineated along the southern edges of Zadloško polje (Mlakar & Čar, 2009).

The thrust–shear deformations in the dolomites of both thrust units can be directly observed along the forest road Ipavšk–Podtisov Vrh on the slope of the Belca valley. The intensity and extent of the thrust–shear crushed zone varies, it is at least 10 to 15 m thick and gradually transitions to a several metres thick zone of less tectonically deformed dolomite. Within the crushed zone, the main thrust plane with a dip of 40 to 20° runs southwards. At Podtisov vrh (724 m), the thrust line veers to the western edges of Zadloško polje. An approximately 200 m wide zone of completely crushed dolomite has formed here as a result of a strong thrust–shear crushed zone intersecting the Podtis fault zone (Fig. 3A). A thrust-fault crushed zone with a tectonic (cataclastic) structure of 'meal, grit and detritus' is exposed in the larger sand quarry, where an intricate interplay of thrust and fault zones can be observed. Due to fault-induced deformations, sections of the thrust plane dip 60° to the southwest (230/60°). The thrust zone continues beneath the anthropogenically levelled and ameliorated bedrock of Zadloško polje and cannot be observed directly. Indirectly, the thrust line can be traced based on a distinctively levelled surface with no bedrock outcrops. Thrust line crosses the complex zone of the Zadlog fault, intersects the less disturbed part of the polje between the Zadlog and the Plestenice fault, and continues to the Črni Vrh fault on the western edge of Zadlog. Its course

dolomitu skrilavih laporastih vložkov ni. Prav enak vpad plasti in velika litološka podobnost med dolomitoma obeh narivnih enot je bil pomemben razlog, da je bila narivnica med Čekovniško krovno lusko in Trnovskim pokrovom doslej izrisana po južnem obrobju Zadloškega polja (Mlakar & Čar, 2009).

Obnarivne deformacije v dolomitih obeh narivnih enot lahko neposredno opazujemo ob gozdni cesti Ipavšk – Podtisov Vrh na pobočju doline Belce. Intenzivnost in obseg obnarivne zdrobljene cone se spreminja; debela je vsaj 10 do 15 m in postopno prehaja v več metrov debelo cono manj pretrtega dolomita. Znotraj zdrobljene cone poteka glavna narivna ploskev z vpadom 40 do 20° proti jugu. Pri Podtisovem Vrhu (724 m) se narivnica previje na zahodno obrobje Zadloškega polja. Tu je nastalo okrog 200 m široko območje povsem zdrobljenega dolomita, ki je rezultat močne obnarivne zdrobljene cone, ki jo seka cona Podtisovega preloma (sl. 3A). Narivno-prelomna zdrobljena cona s tektonsko (kataklastično) strukturo 'moka, zdrob in drobir' je odprta v večjem peskokopu, kjer lahko opazujemo zapleteno prepletanje narivnih in prelomnih con. Zaradi obprelomnih deformacij vpadajo odseki narivne ploskve za 60° proti jugozahodu (230/60°). Narivna cona se nadaljuje pod antropogeno izravnanim in melioriranim dnom Zadloškega polja in jo neposredno ne moremo opazovati. Posredno lahko narivnici sledimo na podlagi izrazito uravnanega terena brez izdankov matične kamnine. Narivnica prečka zapleteno cono Zadloškega preloma, seka manj pretrti del polja med Zadloškim in Plesteniškim prelomom in se nadaljuje do Črnovrškega preloma na zahodnem obrobju Zadloga. Njen potek

Fig. 3. A – thrust-fault crushed zone in a quarry at Podtisov Vrh on the western perimeter of Zadloško polje. B – A thrust crushed zone in a sand quarry at Trebče near Črni Vrh, southeast of Zadloško polje. Photo: Jože Čar.

Sl. 3. A – Narivno-prelomna zdrobljena cona v peskokopu pri Podtisovem Vrhu na zahodnem obodu Zadloškega polja. B – Narivna zdrobljena cona v peskokopu v Trebčah pri Črnem vrhu, jugovzhodno od Zadloškega polja. Foto: Jože Čar.

is also confirmed by the finding of pieces of cataclastic rocks in the field west of the Črni Vrh fault. The thrust line reappears about a kilometre further south in the sand quarry near the hamlet of Trebče at Črni Vrh, on the western side of the Črni Vrh fault, i.e. in the same structural block as in Zadloško polje. Further towards Črni Vrh, the thrust zone runs parallel to the fault zone of the Črni Vrh fault. In the Trebče sand quarry, the thrust line dips 20° to the southwest (Fig. 3B) and has the same dip all the way to Črni Vrh (Fig. 2).

Structural and hydrological conditions

The structural conditions and associated hydrological features of Zadloško polje are evident from the attached cross-section (Fig. 4). In addition to the geological data directly from the line of the cross-section, the geological structure of the wider area of the Črni Vrh plateau has also been taken into account. The profile is a geologically typical cross-section of the Idrija overthrust structure.

The cross-section starts at the Strug tectonic window in the Idrijca valley, where the Idrijca riverbed already cuts into Upper Cretaceous limestone and the overlying Palaeocene-Eocene flysch rocks of the Hrušica nappe. The cross-section then crosses the thrust contact between flysch rocks and Cretaceous limestones of the Koševnik nappe slice. The thrust contact dips approx. 25° to the south and southwest. The Cretaceous limestone underneath Zadloško polje is, based on geological mapping at the Strug tectonic window in Idrijski Log and Predgriže, presumed to be slightly folded into synclinals and anticlinals (Fig. 4). It is overthrust by Norian-Rhaetian dolomite of the Čekovnik nappe slice (Mlakar, 1969; Zagoda, 2004; Mlakar & Čar, 2009; Čar, 2010) (Figs. 1 and 4) with the thrust plane dipping 10 to 15° to the southwest or south. The dolomite constitutes the higher northern edge of Zadlog and the northern part of the Zadloško polje plain, and then the section intersects the thrust line between the Čekovnik nappe slice and the Norian-Rhaetian dolomite of the Trnovo nappe underthrust block. The thrust contact between the two dolomites dips approx. 7° to 10° in general southwards. Southward of here, the geological cross-section continues in the slope of Špičasti vrh (1127 m) (Fig. 2).

The cross-section shows that three strong hydrological retention-deflection structures follow each other vertically below Zadloško polje (Čar, 2018), i.e. flysch rocks, a lithological hydrological retention-deflection zone (marked **a** in the profile), and two thrust–shear hydrological retention-deflection zones with several-metre-thick impermeable cataclastic dolomite rocks (marked **b** & **c** in the profile) (Fig. 4).

potrjuje tudi najdba kosov kataklastičnih kamnin na njivi zahodno od Črnovrškega preloma. Narivnica se ponovno pokaže kak kilometer južneje v peskokopu pri zaselku Trebče pri Črnem Vrhu, na zahodni strani Črnovrškega preloma, torej v istem strukturnem bloku kot na Zadloškem polju. V nadaljevanju proti Črnemu Vrhu poteka narivna cona vzporedno s prelomno cono Črnovrškega preloma. V peskokopu v Trebčah vpada narivnica za 20° proti jugozahodu (sl. 3B) in ima enak vpad vse do Črnega Vrha (sl. 2).

Strukturno-hidrološke razmere

Strukturne razmere in nanje vezane hidrološke značilnosti Zadloškega polja so vidne iz priloženega prereza (sl. 4). Poleg geoloških podatkov neposredno v liniji prereza je pri izrisu upoštevana tudi geološka zgradba širšega območja Črnovrške planote. Profil je v geološkem pogledu značilen presek idrijske narivne zgradbe.

Presek poteka iz Tektonskega okna Strug v dolini Idrijce, kjer je korito reke Idrijce že vrezano v zgornjekrednem apnencu in na njem ležečih paleocensko-eocenskih flišnih kamninah Hrušiškega pokrova. Prerez nato prečka narivni kontakt med flišnimi kamninami in krednimi apnenci Koševniške krovne luske. Narivni stik vpada za okrog 25° proti jugu in jugozahodu. Iz razmer, s kartiranjem ugotovljenih v Tektonskem oknu Strug v Idrijskem Logu in Predgrižah sklepamo, da so kredni apnenci pod Zadloškim poljem rahlo sinklinalno in nato antiklinalno upognjeni (sl. 4). Nanj je narinjen norijsko-retijski dolomit Čekovniške krovne luske (Mlakar, 1969; Zagoda, 2004; Mlakar & Čar, 2009; Čar, 2010) (sl. 1 in 4) z vpadom narivne ploskve od 10 do 15° proti jugozahodu ali jugu. Dolomit gradi višje severno obrobje Zadloga in severni del izravnave Zadloškega polja. V nadaljevanju prerez seka narivnico med Čekovniško krovno lusko in norijsko-retijskim dolomitom spodnjega narivnega bloka Trnovskega pokrova. Narivni kontakt med dolomitoma vpada okrog 7 do 10° v splošnem proti jugu. Južno od tod se geološki prerez nadaljuje v pobočju Špičastega vrha (1127 m) (sl. 2).

Iz preseka vidimo, da si pod Zadloškim poljem v vertikali sledijo tri močne hidrološke zadrževalno-zaporne strukture (Čar, 2018) in sicer flišne kamnine kot litološka hidrološka zadrževalno-zaporna cona (na profilu oznaka **a**) ter dve obnarivno hidrološki zadrževalno-zaporni coni z več-metrskimi neprepustnimi kataklastičnimi dolomitnimi kamninami (na profilu oznaki **b** in **c**) (sl. 4). Flišne kamnine so ob narivnem stiku večkrat iztisnjene tako, da sta na več območjih

Several flysch rocks are pushed out along the thrust contact in such a way that Upper Cretaceous limestone of the Hrušica nappe and Cretaceous limestone of the Koševnik nappe slice are in direct contact with each other. In such cases, water flows almost unimpeded from one thrust unit to the other. Such conditions can be observed in several places in the Strug tectonic window and are most likely also present beneath the Črni Vrh plateau. A smoothed out thrust plane in the limestone in several places and an up to 20 m thick thrust–shear zone of completely crushed dolomite can be observed at the thrust contact between the limestone of the Koševnik nappe slice and the Norian-Rhaetian dolomite of the Čekovnik nappe slice in Strug and Bevk tectonic windows (Fig. 4, mark **b**, Fig. 3B). The thrust–shear cataclastic rocks at the thrust contact of the two dolomites between the Čekovnik nappe slice and Trnovo nappe (Fig. 4, mark **c**) are from some metres up to 15 m thick, in some areas even thicker. Thrust–shear crushed zones may vary in thickness, but do not pinch out in the lateral direction.

There is no direct data available on how deep underneath Zadloško polje the thrust contacts between flysch and limestone, as well as between the dolomite of the Čekovnik nappe slice and the lower thrust block of Trnovo nappe, are located. The dip of the thrust plane between flysch and Upper Cretaceous limestone of Čekovnik nappe slice, and its location underneath Zadloško polje may be inferred from the conditions observed in the Strug tectonic window and from the findings of mapped flysch outcrops in Dolenje Lome east of Črni Vrh (Mlakar & Čar, 2009; Čar, 2010). In the tectonic window, the thrust plane dips 15 to 25° roughly to the south, and then the contact gradually rises and surfaces in expansive outcrops in Dolenje Lome.

The course and nature of the thrust line between Cretaceous limestones of the Koševnik nappe slice and Norian-Rhaetian dolomite of the Čekovnik nappe slice were observed on the plain of Idrijski Log and 1.5 to 2 km east of Zadlog between Idrijski Log and Predgriže (Zagoda, 2004; Čar & Zagoda, 2005) (Fig. 2). The thrust line runs NW–SE and only drops by about 20 m over a distance of 3.5 km. The structural conditions beneath Zadloško polje are presumed to be similar. Taking into account the structural-geological data from the wider surroundings, the thrust contact between limestone and dolomite is only about 100–150 m below the surface of the polje. Based on the conditions in the vicinity of Črni Vrh and Predgriže, the thrust line gently descends towards the Na Sredi site (sinking zones A, B & C) (Fig. 2), and lifts up at reverse faults.

neposredno v stiku zgornjekredni apnenec Hrušiškega pokrova in kredni apnenec Koševniške krovne luske. Voda se v takih primerih skoraj nemoteno pretaka iz ene narivne enote v drugo. Take razmere lahko opazujemo na več mestih v Tektonskem oknu Strug in jih najverjetneje imamo tudi pod Črnovrško planoto. Na narivnem stiku med apnencem Koševniške krovne luske in norijsko-retijskim dolomitom Čekovniške krovne luske (sl. 4, oznaka **b**) opazujemo v tektonskih oknih Strug in Bevk zglajeno narivno ploskev v apnencu in do 20 m debelo obnarivno cono povsem zdrobljenega dolomita. Obnarivne kataklastične kamnine na narivnem stiku dveh dolomitov med Čekovniško krovno lusko in Trnovskim pokrovom (sl. 4, oznaka **c**, sl. 3B) so debele od nekaj metrov do 15 m, ponekod lahko tudi več. Po debelini se obnarivno zdrobljene cone lahko spreminjajo, v horizontalni smeri pa se ne izklinjajo.

Neposrednih podatkov, kako globoko pod Zadloškim poljem se nahajajo narivni stiki med flišem in apnencem, dolomitom Čekovniške krovne luske in spodnjega narivnega bloka Trnovskega pokrova ter apnencem Koševniške in dolomitom Čekovniške krovne luske, nimamo. Na vpad narivne ploskve med flišem in zgornjekrednim apnencem Koševniške krovne luske in njeno lego pod Zadloškim poljem lahko sklepamo na podlagi opazovanih razmer v Tektonskem oknu Strug in ugotovitvah kartiranih izdankov fliša v Dolenjih Lomeh vzhodno od Črnega Vrha (Mlakar & Čar, 2009; Čar, 2010). V tektonskem oknu vpada narivna ploskev od 15 do 25° približno proti jugu, nato se stik postopno dviga in izdanja v obsežnih golicah v Dolenjih Lomeh.

Potek in značaj narivnice med krednimi apnenci Koševniške krovne luske in norijsko-retijskim dolomitom Čekovniške krovne luske opazujemo na izravnavi Idrijskega Loga ter od 1,5 do 2 km vzhodno od Zadloga med Idrijskim Logom in Predgrižami (Zagoda, 2004; Čar & Zagoda, 2005) (sl. 2). Narivnica poteka v smeri SZ-JV in se na dolžini 3,5 km spusti le za okrog 20 m. Predpostavljamo, da imamo podobne strukturne razmere tudi pod Zadloškim poljem. Ob upoštevanju geološko-strukturnih podatkov iz širše okolice se nahaja narivni stik med apnenci in dolomitom le kakih 100 do 150 m pod površjem polja. Sodeč po razmerah v okolici Črnega Vrha in Predgriž se narivnica proti lokaciji Na Sredi rahlo spušča (ponikalna območja A, B, in C) (sl. 2), ob reverznih prelomih pa je dvignjena.

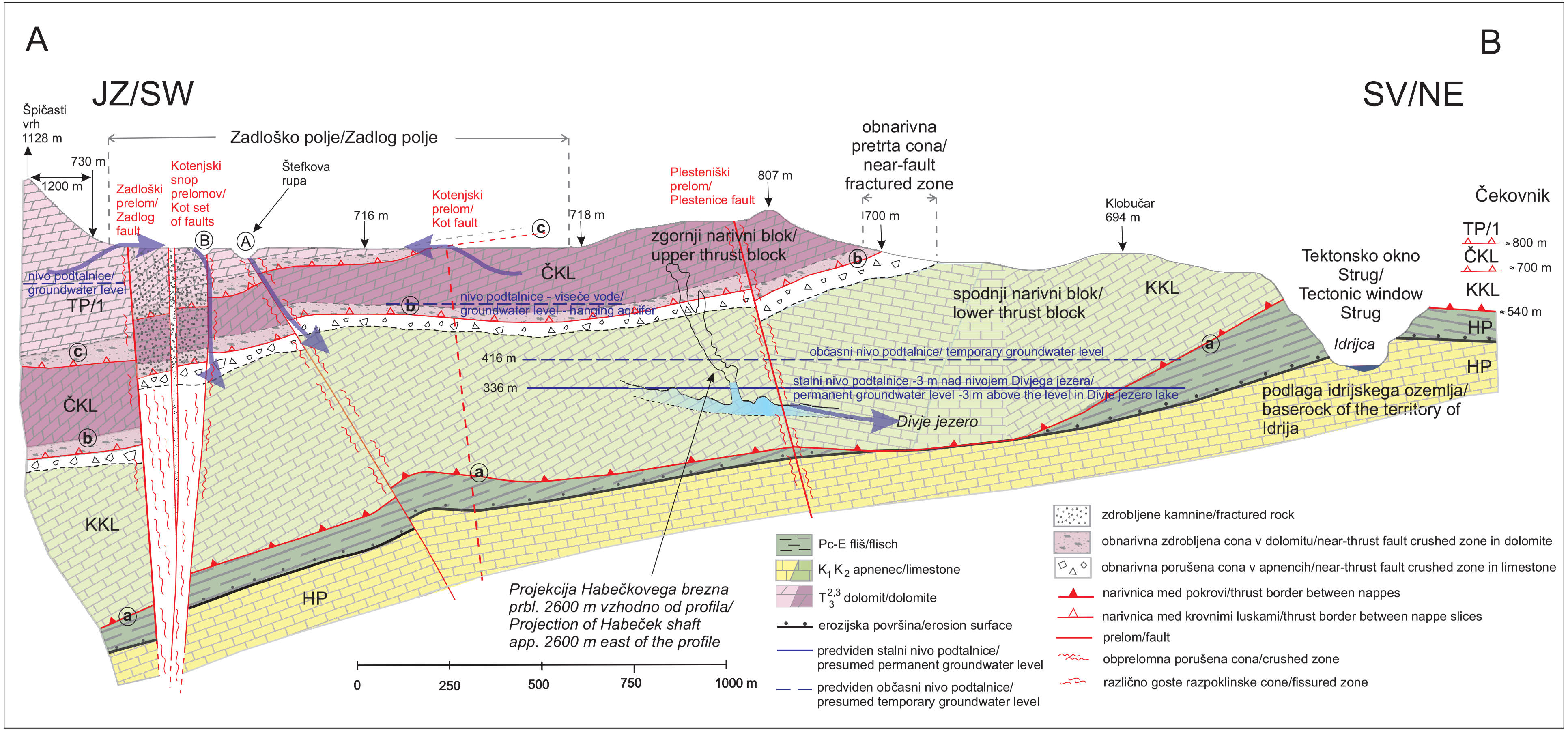

Fig. 4. Hydrogeological cross-section of Zadloško polje. HP – Hrušica nappe, TP/1 – Lower thrust block of Trnovo nappe, ČKL – Čekovnik nappe slice, KKL – Koševnik nappe slice. Ponor zones: A – Štefkova rupa, B – Ponikva. Hydrological retention-deflection structures: a - lithological hydrological retention-deflection zone in flysch, b, c - thrust–shear hydrological retention-deflection zones.

Sl. 4. Strukturno-geološki presek Zadloškega polja s hidrogeološkimi značilnostmi. HP – Hrušiški pokrov, TP/1 – Spodnji narivni blok Trnovskega pokrova, ČKL – Čekovniška krovna luska, KKL – Koševniška krovna luska. Ponikalna območja: A – Štefkova rupa, B – Ponikva. Hidrološke zadrževalno-zaporne strukture: a - litološka hidrološka zadrževalno-zaporna cona v flišu, b, c - obnarivni hidrološki zadrževalno-zaporni coni.

More information is available on the thrust contact between the Norian-Rhaetian dolomites of the Čekovnik nappe slice and the lower part of the Trnovo nappe (TP/1). The thrust zone is visible in the slope above the Belca valley, in the sand quarry at Podtisov vrh and in the Trebče sand quarry (Fig. 3 B), and further towards Črni Vrh. From north to south the thrust line descends at a slight angle of 5 to 7° southward, then almost levels off or even rises slightly. The Norian-Rhaetian dolomite of the Trnovo nappe north of Štefkova rupa is estimated to be only 20 to 30 m thick, depending on the dip of the thrust plane. Its thickness increases on the southwest side of the Zadlog fault.

Hydrological and geomorphological conditions

Weak and temporary springs with a small hydrological catchment area can be found on the southern slopes of Idrijski Log (Fig. 2) while Zadloško polje has no permanent running water.

Morphological analysis of the surface of Zadloško polje showed that its bottom is relatively well levelled out, and lies between 714 and 716 m above sea level. The entire bottom is covered by dolomite eluvium. The perimeter of the basin is covered by colluvium, indicating that the recent maximal flood range is smaller than in the past. The influence of sediment transport from the dolomitic catchment area is most clearly visible in the form of the colluvial fan at Plestenice on the southeastern edge of the basin (Fig. 8). A network of wide and shallow channels formed in the otherwise flat bottom of Zadloško polje. Up to several metres deep erosion ditches formed in fractured zones along the faults (Zadlog, Kot, Plestenice, Klančar faults), while more shallow ones evenly drain the relatively flat bottom. The whole western part that formed in the wider Zadlog fault zone from Podtisov Vrh to the southern edge of the polje, the entire western part (to Plestenice fault towards the east) and the southern and southeastern part of the polje drain towards the ponor zones on the location Na Sredi, which confirms the absence of similar drainage structures in the western and eastern parts of the polje. The NW–SE oriented strike-slip faults and the N–S oriented reverse faults in the central part of the polje that cross the outer fault (crushed and fractured) zone of the Zadlog fault appear to be the key structures allowing water to drain from the major part of the polje to the underground.

During heavy rainfall, the lower parts of the northern structural block of Zadlog quickly become partially flooded from the northern edge of the polje to the thrust line between the Čekovnik nappe slice and the lower thrust block of Trnovsko

O narivnem stiku med norijsko-retijskima dolomitoma Čekovniške krovne luske in spodnjim delom Trnovskega pokrova (TP/1) imamo več podatkov. Narivna cona je vidna v pobočju nad dolino Belce, peskokopu v Podtisovem Vrhu in peskokopu Trebče (sl. 3B) ter dalje proti Črnemu Vrhu. Od severa proti jugu se narivnica spušča pod blagim kotom od 5 do 7° proti jugu, nato skoraj izravna ali celo rahlo dviga. Debelina norijsko-retijskega dolomita Trnovskega pokrova je severno od Štefkove rupe, glede na vpad narivne ploskve, po oceni le 20 do 30 m. Na jugozahodni strani Zadloškega preloma se poveča.

Hidrološke in geomorfološke razmere

Na južnih pobočjih Idrijskega Loga se ob prelomnih conah pojavljajo večinoma občasni in šibki izviri z majhnim hidrološkim zaledjem (sl. 2). Zadloško polje pa nima stalne tekoče vode.

Morfološka analiza površja Zadloškega polja pokaže, da je njegovo dno relativno dobro uravnano, in sicer na višini med 714 in 716 m nad morjem. Dno je med številnimi izdanki dolomita prekrito z dolomitno preperino, ki je nastajala v času ojezeritve. Obod kotline je prekrit s koluvijem, kar kaže na recentno manjši obseg poplav kot v preteklosti. Najbolj jasno se vpliv premeščanja sedimentov z dolomitnih pobočij kaže v obliki vršaja v Plestenicah na jugovzhodnem robu kotline (sl. 8). V sicer ravnem dnu Zadloškega polja se je oblikovala mreža širokih in plitvih kanalov. Do nekaj metrov globoki jarki so nastali v pretrtih conah vzdolž prelomov (Zadloški, Kotenjski, Plesteniški, Klančarjev prelom), plitvejši enakomerno drenirajo relativno ravno površino dna. Zahodni del polja, ki je oblikovan v širši coni Zadloškega preloma od Podtisovega Vrha do južnega obrobja polja, ves osrednji del polja (do Plesteniškega preloma proti vzhodu) ter južni in jugovzhodni del polja drenirajo proti ponikvam na lokaciji Na Sredi, kar potrjuje odsotnost podobnih odvodnih struktur v zahodnem in vzhodnem delu polja. Kaže, da so zmični prelomi z orientacijo SZ-JV in reverzni prelomi v smeri S-J osrednjega dela polja, ki sekajo zunanjo prelomno cono (porušena in razpoklinska cona) Zadloškega preloma ključne strukture, ki omogočajo podzemno odtekanje vode z velikega dela polja.

Ob večjem deževju so nižji deli od severnega roba polja do narivnice med Čekovniško krovno lusko in spodnjim narivnim blokom Trnovskega pokrova razmeroma hitro delno poplavljeni. Glede na geološke podatke (sl. 2 in 4) imamo v tem delu Zadloškega polja nad hidrološko pregrado nappe. According to the geological data (Figs. 2 and 4), there is permanently hanging aquifer in this part of Zadloško polje above the hydrological barrier **b**. Based on the observations, its level rapidly rises to the surface of the polje and floods the lower parts and hollows on the polje (Fig. 1B). The conditions described also show that the dolomite of the Čekovnik nappe slice over the limestone of the Koševnik nappe slice is relatively thin, while the thrust–shear hydrological barrier **b** is largely impermeable and leaks only at the faults intersecting it.

The hydrological conditions south of the thrust zone between the Čekovnik nappe slice and the Trnovo nappe (TP/1), are similar to the conditions to the north of it. We presume that the groundwater here also needs to stay quite high above the hydrological retention-deflection thrust zone **c** at all times, as it starts to relatively rapidly overflow to the surface when it rains. Large amounts of groundwater flow onto Zadloško polje from the south during heavy rainfall (mostly along the layers) due to the extensive and rugged catchment area of Mrzli log with its highest peak Špičasti vrh (1127 m).

Several morphologically distinct, intermittent sinking zones are observed in Zadlog, which are shown in capital letters A to F on the Fig. 2. The largest one – *Štefkova rupa* (mark A, Fig. 6A, B) – is up to 13 m deep, at the Na Sredi site in the central part of Zadlog. From the large sinkhole Štefkova rupa (mark A), a narrow, some 200 m long valley or rather an erosion ditch in the fault zone runs southsoutheastward along the strike-slip fault. A relatively strong temporary spring flows to the surface at its southern part. The water flows northnortheastward down the erosion ditch to the central sinking area Štefkova rupa. At low inflows, the water gradually sinks already in the strike-slip fault zone and does not flow to the central large sinkhole. An extensive larger sinkhole formed at the junction of one of the reverse faults of Kot with the connecting strike-slip fault, which intersect the area between the Zadlog and Plestenice faults. Štefkova rupa does not have an open swallow hole (Fig. 6A, B), but has slightly deepened, bare surface in its NE part where substantial volumes of water sink through. The geological conditions suggest that, due to the uplift along the reverse fault, there are karstified and therefore highly permeable Upper Cretaceous limestones of the Koševnik nappe slice close to the surface. At high groundwater level, the water outflows even sideway from the sinkhole in the crushed zone of Zadlog fault and Kot set of faults.

b stalno ujeto ali visečo podtalnico. Na podlagi opazovanj se njen nivo hitro dvigne in zalije nižje dele in kotanje na polju (sl. 1 B). Opisane razmere tudi kažejo, da je dolomit Čekovniške krovne luske nad apnencem Koševniške krovne luske sorazmerno tanek, obnarivna hidrološka pregrada **b** pa je v večini neprepustna in pušča le ob prelomih, ki jo sekajo.

Južno od poteka narivne cone med Čekovniško krovno lusko in Trnovskim pokrovom (TP/1) imamo podobne hidrogeološke razmere kot severno od nje. Domnevamo, da je podtalnica nad hidrološko zadrževalno zaporno narivno cono **c** stalno dokaj visoko, saj ob deževju začne razmeroma hitro iztekati na površje. Zaradi obsežnega in razgibanega zaledja Mrzlega loga z najvišjim Špičastim vrhom (1127 m) se ob izdatnejšem deževju z južne strani v glavnem medplastno stekajo na Zadloško polje velike količine podtalnice.

V Zadlogu opazujemo več morfološko izstopajočih, občasnih ponikalnih območij, ki so na sliki 2 označeni z velikimi črkami od A do F. Največje je do 13 m globoka *Štefkova rupa* (oznaka A, sl. 6A in B) na lokaciji Na Sredi v osrednjem delu Zadloškega polja. Iz ponikalne globeli Štefkove rupa (oznaka A) poteka ob zmičnem prelomu proti JJV okrog 200 m dolga ozka dolina, ali bolje, razširjen erozijski žleb v prelomni coni. Na njegovem južnem delu je relativno močan občasni izvir. Voda odteka po jarku proti SSZ k osrednjemu ponikalnemu območju Štefkove rupe. Ob nizkih pretokih voda postopno ponikne že v coni zmičnega preloma in ne priteče do osrednje ponikalne globeli. Obsežna ponikalna globel je nastala na stičišču enega izmed Kotenjskih reverznih prelomov z veznim zmičnim prelomom, ki seka območje med Zadloškim in Plesteniškim prelomom. V Štefkovi rupi ni odprtega požiralnika (sl. 6A in B), vendar je v njenem SV delu nekoliko poglobljeno golo območje, skozi katerega poniknejo izredno velike količine vode. Glede na geološke razmere sklepamo, da se zaradi dviga ob reverznem prelomu zakraseli in zato dobro prepustni zgornjekredni apnenci Koševniške krovne luske nahajajo blizu površja. Ob višjih vodah se voda izteka iz globeli tudi bočno v pretrti coni Zadloškega preloma in Kotovega prelomnega snopa.

V podobnih geoloških razmerah sta nastali tudi ponikalni območji *Ponikva* (oznaka B in sl. 5B) in *ponikalno območje pri kmetiji Cigale* (oznaka C) severozahodno od Štefkove rupe v osrednjem delu polja. Ponikalno območje Ponikva je proti vzhodu povezano z erozijskim

The *Ponikva* sinking area (mark B and Fig. 5B) and the *sinking area at the Cigale farm* (mark C) northwest of Štefkova rupa in the central part of the polje formed under similar geological conditions. The Ponikva sinking area is connected to the erosion ditch of Štefkova rupa to the east and on the other side to the inflow area below Tomažon (Fig. 5B), and at high waters it connects to the springing/sinking puddle *Gregorcova lokev*. This is an approx. 400 m long water channel which runs in the NW–SE direction and formed in the Zadlog fault zone. It ends in a large sinkhole where water also flows into from the southeast from the Podgora farm. The extensive sinkhole (mark C) below the Cigale farm extends northward along the reverse fault and drains waters from the wide area under Podtisov Vrh north from the road Na Sredi – Figar and from the northern portion of the central part of the polje. Next is an approx. 15 m deep intermittent swallow hole (mark D) called *Štirnska rupa*. It lies between the two roads leading from the central part of Zadlog towards Šoštar at the crossing towards Črni Vrh (Fig. 2). It formed in the Plestenice fault zone and extends along the Plestenice fault in the NW–SE direction of the fault. Štirnska rupa is approximately 200 m long and has a morphologically distinct swallow hole in its central part. Eastward lies an up to 6 m deep less pronounced sinking zone in the Klančar fault zone (mark E) with numerous sinkholes that are interconnected with shallow lowered passes. The extensive and morphologically less visibly lowered sinking area in the wide broken zone of the Figar fault on the far western edge of Zadloško polje is also worth mentioning (mark F).

During heavy rainfall or rise of the groundwater level, Štefkova rupa fills up and water spills out into its wider surroundings. Gregorcova lokev fills up and water starts to flow along the distinctive and wide erosion ditch towards Ponikva, marked B. Strong temporary springs and water from several scattered interbedded inflows from the wider area below Tomažon join together before the sinking area. Water flows from the northwestern part of Zadloško polje into the wider fault zone of Zadlog and drains at Rovtar into the extensive sinkhole below Cigale. Excess water flows on the southern side of the sinkhole further towards Štefkova rupa. The sinking areas D and E also fill up (Fig. 2). As the groundwater rises in the central and southern parts of the Zadloško polje, even weaker inflows spring up along the permeable fault zones and along the stratification. In the poorly permeable lower parts of dolomite in the Čekovnik nappe slice and the Trnovo nappe water starts to stagnate and the impoundments on Zadloško polje grow and merge. The entire Zadloško

jarkom Štefkovih rup, na drugi strani pa z dotočnim območjem pod Tomažonom (sl. 5B) in ob višjih vodah z izvirno-ponikalno Gregorcovo lokvijo. To je okrog 400 m dolg jarek, ki poteka v smeri SZ-JV in je nastal v coni Zadloškega preloma. Zaključuje se z večjo globeljo, v katero priteka voda tudi od jugovzhoda od kmetije Podgora. V obsežno ponikalno globel pod kmetijo pri Cigaletu (oznaka C), ki je razpotegnjena proti severu ob reverznem prelomu, se stekajo vode z obsežnega območja izpod Podtisovega Vrha severno od ceste Na Sredi – Figar in s severa osrednjega dela polja. Naslednji je okrog 15 m globok občasni požiralnik imenovan *Štirnska rupa* (oznaka D). Leži med obema cestama, ki vodita iz osrednjega dela Zadloga proti Šoštarju na prehodu proti Črnemu vrhu (sl. 2). Nastal je v prelomni coni Plesteniškega preloma in je ob njem podaljšan v prelomni smeri SZ-JV. Štirnska rupa je dolga okrog 200 m z morfološko izrazitim požiralnikom v osrednjem delu. Vzhodno od tod leži v prelomni coni Klančarjevega preloma manj izrazito, do 6 m globoko ponikalno območje (oznaka E) s številnimi globelmi, ki so povezane s plitvimi znižanimi prehodi. Omenimo še obsežno in morfološko manj izrazito znižano ponikalno območje v široki porušeni coni Figarjevega preloma na skrajnem zahodnem obrobju Zadloga (oznaka F).

Ob močnejših nalivih in dvigu podtalnice se Štefkova rupa napolni in voda se razlije v širšo okolico. Napolni se Gregorcova lokev in voda začne po izrazitem in širokem jarku odtekati proti Ponikvi z oznako B. Pred ponikalnim območjem se iz širšega območja pod Tomažonom priključijo močnejši občasni izviri in voda iz številnih razpršenih medplastnih dotokov. Iz severozahodnega dela Zadloškega polja se voda pretaka po širši coni Zadloškega preloma in se pri Rovtarju izteka v ponikalno globel pod Cigaletom. Višek vode odteka na južni strani ponikalne globeli naprej proti Štefkovi rupi. Napolnita se tudi ponikalni območji D in E (sl. 2). Z dviganjem podtalnice se v osrednjem in južnem delu Zadloškega polja aktivirajo še šibkejši dotoki ob prepustnih prelomnih conah in tudi vzdolž plastnatosti. V slabo prepustnih znižanjih na dolomitu Čekovniške krovne luske in Trnovskega pokrova začne voda zastajati, zajezitve na Zadloškem polju se večajo in združujejo. Postopno lahko poplavi celotno Zadloško polje tako, da nastane začasna ojezeritev (sl. 5A) ali, kot pravijo domačini, nastane 'zadloško morje' (Bajec, 2007). Ob izjemnih hidroloških razmerah začne voda odtekati čez nizek prehod polje can gradually become flooded, forming a temporary impoundment (Fig. 5A) or the ‘sea of Zadlog’, as the locals call it (Bajec, 2007). Under exceptional hydrologic conditions, the water starts to flow over a low pass at Šoštar in the eastern part of Zadlog in the Črni Vrh fault zone towards Trebče at Črni Vrh. A particularly high lake impoundment formed in 1923, when the water flowed for three hours over the pass at Šoštar towards Trebče (Bajec, 2007).

pri Šoštarju na vzhodnem delu Zadloškega polja v coni Črnovrškega preloma proti Trebčam pri Črnem Vrhu. Posebno visoka ojezeritev je bila leta 1923, ko je voda kar tri ure tekla čez prelaz pri Šoštarju proti Trebčam (Bajec, 2007).

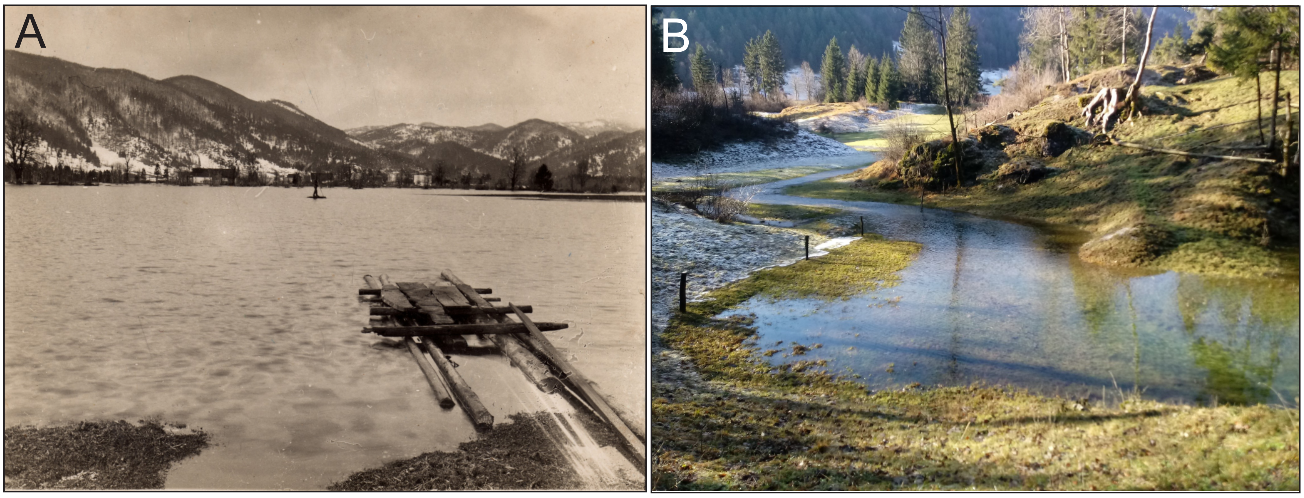

Fig. 5. A – Zadloško polje during temporary lake-formation (‚Zadlog sea‘), view to the west (Figar). Photo: Francka Zagoda B – Inflow into the sinking zone B (Fig. 2). Photo: Jože Čar.

Sl. 5. A – Zadloško polje v času začasne ojezeritve (‚zadloško morje‘), pogled proti zahodu (Figar). Foto: Francka Zagoda B – Dotok v ponikalno območje B (sl. 2). Foto: Jože Čar.

All sinking areas are formed in the dolomite of the Trnovo nappe, where the impermeable thrust–shear deflector zone (thrust–shear and hydrological collector & deflecting structure **c**) between the Čekovnik nappe slice and the Trnovo nappe is intersected by faults. The favourable conditions are apparently the result of relatively weak reverse faults pulling fractured and highly soluble Lower Cretaceous limestones of the Koševnik nappe slice closer to the surface. These are the positions of the sinking zones A, B & C. The prerequisite for the formation of swallets at the Plestenice and Klančar faults are wide fault zones with sufficiently extensive broken and fissure zones.

Water flows from Zadloško polje underground towards the Divje jezero lake and Podroteja in the Idrijca valley through Cretaceous limestones in which extensive cave systems have already formed, as confirmed by cave diving surveys (Vrhovec, 1997).

The permanent groundwater level below Zadloško polje is now 336 m (Habe et al., 1955; Vrhovec, 1997), which is only 3 m above the standing water level at Divje jezero. In flood conditions, the groundwater level in the catchment area of Divje jezero rises by 80 m, which was proven by the traces of stagnating water at the mentioned level in

Vsa ponikalna območja so oblikovana v dolomitu Trnovskega pokrova in sicer na mestih, kjer neprepustno obnarivno zaporno cono (obnarivno-hidrološka zadrževalno-zaporna struktura **c**) med Čekovniško krovno lusko in Trnovskim pokrovom sekajo prelomi. Očitno so ugodni pogoji nastali ob sicer sorazmerno šibkih reverznih prelomih, ki so potegnili pretrte in dobro topne spodnje kredne apnence Koševniške krovne luske bliže površini. Tako lego imajo ponikalna območja A, B, in C. Pogoj za nastanek ponikev ob Plesteniškem in Klančarjevem prelomu sta široki prelomni coni z dovolj obsežnima porušenima in razpoklinskima conama.

Iz Zadloškega polja voda odteka podzemno proti Divjemu jezeru in Podroteji v dolini Idrijce po krednih apnencih, v katerih so že oblikovani obsežni jamski rovi, kar so potrdile potapljaške raziskave (Vrhovec, 1997).

Stalna gladina podzemne vode pod Zadloškim poljem se danes nahaja na koti 336 m (Habe et al., 1955; Vrhovec, 1997), kar je le 3 m nad nivojem stoječe vode v Divjem jezeru. V poplavnih razmerah se podtalnica v zaledju Divjega jezera dvigne za 80 m, kar je bilo dokazano z znaki stagnacije vode na omenjeni višini

Fig. 6. A – The main larger sinkhole of Štefkova rupa. B – The inflow channel to Štefkova rupa formed along the connecting faults in the northeastern outer fault zone of Zadlog. Photo: Jože Čar.

Sl. 6. A – Glavna ponikalna globel Štefkove rupe. B – Dotočni kanal v Štefkovo rupo, nastal ob veznih prelomih v severovzhodni zunanji coni Zadloškega preloma. Foto: Jože Čar.

the Habečkovo brezno shaft (personal communication). Nowadays, the hanging groundwater in ČKL occasionally floods Zadloško polje to the north of the thrust line while the groundwater within the Trnovo nappe (TP/1) floods the polje to the south of the thrust line only during heavy rainfall. Numerous dolomite outcrops that emerge from the sediment-covered bedrock have an average dip of 230/20–30°, which is consistent with the stratification of the underlying dolomites in the wider surrounding. The equilibration of slopes at the thrust front and the emergence of parent rock outcrops in the sinking areas are indicative of the recent decreased capability of hydrologic retention of karst polje and intensive washing out of eluvium. The present hydrological conditions are therefore largely the result of leaching fault zones and clayey eluvium from the polje floor, and the resulting increased drainage capacities. Instead of the accumulation and displacement of material, which took place during the formation of Zadloško polje sediment plain, we now observe a gradual leaching into the subsurface as a result of the new hydrogeological conditions, as well as of the increased karsification and associated flow capacity of the karst subsurface.

Conditions for the formation of Zadloško polje

The detailed structural-geological mapping of Zadloško polje and the analysis of its morphological and hydrological conditions have provided some new insights and interesting benchmarks for further reflection on the origins of karst poljes in the Dinaric Karst. The authors define the karst polje as a large-scale depression of tectonic origin, formed by the selective karstification of regional tectonic structures at the groundwater level, where the

v Habečkovem breznu (ustni vir). Danes viseča podtalnica v ČKL občasno poplavlja Zadloško polje severno od narivnice, južno pa podtalnica v okviru Trnovskega pokrova (TP/1) tako, da poplavi polje le ob močnejšem deževju. Številni dolomitni izdanki, ki izdanjajo iz s sedimenti pokritega dna, imajo vpad plasti povprečno 230/20-30°, kar je skladno s plastovitostjo dolomitov v širši okolici. Pojav uravnovešanja pobočij polja in pojav izdankov matične kamnine na ponikalnih območjih nakazujeta na recentno zmanjšano vodno zadrževalno sposobnost izravnave in intenzivno izpiranje preperine. Današnje hidrološke razmere so torej predvsem posledica izpiranja prelomnih con in glinene preperine iz dna polja in zaradi tega povečanih odtočnih kapacitet. Namesto kopičenja in premeščanja materiala, ki sta potekala v času nastajanja sedimentne uravnave Zadloškega polja, zdaj opazujemo postopno izpiranje v podzemlje, ki je posledica novih hidrogeoloških razmer, pa tudi povečane zakraselosti in s tem povezane pretočnosti kraškega podzemlja.

Razmere za nastanek Zadloškega polja

Podrobno strukturno-geološko kartiranje Zadloškega polja in analiza njegovih morfoloških in hidroloških razmer so podali nekaj novih vpogledov in zanimivih izhodišč za nadaljnje razmišljanje o nastanku kraških polj Dinarskega krasa. Avtorja opredeljujeva kraško polje kot depresijo večjih dimenzij tektonskega nastanka, nastalo s selektivnim zakrasevanjem regionalnih tektonskih struktur na gladini podtalnice, pri čemer se stopnja njene nadaljnje ojezeritve prilagaja danim razmeram v degree of its further capacity for surface water retention is adapted to the given conditions in the dynamic karst hydrological system (Šegina, 2021, 92), which also provides the basis for the formation of Zadloško polje and its evolution presented below.

In accordance with the structural-geological conditions presented in the previous chapters, two types of thrusting were observed in the wider area of Zadloško polje, i.e. thrusts between different lithological units (thrusts of dolomite of the Čekovnik nappe slice onto the limestone of the Koševnik nappe slice) and thrusts within the same lithological unit (thrusts of dolomite of the Trnovo nappe (TP/1) onto the dolomite of the Čekovnik nappe) (Fig. 2). All three thrust packages present a specific, intrinsically characteristicsurface morphology. The Koševnik nappe slice isdensely interspersed with small dolines with an average diameter of 30 m, the surface of the Čekovnik nappe slice is mostly the reflection of denuded and with occasional surface runoff deepened tectonic structures, while the surface of the Trnovo nappe is more strongly dissected, interspersed with few large dolines with an average diameter of 60 m and intermediate conical peaks (Fig. 8).

In the case of both the thrust within the dolomite (TP/1–ČKL) and dolomite thrust over limestone (ČKL–KKL) somewhat similar relief phenomena were observed. Both shall be considered for a better understanding of the impact of thrust structures on the formation of the karst polje, albeit the interest of this research predominantly lies in the thrust within the dolomite in the area of Zadlog.

At the thrust of the lower thrust block of the Trnovo nappe dolomite package onto the Čekovnik nappe slice, a thrust line formed with the corresponding thrust–shear crushed zone in the dolomite. Underneath the thrust front a thrust plain formed in the less permeable, thrust–shear crushed zone in the dolomite as a morphological basis for karst polje (Fig. 7A). This is where groundwater from the nappe block of the Trnovo nappe (TP/1) flowed and stagnated on the surface due to the poor permeability of the crushed thrust–shear zone in the dolomite. During the lake-formation the bottom of the karst polje was covered by the sediment (Fig. 7B). The karts polje expanded laterally along the fractured crushed zone. The main direction of expansion was towards the thrust front, where the dolomite slopes adapted to slope erosion. The perimeter of the hollow gradually cut into the dolomite of the Trnovo nappe southwest of the thrust zone and the Čekovnik nappe slice northeast of it (Fig. 7C). During the formation of fault structures in the NW-SE direction, underground drainage formed in the Trnovo nappe dolomite and the Čekovnik

dinamičnem kraškem hidrološkem sistemu (Šegina, 2021, 92), na čemer tudi temelji v nadaljevanju predstavljen nastanek in razvoj Zadloškega polja.

Soglasno s predstavljenimi strukturno-geološkimi razmerami v predhodnih poglavjih na širšem območju Zadloškega polja opazujemo dve vrsti narivov, in sicer nariv med različnima litološkima enotama (nariv dolomita Čekovniške krovne luske na apnenec Koševniške krovne luske) in nariv znotraj iste litološke enote (nariv dolomita Trnovskega pokrova (TP/1) na dolomit Čekovniške krovne luske) (sl. 2). Vsi trije narivni paketi kažejo specifično, zase značilno morfologijo površja. Na Koševniški krovni luski so gosto posejane manjše vrtače premera povprečno 30 m, površje Čekovniške krovne luske je predvsem odraz denudiranih in z občasnim površinskim odtokom poglobljenih tektonskih struktur, medtem ko je površje na Trnovskem pokrovu močneje razčlenjeno, posejano z redkimi večjimi vrtačami povprečnega premera 60 m in vmesnimi kopastimi vrhovi (sl. 8).

Pri narivu tako znotraj dolomita (TP/1-ČKL), kakor tudi pri narivu dolomita na apnenec (ČKL-KKL) opazujemo do neke mere podobne reliefne pojave. Za boljše razumevanje vpliva narivnih struktur na oblikovanje kraškega polja bomo obravnavali oba, čeravno je v ospredju te raziskave nariv znotraj dolomita na območju Zadloga.

Ob narivu spodnjega narivnega bloka dolomitnega Trnovskega pokrova na dolomit Čekovniške krovne luske se je oblikovala narivnica s pripadajočo obnarivno zdrobljeno cono v dolomitu. V narivni coni se je v slabo prepustni, obnarivni zdrobljeni coni v dolomitu oblikovala narivna izravnava kot morfološka zasnova za kotanjo (sl. 7A). Tja je zatekala podzemna voda iz krovninskega bloka Trnovskega pokrova (TP/1), kjer je zaradi slabe propustnosti zdrobljene obnarivne cone v dolomitu površinsko zastajala. V času ojezeritve je nastalo skoraj povsem uravnano sedimentno dno (sl. 7B). Kotanja se je bočno širila po pretrti zdrobljeni coni. Glavna smer širjenja je bila proti čelu nariva, kjer so se dolomitna pobočja prilagajala spodjedanju pobočij. Postopno je obod kotanje zarezal v dolomit Trnovskega pokrova jugozahodno od narivne cone in Čekovniške krovne luske severovzhodno od nje (sl. 7C). Ob nastanku prelomnih struktur v smeri SZ-JV se je na mestih prelomov v dolomitu Trnovskega pokrova in Čekovniške krovne luske vzpostavil podzemni odtok, nastali so ponori. Skozi oba paketa nappe slice at the faults, and ponors emerged. Surface water drainage and sediment transport to the underground developed through both rock packages, which are now part of the basin floor. This is why parent rock outcrops through the sediments covering the bottom of the karst polje. Similar conditions to those in Zadlog are present in the wider surroundings of Črni Vrh.

kamnine, ki zdaj gradita dno kotline, se je vzpostavilo odtekanje površinskih voda in odnašanje sedimentov v podzemlje, zaradi česar so skozi sediment, ki prekriva kraško polje, pogledali izdanki matične kamnine. Podobne razmere kot v Zadlogu so tudi v širši okolici Črnega Vrha.

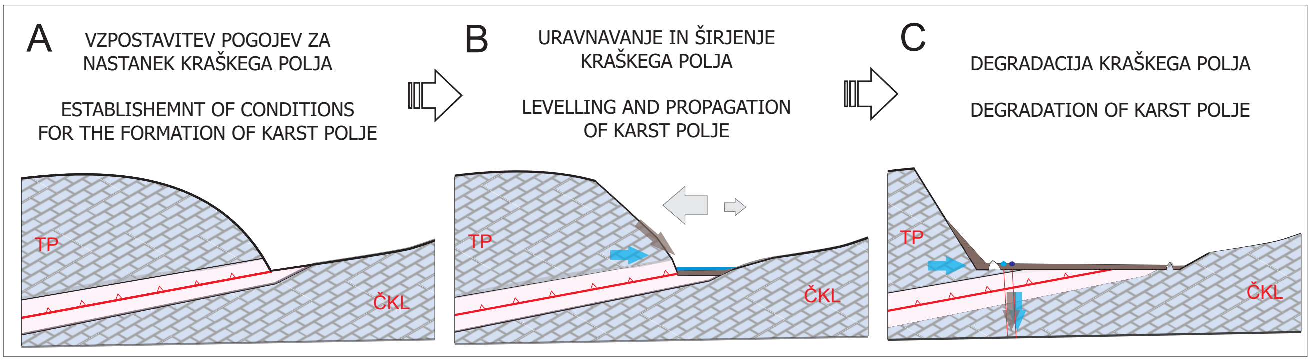

Fig. 7. Formation of a karst polje along a dolomite thrust. A – Thrust tectonics. B – Peneplanation and lake-formation on the poorly permeable fault-induced crushed zones in the dolomite, and lateral expansion of the plain. C – Expansion of the plain into the dolomite, younger fault tectonics and the formation of subsurface drainage of surface water and sediments.

Sl. 7. Razvoj kraškega polja ob narivu v dolomitu. A – Narivna tektonika. B – Uravnavanje in ojezeritev slabo prepustne obprelomne zdrobljene cone v dolomitu in bočno širjenje uravnave. C – Razširitev uravnave v dolomit, mlajša prelomna tektonika in vzpostavitev podzemnega odtoka površinske vode in sedimentov.

The conditions were somewhat different when the dolomite package of the Čekovnik nappe slice was thrust over the limestone of the Koševnik nappe slice. Underneath the thrust front, there was a slopeward displacement of dolomite eluvium from the thrust front and eluvium of the thrust–shear crushed zone, with no water retention on the surface due to limestone contact. Water flowed superficially over poorly permeable eluvium and percolated into well-karstified limestone. Due to erosion of the thrust–shear crushed zone, the slope of the thrust front gradually retreated and the slightly sloped surface covered with sediments spread towards the thrust front. Younger fault tectonics established subsurface drainage and small areas of ponors. The weak springs in the thrust front (rather than in the floor of the plain) suggest that the entire sedimentary plain did not expand beyond the thrust–shear zone, as its potential for lateral expansion is limited only to the levelling of the dolomite slope at the thrust front. Such conditions are present in the area of Idrijski Log and Predgriže. The karst which formed along the thrust belt of dolomite over limestone has its own features. This phenomenon has its specific characteristics which has not yet been explored systematicall so far (Čar, 2001; Čar & Šebela, 2001; Zagoda, 2004; Čar & Zagoda, 2005).

Ob narivu dolomitnega paketa Čekovniške krovne luske na apnenec Koševniške krovne luske so bile razmere nekoliko drugačne. Pod čelom nariva je potekalo pobočno premeščanje dolomitne preperine s čela nariva in preperine obnarivne zdrobljene cone, pri čemer zaradi kontakta z apnencem ni prišlo do površinskega zadrževanja vode. Voda se je po slabo propustni preperini pretakala površinsko in ponikala v dobro zakraselem apnencu. Zaradi erozije obnarivne zdrobljene cone se je pobočje čela nariva postopoma umikalo in blago nagnjeno površje pokrito s sedimenti se je širilo v smeri proti čelu nariva. Mlajša prelomna tektonika je vzpostavila podzemni odtok in nastanek manjših ponornih območij. Šibki izviri v čelu nariva (in ne v dnu uravnave) kažejo na to, da se celotna sedimentna uravnava ni razširila izven obnarivne cone, saj je njen potencial za bočno širjenje povezan zgolj z uravnavanjem dolomitnega pobočja v čelu nariva. Takšne razmere so na območju Idrijskega Loga in Predgriž. Kras, ki je nastal ob narivnem pasu dolomita na apnenec, ima svoje značilnosti, ki pa zaenkrat še niso bile sistematično raziskane (Čar, 2001; Čar & Šebela, 2001; Zagoda, 2004; Čar & Zagoda, 2005).

The Figure (Fig. 8) shows a typical profile of the dolomite-dolomite thrust and dolomite-limestone thrust, illustrating the characteristic and unique features of surface evolution along thrust structures (Fig. 8). Under the given conditions, steep slopes with an inclination of more than 30° formed at the thrust front between dolomite packages (Fig. 8, mark **a**). High inclinations facilitated occasional surface runoff along the fault structures where the removal of fractured dolomite on steep slopes led to the formation of mostly simple, rectilinear gullies. These have contributed additional deposits of dolomitic eluvium to the area of the thrust line. Slightly sloped sedimentary plains at the foot of the thrust block are nowadays made of dolomite eluvium from the thrust front that partially filled in the flattened sedimentary bed along the edges (Fig. 8, mark **b**). In the expanded thrust–shear zone (Fig. 4),

Na sliki 8 je prikazan značilen profil čez nariv dolomita na dolomit in dolomita na apnenec, ki ponazarja značilne in svojstvene značilnosti razvoja površja vzdolž narivnih struktur (sl. 8). V danih razmerah so se na čelu nariva med dolomitnima paketoma oblikovala strma pobočja z naklonom nad 30° (sl. 8, oznaka **a**). Zaradi visokih naklonov se je na njih občasno vzpostavil površinski odtok vzdolž prelomnih struktur, kjer so se zaradi odnašanja pretrtega dolomita po strmih pobočjih oblikovale večinoma enostavne, premočrtne grape. Te so na območje narivnice prispevale dodaten vnos dolomitne preperine. Dolomitna preperina s čela nariva danes gradi rahlo nagnjene obode sedimentnih uravnav ob vznožju narivnega bloka, ki ob robovih deloma prekrivajo uravnano sedimentno dno (sl. 8, oznaka **b**). V razširjeni obnarivni coni

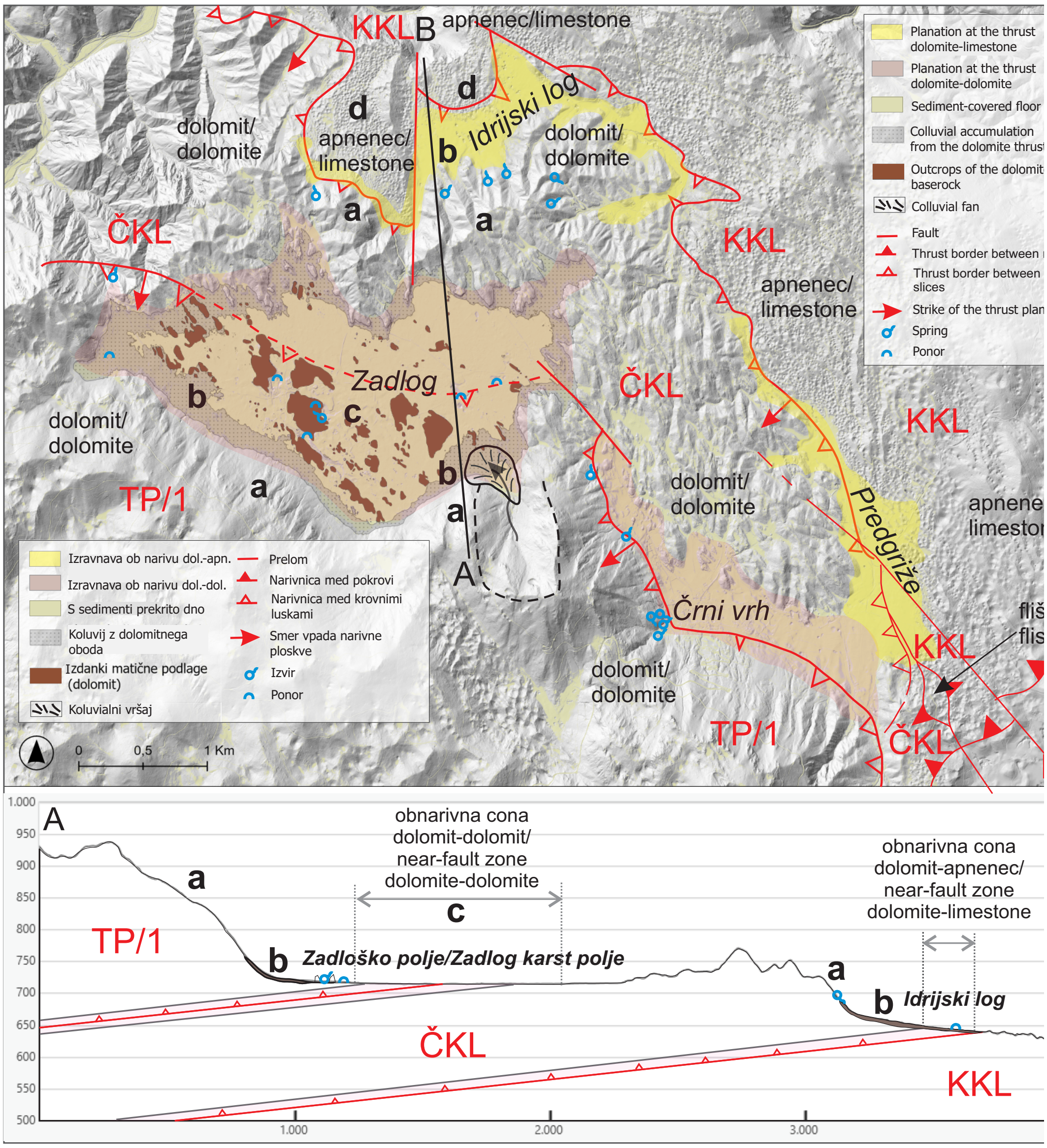

Fig. 8. Thrust–shear surface morphology.

Sl. 8. Obnarivna morfologija površja.

a sediment-covered levelled surface can be observed today (Fig. 8, mark **c**). The absence of outcrops towards the northern part of the polje marks the area of the thrust–shear zone and crushed rocks. There are springs and ponors along the younger faults in the extended bed of the karst polje, which extends beyond the thrust–shear zone.

A steep slope in the dolomite also formed at the thrust front between the dolomite and limestone packages (Fig. 8, mark **a**), where the dolomite eluvium originates from, overlying the expanded area of the thrust–shear zone at a slight inclination (up to 7°) (Fig. 8, mark **b**). It transitions into a classically dissected, morphologically distinct karstified karst surface of the Koševnik nappe slice (Fig. 8, mark **d**). Temporary springs are located in the slope of the thrust front over the dolomite crushed zone. Ponors and dolines formed along the younger faults.

(sl. 4) danes opazujemo s sedimentom prekrito, uravnano površje (sl. 8, oznaka **c**). Odsotnost izdankov proti severnemu delu polja nakazuje na območje obnarivne cone in zdrobjenih kamnin. Ob mlajših prelomih v razširjenem dnu kraškega polja, ki sega izven obnarivne cone, so izviri in ponori.

Na čelu nariva med paketom dolomita in apnenca se je prav tako oblikovalo strmo pobočje v dolomitu (sl. 8, oznaka **a**), od koder izvira dolomitna preperina, ki v blagem naklonu (do 7°) prekriva razširjeno območje obnarivne cone (sl. 8, oznaka **b**). Ta prehaja v klasično razčlenjeno, morfološko izraziteje zakraselo kraško površje Koševniške krovne luske (sl. 8, oznaka **d**). Občasni izviri se nahajajo v pobočju čela nariva nad dolomitno zdrobljeno cono. Ob mlajših prelomih so nastali ponori in vrtače.

Conclusion

With detailed geological mapping on a scale of 1:5000, we found significantly different geological conditions in Zadlog and the surrounding area than those previously drawn on geological maps. Three hydrological retention-deflection levels and numerous, different fault zones intersecting these levels have been identified. The established lithological-structural elements determine the inflow and outflow conditions in Zadloško polje and provide the basis for the formation of karst polje, while present geomorphological and hydrological characteristics indicate recently reduced hydrologic-retention capability of the karst polje and intensive washing out of the eluvium. Denudation, karstification and sediment transport to the underground are the principal processes that, at present, shape the Zadlog karst polje.

Similar thrust and tectonic structures probably occur also in large karst poljes in the Notranjska region. What is the role of thrust tectonics in the formation of these karst poljes and what is the impact on their recent morphological and hydrogeological characteristics will have to be verified with the detailed geological mapping in the future.

Zaključek

S podrobnim geološkim kartiranjem v merilu 1: 5000 smo v Zadlogu in širši okolici ugotovili bistveno drugačne geološke razmere, kot so bile na geoloških kartah izrisane doslej. Ugotovljeni so bili trije zaporno-zadrževalni nivoji in številne, različne prelomne cone, ki te nivoje sekajo. Ugotovljeni litološko-strukturni elementi določajo dotočne in odtočne razmere na Zadloškem polju ter dajejo osnove za oblikovanje kraškega polja, zatečene geomorfološke in hidrološke značilnosti pa kažejo recentno zmanjšano vodno zadrževalno sposobnost kraškega polja in intenzivno izpiranje preperine. Denudacija, zakrasevanje in odnašanje sedimenta v podzemlje so poglavitni procesi, ki trenutno delujejo na območju Zadloškega kraškega polja.

Podobne narivne in tektonske strukture se verjetno pojavljajo tudi na velikih kraških poljih na Notranjskem. Kakšna je njihova vloga pri nastanku, morfološkem oblikovanju in hidrogeoloških značilnostih bo potrebno preveriti z natančnejšim geološkim kartiranjem.

Acknowledgement

The research was funded by the Slovenian Research Agency through grants P1-0419 and project Mladi forum which is co-funded by the Slovenian Research and Innovation Agency within the framework of DFP (Developmental funding pillar).

Zahvale

Članek je bil sofinanciran s strani programske skupine P1-0419 in projekta Mladi forum, ki ga financira Javna agencija za znanstvenoraziskovalno in inovacijsko dejavnost Republike Slovenije v okviru razvojnega stebra (RSF).

References

Bajec, U. 2007: Matuckarjeva pot v Zadlogu. Idrijski razgledi, 2: 100–119.

Buser, S., Grad, K. & Pleničar, M. 1967: Osnovna geološka karta SFRJ 1:100 000. List Postojna. Zvezni geološki zavod, Beograd.

Čar, J. 2001: Structural bases for shaping of dolines – Strukturene osnove oblikovanja vrtač. Acta carsologica, 30/2: 239–256.

Čar, J. 2010: Geološka zgradba idrijsko-cerkljanskega ozemlja. Tolmač h geološki kart idrijski- cerkljanskega hribovja med Stopnikom in Rovtami 1 : 25 000. Geološki zavod Slovenije, Ljubljana: 124 p.

Čar, J. 2018: Geostructural mapping of karstified limestone – Strukturno-geološko kartiranje zakraselih apnencev. Geologija, 61/2: 133–162. https://doi.org/10.5474/geologija.2018.010

Čar, J. & Šebela, S. 2001: Kraške značilnosti narivnega stika apnenec-dolomit pri Predjami – Karst characteristics of thrust contact lemestone-dolomite near Predjama. Acta carsologica, 30/2: 141–156.

Čar, J. & Zagoda, B. 2005: Strukturna lega Habečkovega brezna – Structural position of Habe shaft (Idrijsko, Slovenija). Acta carsologica, 34/1: 113–133. https://doi.org/10.3986/ac.v34i1.282

Čar, J., Jež, J. & Milanič, B. 2021: Strukturne razmere na stiku Južnih Alp in Dinaridov na zahodnem Cerkljanskem – Structural setting at the contact of the Southern Alps and Dinarides in western Cerkljansko region (western Slovenia). Geologija, 64/2: 189–203. https://doi.org/10.5474/geologija.2021.011

Doğan, U., Koçyiğit, A. & Gökkaya, E. 2017: Development of the Kembos and Eynif structural poljes: Morphotectonic evolution of the Upper Manavgat River basin, central Taurides, Turkey. Geomorphology, 278: 105–120. https://doi.org/10.1016/j.geomorph.2016.10.030

Gams, I. 1987: The polje; the problem of definition; with special regard to the Dinaric karst. Zeitschrift für Geomorphologie, 22/2: 170–181.

Gracia, F. J., Gutiérrez, F. & Gutiérrez, M. 2003: The Jiloca karst polje-tectonic graben (Iberian Range, NE Spain). Geomorphology, 52: 215–231. https://doi.org/10.1016/S0169-555X(02)00257-X

Habič, P. 1968: Kraški svet med Idrijco in Vipavo. Inštitut za geografijo SAZU, Ljubljana: 239 p.

Habe, F., Hribar, F. & Štefančič, P. 1955: Habečkovo brezno. Acta carsologica, 27–39.

Janež, J., Čar, J., Habič, P. & Podobnik, J. 1997: Vodno bogastvo Visokega krasa. Ranljivost kraške podzemne vode Banjšic, Trnovskega gozda, Nanosa in Hrušice. Geologija d.o.o. Idrija: 167 p.

Melik, A. 1963: Slovenija, geografski opis 1., splošni del 1, Ljubljana.

Mlakar, I. 1969: Krovna zgradba idrijsko žirovskega ozemlja = Nappe Structure of the Idrija-Žiri Region. Geologija, 12: 5–72.

Mlakar, I. 2002: O nastanku hidrografske mreže in nekaterih kraških pojavih na Idrijskem. On theorigin of the hydrographic net and on some karst phenomena in the Idrija region. Acta carsologica, 31/2: 9–60. https://doi.org/10.3986/ac.v31i2.387

Mlakar, I. & Čar, J. 2009: Geološka karta idrijsko – cerkljanskega hribovja med Stopnikom in Rovtami 1: 25 000. Geološki zavod Slovenija.

Placer, L. 1973: Rekonstrukcija krovne zgradbe idrijsko žirovskega ozemlja = Reconstruction of the Nappe Structure of the Idrija-Žiri Region = Rekonstruktion des Deckenbaus des Idrija-Žiri gebietes. Geologija, 16: 317–334.

Placer, L. 1981: Geološka zgradba jugozahodne Slovenije = Geologic structure of southwestern Slovenia. Geologija, 24/1: 27–60.

Placer, L. 2008: Principles of the tectonic subdivision of Slovenia = Osnove tektonske razčlenitve Slovenije. Geologija, 51/2: 205–217. https://doi.org/10.5474/geologija.2008.021

Pleničar, M., Prestor, M., Rijavec J. & Šribar, L. 1970: Osnovna geološka karta SFRJ 1:100 000. Tolmač lista Postojna. Zvezni geološki zavod, Beograd: 62 p.

Savnik, R. 1959: Ob logaških vratih idrijske pokrajine. Idrijski razgledi, IV/1: 7–9.

Šegina, E. 2021: Spatial Analysis in Karst Geomorphology: An Example from Krk Island, Croatia. Cham: Springer Nature, 183 p. https://doi.org/10.1007/978-3-030-61449-2

Vrabec, M. 1994: Some thoughts on the pull-apart origin of karst poljes along the Idrija strike-slip fault zone in Slovenia. Acta Carsologica, 23: 155–167.

Vrhovec, T. 1997: Potapljaške raziskave v Habečkovem breznu. Naše jame, 39: 145–149.

Zagoda, B. 2004: Karstification along the thrust contact between the dolomite and limestone in Idrijski Log and Koševnik - Zakrasevanje ob narivnem stiku dolomita in apnenca v Idrijskem Logu in Koševniku. Acta carsologica, 33/2: 55–74. https://doi.org/10.3986/ac.v33i2.291

GEOLOGIJA 67/2, 273-284, Ljubljana 2024
https://doi.org/10.5474/geologija.2024.013

Molybdenum, lead and zinc mobility potential in agricultural environments: a case study of the Kočani field, North Macedonia

Mobilnost molibdena, svinca in cinka v kmetijskih okoljih, primer Kočanskega polja (Severna Makedonija)

Nastja ROGAN ŠMUC

University of Ljubljana, Faculty of Natural Sciences and Engineering, Department of Geology, Aškerčeva c. 12, SI–1000 Ljubljana, Slovenia; e-mail: nastja.rogan@ntf.uni-lj.si

Prejeto / Received 11. 7. 2024; Sprejeto / Accepted 15. 11. 2024; Objavljeno na spletu / Published online 16. 12. 2024

Key words: potential toxic elements, soil, mobility potential, environmental assessment, North Macedonia
Ključne besede: potencialno strupeni elementi, tla, mobilnost, okoljska ocena, Severna Makedonija

Abstract

The research focuses on the assessment of potential toxic elements (PTEs) contamination of the soils of the Kočani field (North Macedonia) due to the surrounding past and current polymetallic mining activities. The Zletovska River drains the untreated wastewater from the Pb-Zn mine in the Zletovo-Kratovo region and is unfortunately used to irrigate the surrounding rice fields. Elevated levels of molybdenum (Mo) and especially lead (Pb) and zinc (Zn) were found in the soil samples from the rice fields near the Zletovska River (in the western part of the Kočani field), which are well above the limit and critical emission values for PTEs content in soils. In addition, Mo was consistently bound to water soluble, exchangeable and oxidizable fractions in all samples, while reducible and residual fractions were predominated by Pb and Zn. According to the sum of the water-soluble and exchangeable fractions, the mobility and environmental bioavailability potential of the investigated PTEs in the soil-plant system decreased in the following order: Mo > Pb > Zn. It is therefore very important to emphasize that when assessing the environmental impact of PTEs on the respective surroundings, not only the commonly considered trace and minor PTEs (such as Pb and Zn) that occur in geological materials should be taken into account, but also in lower contents (such as Mo). The translocation of PTEs within the ecosystem does not depend on their total content in the primary geological materials, but on their individual mobility and binding capacity.

Izvleček

Raziskava se osredotoča na onesnaženost tal s potencialno toksičnimi elementi (PTE) na območju Kočanskega polja (Severna Makedonija), ki se nahaja v bližini dveh še vedno aktivnih rudnikov, Sase-Toranice in Zletova-Kratova. V vzorcih tal riževih polj ob reki Zletovski smo odkrili povečane vsebnosti molibdena (Mo) in predvsem kritične vsebnosti svinca (Pb) ter cinka (Zn). Reka Zletovska odvaja neprečiščeno odpadno vodo iz rudnika Pb-Zn Zletovo-Kratovo, na območju Kočanskega polja pa se rečna voda uporablja za intenzivno namakanje riževih polj. S pomočjo rezultatov zaporedne ekstrakcijske analize smo ugotovili, da so deleži Mo večinoma topni v talni raztopini, izmenljivo vezani in vezani na organsko snov, medtem ko so deleži Pb in Zn večinoma vezani na Fe in Mn okside/hidrokside ter v preostanku. Nadalje smo določili mobilnostni potencial in biodostopnost preiskovanih PTE, ki se zmanjšujeta v naslednjem vrstnem redu: Mo > Pb > Zn. Posledično je pomembno poudariti, da pri ocenjevanju okoljskega vpliva PTE ne upoštevamo le splošno obravnavane PTE (kot sta Pb in Zn), temveč tudi tiste, ki se pojavljajo v kamninah, mineralih in tleh v manjših vsebnostih (kot je Mo). Premeščanje PTE v ekosistemu ni odvisna od njihovih celokupnih vsebnosti v primarnih geoloških materialih, ampak od njihovih individualnih lastnosti mobilnosti in vezave.

Introduction

Soil has always been important for people and their existence, especially as a resource that can be used for shelter and food production (Abrahams, 2002; Brevik et al., 2019). Agricultural land today accounts 45 % (48 million km^2) of the world's habitable land (Ritchie & Roser, 2019), and large parts of agricultural land are located near active mines (Wang et al., 2023a). Soil pollution with PTEs has therefore become a widespread global problem over the last four decades, posing a long-term threat to the health and quality of ecosystems (Matong et al., 2016; Wang et al., 2018; Wang et al., 2023a; Yin et al., 2020). The excessive accumulation of PTEs in agricultural soils is of great concern because soil, which contains various essential elements, is a primary nutrient carrier for plants. Food crops grown on contaminated agricultural soils can an accumulate elevated level of PTEs, indicating a potential health risk to the local population and to others if the crops are exported (Adriano, 2001; Pruvot et al., 2006; Wang et al., 2023a; Zhang et al., 2018a; Zhang et al., 2018b; Wang et al., 2023b). Consequently, numerous scientific studies around the world report serious health risks to humans from soils and plants contaminated with PTEs, including Mo (Frascoli & Hudson-Edwards, 2018; Han et al., 2019; Wang et al., 2018; Yin et al., 2020), Pb and Zn (Arenas-Lago et al., 2014; Li et al., 2014; Liu et al., 2022; Zhang et al., 2018a; Wang et al., 2023a).

Environmental risk assessment therefore requires the measurement of the total amount of PTEs in soils and the total amount of PTEs detected in the available/bioavailable fractions (Dean, 2007; Zhang et al., 2014; Kim et al., 2015). A widely used modified method for determining and evaluating the availability or binding forms of PTEs in soils is the sequential extraction method proposed by Tessier et al. (1979), in which the water-soluble and exchangeable fractions represent the most mobile fraction of the individual PTEs (Kabata-Pendias & Pendias, 2001; Dean, 2007).

Compared to the Earth's crust, the PTEs abundance (e.g. Pb and Zn) in various polymetallic ore deposits are generally very high. These naturally occurring elevated PTEs contents are transferred to the immediate surroundings of the ore deposits, where they influence the chemistry of waters, sediments, soils, plants, etc. Primarily through the weathering of the geological background and secondarily through mining and extraction (Bradl et al., 2005; Liu et al., 2013; Zhang et al., 2018a; Wang et al., 2023a). The agricultural area of the Kočani field in North Macedonia, for example, is exposed to the environmental impact of two large mines nearby, Zletovo-Kratovo and Sasa-Toranica, where Pb and Zn have been continuously mined for over 45 years (Balabanova et al., 2014; Rogan Šmuc et al., 2009; Rogan Šmuc et al., 2010; Vrhovnik et al., 2013). Since the ore-mineral association in both mines is very diverse (Rogan Šmuc, 2010) it is necessary to investigate also the presence of other PTEs (for example Mo) and not only Pb and Zn.

In this context, the spatial distribution and possible translocation of Mo in comparison to Pb and Zn in the soils of the Kočani field are investigated. The main objectives of the present study are the following: (1) to estimate the distribution patterns of Mo, Pb and Zn in the soils of the Kočani field and (2) to assess the mobility and environmental bioavailability signature of Mo, Pb and Zn in soil samples.

Materials and methods

Study area

The Kočani field is located in eastern Macedonia, about 32 km from the city of Štip and 115 km from the capital Skopje. With an average length of 35 km and a width of 5 km, the Kočani field is located in the valley of the Bregalnica River between the Osogovo Mountains in the north and the Plačkovica Mountains in the south (Fig. 1).

The wider region is known as an agricultural and mining province (Zletovo Kratovo Pb-Zn and Sasa Toranica Pb-Zn mine). The main agricultural products of the region are rice, corn, tomatoes, cucumbers, peppers and other vegetables.

The Bregalnica River, together with its tributaries, represents the most important drainage system in the study area and is an important water supply for the irrigation of the surrounding rice fields. The main tributaries of the Bregalnica are the Kamenica River in the northeastern part of the study area and the Zletovska River in the west of the Kočani field (Fig. 1). The Kamenica drains the northeastern part of the Bregalnica catchment and flows directly into the artificial Kalimanci Lake, which was constructed to irrigate the rice fields during the dry season. It also drains the untreated mine wastewater from the Sasa Pb-Zn polymetallic ore deposit. The Zletovska River originally drained the central part of the Zletovo-Kratovo volcanic complex as well as the untreated mine wastewater from the Zletovo Pb-Zn mine and its ore processing facilities. The local farmers use both rivers to irrigate the nearby rice fields.

It was assumed that the soil mineral component of the Kočani field originated from a composite material of sediments from igneous, metamorphic and sedimentary rocks in the Kočani region (Dolenec et al., 2007; Aleksandrov et al., 1995). The sedimentary material was transported by the Bregalnica River and its tributaries and deposited in the Kočani depression (Dolenec et al., 2007). The exposed lithologies of the Kočani field consist mainly of acidic to intermediate igneous rocks and to a lesser extent of metamorphic and sedimentary rocks, while the igneous basic lithologies (gabbros and basalts) were found only sporadically (Dolenec et al., 2007; Aleksandrov et al., 1995).

The mineral components of the Kočani soil are closely related to the acidic and intermediate rocks of the Kočani region and consist mainly of

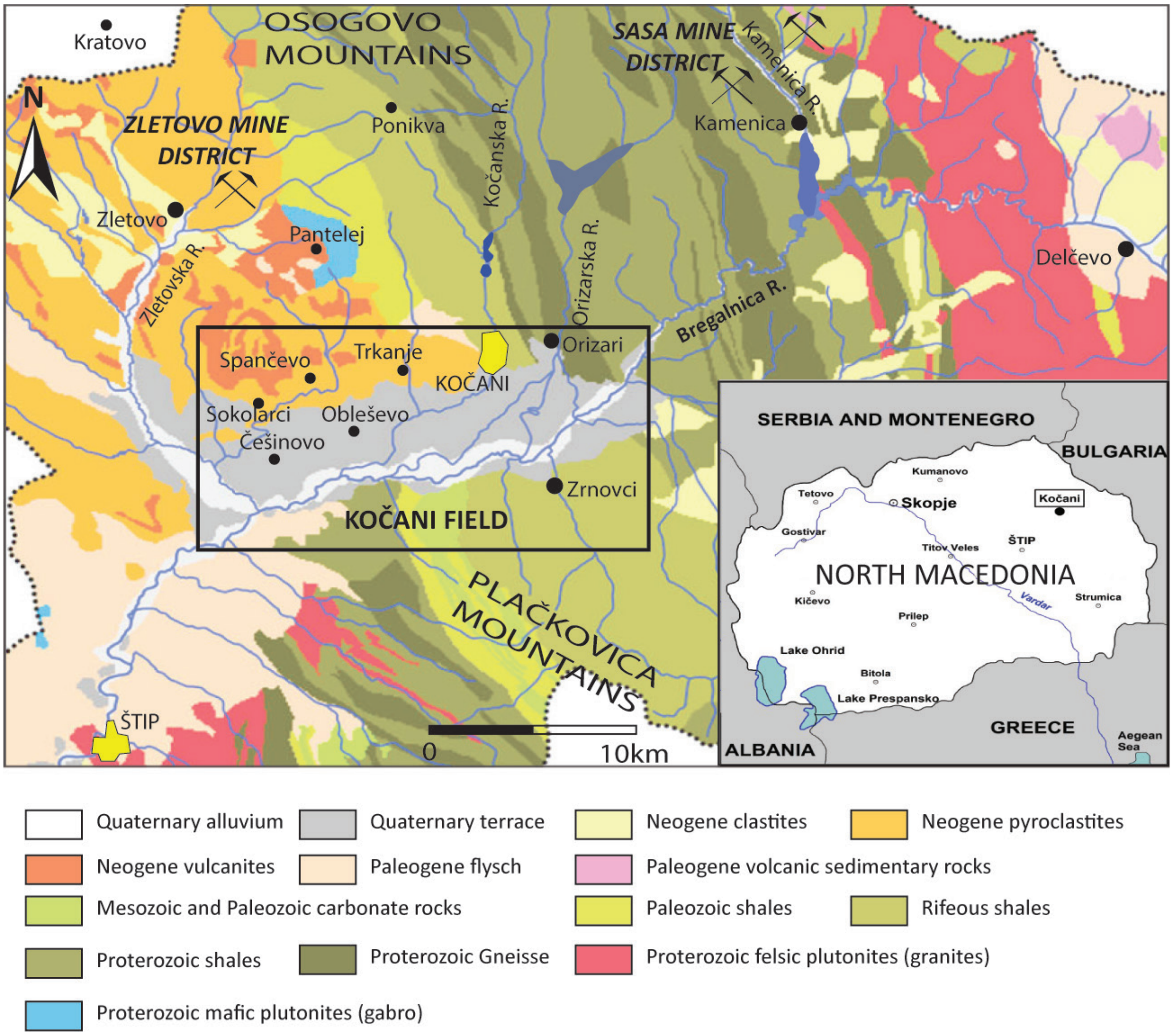

Fig. 1. Study area, Kočani field, North Macedonia. Geological map simplified after Balabanova et al., 2016.

the following minerals: quartz, plagioclase, muscovite-illite, orthoclase and chlorite together with small amounts of amphibole and kaolinite, while traces of calcite and dolomite were found only sporadically (Dolenec et al., 2007). No significant changes in the main soil mineral composition were found throughout the area studied. In addition, a number of secondary products of the soil were detected that originate from the surface-related chemical degradation of the parent material and/or the remobilization of anthropogenic PTEs. These secondary minerals are bixbyite, anglesite, lanarkite, ferrihydrite, clinoclase and chrysocolla (Dolenec et al., 2007; Rogan Šmuc, 2010).

Zletovo-Kratovo ore district

The Zletovo-Kratovo Pb-Zn ore district is located 5 km northwest of the village of Zletovo and about 7 km from the town of Probistip (Fig. 1). It is located in the central part of the Zletovo-Kratovo volcanic complex. The Pb and Zn mineralization occurs in dacitic ignimbrites, the most common volcanic rocks in the area. Ore mineral association includes galena (main ore mineral) and sphalerite, with subordinate pyrite, minor amounts of siderite and chalcopyrite, and occasional pyrrhotite, marcasite and magnetite. Minor occurrences of U-mineralization have also been discovered (pitchblende).

The Zletovo mine has an annual capacity of 400,000 tons of ore, with an average content of 8 % Pb + Zn within the ore (Tasev et al., 2019), and yields significant amounts of Ag, Bi, Cd and Cu (Tasev et al., 2019). The ore is concentrated during the flotation process in Probistip, and the tailings are stored in two tailings ponds in the adjacent valleys (Alderton et al., 2005; Rogan Šmuc, 2010).

Sasa-Toranica ore district

The Sasa-Toranica ore district lies in the Osogovo Mountains, 10 km from the city of Makedonska Kamenica and Lake Kalimanci (Fig. 1). It is established as one of the largest ore districts within the Besna Kobila-Osogovo Tassos metallogenic zone and occupies an area of about 200 km². The important Pb and Zn ore bodies are usually found in quartz/muscovite/graphitic schists, green schists and marbles. The ore mineral association consists of sphalerite, galena, pyrrhotite, pyrite, chalcopyrite, molybdenite, bornite, stibnite and locally cassiterite, accompanied by a series of bismuth and silver minerals as well as non-ore minerals such as skarn minerals, calcites, Mn-calcites and quartz.

The Sasa mine has been in production for over 45 years, yielding 90,000 tons of high quality Pb-Zn concentrate annually and 10 million tons of tailings material (Šajn et al., 2022). The flotation processes in the mine are used to concentrate the ore, and the tailings are stored in a dam in a narrow valley directly below the mine (Alderton et al., 2005; Vrhovnik et al., 2013).

Sampling

Soil samples were taken (year 2006) from 38 locations in seven profiles on the Kočani field (Fig. 2, sections I–VII). The profiles were organized according to the location of the rice fields, as we sampled not only the soil but also the rice. Since we sampled everything at the same time and the samples were agricultural soils, there were no general differences between them in terms of moisture content, soil properties, morphology... The near-surface paddy soils were taken from a depth of 0–20 cm. The soils were sampled with a plastic spade to avoid any metal contamination. Each soil sample consisted of five subsamples taken from an area of 1×1 m². The soil samples were air-dried at 25°C for one week and sieved through a 2 mm thick polyethylene sieve to remove plant debris, pebbles and stones. The samples were then ground to a fine powder in a mechanical agate mill.

Analyses

The **physical and chemical soil properties** (pH, CEC and total organic carbon) were determined at the Slovenian Agricultural Institute. The pH values were measured according to ISO 10390 and with a pH meter. CEC values were measured according to reference NF X31-108 and the Melich method modified according to Peechu et al. using flame atomic absorption spectroscopy (to determine exchangeable cations) and titration (to determine total exchangeable soil acidity). Total organic carbon values were measured using a UV/VIS spectrometer according to ISO 14235.

All soil samples were analysed for **Mo, Pb and Zn content** in a certified (ISO/IEC 17025) commercial Canadian laboratory (Bureau Veritas Mineral Laboratories, Vancouver, B.C., Canada) by one-hour extraction with 2-2-2-HCl-HNO_3-H_2O at 95 °C and ICP-MS. The accuracy and precision of the soil analysis was evaluated using international reference material such as Canadian Certified Reference Material Project (CCRMP) SO-1 (soil) and United

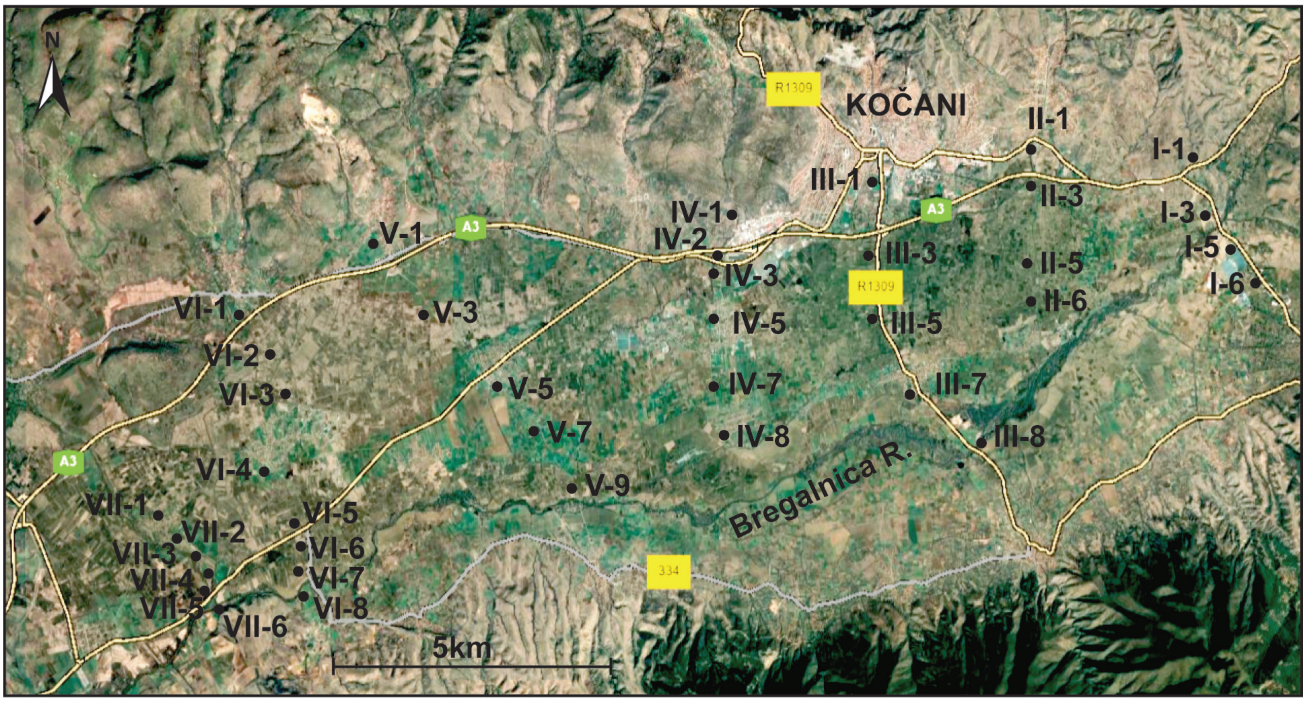

Fig. 2. Map of the locations of the soil samples.

States Geological Survey (USGS) G-1 (granite). The analytical precision and accuracy was better than ±5 % for the elements analysed (minor and trace elements), taking into account the results of duplicate measurements in 10 soil samples and duplicate measurements of the G-1 and SO-1 standards.

Five randomly selected soil samples (I-3, II-6, III-5, VI-4 and VII-2) were also analysed using a sequential extraction procedure to decipher the **Mo, Pb and Zn chemical bonding forms** (Li et al., 1995; Tessier et al., 1979). The 1 g of each soil sample was placed in screw-capped test tubes. A duplicate pulp split and a control sample of WSA (water leach), ESL (Na-acetate), OSL (Na-pyrophosphate), MSL (weak hydroxylamine), or FSL (strong hydroxylamine) monitored the precision and accuracy of each batch of 32 samples. To each sample, 10 ml of leaching solution was added; then the caps were screwed on and the tubes were subjected to an extraction procedure (Bureau Veritas Mineral Laboratories, Vancouver, B.C., Canada). The samples was leached, centrifuged, decanted and washed; the residue was then leached again in a five-step procedure from the weakest to the strongest solution: water → ammonium acetate → sodium pyrophosphate → cold hydroxylamine hydrochloride → hot hydroxylamine hydrochloride. A reagent blank was carried out in parallel with the leaching and analysis steps. The procedure and chemical fractions are listed in Table 1. After the sequential extraction procedure, the content of the analysed elements in the solution were measured using a Perkin Elan 6000 ICP-MS for the determination of over 60 elements (Bureau Veritas Mineral Laboratories, Vancouver, B.C., Canada). A QA/QC protocol included a sample duplicate to monitor analytical precision. A reagent blank was used to measure background and an aliquot of in-house reference material was used to monitor precision. A British Columbia Certified Assayer reviewed the raw and final data.

Tabela 1. Sequential extraction procedure with sequential fractions and chemical reagents.

Step	Fraction	Chemical reagents
1	Water soluble	Demineralized H_2O
2	Exchangeable	1 M sodium acetate
3	Oxidizable	0.1 M sodium pyrophosphate
4	Reducible	Cold 0.1 M hydroxylamine
5	Residual	Hot 0.25 M hydroxylamine

Basic statistical parameters for each element were calculated using Statistica VII. The Mo, Pb and Zn distribution maps were created with the Surfer 6 programme.

Results and discussion

The physico-chemical properties of the soil

The physico-chemical characteristics of the soil are listed in Table 2. All soil samples were characterised by a slightly acidic pH (5.2–6). CEC values were relatively moderate, with an average value of 20.7 mmol/100g. Total organic carbon was between 0.7 and 2.95 %.

Table 2. Information about physico-chemical characteristics of the soil samples from Kočani Field.
Number of measured samples (n) = 25.

	pH	**CEC** (mmol/g)	**TOC** (%)
Range	5.2-6.0	11.4-38.6	0.70-2.95
Mean	5.5	20.7	1.70

Mo, Pb and Zn content in the soil

As there are many samples, I have divided them into three groups according to their Mo, Pb and Zn content. The first group (1) comprises the samples with the lowest Mo, Pb and Zn contents, the second group (2) the samples with the medium Mo, Pb and Zn contents and the last, third group (3) the samples with the highest Mo, Pb and Zn contents.

Table 3 shows the contents of Mo, Pb and Zn determined in the soil samples from the Kočani field based on their descriptive statistical parameters (minimum, maximum, mean, median and standard deviation (SD)) together with the Decree on the limit, warning and critical levels of hazardous substances in soil (Ur. l. RS No. 68/96) and with the Dutch Target and Intervention Values, 2000 (the new Dutch list).

Table 3. Mo, Pb and Zn content (mg/kg) in the soil samples from the Kočani field together with their descriptive statistical parameters and with the proposed values for Mo, Pb and Zn in soil in the Decree on the limit, warning and critical levels of hazardous substances in soil (Ur. l. RS No. 68/96) and with the Dutch Target and Intervention Values, 2000 (the new Dutch list).

The Mo content in the soils was between 0.3 and 1.8 mg/kg (Table 3) and thus far below the limit of 10 mg/kg proposed in Ur. l. RS No. 68/96 and below the target (3 mg/kg) and intervention (200 mg/kg) values proposed in the Dutch Target and Intervention Values, 2000 (the new Dutch list). The Pb content in the soils was between 10.5 and 983 mg/kg, while the Zn content was significantly higher at 53 to 1245 mg/kg (Table 3). The highest Pb and Zn values were predominantly measured in the soil samples from section VII, which had a Pb

Table 3. Mo, Pb and Zn content (mg/kg) in the soil samples from the Kočani field together with their descriptive statistical parameters and with the proposed values for Mo, Pb and Zn in soil in the Decree on the limit, warning and critical levels of hazardous substances in soil (Ur. l. RS No. 68/96) and with the Dutch Target and Intervention Values, 2000 (the new Dutch list).

Statistical data	**n**	**Min**	**Max**	**Mean**	**Median**	**Std. Dev.**
Group/Element	**Mo**	**Mo**	**Mo**	**Mo**	**Mo**	**Mo**
1	12	0.3	0.7	0.48	0.5	0.13
2	20	0.3	1	0.57	0.6	0.14
3	6	0.9	1.8	1.47	1.5	0.34
All groups	38	0.3	1.8	0.68	0.6	0.39
	Pb	**Pb**	**Pb**	**Pb**	**Pb**	**Pb**
1	12	10.5	26.9	18.4	18.5	4.7
2	20	15.4	81.3	29.3	23	15.3
3	6	**295.7**	**983.1**	675.8	723.9	269.4
All groups	38	10.5	983.1	128	22.1	260.3
	Zn	**Zn**	**Zn**	**Zn**	**Zn**	**Zn**
1	12	53	74	67.6	68.5	5.6
2	20	76	162	95.7	94	17.9
3	6	**384**	**1245**	852.5	910.5	335.7
All groups	38	53	1245	206.3	87.5	309.8
Decree on the limit, warning and critical levels of hazardous substances in soil (Official Gazette of RS, No. 68/96)						
Element	**Limit levels (mg/kg)**		**Warning levels (mg/kg)**		**Critical levels (mg/kg)**	
Mo	10		40		200	
Pb	85		100		530	
Zn	200		300		720	
Target values and soil remediation intervention values soil/sediment for metals Dutch Target and Intervention Values, 2000 (the New Dutch List)						
Element	**National background concentration**		**Target values (mg/kg)**		**Intervention values (mg/kg)**	
Mo	0.5		3		200	
Pb	85		85		530	
Zn	140		140		720	

content of 295.7 to 983.1 mg/kg and a Zn content of 384 to 1245 mg/kg (Table 3). The Pb and Zn content of the soil in section VII exceeds all the levels specified in the Ur. l. RS No. 68/96 and the Dutch Target and Intervention Values, 2000 (the new Dutch list) (Fig. 3).

The Kočani field is also surrounded by two large polymetallic mineralized areas, e.g. the Pb-Zn ore districts of Zletovo-Kratovo and Sasa-Toranica. The soils in section VII, which is located near the Zletovska River and the Zletovo-Kratovo ore district, were exposed to a comparatively higher input of anthropogenic PTEs than other parts of the Kočani area. The polymineralic zone of Zletovo Kratovo consists of the main Pb and Zn minerals, galena and sphalerite, while no main Mo mineral is present. In addition to the main minerals mentioned, pyrite occurs in the Zletovo-Kratovo ore mineral association and, as reported by Hu et al. 2019 can also incorporate Mo into its crystal structure. Slightly elevated Mo levels were detected in the soil samples. The difference between the Mo, Pb and Zn contents in section VII and the other sections is shown in box and whisker plots (Fig. 4). The pollution in section VII is undoubtedly related to the irrigation of rice fields with water from the Zletovska River; previous studies have confirmed that the water of the Zletovska River was contaminated with PTEs from untreated mining wastewater (Alderton et. al, 2005; Dolenec et al., 2007; Rogan Šmuc, 2010). Repeated water samples from the Zletovska River showed marked fluctuations in Mo (0.3-0.9 µg/l), Pb (50-80 µg/l) and Zn (101-1250 µg/l) (Alderton et al., 2005; Dolenec et al., 2007; Rogan Šmuc, 2010). Elevated levels of Pb and Zn were also found in other soil sections, especially in sections V and VI. This increase is due to various sources, e.g. phosphate fertilisers (Zn) (Zhou et al., 2021; Alengebawy et al., 2021) and pesticides (Pb) in agriculture (Alengebawy et al.,

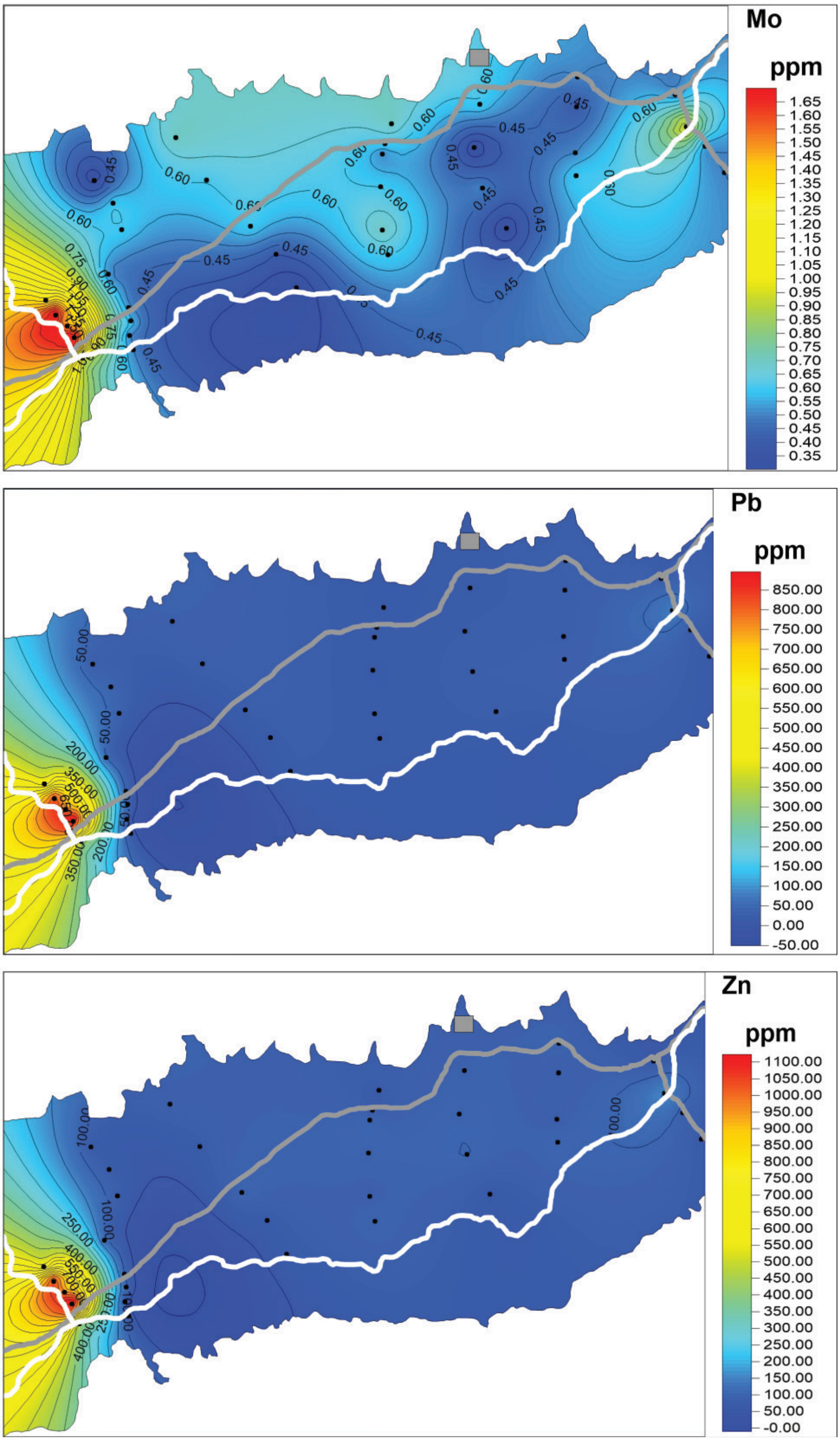

Fig. 3. The spatial distribution of Mo, Pb and Zn content, clearly denoting the enrichment with the investigated elements in the section VII.

2021; Bradl, 2005; Wang et al., 2023a) as well as urban and traffic-related sources (Pb, Zn) (Bradl, 2005; Wang et al., 2023a). It could also originate from the discharge of untreated municipal and domestic wastewater (Bradl, 2005) from the town of Kočani and the village of Orizari into the river systems of the Kočanska and Orizarska rivers, both of which are used for irrigation purposes.

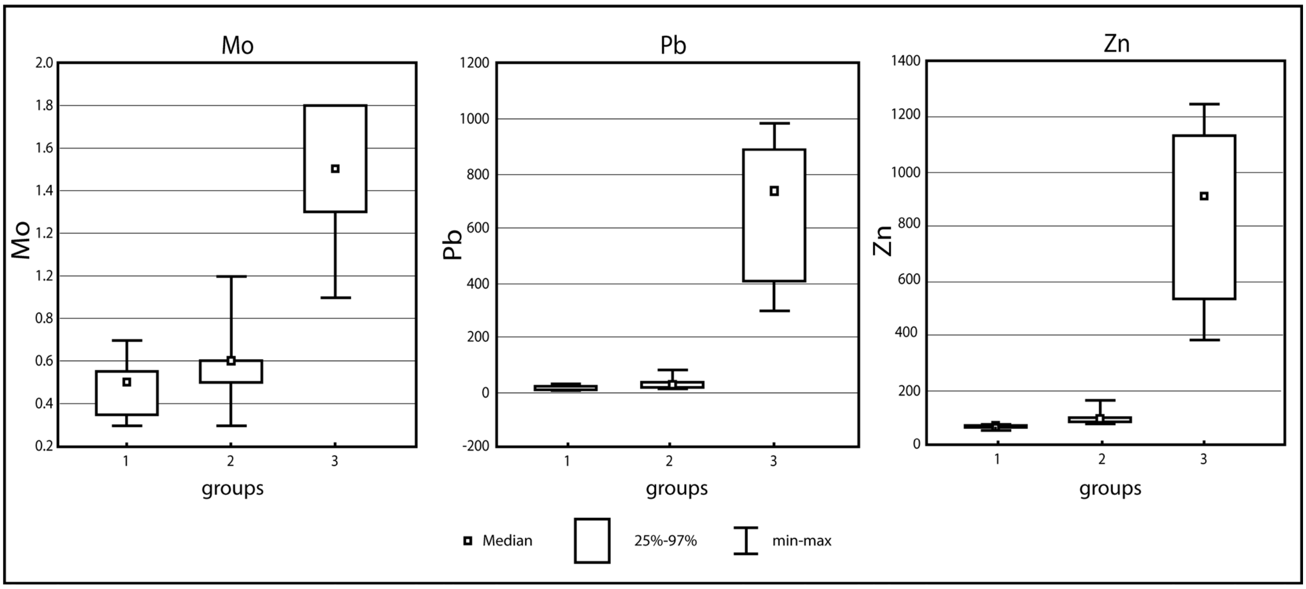

Fig. 4. Box and whisker plots of Mo, Pb and Zn for soil samples from the Kočani field.

Mobility potential and environmental bioavailability of Mo, Pb and Zn from soils

A sequential extraction method was used to assess the mobility potential and environmental bioavailability of Mo, Pb and Zn in the investigated environment. No significant differences were noted in the distribution/partitioning of the elements within the selected samples originating from different sites, but there is an obvious difference in the sequential fractions in which the elements are most abundant.

The most abundant fraction for Mo was the oxidizable fraction, and the other important fractions for Mo were the residual and the water-soluble fractions (Fig. 5). This is supported by the findings of Kabata-Pendias & Pendias (2001), Wichard et al. (2009), Xu et al. (2013), Marks et al. (2015), Matong et al., (2016) and Alvarez-Ayuso & Abad-Valle (2017) that Mo in soil is predominantly associated with organic matter (e.g. organometallic complexes).

Pb and Zn were mainly bound to the residual fraction and the reducible fraction (Fig. 5). The results of Riffaldi et al. (1976), Kabata-Pendias & Pendias (2001), Liu et al. (2013), Nemati et al. (2013), Arenas-Lago et al. (2014), Kennou et al. (2015), Matong et al. (2016) and Zhang et al. (2018) also indicate that Pb is mainly associated with the residual fraction and Mn oxides as well as Fe and Mn hydroxides. The association of Zn with Fe and Mn hydroxides in soils was similarly demonstrated by Kabata-Pendias & Pendias (2001), Arenas-Lago et al. (2014) and Alvarez-Ayuso & Abad-Valle (2017). Rice cultivation in the Kočani rice fields generally requires frequent flooding. Different flooding conditions have different effects on the mobility and environmental bioavailability of PTEs. Fe and Mn oxides are important adsorbents for PTEs in soils under oxidising conditions (Lee, 2006). Under reducing conditions (flooded fields), however, a relatively high proportion of PTEs is detected in the exchangeable fraction, as the PTEs adsorbed on the Fe and Mn oxides release (Charlatchka & Cambier, 2000; Lee, 2006). As the soil samples were taken under oxidising conditions (non-flooded fields), Pb and Zn are mainly associated within the reducible and residual fractions.

The mobility and environmental bioavailability of Mo, Pb and Zn in soils depends primarily on the nature of their binding forms in the soil. The water-soluble and exchangeable fractions are considered to be the most mobile and bioavailable fractions, in contrast to the residual fractions, where the PTEs are strongly bound to the crystalline structures of the minerals present in the soil matrix and are stable (Dean, 2007; Nemati et al., 2013). Mo was consistently bound to bioavailable and leachable fractions (Fig. 5) in all samples, while Pb and Zn predominated in reducible and residual fractions (Fig. 5), indicating a relatively low mobility potential. The sum of the water-soluble and exchangeable fractions for Mo, Pb and Zn detected in the soils of the Kočani field shows that the potential mobility and environmental bioavailability of these elements for plants in the studied area decreases in the following order: **Mo > Zn > Pb.** It is very important to point out that in polymetallic areas exposed to the anthropogenic influence of several PTEs, environmental pollution must be assessed not only for the PTEs that

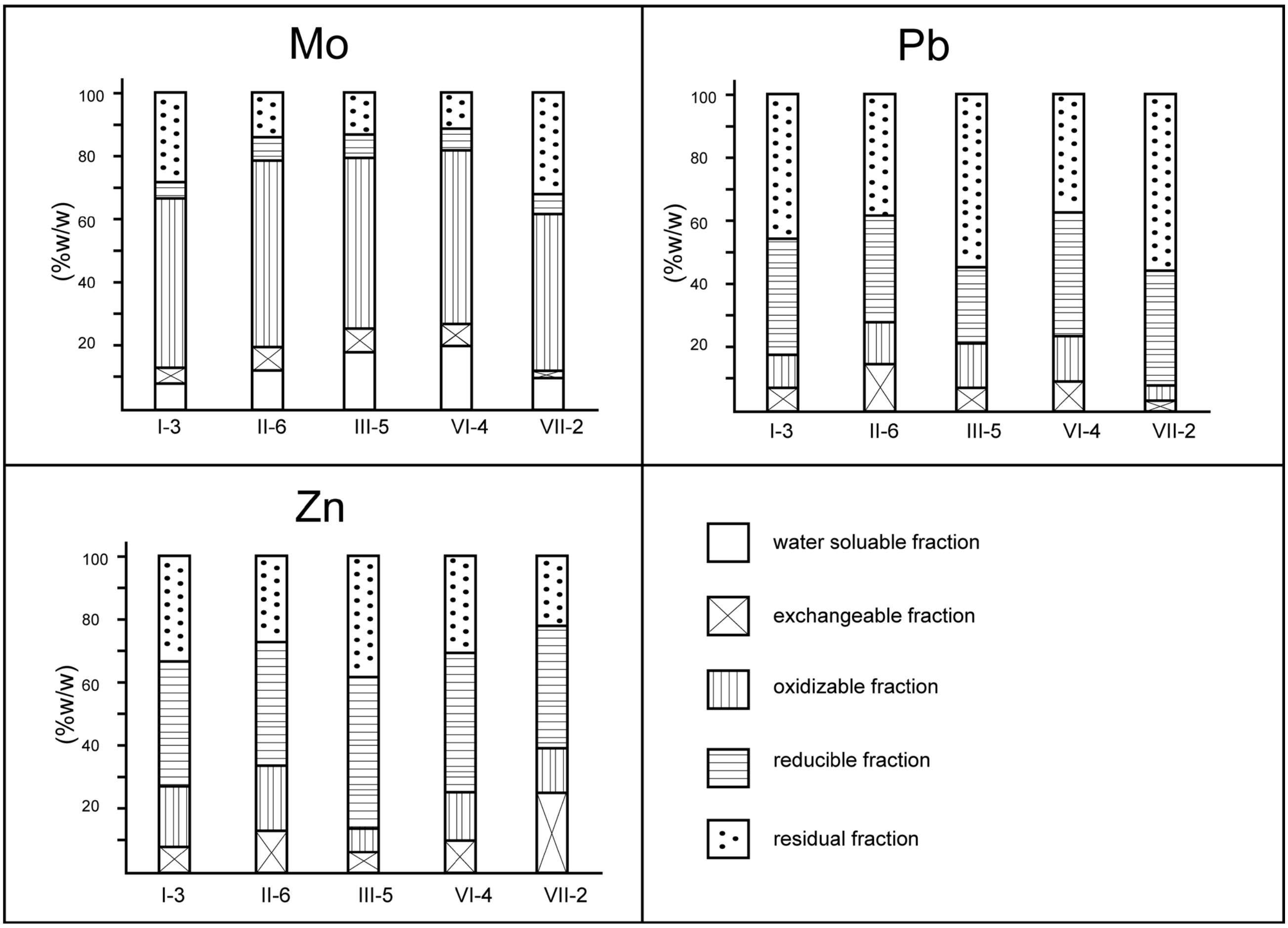

Fig. 5. Mo, Pb and Z binding forms in soil samples from sampling sites I-3, II-6, III-5, VI-4 and VII-2.

are present in high total content, but also for those whose contents are not so high (Kabata-Pendias & Pendias, 2001; Dean, 2007). The mobility potential and environmental bioavailability of PTEs do not depend on their content in the various minerals, ore mineral, rocks, sediments and soils, but on their individual nature and their ability to bind in the different minerals, amorphous materials and organic matter.

Conclusions

The Pb and Zn contents determined in the Kočani soils from section VII were well above the maximum permissible values for the PTEs content of soils (according to Slovenian legislation and new Dutch list). Although the Mo content was below the mentioned limits, its accumulation in the soil samples near the Zletovska River was conspicuous, which confirms the higher anthropogenic PTEs contamination in this area. The mine's wastewater is discharged uncontrolled into the Zletovska River, which therefore contains extremely high concentrations of PTEs (Alderton et al., 2005), and is used to irrigate the nearby rice fields. The Zletovska River is thus considered the most anthropogenically influenced part of the Kočani field. The very high contents of analysed PTEs in agricultural soils are most probably related to past and present mining activities, especially in the Zletovo-Kratovo ore district.

According to the sum of the water-soluble (1) and exchangeable (2) fractions of Mo, Pb and Zn detected in the soils of the Kočani field, the mobility potential and environmental bioavailability of the studied PTEs (from soils to plants) decreased in the following order: Mo > Zn > Pb. For this reason, it is very important to assess the potential mobility of all PTEs in areas exposed to multi-element contamination, as mobility usually depends not only on the amount of PTEs in the minerals, ore mineral, rocks, sediments and soils, but also on their individual nature, their preferential binding and their mobility potential.

Acknowledgements

The research was financially supported by the Slovenian Research and Innovation Agency (ARIS), contract number 1000-05-310229 and as part of the ERC complementary scheme N1-0164.

References

Abrahams, P.W. 2002: Soils: their implications to human health. Science of the Total Environment, 291: 1–32.

Adriano, D.C. 2001: Trace elements in terrestrial environments: biogeochemistry, bioavailability and risks of metals (2nd edition). Springer-Verlag, New York: 867 p.

Aleksandrov, M., Serafimovski, T. & Markov, S. 1995: Major lead-zinc field at Sasa: Mineral associations and morpho-structural types. In: International Workshop, Unesco-IGCP Project 356, Stip Macedonia.

Alengebawy, A., Abdelkhalek, S.T., Qureshi, S.R. & Wang, M.-Q. 2021: Heavy metals and pesticides toxicity in agricultural soil and plant: ecological risks and human health implications. Toxics, 9: 42. https://doi.org/10.3390/toxics9030042

Alderton, D.H.M., Serafimovski, T., Mullen, B., Fairall, K. & James, S. 2005: The chemistry of waters associated with Metal Mining in Macedonia. Mine water and the Environment, 24: 139–149. https://doi.org/10.1007/s10230-005-0085-z

Álvarez-Ayuso, E. & Abad-Valle, P. 2017: Trace element levels in an area impacted by old mining operations and their relationship with beehive products. Science of the Total Environment, 599-600: 671–678. http://dx.doi.org/10.1016/j.scitotenv.2017.05.030

Arenas-Lago, D., Andrade, M.L., Lago-Vila, M., Rodríguez-Seijo, A. & Vega, F.A. 2014: Sequential extraction of heavy metals in soils from a copper mine: Distribution in geochemical fractions. Geoderma, 230–231: 108–118. http://doi.org/10.1016/j.geoderma.2014.04.011

Balabanova, B., Stafilov, T., Šajn, R. & Bačeva Andronovska, K. 2014: Variability assessment of metals distributions due to anthropogenic and geogenic impact in the lead-zinc mine and flotation Zletovo environs (moss biomonitoring). Geologica Macedonica, 28/2: 101–114.

Balabanova, B., Stafilov, T., Šajn, R. & Tănăselia, C. 2016: Multivariate extraction of dominant geochemical markers for deposition of 69 elements in the Bregalnica River basin, Republic of Macedonia (moss biomonitoring). Environmental Science and Pollution Research, 23: 22852–22870. https://doi.org/10.1007/s11356-016-7502-7

Bradl, H.B. 2005: Heavy Metals in the Environment: Origin, Interaction and Remediation. Elsevier Academic Press, Amsterdam-Boston: 282 p.

Brevik, E.C., Pereg, l., Pereira, P., Steffan, J.J., Brugess, L.C. & Gedeon, C.I. 2019: Shelter, clothing and fuel: Often overlooked links between solis, ecosystem services, and human health. Science of the Total Environment, 651: 134–142. https://doi.org/10.1016/j.scitotenv.2018.09.158

Charlatchka, R. & Cambier, P. 2000: Influence of reducing conditions on solubility of trace metals in contaminated soils. Water Air and Soil Pollution, 118/1–2: 143–168. https://dx.doi:10.1023/A: 100519592087

Dean, J.R. 2007: Bioavailability, Bioaccessibility and Mobility of Environmental Contaminants. John Wiley and Sons Ltd., England: 292 p.

Dolenec, T., Serafimovski, T., Tasev, G., Dobnikar, M., Dolenec, M. & Rogan, N. 2007: Major and trace elements in paddy soil contaminated by Pb–Zn mining: a case study of Kočani Field, Macedonia. Environemntal Geochemistry and Health, 29/1: 21–32. https://doi.org/10.1007/s10653-006-9057-x

Dutch Target and Intervention Values, 2000 (the New Dutch List). Annexes. Circular on Target Values and Intervention Values for Soil Remediation. https://support.esdat.net/Environmental%20Standards/dutch/annexs_i2000dutch%20environmental%20standards.pdf

Frascoli, F. & Hudson-Edwards, K. 2018: Geochemistry, Mineralogy and Microbiology of Molybdenum in Mining-Affected Environments. Minerals, 8/2: 42. https://doi.org/10.3390/min8020042

Han, Z., Wan, D., Tian, H., He, W., Wang, Z. & Liu, Q. 2019: Pollution assessment of heavy metals in soils and plants around a molybdenum mine in central China. Polish Journal of Environmental Studies, 28: 123–133. https://doi.org/10.15244/pjoes/83693

Hu, K.-X., Tang, L., Zhang S.-T., Santosh, M., Spencer, C.J., Zhao, Y., Cao, H.-W. & Pei, Q.-M. 2019: *In situ* trace element and sulfur isotope of pyrite constrain ore genesis in the Shapoling molybdenum deposit, East Qinling Orogen, China. Ore Geology Reviews, 105: 123–136. https://doi.org/10.1016/j.oregeorev.2018.12.019

Kabata-Pendias, A. & Pendias, H. 2001: Trace Elements in Soils and Plants (3rd edition). CRC Press, Boca Raton: 432 p.

Kim, R.-Y., Yoon, J.-K., Kim, T.-S., Yang, J.E., Owens, G. & Kim, K.-R. 2015: Bioavailability of heavy metals in soils: definitions and practical implementation – a critical review. Environmental Geochemistry and Soils, 37:

1041–1061. https://doi.org/10.1007/s.10653-015-9695-y

Kennou, B., El Meray, M., Romane A. & Arjouni, Y. 2015: Assessment of heavy metal availability (Pb, Cu, Cr, Cd, Zn) and speciation in contaminated soils and sediment of discharge by sequential extraction. Environmental Earth Sciences, 74: 5849–5858. https://doi.org/10.1007/s12665-015-4609-y

Lee, S. 2006: Geochemistry and partitioning of trace metals in paddy soils affected by metal mine tailings in Korea. Geoderma, 135: 26–37. https://doi.org/10.1016/j.geoderma.2005.11.004

Li, Z., Ma, Z., van der Kuijp, T.J., Yuan, Z. & Huang, L. 2014: A review of soil heavy metal pollution from mines in China: Pollution and health risk assessment. Science of the Total Environment, 468-469: 843–853. https://doi.org/10.1016/j.scitotenv.2013.08.090

Liu, G., Tao, L., Liu, X., Hou, J., Wang, A., & Li, R. 2013: Heavy metal speciation and pollution of agricultural soils along Jishui River in non-ferrous metal mine area in Jiangxi Province, China. Journal of Geochemical Exploration, 132: 156–163. https://doi.org/10.1016/j.gexplo.2013.06.017

Liu, H., Qu, M., Chen, J., G., X., Zhang, J., Liu, M., Kang, J., Zhao, Y. & Huang, B. 2022: Heavy metal accumulation in the surrounding areas affected by mining in China: Spatial distribution patterns, risk assessment, and influencing factors. Science of the Total Environment, 825: 154004. https://doi.org/10.1016/j.scitotenv.2022.154004

Marks, J.A., Perakis, S.S., King, E.K. & Pett-Ridge, J. 2015: Soil organic matter regulates molybdenum storage and mobility in forests. Biogeochemistry, 125: 167–183. https://doi.org/10.1007/s10533-015-0121-4

Matong, J.M., Nyaba, L. & Nomngongo, P.N. 2016: Fractionation of trace elements in agricultural soils using ultrasound assisted sequential extraction prior to inductively coupled plasma mass spectrometric determination. Chemosphere, 154: 249–257. https://doi.org/10.1016/j.chemosphere.2016.03.123

Nemati, K., Bakar, N.K.A., Abas, M.R.B., Sobhanzadeh, E. & Low, K.H. 2013: Comparison of unmodified and modified BCR sequential extraction schemes for the fractionation of heavy metals in shrimp aquaculture sludge from Selangor, Malaysia. Environmental Monitoring Assessment, 176/1–4: 313–320. https://doi.org/10.1007/s10661-010-1584-3

Pruvot, C., Douay, F., Herve, F. & Waterlot, C. 2006: Heavy metals in soil, crops and grass as a source of human exposure in the former mining areas. Journal of Soils and Sediments, 6: 215–20. https://doi.org/10.1065/jss2006.10.186

Ritchie, H. & Roser, M. 2019: Half of the world's habitable land is used for agriculture. Internet: https://ourworldindata.org/global-land-for-agriculture

Riffaldi, R., Levi-Minzi, R. & Soldatini, G.E. 1976: Pb absorption by soils. Water, Air and Soil Pollution, 6: 119–123.

Rogan Šmuc, N., Serafimovski, T., Dolenec, M., Tasev, G. & Dolenec, T. 2009: Heavy metal contamination of paddy soils and rice (Oryza sativa L.) from Kočani field (Macedonia). Environmental geochemistry and health, 31: 439–451. https://doi.org/10.1007/s10653-008-9197-2

Rogan Šmuc, N. 2010: Heavy metal contamination of soils and crops in tertiary basins: A case study of Kočani Field (Macedonia). Doktorska disertacija. Univerza v Ljubljani, Naravoslovnotehniška fakulteta, Ljubljana: 108 p.

Šajn, R., Ristović, I. & Čeplak, B. 2022: Mining and metallurgical waste as potential secondary sources of metals – a case study for the West Balkan Region. Minerals, 12/5: 547. https://doi.org/10.3390/min12050547

Tasev, G., Serafimovski, T., Dolenec, M. & Rogan Šmuc, N. 2019: Contribution to understanding of ore fluids in the Zletovo mine based on the fluid inclusion data. RMZ: Materials and Geoenvironment: periodical for mining, metallurgy and geology, 66/2: 75–86. https://doi.org/10.2478/emzmag-2019-0008

Tessier, A., Campbell, P.G.C. & Bisson, M. 1979: Sequential extraction procedure for the speciation of particulate trace metals. Analytical Chemistry, 51: 844–851.

Uradni list RS, 68/96, 41/04 – ZVO-1 in 44/22 – ZVO-2: Uredba o mejnih, opozorilnih in kritičnih emisijskih vrednostih nevarnih snovi v tleh. https://pisrs.si/pregledPredpisa?id=URED114

Vrhovnik, P., Arrebola, J.P., Serafimovski, T., Dolenec, T., Rogan Smuc, N., Dolenec, M. & Mutch, E. 2013: Potentially toxic contamination of sediments, water and two animal species in Lake Kalimanci, FYR Macedonia: Relevance to human health. Environmental Pollution, 180: 92–100. https://doi.org/10.1016/j.envpol.2013.05.004

Wang, Z., Hong, C., Xing, Y., Wang, K., Li, Y., Feng, L. & Ma, S. 2018: Spatial distribution and sources of heavy metals in natural pasture soil around copper-molybdenum mine in Northeast China. Ecotoxicology and Environmental Safety, 154: 329–336. https://doi.org/10.1016/j.ecoenv.2018.02.048

Wang, C.-C., Zhang, Q.-C., Yan, C.-A., Tang, G.-Y., Zhang, M.-Y., Ma, L.Q., Gu, R.-H. & Xiang, P. 2023a: Heavy metal(loid)s in agriculture soils, rice, and wheat across China: Status assessment and spatiotemporal analysis. Science of the Total Environment, 882: 163361. https://doi.org/10.1016/j.scitotenv.2023.163361

Wang, C., Zhang, Q., Kang, S., Li, M., Zhang, M., Xu, W., Xiang, P. & Ma, L.Q. 2023b: Heavy metal(oid)s in agricultural soil from main grain production regions of China: bioaccessibility and health risks to humans. Science of the Total Environment, 858/2: 159819. https://doi.org/10.1016/j.scitotenv.2022.159819

Wichard, T., Mishra, B., Myneni, S.C.B., Bellenger, J.P. & Kraepiel, A.M.L. 2009: Storage and bioavailability of molybdenum in soils increased by organic matter complexation. Nature Geoscience, 2: 625–629. https://doi.org/10.1038/ngeo589

Xu, N., Braida, W., Christodoulatos, C. & Chen, J. 2013: A review of molybdenum adsorption in soils/bed sediments: speciation, mechanism, and model applications. Soils Sediment Contamination, 22: 912–929. https://doi.org/10.1080/15320383.2013.770438

Yin, K., Shi, Z., Zhang, M. & Li, Y. 2020: Effects of mining on the molybdenum absorption and translocation of plants in the Luanchuan molybdenum mine. PeerJ 8: e9183. https://doi.org/10.7717/peerj.9183

Zhang, C., Yu, Z., Zeng, G., Jiang, M., Yang, Z., Cui, F., Zhu, M., Shen, L. & Hu, L. 2014: Effects of sediment geochemical properties on heavy metal bioavailability. Environment International, 73: 270–281. https://doi.org/10.1016/j.envint.2014.08.010

Zhang, J., Li, H., Zhou, Y., Dou, L., Cai, L., Mo, L. & You, J. 2018a: Bioavailability and soil-to-crop transfer of heavy metals in farmland soils: A case study in the Pearl River Delta, South China. Environmental Pollution, 235: 710–719. https://doi.org/10.1016/j.envpol.2017.12.106

Zhang, S., Song, J., Cheng, Y., Liu, G. & Wallace, A.R. 2018: Trace metal(oid)s exposure through soil-tobacco-human pathway: Availability in metal-contaminated agricultural soil, transfer models and health risk assessment. Ecotoxicology and Environmental Safety, 148: 1034–1041. https://doi.org/10.1016/j.ecoenv.2017.11.043

Zhou, S., Su, S., Meng, L., Liu, X., Zhang, H. & Bi, X. 2021: Potentially toxic trace element pollution in long-term feritlized agricultural soils in China: A meta-analysis. Science of the Total Environment, 789: 14967. https://doi.org/10.1016/j.scitotenv.2021.147967

GEOLOGIJA 67/2, 285-300, Ljubljana 2024
https://doi.org/10.5474/geologija.2024.014

Mineralogy, geochemistry and genesis of low-grade manganese ores of Anujurhi area, Eastern Ghats, India

Mineralogija, geokemija in geneza revnih manganovih rud z območja Anujurhi, Vzhodni Gati, Indija

Sujata PATTNAIK[1]* & Satrughan MAJHI[2]

[1]Geological Survey of India, Eastern Region, Bhu-Bijnan bhawan, DK-6, Karunamayee, Sector-2, Salt Lake, Kolkata-700091;
*corresponding author: suji.pinky@gmail.com
[2]Geological Survey of India, State Unit: Odisha, Unit-8, Nayapalli, Bhubaneswar-751012

Prejeto / Received 18. 3. 2024; Sprejeto / Accepted 12. 11. 2024; Objavljeno na spletu / Published online 16. 12. 2024

Key words: Eastern Ghats Mobile Belt (EGMB), Anujurhi, manganese ore, supergene enrichment
Ključne besede: Vzhodni Gati, Anujurhi, manganova ruda, supergena obogatitev

Abstract

The Anujurhi manganese ores occur in the high-grade gneisses of the Precambrian Eastern Ghats Supergroup in Odisha, India. They are characterized by conformable lenses containing minerals such as cryptomelane, romanechite, pyrolusite, todorokite, and pyrophanite, along with other opaque minerals like graphite, goethite and ilmenite. The gangue minerals associated with these ores include quartz, feldspar, garnet, kaolinite, apatite, sillimanite, zircon, biotite, alunite, and gorceixite. The primary elements present in the ore, Si, Mn, Fe, and Al, average at 16.20 %, 15.06 %, 11.94 %, and 6.6 % respectively. Additionally, trace amounts of P, K, Ti, Mg, Ca, and Na were detected. The average Fe/Mn ratio of 0.81 and the Si *versus* Al plot of the Anujurhi manganese ores suggest a hydrogenous-hydrothermal mixed source for the ferromanganese sediments. The characteristics of the manganese ore bands, absence of carbonate facies of ore, and geochemical association of Mn-Ba together with Na/Mg ratios and CaO-Na_2O-MgO ternary plot of the manganese ores strongly indicate that the mineralization is a metamorphosed shallow marine-lacustrine deposit. Following deposition and diagenesis, the manganese minerals underwent at least two phases of Ultra High Temperature (UHT) and granulite facies metamorphism along with the host rocks. Tectonic uplift, erosion, extended exposure to atmospheric oxygen and percolation of meteoric water led to the supergene alteration and remobilization of the primary manganese minerals in a colloidal state, followed by epigenetic replacement along the structural weak planes of the granulite facies rocks, resulting in the formation of the current deposits. This is evidenced by the observed secondary replacement and colloidal textures in the Mn oxides.

Izvleček

Članek obravnava manganove rude, ki se pojavljajo znotraj visokometamorfnih gnajsov predkambrijske supergrupe Vzhodni Gati na območju Anujurhi v zvezni deželi Odisha, Indija. Zanje so značilne konformne leče, ki vsebujejo minerale, kot so kriptomelan, romanehit, piroluzit, todorokit in pirofanit, skupaj z drugimi neprozornimi minerali, kot so grafit, goethit in ilmenit. Jalovinski minerali v teh rudah vključujejo kremen, glinenec, granat, kaolinit, apatit, silimanit, cirkon, biotit, alunit in gorceiksit. Primarni elementi prisotni v rudi so Si (16,20 %), Mn (15,06 %), Fe (11,94 %) in Al (6,6 %). Dodatno so ugotovili sledne vsebnosti P, K, Ti, Mg, Ca in Na. Povprečno razmerje Fe/Mn, ki znaša 0,81, in diagram primerjave vsebnosti Si z vsebnostmi Al v rudi z območja Anujurhi nakazuje, da feromanganovi sedimenti izvirajo iz mešanih hidrotermalnih virov. Značilnosti manganove rude, kot so odsotnost karbonatnega faciesa rude in geokemična povezava Mn-Ba skupaj z razmerji Na/Mg ter tri komponentnim diagramom CaO-Na_2O-MgO rud jasno kažejo, da gre za metamorfozirano plitvomorsko do jezersko nahajališče. Po odlaganju in diagenezi so manganovi minerali prestali vsaj dve fazi ultra visoke temperature (UHT) in metamorfizma granulitnega faciesa skupaj s prikamnino. Tektonski dvig, erozija, dolga izpostavljenost atmosferskemu kisiku in pronicanju meteorne vode so privedli do supergene spremembe in remobilizacije primarnih manganovih mineralov v koloidnem stanju, čemur je sledila epigenetska zamenjava vzdolž strukturno šibkih površin kamnin granulitnega faciesa, kar je povzročilo nastanek sedanjih ležišč. To dokazujejo opazovane sekundarne zamenjave in koloidne teksture v Mn oksidih.

Introduction

Manganese makes up about 0.1 to 0.2 % of the Earth's crust, ranking as the 10th most abundant element (Post, 1999). It exists in three different oxidation states in natural systems: +2, +3, and +4, leading to a variety of multivalent phases. Manganese oxide minerals have been utilized for many years by ancient civilizations for pigments and to clarify glass. By the mid-nineteenth century, manganese became a crucial component in the steel-making industry, which remains the main consumer of manganese ore. Manganese is the primary component in LMO (Lithium manganese oxide) and NMC (Lithium nickel manganese cobalt) batteries due to its cost-effectiveness compared to other battery metals and its abundant supply (Parrotti et al., 2023). Over 30 manganese oxide/ hydroxide minerals are found in various geological settings (Post, 1999).

The total resources/ reserves of manganese ore in India as of 2015 is 495.87 million tonnes. Odisha tops the total reserves/ resources with a 44 % share, followed by Karnataka at 22 % and Madhya Pradesh at 12 %. During 2018–19, the total production of manganese ore was 2.82 million tonnes with Madhya Pradesh as the leading producer of manganese ore at 33 %, followed by Maharashtra (27 %) and Odisha (16 %). Grade-wise, 68 % of the total production was of lower grade (below 35 % Mn), 21 % of medium grade (35–46 % Mn) and 10 % was of high grade (above 46 % Mn) (Indian Minerals Yearbook 2019).

To fulfill the large supply-demand gap of manganese due to the splurge in demand in the steel industry; the limited availability of high-grade (+44 % Mn) manganese ores coupled with the limitations of the domestic manganese ore, made it obligatory for revision of the threshold value of manganese ores to 10 % Mn in exploration and to exploit low-grade manganese ores. For the development or upgradation of low-grade ores, it is important to characterize or know the nature of the low-grade ores of our country, including the chemistry, mineralogy and correlation that will serve the future industrial development (Manganese Ore: Vision 2020 and beyond, IBM, 2014).

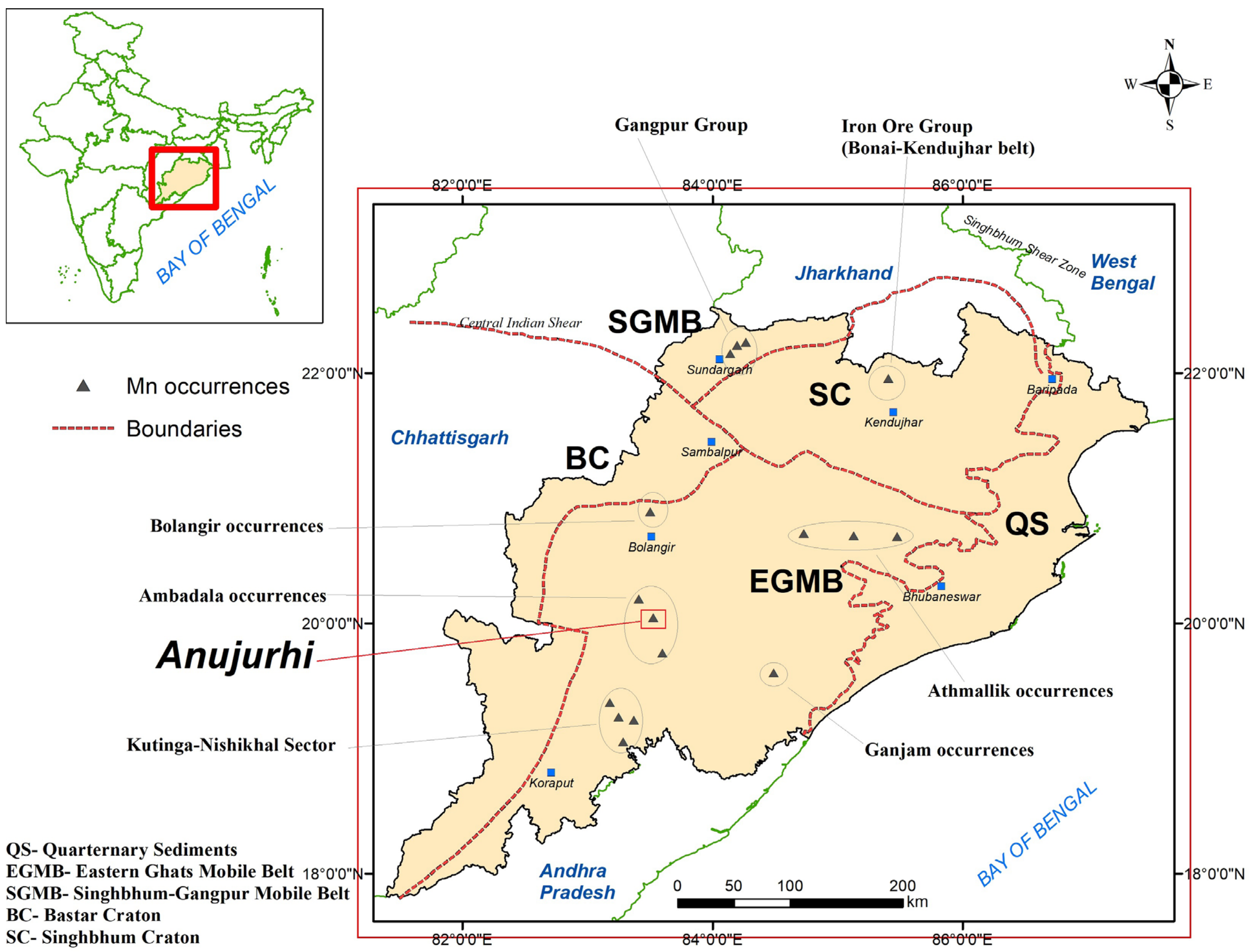

Fig. 1. Map of Odisha state showing the important domains (Cratons, Mobile belts and Quaternary sediment cover) and the known manganese occurrences (Map source- GSI, SU: Odisha).

In the state of Odisha, the manganese ore is found to occur in three stratigraphic horizons and spatially distributed wide apart i.e. Iron Ore Group in Bonai-Keonjhar belt (Roy, 2000), Gangpur Group in Sundergarh district and Eastern Ghats Supergroup in Koraput-Rayagada-Kalahandi-Balangir belt (Roy, 2000; Mishra et al., 2016). The manganese occurrences in the Eastern Ghat Mobile belt have been studied for their economic potential, mineralogical characteristics and evolutional history by several workers like Walker (1902), Dey (1942), Murthy et al. (1971), Narayanswamy (1966, 1975), Acharya et al. (1994, 1997), Ramakrishna et al. (1998), Nanda & Pati (1991), Jena et al. (1995), Rao et al. (2000), Rickers et al. (2001), Dasgupta and Sengupta (2003), Dash et al. (2005), Bhattacharya et al. (2011), Chetty (2014), Karmakar et al. (2009) and others.

The manganese deposits in the Anujurhi-Ambadala-Rukunibori-Loharpadar areas, collectively known as the Ambadala occurrence, confirm the presence of a continuous manganese ore zone spanning 150 km from the Kutinga-Nishikhal sector in the Koraput district of Odisha to the Uchhabapalli-Kanaital sector in the Bolangir district of Odisha (Fig. 1). The explored manganese occurrence is situated approximately 200 m east of Anujurhi village in the Rayagada district of Odisha and falls in Survey of India Toposheet no. 65M/5. This paper will provide an overview of the geology, mineralogy, and geochemistry of the manganese deposits in the Eastern Ghat Supergroup of rocks at Anujurhi, with a focus on characterizing the manganese ores as a potential future economic opportunity. The results obtained will be compared with similar deposits to develop a genetic model that determines the source and formation process of manganese in the Eastern Ghat Mobile Belt.

Geological Setting

The Eastern Ghats Mobile Belt (EGMB) is a Mesoproterozoic collisional orogen (Chetty, 2014), that extends along the east coast of India for over 900 km with a varying width from 50 km in the south to a maximum of 300 km in the north. EGMB or Eastern Ghats Belt (EGB) denotes a contiguous terrain of granulite facies rocks bounded to the north, west and south by the Singhbhum, Bastar and Dharwar Cratons (Dasgupta, 2019), and to the east it disappears underneath alluvial plains and the Bay of Bengal. The EGB consists of an intensely deformed and metamorphosed assemblage of meta-sedimentary and meta-igneous granulite facies rocks, which were subsequently intruded by Proterozoic anorthosite, alkaline rocks and granitoids. The metasedimentary rocks mainly include garnet-sillimanite gneiss (khondalite), quartzites and calc-granulites, while the meta-igneous rocks range from basic to felsic in composition and are essentially hypersthene-bearing charnockites (Chetty, 2014). The protoliths for the Khondalite Group is believed to be dominantly pelitic with subordinate arenaceous and calc- magnesian components (Ramakrishnan et al., 1998; Nanda, 2008) and is indicative of their formation in a shallow water stable shelf milieu (Roy, 2000 & 2006). The minimum age of sedimentation of the Khondalite Group points to an Archean event during 2.8 and 2.6 Ga from the available geochronological data (Roy, 2000).

Ramakrishnan et al. (1998) divided the Eastern Ghats Mobile Belt into four lithotectonic domains longitudinally, viz. Western Charnockite Zone (WCZ), Western Khondalite Zone (WKZ), Central Migmatite Zone (CMZ) and Eastern Khondalite Zone (EKZ). A Transition Zone (TZ) at the contact with the Bastar craton to the west is also marked by a prominent frontal thrust (Dasgupta et al., 2013). Rickers et al. (2001) subdivided EGMB into four crustal domains viz. Domain 1(1A & 1B), Domain 2, Domain 3 and Domain 4, whose boundaries do not match with those of Ramakrishnan et al. (1998) based on Nd-mapping carried out over EGMB. Nd-model ages presented contrasting protolith history in all four crustal domains with domain boundaries marked by prominent shear zones. Later, Dobmeier and Raith (2003) conceptualized EGMB as a collage of four isotopic provinces having distinct geological histories viz. Jeypore, Krishna, Eastern Ghats Province (EGP) and Rengali Province (Fig. 2).

EGB played a dominant role in the configurations of at least three supercontinents Columbia (≈ 1.9-1.4 Ga) (Rogers and Santosh, 2002; Zhao et al., 2002, 2004; Karmakar et al., 2009), Rodinia (≈ 1.0–0.75 Ga) (Li et al., 2008) and Gondwana (≈ 0.55–0.30 Ga). The central domain or EGP (Dobmeier & Raith, 2003) witnessed a prolonged accretion–collision history initiated with rifting and consequent ocean opening and sedimentation at ca. 1.50 Ga during the break-up of Columbia (Upadhyay, 2008; Karmakar et al., 2009) and culminated at ca. 0.90 Ga with the formation of supercontinent Rodinia. The latter united cratonic India with east Antarctica as a separate continent Enderbia that existed until about ca. 0.50 Ga (Karmakar et al., 2009; Dasgupta, 2019).

The metamorphic history of EGP was initiated by a high-T/low-P progressive metamorphism and deformation that eventually led to UHT

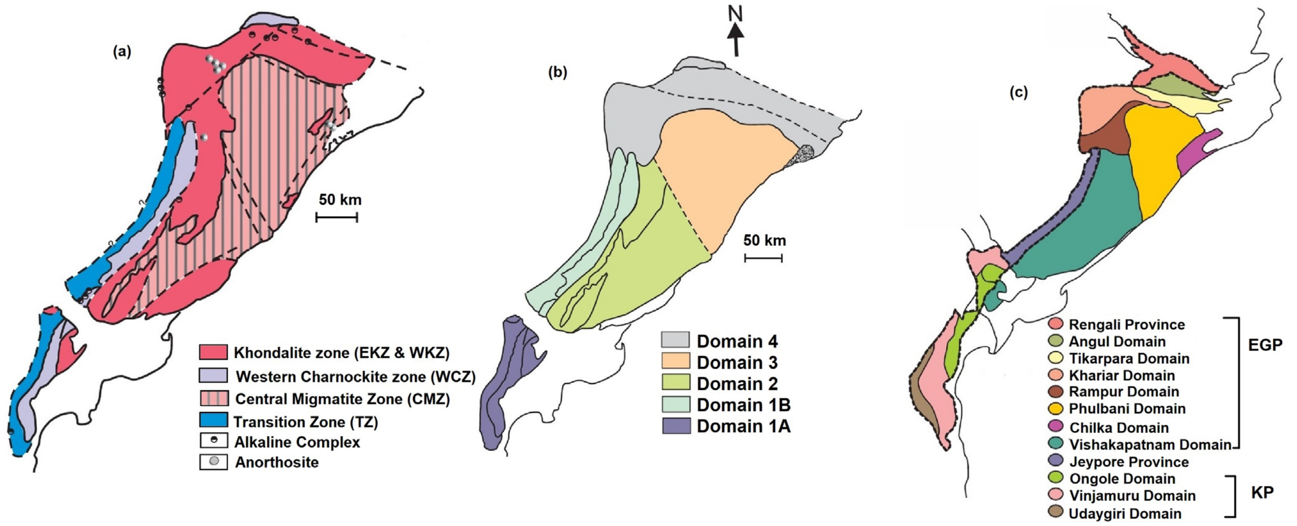

Fig. 2. (a) Geological map of EGB showing lithological divisions by Ramakrishnan et al. (1998), (b) Isotopic domains of EGB of Rickers et al., 2001, (c) Different provinces and domains of EGB by Dobmeier and Raith, 2003 (EGB- Eastern Ghats Belt, EGP- Eastern Ghats Province, KP- Krishna Province).

(~1000 °C) peak (M1-D1) under deep-crustal conditions (8-9 kbar) (Karmakar et al., 2009) ranged from 1.03 Ga (Bose et al., 2011) to 1.13 Ga (Korhonen et al., 2013). A second granulite-grade metamorphism and associated deformation (M2-D2) strongly reworked the deep-crustal granulites and exhumed them to mid-crustal level as evident from decompression-dominated retrogressive segment (Dasgupta & Sengupta, 2003; Dobmeier & Raith, 2003) at 0.95–0.9 Ga with peak conditions of around 7 kbar, 850 °C (Bose et al., 2011; Padmaja et al., 2022). M3 is a weak amphibolite grade overprint and mostly localized along ductile shear zones (Karmakar et al., 2009) constrained at ≈0.55-0.50 Ma (Karmakar et al., 2009). Thermal imprint associated with M3 is manifested by emplacement of pegmatite crosscutting the M2-D2 foliation (Karmakar et al., 2009).

Geology of the Anujurhi area

The area forms a part of the Central Migmatite Zone of Ramakrishnan et al. (1998), Domain 3 of Rickers et al. (2001) and EGP of Dobmeier and Raith (2003). The Khondalite Group comprises a sequence of garnet-sillimanite (± graphite) schists and gneisses (khondalite *senso-stricto*) with relatively minor quartzite and calc-silicate rocks. The manganiferous horizon at Anujurhi is mainly restricted to the contact of quartz-feldspar-garnet-sillimanite gneiss and garnetiferous quartzite.

The manganese mineralization at Anujurhi is both lithologically and structurally controlled and extends for a strike length of about 900 m. The ore zone is continuous with detached outcrops showing varying width ranging from 5 m to 24 m. Five distinct manganese ore lodes were established for the first time at 10 % manganese cut-off in Anujurhi area. The ore bands are narrow, discontinuous and lenticular in shape and parallel to the regional trend of rocks i.e. N20°E–S20°W with moderate dips towards southeast. The area has undergone polyphase deformation with at least three generation viz. F_1 folds are tight to isoclinal folds observed in quartzite/manganiferous quartzite and calc-granulite. The S_1 axial planar cleavage of F_1 folds is parallel to the primary bedding S_0. F_2 folds are mostly open upright mesoscopic folds recorded in calc-granulite and manganiferous quartzite and F_3 folds occur mainly as broad open warps in the khondalites and calc silicates.

Materials and Methods

As a part of the Annual Programme of Geological Survey of India (GSI) during Field Season 2016–2018, the Anujurhi area was investigated for manganese mineralization by way of mapping in detail on 2000 RF in 2 square kilometers to work out the local stratigraphy, structure and disposition of mineralized zones. Subsurface exploration by core drilling was carried out in eleven boreholes to establish the grade, extension and geometry of the ore bodies. Mapping was supported by laboratory studies like whole rock geochemistry, mineral chemistry and petrographic studies of samples from bedrock, pits, trenches and borehole cores. Bedrock samples from *in-situ* manganese ores and manganiferous quartzite were collected with utmost care. Pits and trenches were cut perpendicular to the strike of the ore zone to expose the bedrock and samples were collected by preparing small channels of 50 cm to 1 m in length depending on the width of the zone and mineralogical variation.

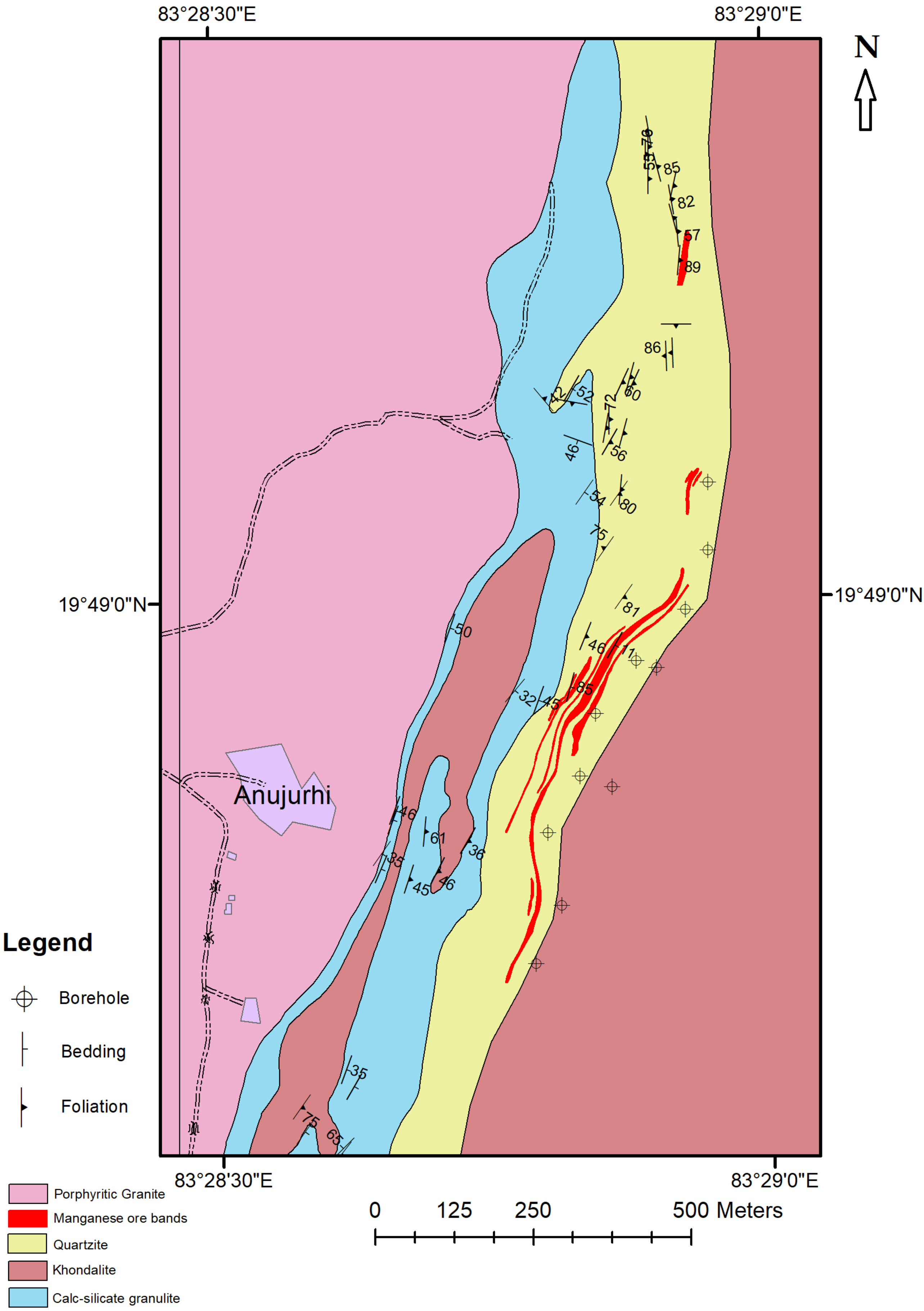

Fig. 3. Geological map of the Anujurhi area showing the manganiferous ore zones.

The core samples of the identified manganiferous zones were collected at a sample interval of 1 m from all the boreholes. Initially, the cores were split into half, half is preserved and the rest is sampled. All the samples collected from bedrock, pit, trench and borehole cores were then powdered manually using mortar and pestle to -120 mesh size. Two sets of samples are prepared by coning and quartering method where one set is submitted for analyses and a duplicate is preserved for future use.

Major element concentrations of 279 whole rock samples were determined through an X-ray fluorescence Spectrometer (Panalytical-ZETIUM) at the Chemical Laboratory, GSI, SU: Odisha by using the pressed pellet technique. The detection limits for this method range from 0.1 % for major and minor elements and 1.0 mg/L for trace elements. Samples from the manganiferous zones were studied under an optical microscope (Leica DM 2500P), the textures exhibited by the manganese ore are of secondary nature mainly replacement and colloform textures.

To confirm the minerals identified in optical microscopy, ten samples from bedrock, trench and cores were analyzed for X-ray diffractometry (XRD), operating at 40 kV and 30 mA with Cu Kα radiation with 1.54 Å wavelength (PANalytical, Model: X'Pert PRO XRD) at Mineral Physics Division, National Centre of Excellence in Geoscience Research, Geological Survey of India, Kolkata. Results are added in Supplementary material (Table 1).

Quantitative chemical analyses of mineral phases have been undertaken at the National Centre of Excellence in Geoscience Research, Geological Survey of India, Kolkata with an automated electron probe microanalyzer (SX 100 CAMECA) with five vertical spectrometers, operating at an acceleration voltage of 15 kV and beam current of 12 nA with beam size of 1 μm. Natural as well as synthetic standards were used during the analyses.

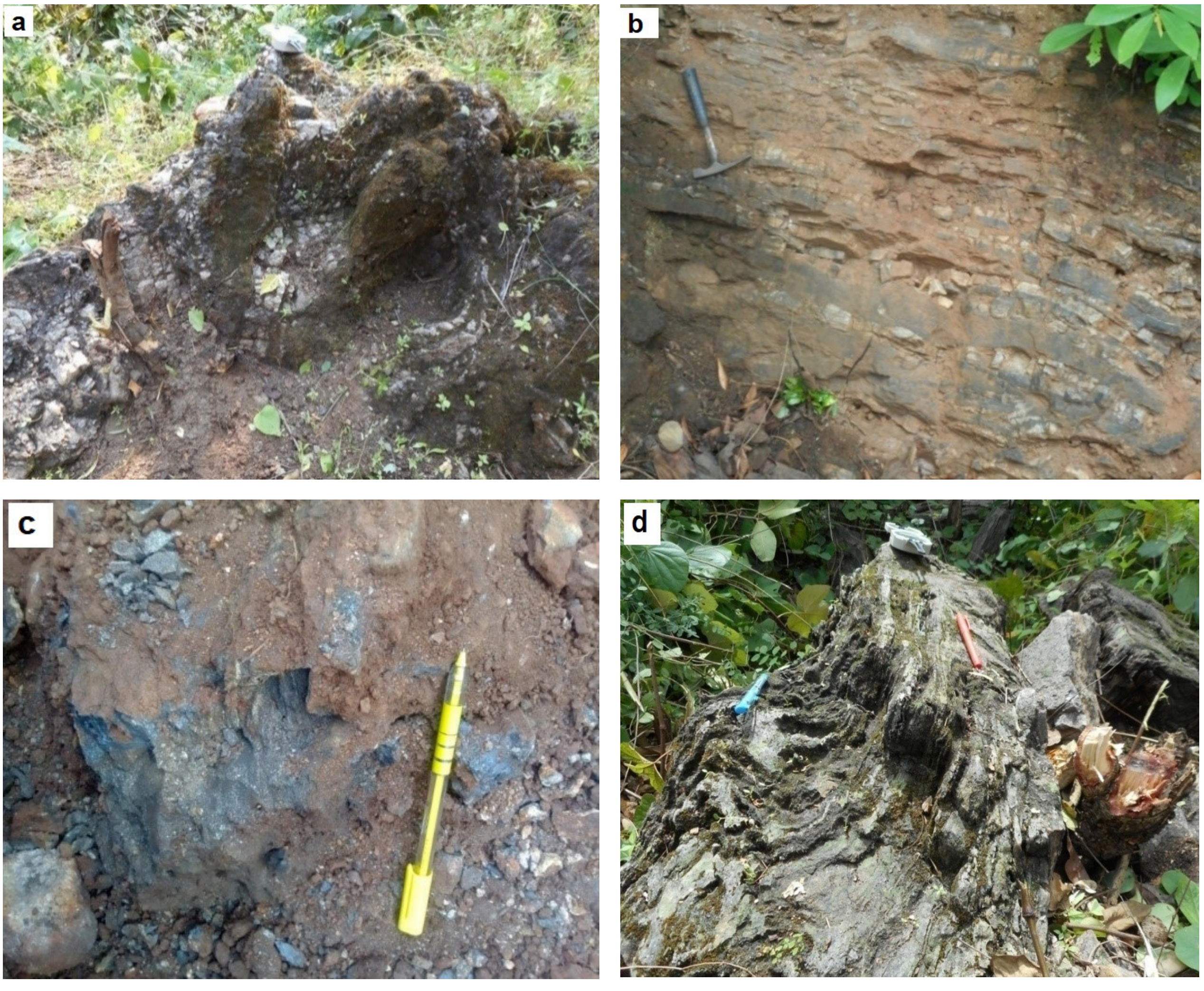

Fig. 4. Disposition of manganese ore zones in Anujurhi area, (a) Folded and silicified manganese ore within quartzite, (b) Fracture filling ore showing parallel bands of manganese ore and silica east of Anujurhi, (c) Soft, friable manganese ore mainly pyrolusite associated with kaolinite east of Anujurhi, (d) Folded manganiferous quartzite.

Results

Field Observations

The ore exhibits a hard, lumpy texture characterized by alternating bands of silica, primarily in the form of recrystallized quartz infilling fractures. In contrast, where associated with clay minerals (e.g. kaolinite) within khondalite, and interfolded with quartzite, the ore becomes soft, friable and powdery. (Fig. 4a, b, c & d).

Ore Petrography

The petrographic analyses revealed a mineral assemblage composed of primary minerals such as quartz (40–50 %), and garnet (10–15 %) respectively followed by Mn-oxides (20–25 %), graphite (5–10 %), goethite (5–10 %), clay minerals (<5 %) and Fe/Mn-Ti oxides (<1 %). The XRD analyses confirm the mineralogy. The chief Mn oxides identified in the area are cryptomelane, romanechite and pyrolusite with minor quantities of todorokite.

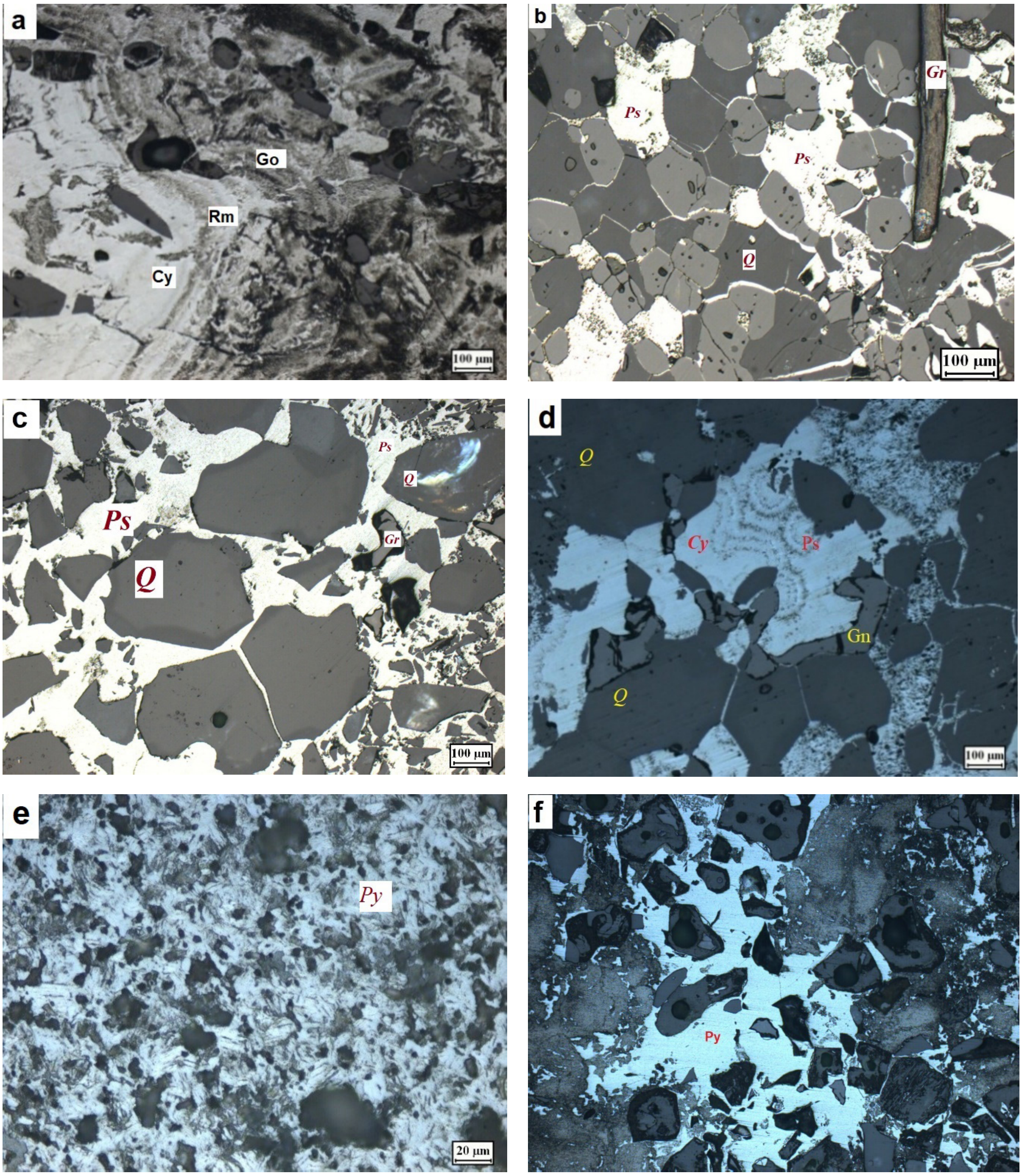

Fig. 5. (a) Colloform bands of cryptomelane (Cy), romanechite (Rm) and goethite (Go), (b) Mosaic grains of quartz & feldspar with fracture filling romanechite (Ps) and flakes of graphite (Gr), (c) Romanechite (Ps) as fracture filling with quartz (Q) and garnet (Gn), (d) Cryptomelane (Cy), Romanechite (Ps) showing colloform banding with quartz (Q) and garnet (Gn) as gangue minerals, (e) Pyrolusite (Py) associated with clay minerals & (f) Pyrolusite (Py) as fracture filling.

The associated gangue minerals are quartz, garnet, graphite, goethite, ilmenite, apatite and zircon, etc.

Since the Mn-oxides share very similar physical and optical characteristics, their identification only with the aid of an optical microscope is difficult, hence, the Mn-oxides were distinguished through EPMA. It is observed that pyrolusite is associated mainly with clay minerals like kaolinite and alunite due to alteration of the quartzo-feldspathic garnet-sillimanite schist or migmatised khondalite. Similarly, a positive correlation is observed between cryptomelane and which is further corroborated by EPMA data. Garnet is generally found as equigranular, mosaic grains associated with quartz and Mn-oxides. The chief ore mineral occupying the intergranular spaces is cryptomelane which forms colloform banding with romanechite and goethite (Fig. 5a, b, c & d). Pyrolusite is mainly confined to the cavity fillings and is often found associated with clay minerals (Fig. 5e & f).

Graphite occurs as scales and flakes within the manganese ores. Goethite is found as gangue showing box work structure, grey with moderate to high reflectivity. Fine crystals of apatite are found embedded in quartz, feldspar and garnet.

Geochemistry

Five representative samples of manganese ore and manganiferous quartzite underwent comprehensive analysis using Electron Probe Microanalysis (EPMA). The results clearly demonstrate that the dominant ore minerals present in the mineralized zones of the Anujurhi area are cryptomelane, romanechite and pyrolusite. Cryptomelane is essentially a potassium-bearing manganese oxide with minor amounts of Ba, Ca, Fe and Al. The K_2O content ranges from 1.93 to 5.24 %. Romanechite occurs together with cryptomelane as a secondary product of alteration of the primary minerals (Fig. 6a & b). BaO content in romanechite is very high which ranges from 16.88 to 18.71 % and Mn content ranges from 46.75 to 49.6 %. Pyrolusite is also present as veins in the host rock, i.e. quartz-feldspar garnet sillimanite schist. Mn content ranges from 60.5 to 61.4 % with minor amounts of Ba, Al and Si. With the EPMA results, the chemical formulae are cryptomlenane–$K_{0.62}(Mn_{7.65},Fe_{0.05},Al_{0.09},Si_{0.02})O_{16}$, romanechite–$(Ba_{0.59},K_{0.01})(Mn_{4.55},Al_{0.04},Si_{0.11})O_{10}$ and pyrolusite-$(Mn_{0.97}Si_{0.01}\ Al_{0.01}Fe_{0.01})O_2$.

The representative EPMA results for cryptomelane & pyrolusite, romanechite, garnet and F-Mn hydroxides are displayed in Table 1 to Table 3.

Garnet is associated with quartz and contains large amounts of Mn (averages of 18.89 %) and Si (averages of 17.47 %). The average Fe and Ca contents were 3.11 wt% and 9.19 wt% respectively. There is an inverse relationship between Mn and (Fe + Ca) results from Mn substitution into spessartines, which have the chemical formulae $[(Mn_{1.9}, Fe_{0.5}, Ca_{0.4})\ Al_2\ (SiO_4)_3]$ and is similar to the spessartine composition of supergene manganese occurrence at Southern Minas Gerais, Brazil (Parrotti, 2023). Two compositional varieties of garnet are reported from the manganese deposits of the Anujurhi area, one variety is rich in spessartine garnet (max. 68 %) whereas the other variety is rich in grossular garnet (max. 46 %) as calculated from the EPMA data. Alteration of the garnet proceeds along the grain boundaries and fractures, often leading to a distinct alteration rim with a

Table 1. Electron microprobe analyses (wt%) of cryptomelane & pyrolusite.

	1	2	3	4	5	6	7	8	9	10	11
SiO_2	0.06	0.1	0.15	0.17	0.1	0.06	0.59	0.15	0.81	0.6	0.69
Al_2O_3	0.31	0.22	0.14	0.24	0.23	0.82	2.68	0.35	0.79	0.86	0.79
MnO	77.84	79.36	78.27	78.4	78.1	75.42	67.39	65.3	78.11	79.32	78.47
MgO	0.07	0.01	0.03	0.01	0.05	0.03	0.04	0.04	0.04	0.06	0.07
Na_2O	0.06	0.17	0.1	0.11	0.07	0.02	0.03	0.13	0.04	0.03	0.02
P_2O_5	0	0	0	0	0	0	0	0	0	0	0
K_2O	4.11	3.98	4.02	4.49	3.9	5.24	4.43	2.3	0.61	0.64	0.59
CaO	0.44	0.49	0.53	0.46	0.45	0.62	0.4	0.48	0.16	0.14	0.19
TiO_2	0	0.02	0	0.02	0	0	0.01	0	0.02	0	0
FeO	0.11	0.11	0.1	0.09	0.2	0.25	3.47	0.02	0.66	0.7	0.53
Cr_2O_3	0	0	0.01	0	0	0	0.1	0	0.31	0.11	0.13
NiO	0	0	0.1	0	0.12	0.14	0.05	0	0.22	0	0.17
BaO	0.29	0.25	0.26	0.21	0.24	0.96	1.5	9.03	1.1	1.04	1.24

Cryptomelane-1 to 8, Pyrolusite-9 to 11

Table 2. Electron microprobe analyses (wt%) of romanechite.

	1	2	3	4	5
SiO_2	0.29	0.64	4.4	0.31	0.47
Al_2O_3	0.46	0.37	0.3	0.51	0.23
MnO	64.06	61.26	61.03	63.85	61.47
MgO	0.05	0.04	0.04	0	0.06
Na_2O	0	0.04	0.04	0.07	0.06
P_2O_5	0	0	0	0	0
K_2O	0.07	0	0.01	0.12	0.15
CaO	0.16	0.25	0.29	0.25	0.38
TiO_2	0	0	0	0	0
FeO	0.13	0.07	0.07	0.19	0.02
Cr_2O_3	0	0	0.2	0.05	0.03
NiO	0.07	0.02	0.01	0	0
BaO	16.88	18.71	17.93	17.2	17.02

central core (Fig. 6c). In rare cases, complete alteration of garnet is also observed. It alters to hydrous oxides/hydroxides of iron and manganese and subsequently cryptomelane (Acharya et al., 1994).

Goethite is a common secondary mineral derived from the alteration of other iron-rich minerals, especially magnetite, pyrite, siderite and hematite under oxidizing conditions. Goethite contains considerable amounts of Al, Si, P and Mn. Phosphorus content is the highest, varying from 0.54 to 2.88 % P_2O_5. Lepidocrocite although less common, has the same origins and they often occur together.

Clay minerals are found in abundance in some sections as a result of deep weathering of host rocks. Gorceixite is a hydrated phosphate ($BaAl_3(PO_4)(PO_3OH)(OH)_6$) that belongs to the alunite group of minerals. It is present as a weathering product of the host rocks like quartz-feldspar-garnet sillimanite schist in the ore zone. In some of the samples, romanechite can be seen altered to gorceixite. P_2O_5 content ranges from 25.43 to 28.76 % and BaO content ranges from 19.1 to 24.47 %. The high amount of phosphorus in samples from Anujurhi can also be attributed to the presence of gorceixite in most samples. Representative EPMA data of gorceixite are given Supplementary material (Table 2).

Pyrophanite in the Eastern Ghats Group of rocks from the Nishikhal area is also reported by Acharya et al. (1994) & in Ambadala area by Pradhan et al. (2016). Pyrophanite is a common accessory mineral associated with metamorphosed manganese-rich rocks. A zoned prismatic grain of ilmenite-pyrophanite is identified in BSE image within cryptomelane with TiO_2 concentration reducing from the center outwards suggesting ilmenite being replaced by Mn-oxides (Fig. 7d). Subhedral prismatic grain of zircons and apatite are rarely found. Representative EPMA data of gorceixite are given in Supplementary material (Table 3).

Table 3. Electron microprobe analyses (wt%) of garnet & Fe-Mn hydroxides.

	1	2	3	4	5	6	7
SiO_2	37.53	37.08	37.61	37.25	2.68	1.17	1.51
Al_2O_3	20.97	20.51	21.31	20.62	2.95	2.1	1.47
MgO	0.22	0.25	0.24	0.9	0.07	0.03	0.03
Na_2O	0.01	0	0.02	0.02	0.09	0.02	0.04
P_2O_5	0	0	0	0	0.54	1.89	2.88
K_2O	0	0.01	0	0	0	0.04	0
CaO	15.99	12.26	18.41	4.8	0.27	0.12	0.04
TiO_2	0.11	0.09	0.03	0.2	0.21	0.07	0.04
FeO	2.63	2.63	1.74	9.03	63.12	68.61	69.97
Cr_2O_3	0.02	0.04	0.03	0	0.07	0.12	0.06
NiO	0	0.02	0	0.1	0.09	0.54	0.22
BaO	0.07	0	0	0.09	0.56	0	0.11
MnO	22.05	27.38	19.45	28.68	7.68	0.9	1.35

Garnet-1 to 4, Fe-Mn hydroxides -5 to 7

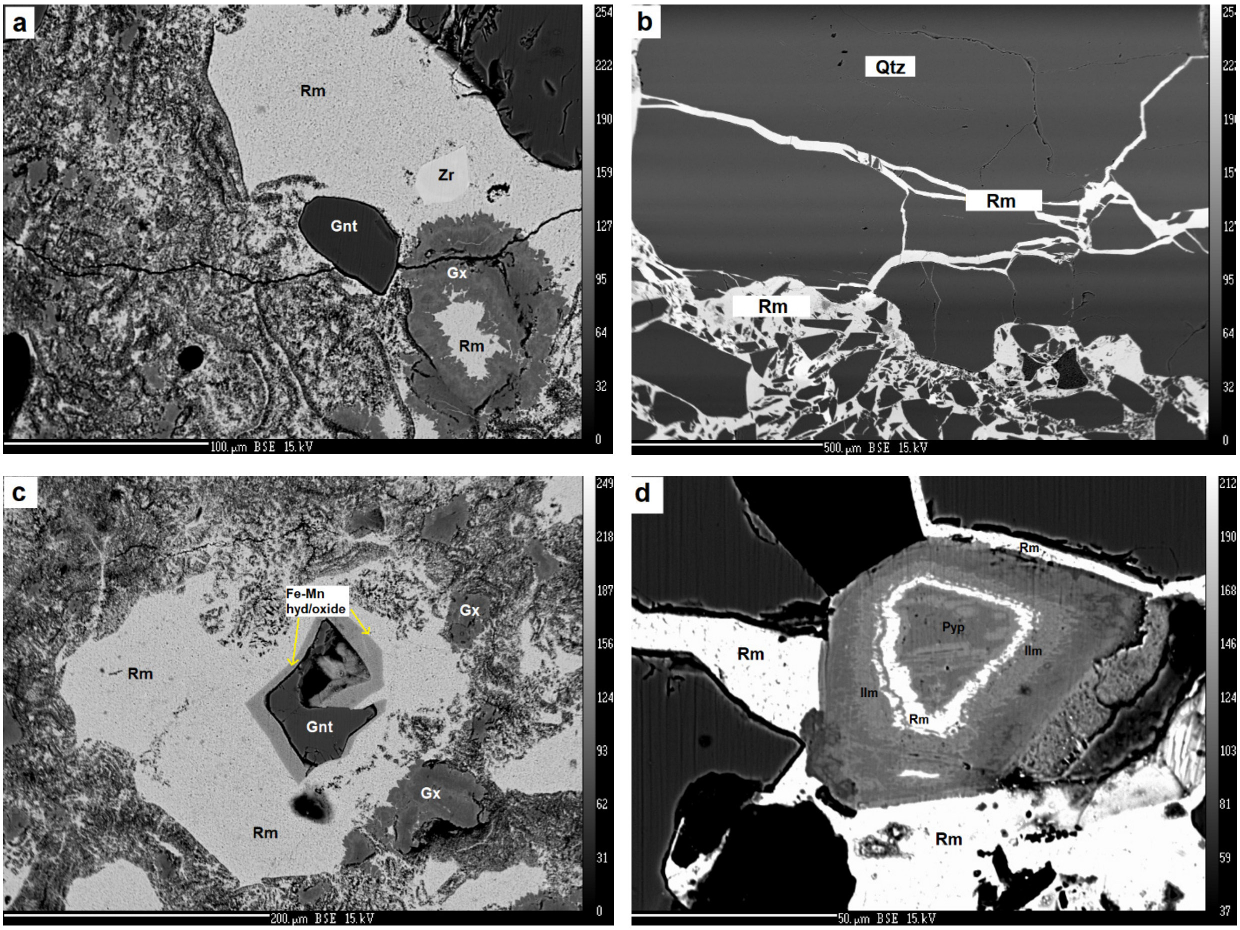

Fig. 6. Back-scattered electron images (EPMA) showing different textures (a) Romanechite (Rm) being altered by clay mineral gorceixite, (b) Romanechite (Rm) as fracture filling in brecciated quartz (qtz), (c) Garnet grains (dark grey) with alteration rims of oxides and/or hydroxides of manganese and iron, enclosed in a matrix of Romanechite (Rm) being altered to Gorceixite (Gx) & (d) ilmenite (Ilm)-pyrophanite (Pyp) zoning within Romanechite (Rm).

Discussion

Diagnostic elemental assemblages of major, minor, and trace metals can be utilized to differentiate manganese deposits formed in various geological environments (Acharya, 1994 & 1997). Such an approach is well established in non-metamorphosed ores (Nicholson, 1992 & 1997) but the application of such diagnostic geochemical signatures to metamorphosed sediments would assume that this signature has been preserved in the meta-sediments of EGB. This argument hinges on the assumption that the original sediment's chemical composition has been retained despite the recrystallization of the mineral assemblage. However, due to the absence of data on minor and trace elements, it was not feasible to accurately define the diagnostic assemblages for different sources of manganese. Upon thorough examination of the chemical data pertaining to the major oxides present in the ores, exhaustive efforts were undertaken to formulate a comprehensive genetic model for the manganese ores located in the Anujurhi area.

The major elements present in the manganese ores of the study area are Si, Mn, Fe and Al, each averaging at 14.82 wt%, 16.60 wt%, 12.42 wt%, and 6.43 wt%, respectively (Table 4). Other elements such as P, K, Ti, Mg, Ca and Na were found to be present in trace amounts (less than 1 wt %). Phosphorous content averaging 0.68 wt % is very high in comparison to other manganese deposits e.g., Noamundi-Koira basin, Odisha (Alvi & Mohd., 2021), Tokoro belt, Japan (Choi & Hariya, 1992) and is a distinguishing property of the manganese ores of EGMB. Phosphorus is either present as definite mineral phases such as apatite, fluor-apatite which is evident from strong positive correlation with Ca (Fig. 7) and gorceixite or in adsorbed state. In adsorbed state phosphorus also occurs within various manganese and associated iron mineral phases like cryptomelane and goethite (Rao et al., 2000). There is enrichment of Na-K-Ca-Mg in Anujurhi manganese ores which is diagnostic assemblage for marine manganese oxides (Nicholson, 1992).

Table 4. Representative chemical composition of manganese ores (wt%).

Sample	ANJ/1	ANJ/2	ANJ/3	ANJ/4	ANJ/5	ANJ/6	ANJ/7	ANJ/8	ANJ/9	ANJ/10
Si	12.53	17.37	16.56	20.35	14.52	15.11	8.69	5.40	17.12	14.91
Al	13.01	13.64	12.04	5.93	5.46	14.31	3.02	5.73	3.95	3.68
Mn	10.94	10.33	11.4	13.58	25.29	10.65	17.06	19.30	12.78	15.37
Fe (T)	8.64	6.35	8.37	11.54	4.03	6.69	27.25	24.54	16.61	18.26
Mg	0.16	0.19	0.20	0.14	0.20	0.14	0.07	0.22	0.02	0.03
Na	0.36	0.27	0.20	0.18	0.17	0.16	0.04	0.04	0.00	0.00
Ti	1.04	0.86	0.72	0.17	0.25	0.84	0.06	0.23	0.22	0.19
Ca	0.69	0.36	0.24	0.24	3.31	0.21	0.10	0.69	0.54	0.64
P	1.41	0.47	0.32	0.29	1.65	0.31	0.68	0.53	0.87	0.60
Mn/Fe	1.27	1.63	1.36	1.18	6.28	1.59	0.63	0.79	0.77	0.84
Si/Al	0.96	1.27	1.38	3.43	2.66	1.06	2.87	0.94	4.33	4.05

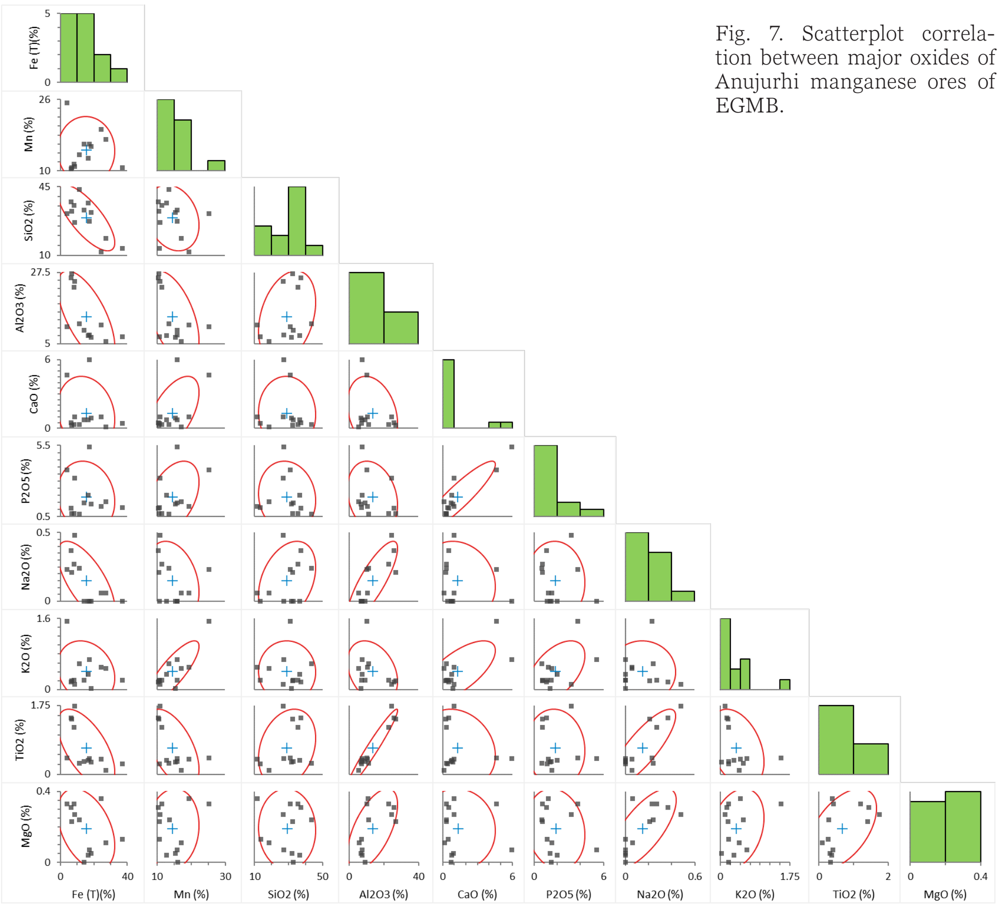

Fig. 7. Scatterplot correlation between major oxides of Anujurhi manganese ores of EGMB.

Genesis of manganese ores

The four sources of material for sedimentary manganese deposits are hydrothermal, hydrogenous, detrital, and diagenetic. Sea-floor hydrothermal crusts typically have fractionated Fe and Mn concentrations, resulting in either Fe-rich (Fe/Mn > 10) or Mn-rich (Fe/Mn < 0.1) deposits. On the other hand, the Fe/Mn ratio of hydrogenous ferromanganese sediments, such as deep-sea manganese nodules, averages about unity (Crerar et al., 1982). The Anujurhi manganese ores have an average Fe/Mn ratio of 0.81, ranging from 0.06 to 3.48, suggesting that the major source is hydrogenous ferromanganese sediments. Hydrogenous deposits are formed by the slow precipitation of Fe and Mn from seawater and are characterized by Mn/Fe ratios between 0.5 to 5 and a relatively high content of trace metals (Bonatti, 1972; Glasby, 1997), similar to that of the Nishikhal manganese ores (Acharya, 1997).

The Si/Al ratio can be used to differentiate between hydrothermal, hydrogenous, and detrital materials and sources (Crerar et al., 1982; Choi and Hariya, 1992). Hydrogenous ferromanganese nodules typically have a Si/Al ratio of about 3, which is characteristic of marine sediment. Ferromanganese crusts have a mean Si/Al ratio of 5.1, while iron-rich hydrothermal crusts exhibit exceptionally high Si/Al ratios ranging from 600 to 900, suggesting an additional source of Si in these deposits. Some hydrothermal manganese-rich crusts also show high Si/Al ratios, ranging from 10 to 20 (Toth, 1980). The Si/Al ratio in the studied manganese ore ranges from 0.82 to 37.76, with a mean ratio of 3.38 (Fig. 8). Most samples fall within the hydrogenous field, indicating a source from ferromanganese crusts and marine sediments. However, a few samples with high Si/Al ratios fall within the hydrothermal field, suggesting a possible hydrothermal source for some manganese ores. The significant presence of alumina in certain samples can be attributed to the abundant clay minerals resulting from the chemical weathering of host rocks.

The scatter plots of Na against Mg clearly distinguishes manganese oxides deposited in marine, shallow marine and freshwater environments (Nicholson, 1992). The plots of Na *versus* Mg (Fig. 9) lie in the freshwater field of Nicholson (1992) similar to the samples of Nishikhal & Kutinga areas (Acharya, 1994 & 1997). The association of Mn-Ba indicates a probable freshwater origin (Nicholson, 1992). Nonetheless, it's crucial to acknowledge that Ba is also enriched in hydrothermal mineralization (Nicholson, 1992).

The CaO-Na_2O-MgO ternary plot (after Dasgupta et al., 1999) shows that the Mn oxide ores are associated to both marine sedimentary environments and freshwater sedimentation in lakes (Fig. 10). In the Anujurhi area, the prevalence of oxide facies without any manganese carbonate mineral further suggests that the ores were deposited in highly oxidizing environments in shallow water, near shore, or shelf settings (Roy, 1981; Dasgupta et al., 1993; Nicholson et al., 1997). Additionally, the Fe-Si^{x}2-Mn ternary plot after Toth, 1980 also indicates that manganese originated from Fe-Mn crusts and nodules (Fig. 11). Ti is typically not mobile in hydrothermal solutions and is used to gauge the amount of clastic input (Choi & Hariya, 1992). A high concentration of Ti indicates the mixing of detrital material during precipitation, which is backed by a strong correlation between aluminum (Al) and titanium (Ti) as shown in Figure 12.

The khondalite succession consists mainly of shallow-water sediments including orthoquartzite-carbonate suite, arkoses, and semi-pelites, with manganese beds indicating a passive continental margin assemblage (Acharya, 1997; Ramakrishnan et al., 1998; Roy, 2006; Nanda, 2008). In the Anujurhi area, well-defined bands of manganese ore occur with the same strike and dip as the dominant foliation in the quartzite and quartz-feldspar-garnet-sillimanite gneiss. Additionally, the similar imprints of different phases of folds in manganese ore bodies and the country rocks strongly suggest that the manganese ores have developed as a syngenetic part of the metasedimentary sequence of the Eastern Ghats complex.

The sediments, primarily resulting from continental weathering and containing iron and manganese, were transported to deposition sites such as lakes or shallow seas through various mechanisms. These include being carried as finely divided particles in river waters, as adsorbed compounds on clay particles, and as sols and gels. The precipitation of iron and manganese in sedimentary

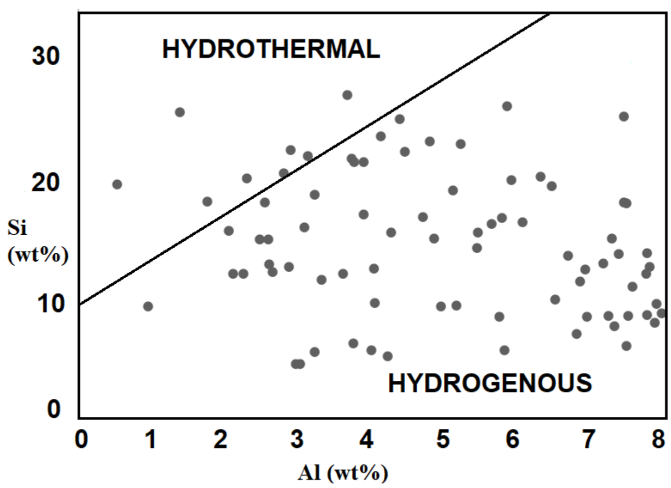

Fig. 8. Plots of Aujurhi manganese ore samples in the Si vs Al graph (Choi & Hariya 1992).

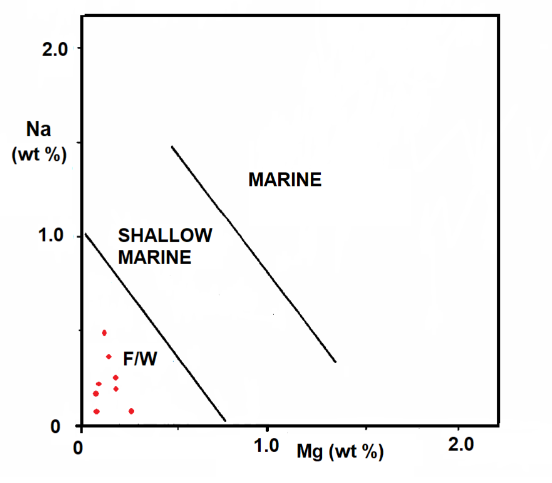

Fig. 9. Na vs Mg discrimination diagram of Nicholson (1992) showing Anujurhi manganese ore samples.

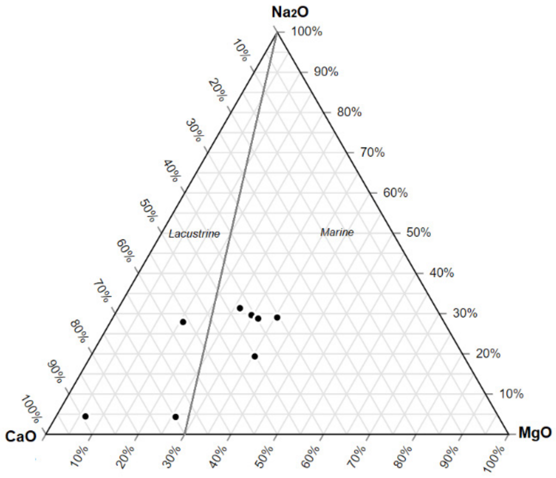

Fig. 10. CaO-Na_2O-MgO ternary plot after Dasgupta et al., 1999 shows majority samples falling in marine field for the manganese ore samples of Anujurhi, EGMB, Odisha.

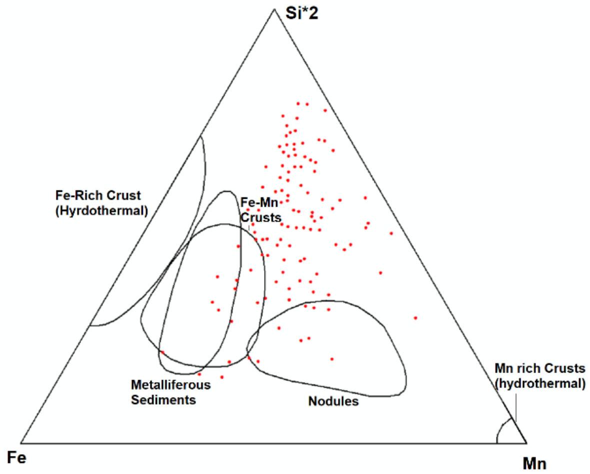

Fig. 11. Fe-Si*2-Mn ternary plot after Toth, 1980 showing the manganese ore samples showing affiliation towards Fe-Mn crusts and nodules.

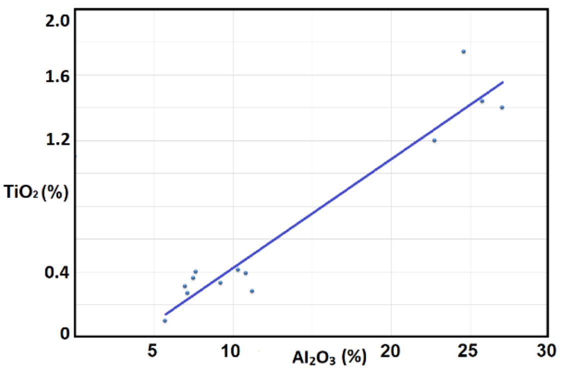

Fig. 12. TiO_2-Al_2O_3 diagram showing positive correlation for the Anujurhi samples.

environments is significantly influenced by Eh-pH conditions. Manganese is soluble at low Eh and precipitates with increasing Eh (under strongly oxidizing conditions) at a pH ranging from 5–8, which corresponds to the pH of surface water to seawater (Maynard, 1983; Nicholson et al., 1997). Iron and manganese may have precipitated as iron and manganese hydroxides and oxides (Mn^{4+}) in the presence of free oxygen. During early diagenesis, Mn^{4+} oxides are reduced to Mn^{2+} oxides through anaerobic reduction.

The model is supported by geochronological data indicating that the protolith ages of the meta-sedimentary rocks of Domain 3 in Eastern Ghats are approximately ≈ 2.2 Ga to 1.8 Ga (Rickers et al., 2001). This coincides with the worldwide first major deposition of sedimentary manganese during the early Paleoproterozoic era, lasting until 1.8 Ga, which occurred concurrently with the Great Oxygenation Event (GOE) between 2.45 Ga to 2.1 Ga (Spinks, 2018). These manganese ores have undergone multiple phases of deformation along with the host rocks, as evidenced by the folding of manganese ore bands and their parallel disposition to the S_2 foliation.

The manganese formations and associated host rocks have experienced at least two phases of ultra-high temperature (UHT) metamorphism at around 1100 Ma and granulite facies metamorphism at approximately 950-900 Ma, which are related to the breakup of the Supercontinent Columbia and the assembly of the Supercontinent Rodinia (Karmakar et al., 2009; Bose et al., 201; Dasgupta, 2019). With an increase in pressure and temperature during metamorphism, the manganese minerals of higher valency states were transformed into oxides of relatively lower valency (Roy, 1981; Acharya, 1997).

After the post-metamorphic period around 950-900 Ma, the Eastern Ghats and Rayner Complex amalgamated during the formation of the Supercontinent Rodinia (Karmakar et al., 2009). This caused tectonic uplift and prolonged exposure to atmospheric oxygen and percolation of meteoric water, leading to the alteration of primary minerals through supergene enrichment. The primary manganese oxide minerals were largely obliterated, evident from the absence of primary manganese oxides and alteration of Mn- silicate like spessartine. Under these supergene conditions, the strong oxidation effects caused a transformation of the lower valency manganese oxides (primary minerals) into higher valency oxides such as cryptomelane, romanechite, and pyrolusite (Acharya et al., 1994). An intriguing example of this transformation is the development of romanechite and/or cryptomelane and goethite from the manganese garnet (spessartine) i.e. supported by petrography and EPMA. The mineral-rich fluid may have journeyed through surface run-off or meteoric water to structurally weak planes like shear and fracture planes of the meta-sedimentaries, where Mn and

Fe reprecipitated as cavity filling and replacement deposits, predominantly containing quartz and feldspar. The replacement and colloidal textures of the secondary manganese oxides provide compelling evidence for this origin.

The remobilized supergene manganese ores occur as lensoidal ore bodies within the granulite facies of rocks of EGB, persisting for a significant strike length. These ore bodies have been confirmed to exist up to a depth of 30–35 m from the surface through drilling. The manganese content in these EGB ores, averaging around 15 %, is lower than that of the Iron Ore Group (Mohapatra et al., 2009) and can be classified as ferruginous manganese ore. The high phosphorus content in these ores presents a challenge for commercial recovery, as evidenced in the case of Kutinga-Nishikhal ores (Acharya et al., 1994 & 1997; Rao et al., 2000). However, characterizing these low-grade ores for their mineralogy and association could unlock promising prospects for future utilization. Hence, a thorough study of these ores in the future could be undertaken using Raman Spectroscopy in conjunction with Scanning Electron Microscope (SEM) studies, accompanied by trace element geochemistry analysis. This approach is expected to provide detailed insights into the mineralogy and geochemical behavior of the processes involved during the supergene enrichment and subsequent mobilization to form commercially viable deposits.

Acknowledgements

The authors would like to express their gratitude to the Deputy Director General of the Geological Survey of India, State Unit: Odisha, for providing administrative and financial support to this work between 2016 and 2018. The study was conducted as part of the mineral exploration project (FSPID: ME/ER/ODS/2016/008 & M2AFGBM-MEP/NC/ER/SU-ODS/2017/12919). The authors are also thankful to Shri Bijay Kumar Sahu, Retired Deputy Director General, GSI, and Shri Manoj Kumar Patel, Retired Deputy Director General, GSI, for their suggestions, guidance, and supervision during fieldwork. The authors express their appreciation to the personnel working in Petrological Lab of Odisha, the Chemical Lab of Eastern Region, Mineral Physics Division and EPMA lab of NCEGR at Central Headquarters, GSI, Kolkata, for their timely submission of results and cooperation during lab work.

Conflict of interest

The authors certify that there is no conflict of interest with any individual or any organization.

References

Acharya, B.C., Rao, D.S. & Sahoo, R.K. 1997: Mineralogy, geochemistry and genesis of Nishikhal manganese ore deposit, South Orissa, India. Min. Deposita, 32, 79–93. https://doi.org/10.1007/s001260050074

Acharya, B.C., Rao, D.S & Sahoo, R.K. 1994: Mineralogy and genesis of Kutinga manganese deposit, South Orissa, India. J. Min. Petr. Econ. Geol. 89: 317–328. https://doi.org/10.2465/ganko.89.317

Alvi, S.H. & Shaif Mohd. 2021: Geochemical signatures of manganese ores around Barbil, Noamundi-Koira basin, Singhbhum Craton, Eastern India. Geology, Ecology, and Landscapes, 5/4: 260–268. https://doi.org/10.1080/24749508.2020.1720489

Bhattacharya, S., Kar, S., Saw, A.K., Das & P. 2011: Relative Chronology in High-Grade Crystalline Terrain of the Eastern Ghats, India: New Insights. Int. Jour. Geosciences, 2: 398–405

Bhattacharya, A. & Gupta, S. 2001: A reappraisal of polymetamorphism in the Eastern Ghats belt – A view from north of the Godavari rift. Proc. Indian Acad. Sci, 110/4: 369–383. https://doi.org/10.1007/BF02702901

Bose, S., Dunkley, D.J., Dasgupta, S., Das, K. & Arima, M. 2011: India–Antarctica– Australia–Laurentia connection in the Paleo Mesoproterozoic revisited: evidence from new zircon U–Pb and monazite chemical age data from the Eastern Ghats Belt, India. Geol. Soc. of America Bulletin, 123: 2031–2049.

Chetty, T.R.K. 2014: Deep crustal Shear Zones in the Eastern Ghats Mobile Belt, India: Gondwana correlations. J. Ind. Geophysics. Union, 18, 19–56

Choi, J.H. & Hariya, Y. 1992: Geochemistry and depositional environment of manganese oxide deposits in Tokoro belt, northeastern Hokkaido, Japan. Econ. Geol. 87/5: 1265–1274. https://doi.org/10.2113/gsecongeo.87.5.1265

Crerar, D.A., Namson, J., Chyi, M.S., Williams, L. & Feigenson, M.D. 1982: Manganiferous Cherts of the Franciscan Assemblage: I. General Geology, Ancient and Modern Analogues, and Implications for Hydrothermal Convection at Oceanic Spreading Centers. Economic Geology, 77/3: 519–540. https://doi.org/10.2113/gsecongeo.77.3.519

Dash, C., Behera, S.N. & Patel, S.N. 2009: Delineation of potential Manganese ore bands/bodies within the Manganiferous horizon of the central sector of the Eastern Ghats Granulite Belt in Orissa covering parts of Bolangir, Kalahan-

di and Rayagada districts (P-II). Unpublised G.S.I report (2003-2005).
Dash, C. & Behera, S.N. 2009: Search for potential manganese ore bands/bodies within the manganiferous horizon of the eastern part of the Eastern Ghats granulite belt in Orissa covering parts of Angul and Boudh district s, (P - I). Unpublised G.S.I report.
Dasgupta, H.C., Sambasiva Rao, V.V. & Krishna, C. 1999: Geology, geochemistry and genesis of the freshwater, precambrian manganese deposit of the iron ore group from Noamundi basin, Eastern India. Indian J. Geol., 71: 247–264
Dasgupta, S. & Sengupta, P. 2003: Indo-Antarctic correlation: a perspective from the Eastern Ghats Granulite Belt, India. In: Yoshida, M., Windley, B.F. & Dasgupta, S. (eds.): Proterozoic East Gondwana: Supercontinent Assembly and Breakup. Geological Society, London, Special Publications, 206: 131–143.
Dasgupta, S. 2019: Petrological evolution of the Eastern Ghats Belt- Current status and future directions. IUGS, 43/1: 124–131. https://doi.org/10.18814/epiiugs/2020/020007
Dasgupta. S., Bose, S. & Das, K. 2013: Tectonic evolution of the Eastern Ghats Belt, India. Prec. Res., 227: 247–258. https://doi.org/10.1016/j.precamres.2012.04.005
Dobmeier, C.J. & Raith, M.M. 2013: Crustal architecture and evolution of the Eastern Ghats Belt and adjacent regions of India, Geol. Soc. Spec. Publ., 206: 145–168. https://doi.org/10.1144/GSL.SP.2003.206.01.09
Glasby, G.P. 1977: Marine manganese deposits. Elsevier Oceanography Series, 15. New Zealand: 45–52.
Jena, S.K., Devdas, V. & Bhattacharya, S.K. 2001: Final report on the exploration for manganese ore in Kutinga block and adjoining areas of Koraput, Rayagada and Bolangir districts, Orissa. Unpublished G.S.I report
Karmakar, S., Bose, S. & Dasgupta, S. 2009: Proterozoic Eastern Ghats Belt, India – a witness of multiple orogenies and its lineage with ancient supercontinents. Journal of the Virtual Explorer, Electronic Edition, 32, paper 3.
Korhonen, F.J., Clarke, C., Brown, M., Bhattacharya, S. & Taylor, R. 2013: How long-lived is ultrahigh temperature (UHT) metamorphism? Constraints from zircon and monazite geochronology in the Eastern Ghats orogenic belt, India. Prec. Res. 234: 322–350. https://doi.org/10.1016/j.precamres.2012.12.001
Li, Z.X., Bogdanova, S.V., Collins, A.S., Davidson, A., De Waele, B., Ernst, R.E., Fitzsimons, I.C.W., Fuck, R.A., Gladkochub, D.P., Jacobs, J., Karlstrom, K.E., Lu, S., Natapov, L.M., Pease, V., Pisarevsky, S.A., Thrane, K. & Vernikovsky, V. 2008: Assembly, configuration, and breakup history of Rodinia: A synthesis. Prec. Res., 160: 179–210. https://doi.org/10.1016/j.precamres.2007.04.021
Manganese Ore: Vision 2020 and Beyond 2014: Indian Bureau of Mines, Govt. of India, Ministry of Mines.
Maynard, J.B. 1983: Geochemistry of Sedimentary Ore Deposits. Springer-Verlag New York Inc.: 121–145
Nanda, J.K. 2008: Tectonic Framework of Eastern Ghats Mobile Belt. An Overview. Memoir Geological Society of India, 74: 63—87.
Nicholson, K. 1992: Contrasting mineralogical-geochemical signatures of manganese oxides: Guides to metallogenesis. Economic Geology, 87/5: 1253–1264.
Nicholson, K., Hein, J.R., Buhn, B. & Dasgupta, S. 1997: Manganese Mineralization: Geochemistry and Mineralogy of Terrestrial and Marine Deposits. The Geological Society Special Publication, 119.
Padmaja, J., Sarkar, T., Sorcar, N., Mukherjee, S., Das, N. & Dasgupta S. 2022: Petrochronological evolution of Mg-Al granulites and associated metapelites from the contact zone of the Archean Bastar Craton and Proterozoic Eastern Ghats Province, and its implications. Geosystems and Geoenvironment, 1/4: 100041. https://doi.org/10.1016/j.geogeo.2022.100041
Parrotti, D.D., da Conceição, F.T. & Navarro, G.R.B. 2023: The Mineralogy, Geochemistry and Origin of the Supergene Manganese Occurrences in the Southern Minas Gerais, Brazil. Minerals, 13/9: 1216. https://doi.org/10.3390/min13091216
Post, J.E. 1999: Manganese oxide minerals: Crystal structures and economic and environmental significance. Proc. Natl. Acad. Sci. USA, 96/7: 3447–3454. https://doi.org/10.1073/pnas.96.7.3447
Pradhan, S., Mishra, P.P., Dash, N., Mishra, P.C., Khaoash, S. & Mohapatra, B.K. 2016: Manganese mineralization in parts of Eastern Ghats around Ambadola, Rayagada District, Odisha. Vistas in Geological Research, Special Publication in Geology, 14: 42–48.
Ramakrishnan, M., Nanda, J.K. & Augustine, P.F. 1998: Geological evolution of the Proterozoic Eastern Ghats mobile belt. Proc. Workshop on Eastern Ghats Mobile Belt, Geol. Surv. Ind., Spec. Publ: 44.

Rao, D.S., Acharya, B.C., Sahoo & R.K. 2000: Role of mineralogy, mineral chemistry and geochemistry in mineral processing: A case study for high phosphorus manganese ores of Nishikhal, South Orissa, India. Processing of Fines, 2: 25–40.

Rickers, K., Mezger, K. & Raith, M.M. 2001a: Evolution of the continental crust in the proterozoic Eastern Ghats belt, India and new constraints for rodinia reconstruction: implications from Sm-Nd, Rb-Sr and Pb-Pb isotopes. Prec. Res. 112: 183–210.

Rogers, J.J.W. & Santosh, M. 2002: Configuration of Columbia, a Mesoproterozoic supercontinent. Gond. Res., 5: 5–22.

Roy, S. 1981: Manganese Deposits. Academic Press, London.

Roy, S. 2000: Late Archean initiation of manganese metallogenesis: its significance and environmental controls. Ore Geol. Rev., 17: 179–198.

Roy, S. 2006: Sedimentary manganese metallogenesis in response to the evolution of the Earth system. Earth-Science Reviews, 77: 273–305.

Spinks, S.C., Thorne, R.L., Sperling, E., White, A., Armstrong, J., leGras, M., Birchall, R. & Munday, T. 2018: Sedimentary Manganese as Precursors to the Supergene Manganese Deposits of the Collier Group; Capricorn Orogen, Western Australia. CSIRO, Australia. EP18235. 36.

Toth, J.R. 1980: Deposition of submarine crusts rich in manganese and iron. Geological Society of America Bulletin, Part I, V. 91: 44–57. https://doi.org/10.1130/0016-7606(1980)91%3C44:DOSCRI%3E2.0.CO;2

Upadhyay, D. 2008: Alkaline magmatism along the southeastern margin of the Indian shield: implications for regional geodynamics and constraints on craton-Eastern Ghats Belt suturing. Prec. Res. 162: 59–69. https://doi.org/10.1016/j.precamres.2007.07.012

Walker, T.L. 1902: Geology of Kalahandi State, Central Provinces. Memoir, Geological Survey of India, 33: 1–22.

Zhao, G., Cawood, P.A., Wilde, S.A. & Sun, M. 2002: Review of global 2.1-1.8 Ga orogens: implications for a pre Rodinia supercontinent. Earth Sci. Rev., 59/1–4: 125–162. https://doi.org/10.1016/S0012-8252(02)00073-9

Zhao, G., Sun, M, Wilde, S.A. & Li, S. 2004: A Paleo Mesoproterozoic supercontinent: assembly, growth and breakup. Earth Sci. Rev., 67: 91–123. https://doi.org/10.1016/j.earscirev.2004.02.003

GEOLOGIJA 67/2, 301-315, Ljubljana 2024
https://doi.org/10.5474/geologija.2024.015

Localised multi-hazard risk assessment in Kyrgyz Republic

Ocena tveganja večkratnih nevarnosti v Kirgiški republiki

Ruslan UMARALIEV[1], Vitalii ZAGINAEV[2], Daurbek SAKYEV[3], Dimitar TOCKOV[4], Madina AMANOVA[3], Zarangez MAKHMUDOVA[1], Kydyr NAZARKULO[1], Kanatbek ABDRAKHMATOV[5], Abdurashit NIZAMIEV[6], Rui MOURA[7] & Kevin BLANCHARD[1*]

[1]United Nations World Food Programme, Country Office in the Kyrgyz Republic (UN WFP); *corresponding author: kevin.blanchard@wfp.org
[2]Mountain Societies Research Institute, University of Central Asia, Kyrgyz Republic (UCA)
[3]Emergency Monitoring and Forecasting Department, Ministry of Emergency Situations of the Kyrgyz Republic (MES)
[4]United Nations Office for Disaster Risk Reduction (UNDRR)
[5]Institute of Seismology of the National Academy of Sciences of the Kyrgyz Republic (ISNASKR)
[6]Osh State University, Kyrgyz Republic (OSU)
[7]University of Aveiro, Portugal (UAVR)

Prejeto / Received 17. 9. 2024; Sprejeto / Accepted 21. 11. 2024; Objavljeno na spletu / Published online 16. 12. 2024

Key words: Natural hazard, Risk, Exposure, Vulnerability, disaster risk reduction, disaster risk management, Suzak district

Ključne besede: Naravne nevarnosti, tveganje, izpostavljenost, ranljivost, zmanjševanje tveganja nesreč, obvladovanje tveganja nesreč, obmoje Suzak

Abstract

One of the key tasks in ensuring national security is the ability of the state and society to recognise and effectively assess the conditions for disasters, and to prevent them from threatening the sustainable development of the country. The Kyrgyz Republic is highly vulnerable to the influence of climate change, which in turn affects the frequency and intensity of disasters. The Kyrgyz Republic is exposed to almost all types of geological and man-made hazards, including earthquakes, landslides, debris flows, flash floods, outbursts of mountain lakes, dam failures, avalanches, droughts, extreme temperature, epidemics and releases of hazardous substances. Analysis of information on existing risks and their control systems used to reduce their negative impact makes it possible to assess the degree of probability, the expected consequences of threats, determine the degree of risk, the adaptive potential of communities and select appropriate protective measures. Therefore, this study is conducted to assess the hazard, vulnerability and exposure of Suzak district (Jalal-Abad oblast) in order to quantify the risk of the study area using multi-parameter holistic assessment with field collecting of primary data and utilizing Index-based Risk Assessment approach based on applying INFORM Risk model. Collected data was used to downscale subnational INFORM Risk model for municipal and district level using a multi-layered structure. A risk score is calculated by combining 72 indicators that measure three main dimensions: hazard & exposure, vulnerability, and lack of coping capacity. These findings provide an opportunity to develop a more effective disaster risk management at the local and national levels, by prioritizing relevant actions and investments for municipalities – districts which are demonstrated relatively highest risk scores. Also, the possibility of applying localized risk assessment procedures provides an opportunity to obtain more accurate sub-national (district/oblast based) and national levels with effective assessing dynamics of risk.

Izvleček

Ena izmed ključnih nalog pri zagotavljanju nacionalne varnosti je sposobnost države in družbe, da prepoznata in učinkovito ocenita pogoje za nesreče ter preprečita, da bi te ogrozile trajnostni razvoj države. Kirgizistan je zelo ranljiv za vplive podnebnih sprememb, ki vplivajo na pogostost in intenzivnost nesreč. Izpostavljen je skoraj vsem vrstam geoloških nevarnosti in tudi nevarnostim, ki jih povzroči človek, vključno s potresi, zemeljskimi plazovi, blatnimi tokovi, hudourniki, izbruhi gorskih jezer, porušenji jezov, snežnimi plazovi, sušami, ekstremnimi temperaturami, epidemijami in sproščanjem nevarnih snovi. Analiza informacij o obstoječih tveganjih in njihovih nadzornih sistemih, ki se uporabljajo za zmanjšanje njihovega negativnega vpliva, omogoča oceno stopnje verjetnosti, pričakovanih posledic, določitev stopnje tveganja, prilagoditvenega potenciala skupnosti in izbiro ustreznih zaščitnih ukrepov. V tem članku prikazujemo oceno nevarnosti, ranljivosti in izpostavljenosti okrožja Suzak (v regiji Džalal-Abad) z namenom kvantificiranja tveganja z uporabo večparametrske celostne ocene z zbiranjem primarnih podatkov na terenu in uporabo pristopa ocenjevanja tveganja na podlagi indeksa INFORM. Zbrani podatki so bili uporabljeni za prilagoditev regionalnega modela tveganja INFORM za občinsko in okrožno raven z uporabo večplastne strukture. Ocena tveganja je izračunana s kombinacijo 72 kazalnikov, ki merijo tri glavne dimenzije: nevarnost in izpostavljenost, ranljivost in pomanjkanje sposobnosti obvladovanja. Ti rezultati omogočajo razvoj učinkovitejšega upravljanja tveganj nesreč na lokalni in nacionalni ravni, s prednostnim določanjem ustreznih ukrepov in naložb za občine – okrožja, ki imajo relativno najvišje ocene tveganja. Možnost uporabe lokaliziranih postopkov ocenjevanja tveganja omogoča pridobitev natančnejših ocen tveganja na regionalni (okrožni/območni) in nacionalni ravni z učinkovitim ocenjevanjem dinamike tveganja.

Introduction

In recent years, many countries have experienced significant negative impacts from disasters related to the effects of climate change, particularly in the high mountain regions of Asia (Liu et al., 2021; Khanal et al., 2023; Havenith et al., 2017). The Kyrgyz Republic is affected by landslides, especially in the southern regions (Golovko et al., 2017). Catastrophic debris and mud flows affect communities in mountains and valleys, especially in the northern Tien-Shan (Erokhin et al., 2018; Zaginaev et al., 2019). The entire territory of the Kyrgyz Republic is located in a high seismic zone (Kalmetieva et al., 2009). The last major landslide (estimated volume was 10^6 m^3) event in Aysai village (29.04.2017), Uzgen district (Osh oblast) damaged 7 houses and killed 24 people. Recent flash floods in the south of the Kyrgyz Republic (Jalal-Abad oblast) in May 2022 and 2024 damaged facilities and eroded agricultural fields worth tens of thousands of USD. The occurrence of rockfalls and rockslides represents a significant risk to the stability of critical infrastructure, including road and railway networks. On all strategic roads within the Kyrgyz Republic, which connect the various regions, geological hazards present a considerable threat. The potential for rockslides in Boom Gorge on the Bishkek-Karakol road represents a particular concern, given its role as the only direct route connecting the Issyk Kul and Chui oblast, and the potential impact on food security.

To minimize potential losses from disasters, it is necessary to develop effective strategies for disaster risk reduction (DRR) and resilient systems based on risk assessment (Peduzzi et al., 2009). It is important to note that a large majority of worldwide disasters occur in developing countries, where the effect of disasters tends to cancel out real growth in the countries (Long, 1978).

The importance of implementing effective risk reduction practices is confirmed by modern global concepts of sustainable development and the Sendai Framework for Disaster Risk Reduction 2015-2030 in the climate change context (Kelman, 2015). By applying effective DRR practices, even countries with low levels of economic capacity can achieve tangible results in building resilience, ensuring the stability of effective growth even when disasters strike. At the same time, the resources, preserved from possible destruction are directed towards ensuring the most important sectors of development - healthcare, education, social protection, etc., thereby protecting the development gains from the risk of disaster.

To monitor the development of hazardous natural processes in the Kyrgyz Republic, specialized work is regularly carried out by various scientific institutions and agencies within the system of integrated disaster monitoring as part of the disaster risk management policy implemented by the Ministry of Emergency Situations of the Kyrgyz Republic (MES). However, a major challenge is the lack of sufficient information for comprehensive risk assessments at the local level, which hampers the implementation of preventive measures. In order to better understand and assess the risk, a comprehensive approach was taken to collect all locally available information for a pre-selected pilot site. The Suzak district of Jalal-Abad oblast was selected as the pilot site because it is the most exposed to natural hazards, both in terms of the number of disasters registered over the last 30 years and the frequency of occurrence. Considering the population growth rate in the Fergana Valley (Rahmonov, 2022) and the lack of arable land, there is a risk that urban agglomerations will expand into the development zones of hazardous exogenous geological processes.

Study site

The Kyrgyz Republic (KR) is a mountainous, land-locked, lower-middle-income country in Central Asia that has abundant natural resources and potential for the expansion of its hydroelectricity production, agriculture sector, and tourism industry (UN WFP, 2020). The territory is located between two major mountain systems, the Tien Shan and the Pamir. The total area of Kyrgyz Republic is about 199 900 km^2. The Kyrgyz Republic is bordered by Kazakhstan to the north, Uzbekistan to the west, Tajikistan to the southwest, and China to the east. Approximately 94 % of the country is above 1,000 m elevation, and 40 % is above 3,000 m. Over 80 % of the country is within the Tian Shan Mountain chain and 4 % is permanently under ice and snow. The Kyrgyz Republic had a population of 7.3 million in 2023. Most of population lives in the foothills of the mountains and is centered around two urban conurbations, the capital Bishkek and Chuy Valley in the north, and in the south of the country between Osh and Jalal-Abad cities and the eastern edge of the Ferghana Valley. A widespread use of small-scale family-based farms coupled with land degradation makes the agricultural sector rather inefficient (UN ESCAP, 2018). As a result, the country faces moderate to severe food insecurity touching nearly 24 % of the total population and a high dependence on imports of basic food items (UN WFP, 2020).

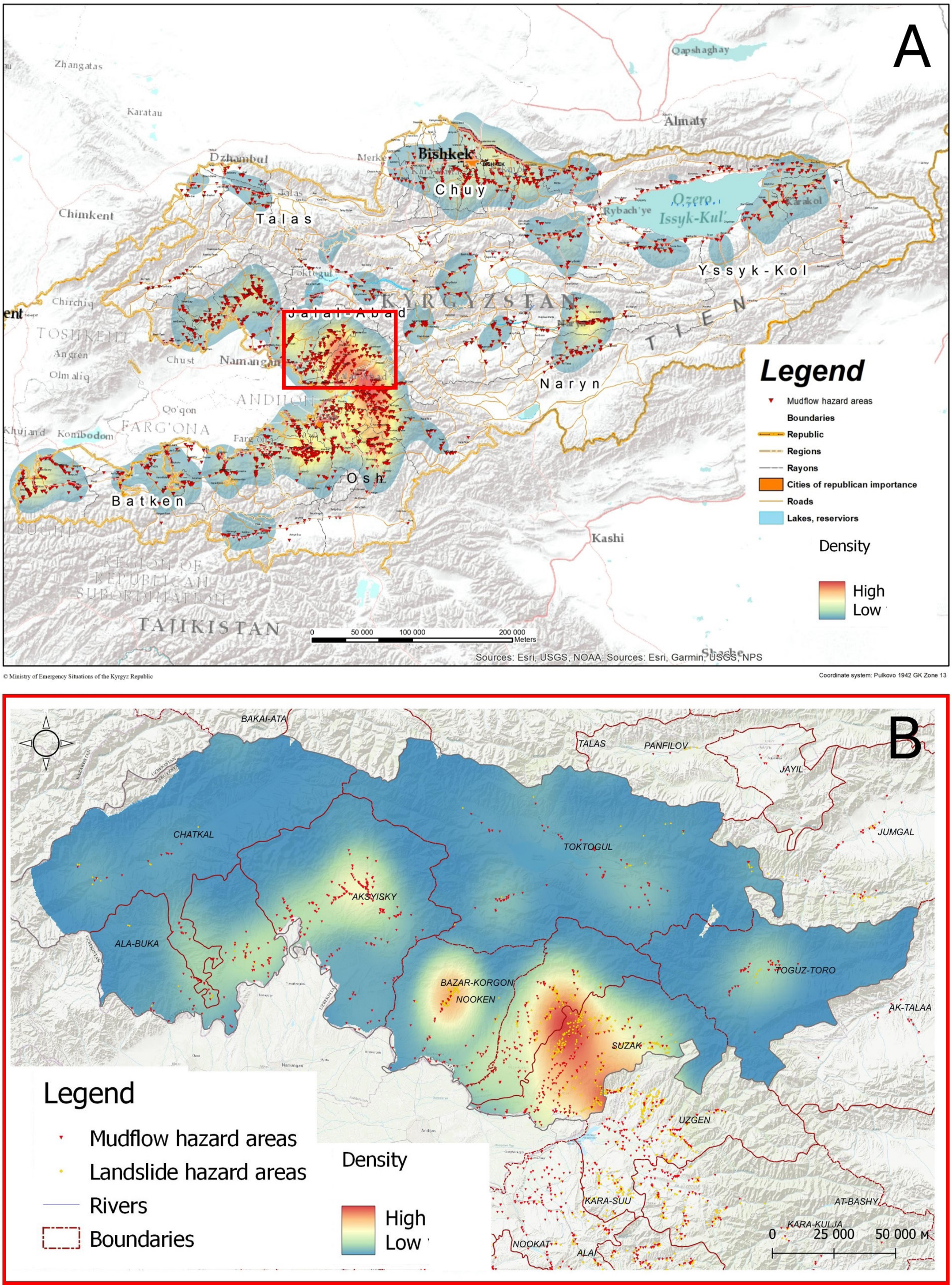

Fig. 1. Susceptibility map by debris and mud floods and landslides of A. Kyrgyzstan, B. Jalal-Abad oblast (data from MES KR).

The Kyrgyz Republic is highly susceptible to natural hazards such as debris and mud floods, landslides, avalanches and earthquakes. According to different estimates, the total absolute multi-hazard Average Annual Loss (AAS) for the Kyrgyz Republic is between USD 92.68 million (UN ESCAP, 2018) and USD 146 million (World Bank, 2011). Of this total multi-hazard AAS, earthquakes contribute 67.54 % and riverine floods 32.46 %. The multi-hazard AAL is heavily concentrated in the southern part of the country - in Osh and Jalal-Abad oblasts (provinces) that together account for almost 50 % of the total multi-hazard AAL (28.86 % and 20.49 % respectively), followed by the Chuy oblast (13.91 %) and Bishkek (10.27 %). Kyrgyz Republic's aggregate loss as a percentage of gross national income is the highest among all Central Asian countries (World Bank, 2011).

Figure 1 A shows a map of Kyrgyzstan with zones based on the occurrence of emergency situations (the most common hazard processes: mudflows and landslides) for the period from 1991 to 2023. The zones with the highest density of debris and mud flows and landslides are located in the southern part of the country: Jalal-Abad and Osh oblasts (Fig. 1 A).

Figure 1B shows the events analysed for the Jalal-Abad oblast. The most affected district in Jalal-Abad oblast is Suzak district, total area of Suzak district is about 3 019 km².

To analyze the existing hazard and risk assessment mechanisms at the local and national levels, a study was conducted to analyze the range of environmental conditions in one of the most hazard-prone regions of the Kyrgyz Republic - Suzak district (Jalal-Abad oblast) on Figure 2, located in the foothills surrounding the Fergana Valley on

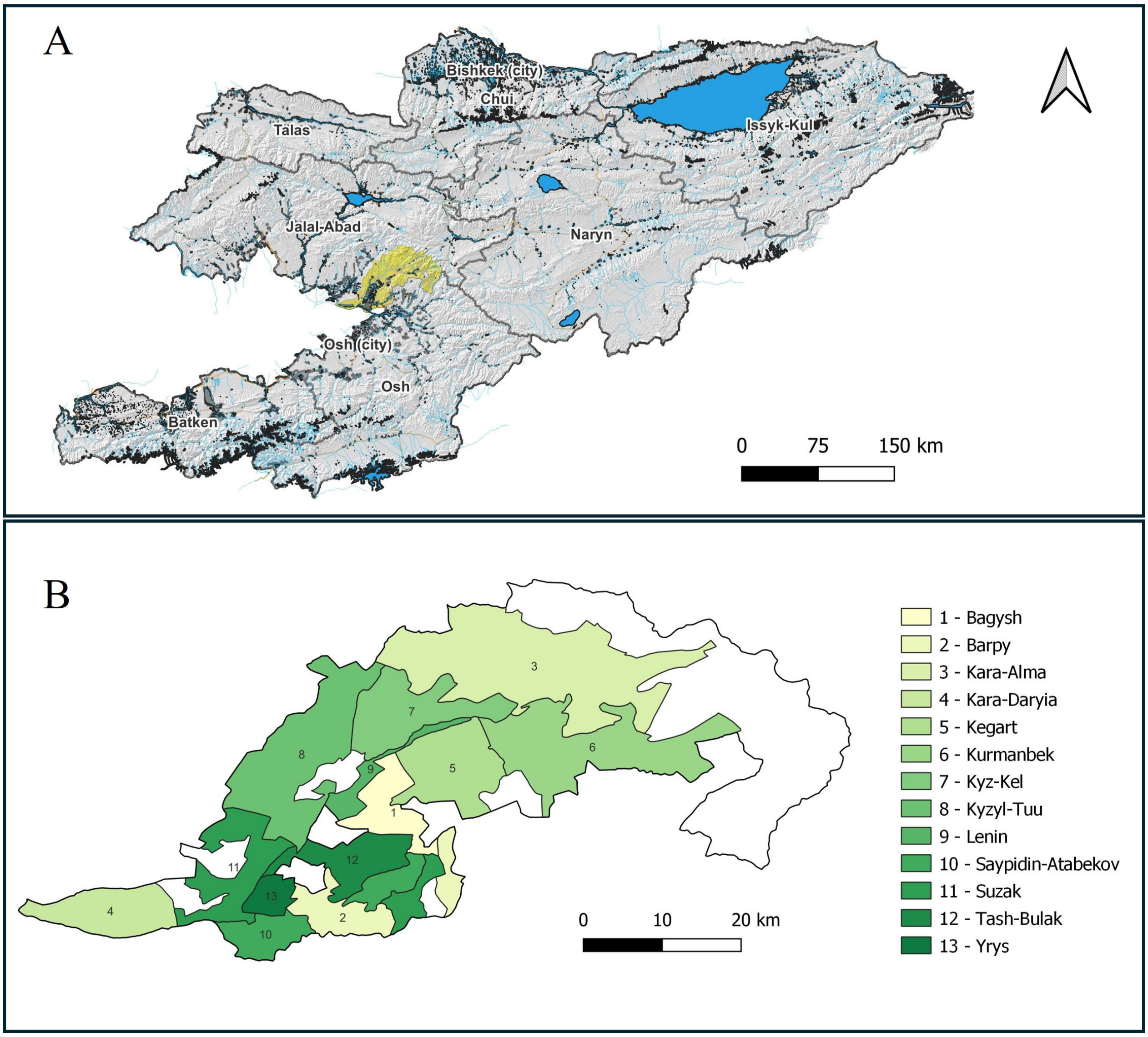

Fig. 2. A. Location of Suzak district; B. Municipalities of Suzak district.

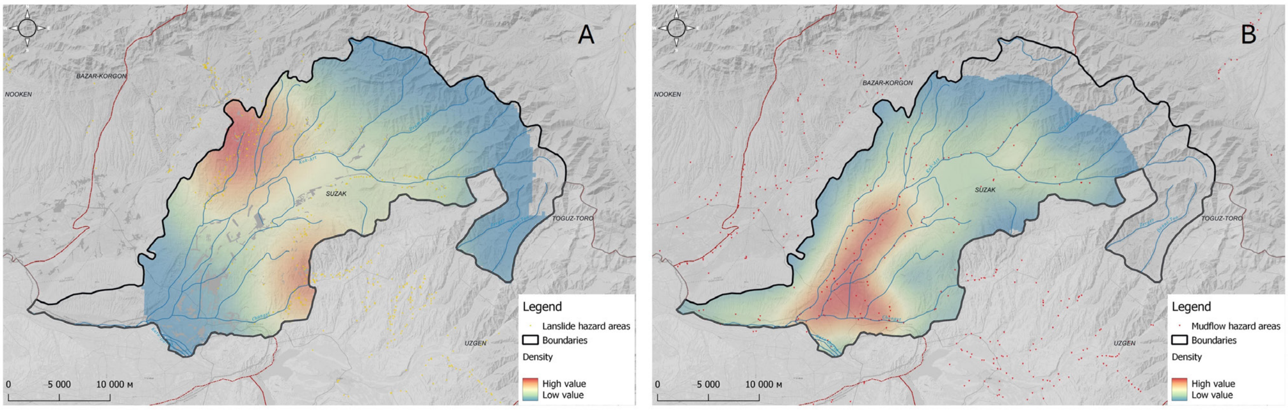

Fig. 3. A. landslide hazard B. Debris and mudflow hazard (Suzak district, Jalal-Abad oblast).

the northeast. In the spectrum of hazards, the territory of the district is most exposed to mudflows and landslides, these are the most developed types of hazards and disasters for the Kyrgyz Republic (in terms of the cases, damage, and losses).

In Figure 3, can be observed that all the settlements (grey blocks) are located in the most hazardous landslide and debris and mudflow areas.

The study area is also characterized by the highest underlying vulnerability indicators - large population, high density, and poverty levels - that increase the level of risk.

Material and methods

This work was carried out in three stages, with the initial field collection and preliminary quantitative analyses of several indicators characterizing hazard, exposure and vulnerability (based on the current methodological experience of the MES), and the subsequent selection of the most relevant indicators that can integrally represent each risk factor (based on the INFORM Risk model (Marin-Ferrer, 2017) developed by the European Union Joint Research Centre (EU JRC)). The INFORM Risk model was chosen for adaptation in this study - as one of the most informative and visually effective methods of presenting data, based on the classical principles of risk assessment and having a well-developed principle of demonstrating and visualizing the risk assessment mechanism. However, the study collected baseline data and compiled a database of 73 different risk components on municipal level within one district. Data were collected in various ways (ground observations, measurements and mapping using UAVs, instrumental measurements, various modelling techniques, statistical data analysis). Based on these data, an initial quantitative assessment of hazard, exposure, and vulnerability have been conducted. As part of these actions, the existing level of understanding and practice of risk assessment and its main factors in the state system (Ministry of Emergency Situations (MES) and local self-government bodies), the technical capabilities of the state system to ensure rapid and centralized collection of the necessary data to produce centralized analysis of multi-risk data were also assessed.

Over the past decade, several quantitative and index-based approaches to risk assessment have been developed. All these approaches are based on the conceptual disaster risk equations developed by Blaikie (Blaikie, 2014), Alexander (Alexander, 2000), Dilley (Dilley, 2005), Van Westen (Van Westen. 2009), Umaraliev (Umaraliev, 2020) and the risk assessment principles of the European Commission (EU strategy, 2009) and the United Nations (UNISDR, 2015). The applied conceptual equation of disaster risk was considered as a function of hazard, vulnerability and exposure:

$$Risk = Hazard\ (H) \times Vulnerability\ (V) \times Exposure\ (Ex) \quad (1)$$

Alternatively, considering the contribution of resilience (UNISDR, 2015), this equation less common than (1):

$$Risk = \frac{Hazard\ (H) \times Vulnerability\ (V) \times Exposures\ (Ex)}{Resilience\ (Rs)} \quad (2)$$

The INFORM Risk model also has three dimensions: Hazard & Exposure, Vulnerability and Lack of Coping Capacity. Each dimension includes different categories, which are user-driven concepts related to the needs of humanitarian and resilience actors. The INFORM Risk Model is based on the risk concepts described above and includes three dimensions of risk: Hazards & Exposure, Vulnerability and Lack of Coping Capacity. They are conceptualized in a reciprocal relationship: the risk of what (natural and human hazards) and the risk to what (population).

The INFORM Risk model balances two major forces: the hazard & exposure dimension on one side, and the vulnerability and the lack of coping capacity dimensions on the other side. Hazard dependent factors are treated in the hazard & exposure dimension, while hazard independent factors are divided into two dimensions: the vulnerability dimension that considers the strength of the individuals and households relative to a crisis situation, and the lack of coping capacity dimension that considers factors of institutional strength. The INFORM Risk model adopts the three aspects of vulnerability reflected in the UNDRR definition. The aspects of physical exposure and physical vulnerability are integrated in the hazard & exposure dimension, the aspect of fragility of the socio-economic system becomes INFORM Risk's vulnerability dimension while lack of resilience to

Table 1. Overview of localised (municipality level) Risk for Suzak district components and indicators under the Hazard and Exposure dimension.

Category	Component	Indicators	Source
Natural	Earthquakes	Number of significant earthquakes in the last 10 years	MES, Field-works, UAV assessment
	Floods	Coastal erosion in the last 10 years, quantity	
		Coastal erosion in the last ten years, km	
		Debris and mud flows	
		Landslide (area)	
		Landslide (number)	
	Landslides	Activity of mudflow-prone rivers	WFP/MES Study on "Conducting a set of research works on vulnerability and hazard assessment in order to integrate effective principles of disaster risk assessment into the national disaster monitoring system of Suzak district of Jalal-Abad oblast"
		Presence of forest plantations on landslide-prone slopes	
		Presence of floodplain forests	
		Rockfalls and rockslides, in the last 10 years, number	MES statistic, Field-works, UAV assessment
		Avalanches, in the last 10 years, number	
	Climate change	Climatic water deficit	FAO Eath Map
		Aridity Index	
	Wildfires	Incidence of wildfires (including forest fires)	MES statistic
		Total number of people dead due to forest fires	
	Population	Presence of dangerous infections (plague, cholera, anthrax, malaria)	WFP/MES Study on "Conducting a set of research works on vulnerability and hazard assessment in order to integrate effective principles of disaster risk assessment into the national disaster monitoring system of Suzak district of Jalal-Abad oblast"
		Population density (people per sq. km of land area)	National Statistical Committee of Kyrgyzstan
		Average household size	
		Children under 5 (% of total population)	
		Availability of educational institutions in the municipality in case of emergency	WFP/MES Study on "Conducting a set of research works on vulnerability and hazard assessment in order to integrate effective principles of disaster risk assessment into the national disaster monitoring system of Suzak district of Jalal-Abad oblast"
Human	Transport accidents	Transport accidents in the last 10 years	MES statistic
		People dead due to transport accidents in the last 10 years	
	Technological hazards	Number of dumpsites	Zoï Environmental Network
		Approximate air distance from pesticides dumpsite	
		Potential Hazardous Lakes	MES statistic
		Presence of industries that may pose risks of climate change	WFP/MES Study on "Conducting a set of research works on vulnerability and hazard assessment in order to integrate effective principles of disaster risk assessment into the national disaster monitoring system of Suzak district of Jalal-Abad oblast"

cope and recover is treated under the lack of coping capacity dimension. The split of vulnerability in three components is particularly useful for tracking the results of disaster reduction strategies over time. Disaster risk reduction activities are often localized and address particular community-level vulnerabilities and capacities.

To accommodate the INFORM Risk methodology, where the vulnerability variable is split among three dimensions, the equation is updated to:

$$Risk = Hazard\&Exposure^{1/3} \times Vulnerability^{1/3} \times Lack\ of\ coping\ capacity^{1/3} \quad (3)$$

This is a multiplicative equation where the risk equals zero if any of the three dimensions is zero. Theoretically, in case of debris and mudflows there is no risk if there is no likelihood of a debris flows to occur or/and the hazard zone is not populated or/and if the population is not vulnerable (e.g., all people have high level of education and live in high level of health and livelihood condition as well as they can afford protective houses/livelihoods) or/and if the resilience of the country to cope and recover is ideal.

Hazard & Exposure

The hazard & exposure dimension reflects the probability of physical exposure associated with specific hazards. There is no risk if there is no physical exposure, no matter how severe the hazard event is. Therefore, the hazard and exposure dimensions are merged into hazard & exposure dimension. As such it represents the load that the community has to deal with when exposed to a hazard event. The disaster risk analysis based on a large number of studies, data and sources, including such key indicators as exposure - the location of people, infrastructure, housing, production facilities and other tangible human assets in areas prone to threats, vulnerability - conditions that increase the susceptibility of a person, community, property or systems to the impact of threats, long-term statistics of emergencies that resulted in loss of life, harm to human health or the environment, significant economic damage and disruption of human life conditions, indicate that the prevailing risk disasters for the population. The dimension comprises two categories: natural hazards and human-induced hazards, aggregated with the geometric mean, where both indexes carry equal weight within the dimension. The Natural Hazard category encompasses physical exposures to primary disasters like earthquakes, floods, landslides, climate change, and wildfires. Conversely, the Human Hazard category quantifies risks using normalized values from transport and industrial accidents. The table below provides an overview of the components and indicators used to populate the localised Risk Index for Suzak district, specifically for the hazard and exposure dimension, as well as the calculation of INFORM categories and dimensions (Table 1).

Vulnerability

Humanitarian organizations primarily focus on people, who constitute the ‘at-risk’ element in the Risk composite index. The impact of disasters on people in terms of number of people killed, injured, and made homeless is predominantly felt in developing countries while the economic costs of disasters are concentrated in the industrialized world. The Vulnerability dimension addresses the intrinsic predispositions of an exposed population to be affected, or to be susceptible to the damaging effects of a hazard, even though the assessment is made through hazard independent indicators. So, the vulnerability dimension represents economic, political and social characteristics of the community that can be destabilized in case of a hazard event. Physical vulnerability, which is a hazard dependent characteristic, is dealt with separately in the hazard & exposure dimension. There are two categories aggregated through the geometric average, socio-economic vulnerability and vulnerable groups. Socio-economic component incorporates components of Development & Deprivation, Gender Inequality, Agriculture and Economy to calculate the normalized index. The indicators used in each category are different in time variability and the social groups considered in each category are the target of different humanitarian organizations. The second category of the applied Vulnerability assessment includes Children under five, Disaster preparedness, Uprooted people, Other vulnerable groups, and Food Security. If the first category refers more to the demography of a country in general, the vulnerable group category captures social groups with limited access to social and health care systems. The following table present an overview of components and indicators used for filling the Risk Index for Suzak district indexes (vulnerability dimension adopted from INFORM Risk model), and calculation of risk categories and dimensions (Table 2).

Table 2. Overview of localized (municipality level) Risk components and indicators under the Vulnerability dimension piloted in target district.

Category	Component	Indicators	Source
Socio-Economic Vulnerability	Development & Deprivation	Share of population that has income below the poverty line	Ministry of Labour, Social Security and Migration of the Kyrgyz Republic (MLSSM)
	Gender equality	Share of women (as % of total population)	National Statistical Committee of Kyrgyzstan (NSC)
		Women educational attainment	
	Agriculture	Energy and energy efficiency Index	WFP/MES Study on "Conducting a set of research works on vulnerability and hazard assessment in order to integrate effective principles of disaster risk assessment into the national disaster monitoring system of Suzak district of Jalal-Abad oblast"
		Number of households dependent on the condition of pastures as a percentage	
		Number of households dependent on soil conditions (farming)	
		Adequacy of sown areas	
		Water sufficiency for irrigation	
	Economy	Availability of tourist places and destinations to accommodate tourists in the municipality	WFP/MES Study on "Conducting a set of research works on vulnerability and hazard assessment in order to integrate effective principles of disaster risk assessment into the national disaster monitoring system of Suzak district of Jalal-Abad oblast"
		Rainfall in summer destroys pasture infrastructure	
		Heavy snowfalls block passes and roads, limiting life support and access to medical care	
		Unemployment rate (people unemployed in total population)	Ministry of Labour, Social Security and Migration of the Kyrgyz Republic (MLSSM)
		Dependency of population from remittances	WFP/MES Study on "Conducting a set of research works on vulnerability and hazard assessment in order to integrate effective principles of disaster risk assessment into the national disaster monitoring system of Suzak district of Jalal-Abad oblast"
Vulnerable Groups	Children U5	Child Mortality	National Statistical Committee of Kyrgyzstan (NSC)
	Disaster preparedness	Victims or deaths in the municipality as a result of disasters	WFP/MES Study on "Conducting a set of research works on vulnerability and hazard assessment in order to integrate effective principles of disaster risk assessment into the national disaster monitoring system of Suzak district of Jalal-Abad oblast"
		Number of large-scale emergency situations in the last 10 years	MES
	Uprooted people	Number of migrants (internal and external)	National Statistical Committee of Kyrgyzstan (NSC)
	Other vulnerable groups	Number of families with disabled people	Ministry of Labour, Social Security and Migration of the Kyrgyz Republic (MLSSM)
	Food Security	Food availability score	WFP
		Food access score	
		Food utilization score	
		Food stability score	

Lack of Coping Capacity

For the coping capacity dimension, the question is which issues the government has addressed to increase the resilience of the society and how successful their implementation is. The coping capacity dimension measures the ability of a country to cope with disasters in terms of formal, organized activities and the effort of the country's government as well as the existing infrastructure which contribute to the reduction of disaster risk. It is aggregated by a geometric mean of two categories: institutional and infrastructural. The difference between the categories is in the stages of the disaster management cycle that they are focusing on. The 'Institutional' category focuses on DRR programs targeting mitigation and the preparedness/ early warning phases, while the 'Infrastructural' category assesses capacities for emergency response and recovery. Institutional category incorporates components of Governance, Disaster risk reduction and humanitarian, while Infrastructure category is consistent of: Communication, Physical

Table 3. Overview of localised (municipality level) Risk components and indicators under the Lack of Coping Capacity dimension piloted in target district.

Category	Component	Indicators	Source
Institutional	Governance	Self-organization and potential of the local community	WFP/MES Study on "Conducting a set of research works on vulnerability and hazard assessment in order to integrate effective principles of disaster risk assessment into the national disaster monitoring system of Suzak district of Jalal-Abad oblast"
		Share of population covered by emergency training	
		Availability of qualified emergency personnel and training centers	
	DRR	Availability of recommendations from the MES and whether work is being done to improve safety	
		Emergency response exercises	
	Humanitarian	Availability of local volunteer teams	
Infrastructure	Communication	Individuals using the Internet (% of population)	
		Mobile cellular subscriptions (per 100 people)	
	Physical Connectivity	Road density coefficient	
		Roads' density (field and muddy roads)	
		Roads density (automobile roads)	
	Water and Sanitation	Frequency of power outages	
		Availability of a central water supply system	
		Quality of drinking water	
		Sufficiency of water supply sources	
		Interruptions in drinking water	
	Access to health care	Availability of healthcare services (availability of primary care facilities)	
		Staffing with medical workers	
		Mortality of the population	
	Ecology	Greening of the locality	
		Presence of forest shelterbelts along roads and highways	
		Air quality in the municipality (winter)	
		Air quality in the municipality (summer)	
		Street lighting	

Connectivity, Water and Sanitation, Access to health care and Ecology. The table below presents an overview of the components and indicators used to populate the localised Risk Index for Suzak district, specifically focusing on the lack of coping capacity dimension, along with the calculation of risk categories and dimensions adopted from INFORM Risk model (Table 3).

Results

Hazard and Exposure of the municipalities of Suzak district

The territory of Suzak district is primarily associated with earthquakes, floods, mudflows, droughts, landslides, industrial and transport accidents, large fires, epidemics, mass infectious diseases of people. The greatest number of victims, as well as significant material losses, are caused by droughts, floods and earthquakes, as well as massive infectious diseases of people (for example, the COVID-19 pandemic, limiting the coping capacities of the healthcare systems throughout the district), however the epidemics effect is measured indirectly by measuring mortality and health capacity across municipalities (included in Population component). The results of assessment represented in Table 4.

Based on the assessment results - Kyz-Kel face the highest risk due to very high risk in the natural and human category of the hazard and exposure dimension. When broken down by components, Kyz-Kel exhibits very high risk across the board, except in the areas of transport accidents, wildfires, and population-related factors. Barpy experiences high risk primarily from the natural hazard category, notably from high earthquake exposure. Conversely, Kegart's high risk stems from the human hazard category, due to numerous dumpsites, proximity to the country's largest pesticide dumpsite, and nearby potentially hazardous lakes. Kara-Daryia and Kurmanbek face medium

Table 4. Localized (municipality level) indexes of Hazard and Exposure.

	Earthquakes	Floods	Landslides	Climate change	Wildfires	Population	**Natural**	Transport accidents	Technological hazards	**Human**	**HAZARD & EXPOSURE**
Municipalities	**(0-10)**	**(0-10)**	**(0-10)**	**(0-10)**	**(0-10)**	**(0-10)**	**(0-10)**	**(0-10)**	**(0-10)**	**(0-10)**	**(0-10)**
Bagysh	1.7	6.1	3.1	8.7	4.5	3.8	**4.7**	3.9	3.1	**3.5**	**4.1**
Barpy	10.0	6.7	2.7	7.2	4.5	5.0	**6.3**	3.9	2.8	**3.4**	**5.0**
Kara-Alma	0.0	0.0	1.1	1.7	4.5	5.0	**1.4**	3.9	7.4	**5.9**	**4.0**
Kara-Daryia	0.0	3.4	3.0	5.0	4.5	6.3	**2.9**	3.9	7.2	**5.8**	**4.5**
Kegart	0.8	0.8	3.5	8.6	4.5	3.8	**3.8**	3.9	8.1	**6.5**	**5.3**
Kurmanbek	0.0	2.8	4.0	7.6	4.5	5.0	**3.7**	3.9	6.2	**5.2**	**4.5**
Kyz-Kel	10.0	5.8	6.3	6.5	4.5	3.8	**6.5**	3.9	6.2	**5.2**	**5.9**
Kyzyl-Tuu	0.8	1.2	3.8	5.9	4.5	3.8	**3.0**	3.9	6.2	**5.2**	**4.2**
Lenin	0.0	0.5	2.7	5.8	4.5	3.8	**2.6**	3.9	2.7	**3.3**	**3.0**
Saipidin-Atabek	0.0	2.2	3.9	0.0	4.5	6.3	**2.0**	3.9	3.2	**3.6**	**2.8**
Suzak	0.0	0.0	2.5	5.7	4.5	7.5	**2.4**	3.9	2.4	**3.2**	**2.8**
Tash-Bulak	1.7	2.2	3.2	6.1	4.5	3.8	**3.2**	3.9	4.5	**4.2**	**3.7**
Yrys	0.0	3.3	1.9	3.6	4.5	6.3	**2.4**	3.9	2.3	**3.1**	**2.8**

levels of hazard and exposure risk. Kara-Daryia's risk is elevated due to technological accidents, while Kurmanbek experiences the highest climate change risk among the municipalities, driven by high exposure to climatic water deficits. Other municipalities experience varying levels of risk, ranging from low to very low, in both human and natural hazard categories.

Table 5. Localized (municipality level) indexes of Vulnerability.

	Development & Deprivation	Gender equality	Agriculture	Economy	**Socio-Economic Vulnerability**	Children U5	Disaster preparedness	Uprooted people	Other vulnerable groups	Food Security	**Vulnerable Groups**	**VULNERABILITY**
Municipalities	**(0-10)**	**(0-10)**	**(0-10)**	**(0-10)**	**(0-10)**	**(0-10)**	**(0-10)**	**(0-10)**	**(0-10)**	**(0-10)**	**(0-10)**	**(0-10)**
Bagysh	0.0	6.7	4.2	6.0	**4.2**	5.6	1.5	7.8	5.7	3.8	**5.2**	**4.7**
Barpy	0.0	7.2	7.4	7.2	**5.5**	5.6	5.0	3.1	3.3	5.0	**4.5**	**5.0**
Kara-Alma	10.0	6.7	4.8	5.3	**6.7**	5.6	5.0	5.2	10.0	5.0	**6.9**	**6.8**
Kara-Daryia	9.8	2.2	4.8	7.1	**6.0**	5.6	5.0	8.6	2.0	6.3	**5.9**	**6.0**
Kegart	2.1	7.2	5.3	4.8	**4.9**	5.6	3.8	8.0	5.3	3.8	**5.5**	**5.2**
Kurmanbek	4.6	6.7	5.2	4.5	**5.3**	5.6	5.0	8.1	5.0	5.0	**5.9**	**5.6**
Kyz-Kel	7.5	5.0	6.6	5.4	**6.1**	5.6	8.3	0.0	0.0	3.8	**4.4**	**5.3**
Kyzyl-Tuu	1.5	6.7	5.3	3.7	**4.3**	5.6	10.0	1.4	0.0	3.8	**5.7**	**5.0**
Lenin	1.4	6.7	6.4	4.8	**4.8**	5.6	1.3	0.0	8.8	3.8	**4.8**	**4.8**
Saipidin-Atabek	5.4	2.2	3.0	2.8	**3.4**	5.6	0.0	10.0	5.7	6.3	**6.6**	**5.2**
Suzak	10.0	5.0	2.0	7.2	**6.1**	5.6	3.8	6.0	8.3	7.5	**6.5**	**6.3**
Tash-Bulak	1.5	5.5	5.7	3.4	**4.0**	5.6	5.0	10.0	10.0	3.8	**8.0**	**6.4**
Yrys	3.2	7.2	2.7	8.0	**5.3**	5.6	3.8	8.4	6.1	6.3	**6.3**	**5.8**

Table 6. Localized (municipality level) indexes of Coping capacity.

	Governance	DRR	Humanitarian	Institutional	Communication	Physical Connectivity	Water and Sanitation	Access to health care	Ecology	**Infrastructure**	**LACK OF COPING CAPACITY**
Municipalities	(0-10)	(0-10)	(0-10)	(0-10)	(0-10)	(0-10)	(0-10)	(0-10)	(0-10)	(0-10)	(0-10)
Bagysh	4.0	7.8	0.0	**3.9**	0.0	10.0	2.0	4.4	2.7	**5.6**	**4.8**
Barpy	7.0	0.3	0.0	**2.4**	0.0	7.2	4.3	2.9	2.3	**3.4**	**2.9**
Kara-Alma	3.3	0.0	8.3	**3.9**	0.0	10.0	2.8	8.3	3.9	**6.7**	**5.5**
Kara-Daryia	3.3	0.0	0.0	**1.1**	0.0	6.2	4.8	1.5	0.0	**1.6**	**1.4**
Kegart	0.0	0.0	10.0	**3.3**	0.0	6.7	0.0	5.0	0.8	**4.4**	**3.9**
Kurmanbek	0.0	0.0	10.0	**3.3**	0.0	1.1	4.8	1.5	6.0	**1.7**	**2.5**
Kyz-Kel	3.3	0.0	0.0	**1.1**	0.0	2.3	8.0	3.2	5.1	**2.0**	**1.6**
Kyzyl-Tuu	4.6	8.8	3.3	**5.6**	0.0	3.3	0.0	6.7	4.3	**5.5**	**5.6**
Lenin	1.1	0.5	0.0	**0.5**	0.0	3.3	1.2	0.0	1.6	**0.9**	**0.7**
Saipidin-Atabek	5.2	0.5	5.3	**3.7**	0.0	2.6	0.0	8.9	0.8	**5.6**	**4.7**
Suzak	1.9	7.3	0.0	**3.1**	0.0	7.6	2.0	6.1	2.4	**5.7**	**4.5**
Tash-Bulak	8.7	5.5	10.0	**8.1**	0.0	2.4	5.3	6.5	5.4	**3.9**	**6.5**
Yrys	9.5	0.0	0.0	**3.2**	0.0	6.0	2.0	5.6	3.3	**4.1**	**3.7**

Vulnerability of the municipalities of Suzak district

Based on assessment results - Kara-Alma face the highest vulnerability risk due to both, socio-economic and vulnerable groups categories high risk. High proportion of people below poverty line in the socio-economic category and high proportion of families living with disability were among the main contributors to elevated risk. At the same time, Kara-Daryia, Kurmanbek, Suzak and Tash-Bulak municipalities face high risk due to individual factors. While all vulnerability components contributed to the high risk in Kurmanbek, the high risk in Kara-Daryia is a result of elevated risk in the poverty and uprooted people components. High risk in Tash-Bulak and Suzak municipalities, from other side is a result of increased risk of uprooted people and disability, coupled with economic risk (low number of tourist places and rainfall damages) in Suzak municipality. The rest of the municipalities face medium to low risk, although notably higher than in the rest of the dimensions (hazard and exposure and coping capacity). A higher proportion of people facing poverty, unemployment, or disability, in addition to higher risk of child mortality has contributed to the higher risk in the vulnerability dimension (Table 5).

Coping capacity of the municipalities of Suzak district

Based on assessment results, the risk in the coping capacity dimension is the lowest in comparison to the other dimensions, due to low risk in the communications, water and sanitation and DRR components. However, Tash-Bulak faces very high coping capacity risk due to increased institutional risk (lack of emergency response exercises, training and low self-organizational capacity), while the risk in the infrastructure category mitigated the further increase of overall coping capacity risk. Kara-Alma and Kyzyl-Tuu face somewhat high risk among the municipalities due to poor access to health care (staffing of medical facilities and availability of healthcare facilities), coupled with poor road connectivity in Kara-Alma and lack of sufficient emergency response exercises in Kyzyl-Tuu (Table 6).

Risk of the municipalities of Suzak district

Risk Index for municipalities of Suzak district provide a risk overview by ranking the municipalities in the district from very low to very high risk, based on cluster analysis.

Based on the analysis, most of the municipalities face medium risk (5 municipalities: Barpy, Kurmanbek, Saipidin-Atabek, Yrys and Suzak), 2 of the municipalities face low (Kyz-Kel and Kara-Daryia) while one municipality (Lenin) very low risk. Very low to medium overall risk is a result of very low risk in the coping capacity dimension, even though Kyz-Kel and Barpy face high hazard risk. Vulnerability risk is elevated in almost all municipalities, contributing to increase of overall risk across all municipalities. Three of the municipalities face high risk: Kegart (due to high risk in the hazard and exposure and vulnerabilities dimensions), Kyzyl-Tuu (due to high coping capacity and vulnerability risk), while in Bagysh the high risk is a result of elevated risk in all of the dimensions of INFORM. At the same time, Kara-Alma and Tash-Bulak face the highest risk due to very high risk in the lack of coping capacity and vulnerability dimensions (Table 7).

Based on the results of the calculated indexes, thematic maps were prepared at the district level (Figure 4) for the risk and three main calculated indicators (hazard and exposure, vulnerability and lack of coping capacity) based on the collected field material and available generalised data.

Table 7. Localized (municipality level) indexes of Risk.

	HAZARD & EXPOSURE	VULNERABILITY	LACK OF COPING CAPACITY	RISK	RISK CLASS
Municipalities	**(0-10)**	**(0-10)**	**(0-10)**	**(0-10)**	**(V.Low-V. High)**
Bagysh	4.1	4.7	4.8	4.5	High
Barpy	5.0	5.0	2.9	4.2	Medium
Kara-Alma	4.0	6.8	5.5	5.3	Very High
Kara-Daryia	4.5	6.0	1.4	3.4	Low
Kegart	5.3	5.2	3.9	4.8	High
Kurmanbek	4.5	5.6	2.5	4.0	Medium
Kyz-Kel	5.9	5.3	1.6	3.7	Low
Kyzyl-Tuu	4.2	5.0	5.6	4.9	High
Lenin	3.0	4.8	0.7	2.2	Very Low
Saipidin-Atabek	2.8	5.2	4.7	4.1	Medium
Suzak	2.8	6.3	4.5	4.3	Medium
Tash-Bulak	3.7	6.4	6.5	5.4	Very High
Yrys	2.8	5.8	3.7	3.9	Medium

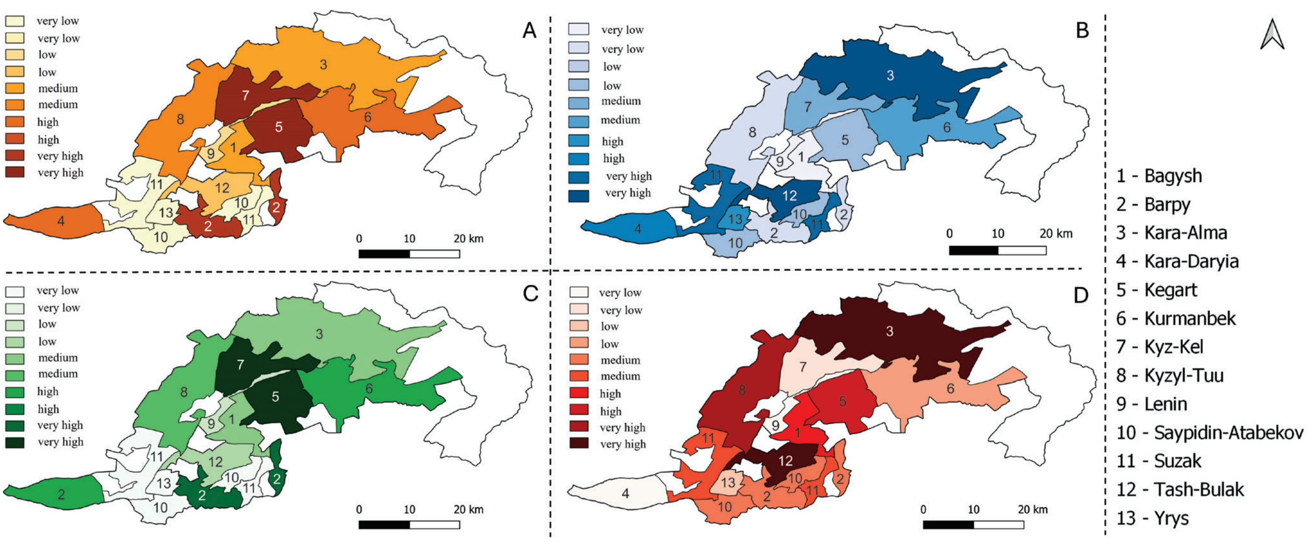

Fig. 4. A. Hazard and exposure B. Vulnerability, C. Lack of coping capacity D. Integrated risk assessment.

Discussion

A deeper understanding of the risk mechanism allows us to establish and develop effective models for its management, which will generally ensure risk reduction, community resilience, and more effective rates of development. Despite the importance of modern knowledge about disaster risk, and the definition of disaster risk, unfortunately current concepts for considering and studying disasters in the Kyrgyz Republic are still predominantly based on the old paradigm of risk where the "risk" is considered equal to "hazard". Furthermore, descriptive and qualitative assessment methods dominate over mathematical and quantitative models, making them less evidence-based and less compelling for the interdisciplinary community of disaster management specialists. Another important disadvantage of the existing approaches to risk and hazard assessment applied in national practices in the Kyrgyz Republic is the absence or separate consideration of vulnerability processes (in which the components of hazard are centrally analyzed by the MES, and the components of vulnerability by the MLSSM). This situation complicates the process of adequate perception and understanding of risk - as potential disaster losses, in lives, health status, livelihoods, assets, and services, which could occur to a particular community or a society over some specified future time and complicates identify effective disaster risk reduction mechanisms.

The risk indexes calculated for the smallest administrative units can significantly enhance governance. They support land use planning, disaster insurance, anticipatory actions, disaster preparedness, and DRM-DRR and civil protection policies. In addition, data from localized risk assessment (municipality based) will provide valid and accurate assessment results at the subnational (district, oblast) and national levels. Using our target area as an example, the risk level of Suzak district can be taken as the average risk of all municipalities, which will be 4.2. However, the risk value of an oblast will make sense if the assessment fully covers all municipalities and districts of one administrative oblast. The same procedure can be applied to oblasts, when many risk values of oblasts will form a reasonable risk index of the entire country for comparisons of its risk level with other countries in the region and the world - in system of unified principles.

This set of works is planned to be implemented during next stage of research. It is envisaged that the authors of this paper will present the assessment results to the Kyrgyz government as a model for potential integration into the national 'Concept for the Development of a Unified Integrated Disaster Monitoring and Forecasting System in the Kyrgyz Republic until 2030'. The model will be developed considering possible replication and scaling at the national level.

The introduction of this mechanism into the national DRM system should also be accompanied by the development of initiatives aimed on improvement of digital data exchange mechanisms. It is also important to note that the identified risk parameters are not constant, they could be changed in the future due to various reasons, including environmental, social, or technical factors (disasters, climate change, industrial activities, the change in DRR education, reconstruction, wear and tear of the facilities, mitigation measures etc.). Therefore, to assess the real status of risk, it would be important to implement risk assessment periodicity. The quantitative multi-risk assessment approach also clearly illustrates the interaction between physical, environmental, and social factors of disaster risk and how they contribute to the risk values (Umaraliev, 2020). Thus, outcomes of research also contributed to raising awareness that the disasters could, in fact, be reduced, if not even prevented (Birkmann & Pelling, 2006) and created a suitable basis for formulating effective strategies for mitigation of their impact on people, communities, and economies.

The quantitative multi-risk assessment procedures can also be effectively integrated into disaster risk financing systems and particularly into disaster insurance programs. Thus, disaster insurance programs occupy an increasingly important place in the structure of DRR because they are strengthening financial resilience (ensure that national financial system and population are financially protected in the disaster events) and because they reduce dependence on post-disaster external aid (or improve the effectiveness of governance). Unfortunately, the disaster insurance sector is one of the least developed DRR mechanisms in Central Asia (CA). In modern times (after the Collapse of the Soviet Union in 1991), in the Kyrgyz Republic the national disaster insurance program was only initiated in 2015 (Law of KR, 2016). Development of an index-based insurance policy is very important in developing countries with limited resources, weak governance, systemic corruption, and high poverty, where big differences in incomes between different socio-economic groups and geographical areas exist and the Kyrgyz Republic is one of those regions, where these environmental and socio-economic issues are particularly acute (UNISDR, 2010).

Conclusion

The study results highlighted practitioners' understanding of 'risk' and 'disaster' concepts, specifically their ability to differentiate the critical risk dimensions: hazard, exposure, and vulnerability.

The localized Risk model for Suzak district uses subnational level indicators of INFORM Risk model applied for 13 municipalities. The national and UN data sources used to construct the model meet four basic criteria: (1) the data is free, publicly available and transparent, (2) the data provides sufficient municipality coverage, (3) the data is reliable (4) and the data allows comparison between municipalities.

The study revealed that the MES's standard monitoring procedures lack a methodological basis for comprehensive risk identification. They focus solely on hazard and exposure without considering their interrelationships or including vulnerability analysis. In this context, current research practice mainly provides a statement of the situation but cannot provide information on the use of which will reduce risk and build resilience.

The localised Risk index for Suzak district represents a final stage of piloting the institutionalization of local risk assessment procedures in Kyrgyz Republic. The Index gathered data from 13 municipalities of Suzak district, Jalal-Abad oblast. A total of 72 indicators have been collected and indexed by following the INFORM Risk model (26 indicators – hazard and exposure, 22 – vulnerability, 24 – lack of coping capacity). The process of development in collaboration between central and local governments, international and research institutions. The risk score combines 72 indicators across three dimensions–hazard and exposure, vulnerability, and lack of coping capacity–to calculate each municipality's risk level. Every municipality has a rating between 0 and 10 for risk and all of its dimensions, categories, and components. The low values of the index represent a better condition (e.g. lower risk / strong or good resilience), and the high values of the index represent a worse condition (e.g. higher risk / weak or bad resilience). The indexes allow a relative comparison of the risk and components between municipalities and of different components within a municipality. Of the 13 municipalities, 2 demonstrated very high risk indexes (Kara-Alma, Tash-Bulak) and 3 are high risk indexes (Bagysh, Kegart, Kyzyl-Tuu) and only one municipality is demonstrated very low risk index (Lenin).

At the next stage of our study, we plan to apply INFORM Risk model with its adaptation to the local context at the level of other rural (Aiyl Aimak) or urban (town administration) municipalities of the Kyrgyz Republic. Adaptation of this method will be developed through the following stages:

- Determination of the optimal set of risk criteria (based on INFORM Risk model standards and the capabilities of the national data and statistics system). Clarifying the existing risk criteria (the form of their mathematical-numerical representation).
- Normalization of risk criteria (categories and components) in a unified system and index standard.
- Calculation of risk components with subsequent assessment of the Risk index.
- Risk mapping and providing information for end-users.

Acknowledgment

This work was supported by the Swiss Agency for Development and Cooperation and implemented by the UN World Food Programme (UN WFP) in close collaboration with the United Nations Office for Disaster Risk Reduction (UNDRR), local authorities and research institutions with the participation of experts and based on the request of the Ministry of Emergency Situations of the Kyrgyz Republic.

References

Alexander, D. 2000: Confronting catastrophe: new perspectives on natural disasters. Liverpool University Press: 288 p.

Birkmann, J. & Pelling, M. 2006: Measuring vulnerability to natural hazards: towards disaster resilient societies. United Nations University: 688 p.

Blaikie, P., Cannon, T., Davis, I. & Wisner, B. 2004: At risk: natural hazards, people's vulnerability and disasters. (2nd Edition). Routledge: 496 p.

Dilley, M. 2005: Natural disaster hotspots: a global risk analysis. World Bank Publications. 5: 148 p.

Golovko, D., Roessner, S., Behling, R. & Kleinschmit, B. 2017: Automated derivation and spatio-temporal analysis of landslide properties in southern Kyrgyzstan. Natural Hazards, 85: 1461–1488. https://doi.org/10.1007/s11069-016-2636-y

Erokhin, S.A., Zaginaev, V.V., Meleshko, A.A., Ruiz-Villanueva, V., Petrakov, D.A., Chernomorets, S.S. & Stoffel, M. 2018: Debris flows triggered from non-stationary glacier lake outbursts: the case of the Teztor Lake complex (Northern Tian Shan, Kyrgyzstan). Landslides, 15: 83–98. https://doi.org/10.1007/s10346-017-0862-3

Havenith, H.B., Umaraliev, R., Schlögel, R., & Torgoev, I. 2017: Past and Potential Future Socioeconomic Impacts of Environmental Hazards in Kyrgyzstan. In: Perry. O.A. (ed.): Kyrgyzstan: political, economic and social issues. NOVA Science Publishers, NY, USA. 2: 63–113.

Kalmetieva, Z.A., Mikolaichuk, A.V., Moldobekov, B.D., Meleshko, A.V., Jantaev, M.M., Zubovich, A.V. & Havenith, H.B. 2009: Atlas of earthquakes in Kyrgyzstan. CAIAG, Bishkek:76 p.

Kelman, I. 2015 Climate change and the Sendai framework for disaster risk reduction. International Journal of Disaster Risk Science, 6: 117–127. https://doi.org/10.1007/s13753-015-0046-5

Khanal, S., Tiwari, S., Lutz, A.F., Hurk, B.V.D. & Immerzeel, W.W. 2023: Historical climate trends over High Mountain Asia Derived from ERA5 reanalysis data. Journal of Applied Meteorology and Climatology, 62/2: 263–288. https://doi.org/10.1175/JAMC-D-21-0045.1

Law of Kyrgyz Republic 2016: On compulsory insurance of residential premises against fire and natural disasters.

Liu, J., Wu, Y. & Gao, X. 2021: Increase in occurrence of large glacier-related landslides in the high mountains of Asia. Scientific Reports, 11/1: 1635. https://doi.org/10.1038/s41598-021-81212-9

Long, F. 1978: The Impact of Natural Disasters on Third World Agriculture.American Journal of Economics and Sociology, 37/2: 149–163. https://doi.org/10.1111/j.1536-7150.1978.tb02809.x

Marin-Ferrer, M., Vernaccini, L. & Poljansek, K. 2017: INFORM Index for Risk Management, Concept and Methodology. Publications Office of the European Union: 90 p.

Peduzzi, P., Dao, H., Herold, C. & Mouton, F. 2009: Assessing global exposure and vulnerability towards natural hazards: The Disaster Risk Index. Natural Hazards and Earth System Science, 9/4:1149–1159. https://doi.org/10.5194/nhess-9-1149-2009

Rahmonov, E.A. 2022: Factors affecting the socio-economic condition of the population in the Fergana valley in the years of independence. American Journal of Research in Humanities and Social Sciences, 7: 71–74.

UN WFP, Annual Country Reports – Kyrgyzstan. 2020: Internet: https://www.wfp.org/publications/annual-country-reports-kyrgyzstan

UN ESCAP, Kyrgyz Republic: Risk Profile, 2018: Internet: https://www.unescap.org/sites/default/files/Kyrgyzstan%20Disaster%20Risk%20Profile.pdf

Umaraliev, R., Moura, R., Havenith, H.-B., Almeida, F. & Nizamiev, A. 2020: Disaster Risk in Central Asia: Socio-Economic Vulnerability Context and Pilot-Study of Multi-Risk Assessment in a Remote Mountain Area of Kyrgyz Republic. European Journal of Engineering Research and Science, 5/3: 234–244. https://doi.org/10.24018/ejeng.2020.5.3.1772

Van Westen, C.J. 2009: Multi-hazard risk assessment. UNU-ITC DGIM. Internet: http://www.itc.nl/EU strategy for supporting disaster risk reduction in developing countries. 2009: Internet: https://eur-lex.europa.eu/LexUriServ/LexUriServ.do?uri=COM:2009:0084:FIN:EN:PDF

UNISDR (United Nations International Strategy for Disaster Reduction). 2015: Sendai framework for disaster risk reduction 2015–2030. Internet: http://www.wcdrr.org/uploads/Sendai_Framework_for_Disaster_Risk_Reduction_2015-2030.pdf. Accessed Apr 2015.

UNISDR, In-depth Review of Disaster Risk Reduction in the Kyrgyz Republic, 2010: Internet: https://www.preventionweb.net/files/14436_14436INDEPTHREVIEWOFDRRINKRfinal1.pdf

World Bank, Kyrgyz Republic: Vulnerability, Risk Reduction, and Adaptation to Climate Change. 2011: Internet: https://climateknowledgeportal.worldbank.org/sites/default/files/2018-10/wb_gfdrr_climate_change_country_profile_for_KGZ.pdf

Zaginaev, V., Falatkova, K., Jansky, B., Sobr, M. & Erokhin, S. 2019: Development of a potentially hazardous pro-glacial lake in Aksay Valley, Kyrgyz range, Northern Tien Shan. Hydrology, 6/1: 3. https://doi.org/10.3390/hydrology6010003

GEOLOGIJA 67/2, 317-332, Ljubljana 2024
https://doi.org/10.5474/geologija.2024.016

Geokemična porazdelitev elementov v okoljskih medijih iz okolice degradiranih območij površinskih kopov

Geochemical distribution of elements in the environmental media from the surroundings of open pit areas

Špela BAVEC[1]*, Sonja CERAR[1], Martin GABERŠEK[1] & Željko POGAČNIK[2]

[1]Geološki zavod Slovenije, Dimičeva ulica 14, SI-1000 Ljubljana, Slovenija; *corresponding author: spela.bavec@geo-zs.si
[2]Georudeko d.o.o., Anhovo, SI-5210 Deskle, Slovenija

Prejeto / Received 9. 10. 2024; Sprejeto / Accepted 2. 12. 2024; Objavljeno na spletu / Published online 16. 12. 2024

Ključne besede: geokemična porazdelitev, tla, matična podlaga, potočni sediment, površinska voda, površinski kop
Key words: geochemical distribution, soil, bedrock, stream sediment, surface water, open pit

Izvleček

Predstavljeni so rezultati geokemičnih preiskav v okolici površinskih kopov Kopriva (nahajališče naravnega kamna-apnenec) in Lipovški vrh (nahajališče apnenca za industrijske namene). Izvedli smo jih v okviru evropskega projekta LIFE IP RESTART. V sklopu omenjenega projekta se na degradiranih površinah omenjenih kopov, z namenom njihove revitalizacije, predvideva vzpostavitev testnih območij vgradnje sekundarnih materialov (mešanice recikliranih materialov in mineralnih surovin). Glavni cilj te študije je opredeliti izhodiščno stanje geokemične porazdelitve elementov v okoljskih materialih (kamninah, tleh, potočnih sedimentih in površinskih vodah) pred vzpostavitvijo testnih območij. Določene vsebnosti elementov bodo podlaga za spremljanje morebitnih okoljskih vplivov vgrajenih sekundarnih materialov. Rezultati so pokazali, da v kamninah zaradi geološke sestave (pretežno apnenec) med elementi prevladuje vsebnost Ca. Glede na zakonodajne smernice za tla smo ugotovili preseganja vsebnosti Pb v enem vzorcu (izvor je lahko antropogen ali naraven) in Ni v dveh vzorcih (predvidoma naraven izvor) v Koprivi. Na območju Lipovškega vrha so v Suhem potoku v dolvodnem sedimentu vsebnosti za elemente Mg, Na, Sr, Ca, Mn in S višje kot v gorvodnem sedimentu. Višje vsebnosti pripisujemo povečanemu antropogenemu doprinosu karbonatnega materiala vzdolž potoka (izpiranje materiala iz bližnjega kamnoloma in cest). V površinski vodi Suhega potoka smo ugotovili višje vsebnosti elementov S, Sr, B, U in Zn, ki niso presegle zakonodajnih smernic.

Abstract

The results of geochemical investigations - carried out within the framework of the European project LIFE IP RESTART - in the degraded areas of the Kopriva (deposit of natural stone-limestone) and Lipovški vrh (deposit of limestone for industrial purposes) open pits are presented. There test sites of the installation of secondary raw materials (a mixture of recycled materials and mineral raw materials) with the aim of revitalizing degraded surfaces are planned. The main goal of this study is to define the baseline geochemical distribution of elements in environmental materials (rocks, soil, stream sediment and surface water) for the purpose of monitoring the potential environmental impacts of installed secondary raw materials. In rocks Ca content predominates due to the geological setting (predominantly limestone) of the studied areas. According to the legislative guidelines for soil, exceedances have been found for Pb in one sample (origin can be natural or anthropogenic) and Ni in two samples (presumably natural origin) from the area of Kopriva. In the area of Lipovški vrh in the stream Suhi Potok, higher contents of Mg, Na, Sr, Ca, Mn and S occur in the downstream sediment compared to upstream sediment. It is assumed higher contents occur due to anthropogenic contribution of carbonate material along the stream (washing of materials from nearby open pit and road). In the surface water of Suhi Potok, higher concentrations of S, Sr, B, U and Zn were determined. However, the concentrations did not exceed the legislative guidelines.

Uvod

Geokemična sestava površinskih materialov vpliva na biosfero, zato je njeno poznavanje ključno za razumevanje kroženja kemičnih prvin v okolju (Darnley et al., 1995). Porazdelitve elementov v površinskih materialih geosfere so opredeljene z njihovimi naravnimi variabilnostmi oziroma geokemičnim ozadjem (Darnley et al., 1995; Salminen et al., 2005; Gosar et al., 2019; Gassama et al., 2021). Poznavanje geokemičnega ozadja je sprva služilo predvsem odkrivanju novih mineralnih nahajališč (Hawkes, 1957). Kasneje je postalo bistvenega pomena za opredelitev in identifikacijo virov onesnaženja ter za vzpostavitev zanesljivih okoljskih meril kakovosti za tla, sedimente in površinske vode (Gałuszka & Migaszewski, 2011). Kakovost površinskih materialov skozi čas ugotavljamo z okoljskim monitoringom, ki predstavlja ključno orodje za zaščito okolja in zdravja biosfere, vključno s človekom (Artiola & Brusseau, 2006). Med najpomembnejše antropogene dejavnosti, ki povzročijo degradacijo naravnih okolij, spada izkoriščanje mineralnih surovin (Koščová et al., 2018). Slednje povzroča številne negativne vplive na okoliško krajino in prebivalstvo, kot so onesnaženje zraka, vod in tal (Šajn & Gosar, 2004; Bavec et al., 2015; Bavec & Gosar, 2016; Miler & Gosar, 2019; Miler et al., 2022). Z namenom preučitve možnih negativnih vplivov na okolje, ki bi lahko bili posledica nekdanjih rudarskih dejavnosti, je bil za Slovenijo izdelan inventar, ki vključuje informacije o 33 rudnikih kovin, 43 premogovnikih, 51 rudnikih nekovinskih mineralnih surovin, 156 odlagališčih odpadkov iz rudnikov kovin in 18 odlagališčih odpadkov iz premogovnikov (Gosar et al., 2020). Reševanje negativnih posledic zaprtih in opuščenih rudnikov ostaja v večji meri breme države (Uradni list SRS, št. 5/88; Uradni list RS, št. 26/05 – uradno prečiščeno besedilo, 43/10, 49/10 – popr., 40/12 – ZUJF, 25/14, 46/14, 82/15, 84/18 in 204/21; Uradni list RS, št. 26/05 – uradno prečiščeno besedilo; Uradni list RS, št. 22/06 – uradno prečiščeno besedilo). V letu 2022 je bilo aktivnih skupno 158 nahajališč s 180 pridobivalnimi prostori z rudarsko pravico za izkoriščanje 24 različnih mineralnih surovin, med katerimi prevladujejo prod in pesek ter tehnični in naravni kamen (Senegačnik et al., 2023). Dokončna sanacija okolja in odprava posledic rudarskih del aktivnih rudnikov je zakonsko urejena (Uradni list RS, št. 14/14 – uradno prečiščeno besedilo, 61/17 – GZ, 54/22 in 78/23 – ZUNPEOVE in 81/24) in v celoti bremeni nosilca rudarske pravice. Sanacija vključuje zapolnitev degradiranih površin z lastno inertno jalovino in odkrivko ter materiali (zemeljski izkop in umetno pripravljena zemljina), ki so skladni z merili okoljske zakonodaje. Ker materialov za sanacijo primanjkuje, se v sozvočju s prehodom na krožno gospodarstvo za zapolnitev degradiranih površin uporabljajo tudi t.i. geotehničnimi kompoziti iz recikliranih odpadkov (Turk et al., 2020; Đurić et al., 2023). Le ti lahko ob neustrezni izvedbi vplivajo na okolje v obliki emisij potencialno nevarnih snovi (Cerar & Bavec, 2019).

Razvoj okoljsko sprejemljivih t.i. sekundarnih materialov za zapolnitev degradiranih površin pridobivalnih prostorov je ena izmed nalog projekta LIFE IP RESTART. Namen omenjenega projekta je premostiti ovire povezane z recikliranjem odpadkov v Sloveniji, vključno s pomanjkanjem usklajene zakonodaje, nezadostnimi zmogljivostmi za recikliranje ter nizko družbeno sprejemljivostjo postopkov recikliranja in nastalih proizvodov (Internet 1). Testna območja vgradnje sekundarnih materialov z namenom revitalizacije degradiranih površin bodo vzpostavljena na območjih površinskih kopov Kopriva in Lipovški vrh.

Glavni cilj tega prispevka je določitev izhodiščnega stanja geokemične porazdelitve elementov v kamninah, tleh, potočnih sedimentih in površinskih vodah iz okolice degradiranih površin pridobivalnih prostorov Kopriva in Lipovški vrh pred vzpostavitvijo testnih območij. Izhodiščne vsebnosti elementov v obravnavanih materialih bodo osnova za dolgoročno spremljanje morebitnih okoljskih vplivov vgrajenih sekundarnih surovin.

Metode

Študijsko območje

Kopriva

Površinski kop Kopriva (sl. 1) se nahaja v občini Sežana približno 1,5 km severno od naselja Kopriva, ki leži približno 60 km jugozahodno od Ljubljane na nadmorski višini okoli 285 m. V pridobivalnem prostoru Kopriva ter Kopriva 2 so izkoriščali oz. izkoriščajo naravni kamen-apnenec (Senegačnik et al., 2023). Glede na Geološko karto Krasa 1:100.000 (Jurkovšek, 2013) širše območje kamnoloma gradijo plastnati mikritni apnenci z roženci in pelagičnimi mikrofosili Repenske formacije. Sam kamnolom in območje južno od njega gradi člen Repen/Kopriva, sestavljen iz masivnega apnenca, ki vsebuje zdrobljene lupine mehkužcev, pretežno rudistov. Glede na digitalno Pedološko karto 1:25.000 (TIS/ICPVO, 1999-2010) se v ožji okolici površinskega kopa pojavljajo rendzina na apnencu in dolomitu ter rjava pokarbonatna tla na

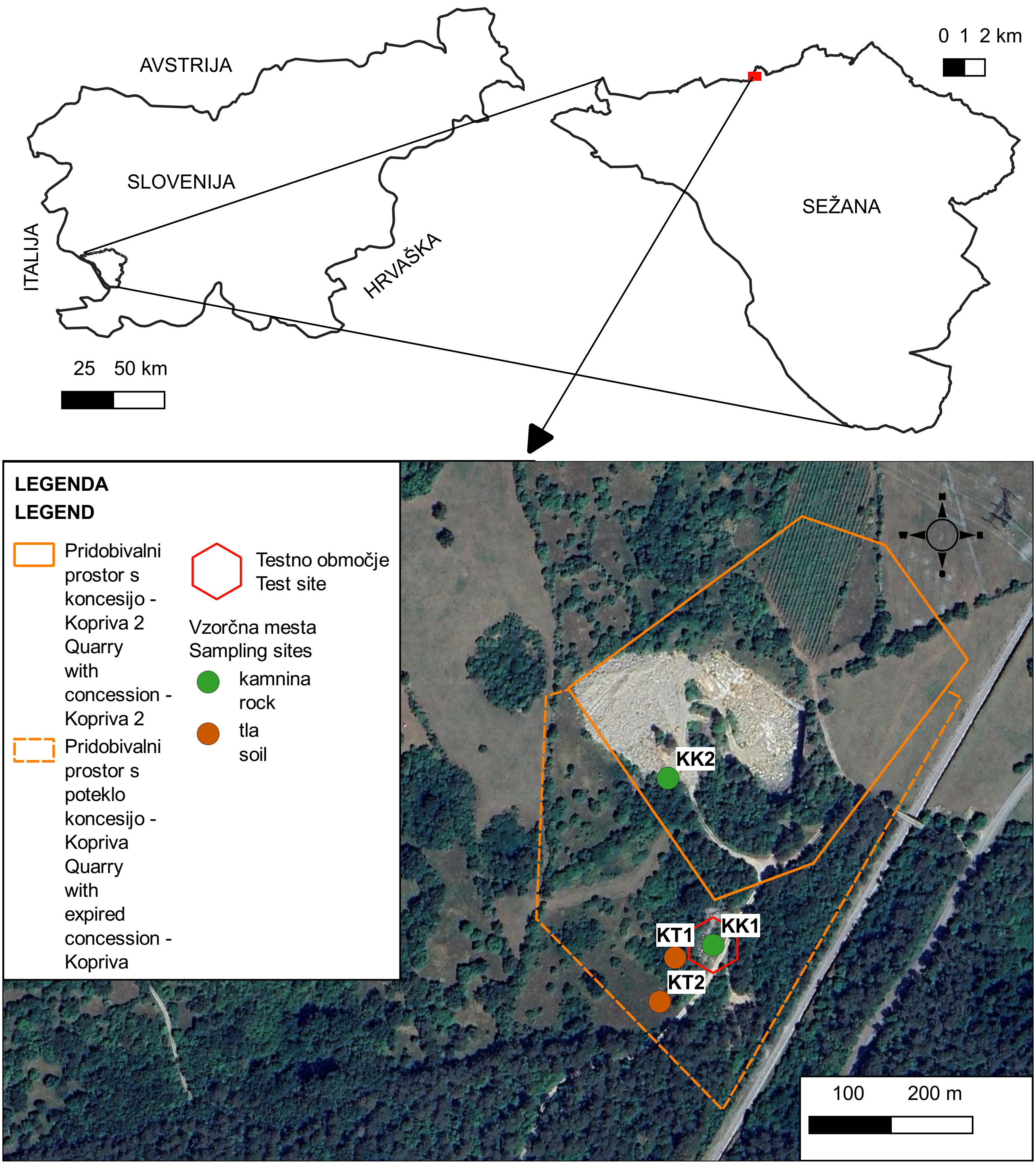

Sl. 1. Prikaz obravnavanega območja (Kopriva) skupaj z lokacijami vzorčnih mest in predvideno lokacijo testnega območja (Podlage: Ortofoto (Geodetska uprava Republike Slovenije); Linijski podatkovni sloj hidrografije – površinske vode (Ministrstvo za okolje podnebje in energijo, Direkcija Republike Slovenije za vode); meje pridobivalnega prostora (Zbirka rudarskih podatkov)).

Fig. 1. Display of study area (Kopriva) together with sampling locations and foreseen test site location (Layers: Ortophoto Geodetic administration of Slovenia); Line data layer of hydrography - surface waters (Ministry of the Environment, Climate and Energy, Slovenian Water Agency); Quarry boundaries (Mining data registry)).

apnencu in dolomitu. Skladno z enotno državno evidenco o dejanski rabi zemljišč (MKGP, 2022) tla v ožji okolici površinskega kopa glede na rabo uvrščamo med trajne travnike, kmetijska zemljišča, porasla z gozdnim drevjem ali v zaraščanju, drevesa in grmičevje ter gozd.

Območje kamnoloma Kopriva je del vodnega telesa podzemne vode »VTPodV 5019 Obala in Kras z Brkini« in vodonosnega sistema »50621 Brestovica – Timav«. Po IAH hidrogeološki klasifikaciji leži na območju lokalnega vodonosnika ali vodonosnika s spremenljivo izdatnostjo, ali obširnega vendar največ srednje izdatnega vodonosnika (II.b). Vodonosnik gradi zgoraj omenjeni zgornjekredni člen Repen/Kopriva. Gre za hidrodinamsko odprt kraško-razpoklinski vodonosnik z dobro do zelo dobro vodoprepustnostjo dobro zakraselih kamnin. Gladina podzemne vode zaradi kraško-razpoklinske poroznosti ni zvezna, globina do podzemne vode na ožjem območju zaradi odsotnosti vrtin in vodnjakov ni znana. Podzemna voda se na tem območju pojavlja na globini okoli 200 m pod površjem (ustni vir: Jasmina Rijavec). Napajalno zaledje vodonosnika predstavlja območje severovzhodno od obravnavanega območja. Generalna smer toka podzemne vode na območju vodonosnika Brestovica – Timav je od severovzhoda proti zahodu – jugozahodu. Glavno napajanje vodonosnika predstavljajo padavine (Mali et al., 2023). Ker gre za kraško območje, površinska voda v okolici kamnoloma ni prisotna.

Lipovški vrh

Površinski kop Lipovški vrh (sl. 2) se nahaja približno 500 m severno od naselja Briše v občini Zagorje ob Savi, ki leži približno 30 km severovzhodno od Ljubljane na nadmorski višini okoli 480 m. V pridobivalnem prostoru Lipovški vrh izkoriščajo apnenec za industrijske namene (Senegačnik et al., 2023). Širše območje kamnoloma sestavljajo miocenske sedimentne kamnine (apneno-kremenovi konglomerati, ki prehajajo v peščenjak, laporovci in apnenci) ter sedimenti (prod, pesek, melj in glina), ki so se odlagali v plitvem Panonskem bazenu. Ožje območje kamnoloma gradijo srednjemiocenske (badenijske) Laške plasti, pretežno litotamnijski apnenec ter apnenčevi peščenjaki in laporovci (Premru, 1980; Križnar & Mikuž, 2014; Pogačnik, 2022). Glede na digitalno Pedološko karto 1:25.000 (TIS/ICPVO, 1999-2010) se v ožji okolici površinskega kopa pojavljajo evtrična rjava tla na različnih bazičnih kamninah in distrična rjava tla na miocenskih peskih, peščenjakih in konglomeratih. Skladno z enotno državno evidenco o dejanski rabi zemljišč (MKGP, 2022) tla v ožji okolici površinskega kopa glede na rabo uvrščamo med trajne travnike, njive, neobdelana kmetijska zemljišča, drevesa in grmičevje ter gozd.

Območje kamnoloma Lipovški vrh je del vodnega telesa podzemne vode »VTPodV 1008 Posavsko hribovje do osrednje Sotle« in vodonosnega sistema »12320 Od Litije do Zidanega mostu«. Po IAH hidrogeološki klasifikaciji leži na območju lokalnega vodonosnika ali vodonosnika s spremenljivo izdatnostjo, ali obširnega vendar največ srednje izdatnega vodonosnika (II.b). Severno in južno so manjši vodonosniki z lokalnimi ali omejenimi viri podzemne vode (III.a). Vodonosnik gradijo srednjemiocenske (badenijske) Laške plasti, pretežno litotamnijski apnenec ter apnenčevi peščenjaki in laporovci. Gre za hidrodinamsko odprt kraško-razpoklinski vodonosnik s srednje do slabšo vodoprepustnostjo. Gladina podzemne vode zaradi kraško-razpoklinske poroznosti ni zvezna, globina do podzemne vode pa zaradi pomanjkanja podatkov (vrtin/vodnjakov) ni znana. Napajalno zaledje vodonosnika predstavlja območje hriba Vrhlja, severno od obravnavanega območja. Glavno napajanje vodonosnika so padavine. V neposredni bližini obravnavanega območja tečeta potoka Kolovratščica na zahodu in Medija na jugu ter občasni vodotok (Suhi potok) na vzhodni strani kamnoloma. Kota struge potoka Kolovratščica je glede na podatke Atlasa okolja okoli 370 m n.v., širina struge je 2–5 m. Vodotok je stalen. Severozahodno od kamnoloma potok teče po naravni strugi površinsko. Ob zahodnem robu kamnoloma, vse do izliva v potok Medija, teče ob vznožju hribovja skozi pokrit kanal ob cesti. Odsek Kolovratščice je po kategorizaciji urejanja vodotokov uvrščen v 2. razred, tj. med sonaravno urejene vodotoke. Južno od kamnoloma teče stalen potok Medija v katerega dolvodno od naselja Briše doteka tudi občasen vodotok (Suhi potok), ki teče vzhodno od kamnoloma.

Vzorčenje

Da bi ugotovili izhodiščno geokemično porazdelitev vsebnosti elementov v okoljskih materialih, smo na obeh območjih vzorčili matično podlago in tla, na območju Lipovškega vrha pa še potočni sediment in površinsko vodo. Karbonatno matično podlago, ki je podrobneje opisana v prejšnjem poglavju, smo vzorčili z odvzemom svežih kosov kamnin znotraj obeh kamnolomov (v Koprivi vzorčno mesto KK2, v Lipovškem vrhu vzorčni mesti LK1, LK2). V Koprivi bo testno območje locirano ob obstoječem odprtem kopu, na manjšem odlagališču karbonantnega jalovinskega materiala, zato smo kose kamnin vzorčili tudi znotraj tega območja (vzorčno mesto KK1).

V okolici površinskega kopa Kopriva smo dve vzorčni mesti za tla (KT1 in KT2) (sl. 1) določili v neposredni bližini testnega območja, kjer pričakujemo, da bodo morebitni vplivi (potencialno onesnaženje predvsem zaradi delovanja vetra in padavin) najbolj izraženi.

V okolici površinskega kopa Lipovški vrh smo določili tri vzorčna mesta za tla (LT1, LT2 in LT3) ter gorvodno in dolvodno vzorčno mesto (glede na lokacijo kamnoloma) potočnih sedimentov in površinskih vod v vodotokih Suhi potok (LS1/LV1,

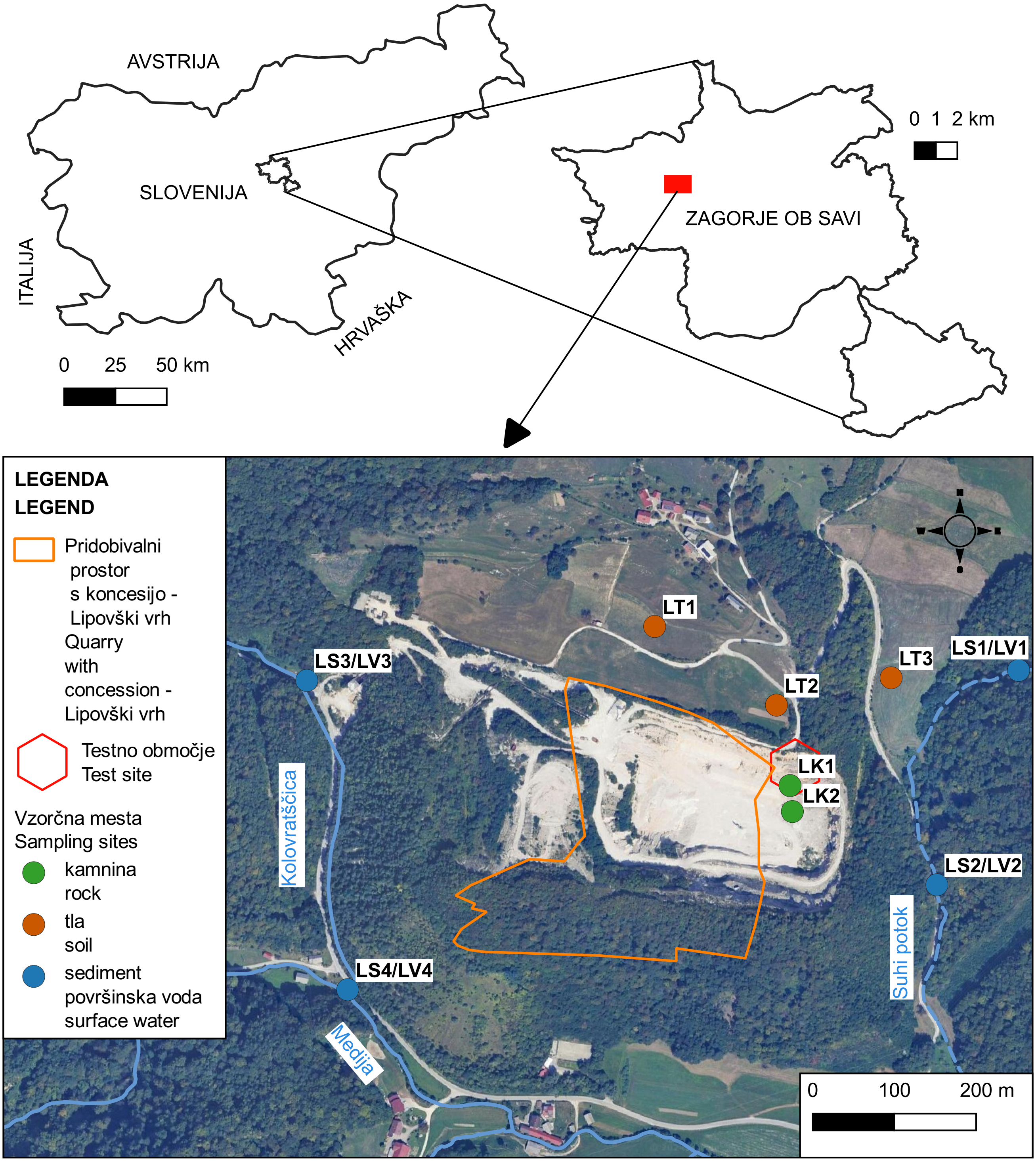

Sl. 2. Prikaz obravnavanega območja (Lipovški vrh) skupaj z lokacijami vzorčnih mest in predvideno lokacijo testnega območja (Podlage: Ortofoto (Geodetska uprava Republike Slovenije); Linijski podatkovni sloj hidrografije – površinske vode (Ministrstvo za okolje podnebje in energijo, Direkcija Republike Slovenije za vode); meje pridobivalnega prostora (Zbirka rudarskih podatkov)).

Fig. 2. Display of study area (Lipovški vrh) together with sampling locations and foreseen test site location (Layers: Ortophoto Geodetic administration of Slovenia); Line data layer of hydrography - surface waters (Ministry of the Environment, Climate and Energy, Slovenian Water Agency); Quarry boundaries (Mining data registry)).

LS2/LV2) in Kolovratščica (LS3/LV3 in LS4/LV4) (sl. 2). Vzorčnih mest za tla v neposredni bližini testnega območja ni bilo mogoče vzpostaviti, saj je testno območje predvideno znotraj opuščenega območja pridobivalnega prostora, kjer so bila tla odstranjena zaradi pridobivanja mineralnih surovin. Zaradi tega smo vzorčne lokacije določili v bližnji okolici (sl. 2), kjer predvidevamo možnost potencialnega onesnaženja. Slednje je kratkoročno gledano možno tekom transporta in vgradnje sekundarnih materialov, dolgoročno pa zaradi delovanja vremenskih dejavnikov.

Tla smo vzorčili na površinah travnikov, z izjemo vzorčnega mesta KT1 (območje Koprive), ki je bilo izvedeno na dnu vrtače, poraščeno z gostim grmičevjem. Skladno s smernicami SIST ISO 18400-205:2019 in SIST ISO 18400-104/2019 smo odvzeli prostorske kompozitne vzorce v enakomerni vzorčni mreži. Na ta način smo pridobili informacije o povprečnih geokemičnih lastnostih tal v ožji okolici preiskovanih območij. Na vzorčnih mestih KT1 in KT2 (območje Kopriva), kjer se glede na Pedološko karto Slovenije pojavlja rendzina na apnencu in dolomitu, ter LT1 (območje Lipovški vrh), kjer se glede na Pedološko karto Slovenije pojavljajo evtrična rjava tla na različnih bazičnih kamninah, smo izkopali po 3 talne profile (do globine 40 m) v medsebojni razdalji 5 m. Vzorčili smo dve globini, in sicer zgornji sloj tal (0–10 cm; oznaka G1) ter spodnji sloj tal (20–30 cm; oznaka G2), pri čemer smo posamezne sloje iz treh talnih profilov združili v skupni vzorec. Dve globini smo vzorčili z namenom ugotavljanja variabilnosti parametrov z globino. Na vzorčnih mestih LT2 in LT3 (območje Lipovški vrh) smo ugotovili, da so tla antropogena in plitva, zato smo odvzeli le zgornji sloj tal (0–5 cm), pri čemer smo v skupni vzorec združili podvzorce iz 6 lokacij v medsebojni razdalji 5 m. Pod tlemi se nahaja antropogeno nasutje (karbonaten gramoz). Organski horizont Oh smo pred vzorčenjem odstranili. Odvzeli smo 5 kg posameznega vzorca tal.

Potočni sediment smo vzorčili na istem vzorčnem mestu kot površinsko vodo. Odvzet je bil kompozitni vzorec, število podvzorcev je bilo odvisno od naravnih danosti, to je količine posameznih žepov drobnozrnatega sedimenta znotraj struge. Podvzorci so bili odvzeti s plastično lopatko do 10 m po strugi navzdol od lokacije vzorčenja površinske vode. Odvzem vzorcev površinske vode smo izvedli skladno s standardom SIST ISO 5667-10:1996, upoštevajoč potrebna določila SIST EN ISO 5667-6:2015. Pred vzorčenjem smo izvedli meritve terenskih fizikalno-kemičnih parametrov vode (temperatura vode, pH, specifična električna prevodnost, raztopljeni kisik, nasičenost s kisikom in redoks potencial) z uporabo vodoodpornega multimetra HI98194 proizvajalca HANNA instruments Inc (Hanna instruments, 2020a). Točnost meritev terenskih parametrov, ki je podana v priloženem gradivu o lastnostih uporabljenega instrumenta (Hanna instruments, 2020a) znaša za pH ± 0,02, za temperaturo vode ± 0,15 °C, za električno prevodnost ± 1 %, raztopljeni kisik oziroma nasičenost s kisikom ± 1,5–3 %, in redoks potencial ± 1 mV.

Vzorce tal in potočnih sedimentov smo shranili v 3 L polietilenske (PE) posode, vzorce površinske vode pa v steklenice, plastenke in viale različnih dimenzij, pri čemer so bile za določene parametre dodane ustrezne tekočine (kisline ali baze) za stabilizacijo. Vzorce vod smo na terenu vseskozi hladili v hladilnih torbah. Vzorce vod smo do pošiljanja v laboratorij hranili v hladilniku, vzorce kamnin, tal in sedimentov pa v temnem prostoru na temperaturi < 10 °C.

Priprava vzorcev in kemijske analize

Priprava vzorcev in kemijske analize so bile opravljene v akreditiranem laboratoriju ALS Czech Republic, s.r.o. Kvaliteta analitike v laboratoriju ALS Czech Republic s.r.o. je skladna z ISO/IEC 17025:2017.

Za določitev vsebnosti elementov v trdnih materialih so bili vzorci pripravljeni z razklopom z zlatotopko (HNO_3:HCl=1:3). Za določitev mobilnih vsebnosti elementov v trdnih materialih so bili pripravljeni vodni izlužki v razmerju 10 litrov vode na 1 kg vzorca v skladu s standardom za izluček odpadka (EN 12457-4). Vzorci površinskih vod so bili pred analizo filtrirani (0,45 μm) in homogenizirani ter mineralizirani z dušikovo kislino v avtoklavu pod visokim pritiskom in temperaturo.

Vsebnosti elementov (Ag, Al, As, B, Ba, Be, Bi, Ca, Cd, Ce, Co, Cr, Cu, Fe, Hg, K, La, Li, Mg, Mn, Mo, Na, Nb, Ni, P, Pb, S, Sb, Se, Sn, Sr, Te, Ti, Tl, V W, Zn in Zr) v vzorcih kamnin, tal in potočnih sedimentov po razklopu z zlatotopko in v vodnem izlužku (EN 12457-4) so bile izmerjene z metodo ICP-OES (Induktivno sklopljena plazma z optično emisijsko spektroskopijo) oziroma ICP-MS (Induktivno sklopljena plazma z masno spektroskopijo). Z omenjenima metodama so bile izmerjene tudi vsebnosti elementov v raztopljeni obliki in v obliki trdnih delcev v površinski vodi. Vrednosti Hg so bile v vseh vzorcih izmerjene z AFS (atomska fluorescentna spektrometrija). Vsebnosti Cr(VI) so bile določene z ionsko kromatografijo s spektrofotometrično detekcijo in izračunom trivalentnega kroma iz izmerjene vrednosti. Kvaliteta analize je bila sledeča. Vsebnosti v slepih vzorcih so bile zanemarljive oziroma pod mejo določljivosti. Točnost (izkoristek %) analitike vseh obravnavanih vzorcev po razklopu z zlatotopko, v vodnih izlužkih, kot tudi v raztopljeni obliki in obliki trdnih delcev v vodi, je bila dobra (90–110 %). Ponovljivost (relativna odstotna razlika oziroma RPD) je bila za večino elementov ter za Cr(VI) v vseh obravnavanih materialih dobra (<10 %). Izjeme so Ba, Ca, Li, P, Sr, S in V v trdnih materialih po razklopu z zlatotopko ter Ba in Zn v vodnih izlužkih, kjer je bila ponovljivost zadovoljiva (<20 %). Ponovljivost je bila slaba za Zn v obliki trdnih delcev v površinski vodi (44 %).

Vrednotenje rezultatov

Izmerjene vsebnosti v tleh smo primerjali z medianami in geokemičnimi zgornjimi mejami naravne variabilnosti (P97,5 oz. 97,5. percentil) (Gosar et al., 2019). Geokemična zgornja meja naravne variabilnosti se uporablja za določitev območij z nenavadno visokimi vsebnostmi elementov. Z geokemičnimi zgornjimi mejami naravne variabilnosti izdvojimo območja tal, ki zahtevajo večjo pozornost in morda nadaljnje analize in študije (Reimann et al., 2018). Za oceno stanja tal smo rezultate celokupnih vrednosti ovrednotili z opozorilnimi in kritičnimi imisijskimi vrednostmi nevarnih snovi v tleh, ki so določene v Prilogi 1 Uredbe o mejnih, opozorilnih in kritičnih imisijskih vrednostih nevarnih snovi v tleh (Ur. l. RS št. 68/96, 41/04-ZVO-1 in 44/22 – ZVO-2). Opozorilna imisijska vrednost (v nadaljnjem besedilu: opozorilna vrednost) je gostota posamezne nevarne snovi v tleh, ki pomeni pri določenih vrstah rabe tal verjetnost škodljivih učinkov ali vplivov na zdravje človeka ali okolje. Kritična imisijska vrednost (v nadaljnjem besedilu: kritična vrednost) je gostota posamezne nevarne snovi v tleh, pri kateri zaradi škodljivih učinkov ali vplivov na človeka in okolje onesnažena tla niso primerna za pridelavo rastlin, namenjenih prehrani ljudi ali živali ter za zadrževanje ali filtriranje vode. V uredbi (Ur. l. RS št. 68/96, 41/04-ZVO-1 in 44/22 – ZVO-2) so sicer podane tudi mejne vrednosti, pri katerih se ne poslabšuje kakovost podzemne vode ter rodovitnost tal oz. so učinki ali vplivi na zdravje človeka ali okolje še sprejemljivi, zato teh vrednosti nismo vključili v obdelavo podatkov.

Razliko vsebnosti elementov v potočnih sedimentih in v površinski vodi na dolvodni lokaciji v primerjavi z gorvodno lokacijo smo izračunali kot obogatitveno razmerje (ER), in sicer s količnikom med vsebnostjo v potočnem sedimentu oziroma površinski vodi dolvodno in koncentracijo v potočnem sedimentu oziroma površinski vodi gorvodno. Za vrednosti pod mejo določljivosti merilne metode (LOQ) smo za izračun uporabili polovično vrednost LOQ.

Za oceno stanja površinske vode smo rezultate ovrednotili glede na najvišje dovoljene koncentracije okoljskega standarda kakovosti (NDK-OSK), ki so določene z Uredbo o stanju površinskih voda (Ur. l. RS št. 14/09, 98/10, 96/13, 24/16 in 44/22 – ZVO-2).

Rezultati in razprava

Vrednosti, ki so bile izmerjene > LOQ so podane v tabelah, in sicer v tabeli 1 za kamnine, tabeli 2 za tla, v tabeli 3 za potočne sedimente, v tabeli 4 za površinske vode in v tabeli 5 za izlužke kamnin, tal in potočnih sedimentov.

Geokemična porazdelitev elementov

Na območju Koprive so vsebnosti elementov v kamninah (tabela 1), ki so bile odvzete iz odlagališča jalovine, kjer je predvideno testno območje, podobne vsebnostim elementov v svežih vzorcih kamnin iz pridobivalnega prostora. Analize potrjujejo, da je material v podlagi, na katerem bo vzpostavljeno testno območje, jalovina iz pridobivalnega prostora. Vsebnosti elementov so si podobne tudi v obeh vzorcih na območju Lipovškega vrha. V vzorcih kamnin iz Koprive in Lipovškega vrha vsebnosti Ca znatno prevladujejo (tabela 1). Geološko podlago obravnavanih območij pretežno gradijo apnenci (Repen/Kopriva masivni apnenec v Koprivi in Litotamnijski apnenec ter apnenčevi peščenjaki in laporovci v Lipovškem vrhu). Analize vodnih izlužkov so pokazale, da se iz kamnin v vodo izlužujejo Ca, Mg, Sr, Al, Ba, V in Zn (tabela 5). Iz kamnin iz območja Koprive se izlužuje še Na, iz kamnin iz Lipovškega vrha pa K.

V vzorcih tal so na splošno na obeh obravnavanih območjih vsebnosti elementov višje od median za slovenska tla (Gosar et al., 2019), z izjemo Hg v vseh vzorcih (z izjemo vzorčnega mesta LT2G1), P v vseh vzorcih (z izjemo vzorčnega mesta LT2G1) in Mg v vzorcih iz Koprive, katerih izmerjene vsebnosti so nekoliko nižje.

Glede na zgornje meje naravne variabilnosti za Slovenijo (Gosar et al., 2019) so izmerjene vrednosti na območju Koprive višje na vzorčnem mestu KT1 in KT2 v obeh slojih za elementa Al in Li, ter za Be in Fe v KT2. Fe in K sta povišana tudi v spodnjem sloju KT1. V zgornjem sloju KT2 sta povišana Cr in Pb. V Lipovškem vrhu so vsebnosti na vzorčnem mestu LT1 višje za Li v obeh slojih in La v spodnjem sloju. Na vzorčnem mestu LT2 je povišan B in na vzorčnem mestu LT3 je povišan Sr. Na obeh obravnavanih območjih se iz tal v vodo izlužujejo Al, Ba, Ca, Fe, Hg, Mg, Mn, Na in Sr (tabela 5). V posameznih vzorcih so bili v vodnem izlužku zaznani tudi Cu (KT1G1, LT1G1, LT3G1), K (LT1G1, LT2G1, LT3G1), V (KT2G2, LT2G1) in Zn (KT2G1, KT2G2, LT1G1).

Za vsa zgoraj navedena preseganja elementov (z izjemo Pb v Koprivi in B v Lipovškem vrhu) predvidevamo, da so naravnega izvora, na kar nakazujejo naslednja dejstva. Vsi obravnavani vzorci tal na območju Koprive ter vzorec tal na vzorčnem mestu

Tabela 1. Vsebnosti elementov v kamnini.
Table 1. Element contents in rock.

Element	Enota / Unit	LOQ[1]	Kopriva		Lipovški vrh	
			KK1	KK2	LK1	LK2
Al	%	0,0001	0,02	0,03	0,22	0,23
As	mg/kg	0,50	<LOQ	0,76	1,50	1,95
B	mg/kg	1,0	<LOQ	1,9	2,6	2,4
Ba	mg/kg	0,20	1,3	1,3	6,1	5,9
Be	mg/kg	0,01	<LOQ	0,01	0,09	0,09
Ca	%	0,005	31,9	33,0	32,4	31,8
Ce	mg/kg	0,500	<LOQ	<LOQ	4,4	3,7
Co	mg/kg	0,20	<LOQ	<LOQ	0,54	0,51
Cr	mg/kg	0,50	0,76	0,64	6,69	6,68
Cr(VI)	mg/kg	0,060	<LOQ	<LOQ	0,064	0,221
Cu	mg/kg	1,0	<LOQ	3,3	3,6	2,9
Fe	%	0,0010	0,02	0,02	0,15	0,17
K	%	0,0005	0,0048	0,0047	0,0382	0,0370
La	mg/kg	0,50	<LOQ	<LOQ	3,0	2,8
Li	mg/kg	1,0	<LOQ	<LOQ	6,2	7,3
Mg	%	0,0005	1,15	1,09	0,43	0,32
Mn	mg/kg	0,50	16,6	11,2	24,6	21,8
Na	%	0,0015	0,0155	0,0216	0,0249	0,0249
Ni	mg/kg	1,0	<LOQ	<LOQ	4,8	5,6
P	mg/kg	5,0	20,5	14	366	391
Pb	mg/kg	1,0	<LOQ	<LOQ	1,8	2,0
S	mg/kg	30	101	119	232	184
Sr	mg/kg	0,10	244	276	709	663
Ti	mg/kg	0,20	3,86	4,03	24	21,9
V	mg/kg	0,10	0,94	1,06	6,79	6,61
Zn	mg/kg	3,0	<LOQ	<LOQ	5,6	5,7

[1]Meja kvantifikacije / Limit of Quantification;

LT1 v Lipovškem vrhu so bili odvzeti v tleh, ki ležijo na prvotni matični podlagi. Matično podlago v Lipovškem vrhu glede na OGK List Ljubljana predstavlja Litotamnijski apnenec (tortonij) (Premru, 1983) v Koprivi pa glede na OGK List Gorica (Buser, 1968) temno siv gost skladovit apnenec v menjavi z rudistnim apnencem (tortonij). Tla, ki so bila odvzeta na vzorčnih mestih LT2 in LT3 (Lipovški vrh), so antropogena, ki ležijo na antropogenem nasutju, in sicer jalovini iz bližnjega pridobivalnega prostora. Vsebnosti elementov v antropogenih tleh LT2 so zelo podobne vsebnostim elementov v tleh iz vzorčnega mesta LT1. Vsebnosti elementov v antropogenih tleh LT3 se za večino elementov precej razlikujejo od tistih v vzorcih tal iz vzorčnih mest LT2 in LT1 (tabela 2). Geokemična porazdelitev elementov v vzorcu antropogenih tal LT2G1 nakazuje, da gre verjetno za premeščen talni material iz lokalnega okolja, v vzorcu antropogenih tal LT3G1 pa, da gre za premeščen talni material, ki ni iz lokalnega okolja.

Pučko in sodelavci (2024) so na podlagi primerjave porazdelitve elementov v zgornjem in spodnjem sloju v tleh Slovenije ugotovili, da so v spodnjem sloju tal Slovenije povišane vsebnosti elementov, kot so Th, Na, Cs, Sc, Co, Rb, Al, La, Fe, Li, Mn, itd., ki so tipični gradniki mineralov v kamninah, naravnega izvora (matična podlaga). Poleg tega so za tla, ki ležijo na karbonatni matični podlagi, značilne nekoliko višje vsebnosti nekaterih elementov v sledovih, kot so na primer Mo, Ni, As, V, Hg, Sb, Bi, U, Cu, Li, Cr, Co (Gosar, 2007). Preiskave tal, ki se nahajajo na različnih apnenčastih karbonatnih podlagah (Sežanska, Lipiška in Liburnijska formacija), so pokazale, da porazdelitev elementov v tleh na splošno odraža porazdelitev elementov v matični kamnini, vendar pa ni zgolj odraz netopnega ostanka karbonatne

Tabela 2. Vsebnosti elementov v tleh skupaj z zakonodajnimi vrednostmi in vrednostmi ozadja za tla Slovenije.
Table 2. Element contents in soil together with legislation values and Slovenian soil background concentrations.

Element	Enota / Unit	LOQ[1]	Kopriva				Lipovški vrh				opozorilna & kritična[2] / warning & critical[2]	Md[3] Slo	GT[4] Slo
			KT1G1	KT1G2	KT2G1	KT2G2	LT1G1	LT1G2	LT2G1	LT3G1			
Al	%	0,0001	3,7	4,2	5,1	5,1	3	3,3	3,4	0,5	-	1,8	3,5
As	mg/kg	0,5	18,1	23,6	23,6	25,6	13,8	14,5	17,8	8,8	30 / 55	11	34
B	mg/kg	1	6,2	5,3	5,4	5	7,3	6,5	10,3	4,4	-	2	9,5
Ba	mg/kg	0,2	127	143	132	130	111	114	112	16,2	-	75	200
Be	mg/kg	0,01	2	2,3	2,5	2,7	1,6	1,6	1,6	0,2	-	0,9	2,4
Ca	%	0,005	0,76	0,65	0,51	0,64	0,73	0,71	1,29	20	-	0,4	14
Cd	mg/kg	0,4	0,74	0,73	0,76	0,76	1,4	1,2	1,98	0,47	2 / 12	0,5	4
Ce	mg/kg	0,5	58,9	66,1	54,3	59	64,4	71,4	56,2	8,9	-	38	80
Co	mg/kg	0,2	22,3	24,1	21	21,4	18,4	17,3	15,3	4,09	50 / 240	14	38
Cr	mg/kg	0,5	71,3	79,6	98,7	96,5	56,4	61,5	59,6	10,5	150 / 380	34	89
Cr(VI)	mg/kg	0,06	<LOQ	0,206	<LOQ	<LOQ	<LOQ	<LOQ	0,224	<LOQ	- / 25	-	-
Cu	mg/kg	1	42,4	51,3	40,1	39,8	24,3	23,1	33	11,6	100 / 300	20	68
Fe	%	0,001	4,4	4,9	5,5	5,9	3,7	3,9	3,9	1,2	-	2,9	4,5
Hg	mg/kg	0,2	0,09	0,07	0,08	0,08	0,05	0,05	0,14	0,09	2 / 10	0,10	0,66
K	%	0,005	0,3	0,33	0,3	0,3	0,27	0,28	0,33	0,11	-	0,1	0,32
La	mg/kg	0,5	30,7	35	30	32,4	36,7	40,7	32,2	5,2	-	17	39
Li	mg/kg	1	54,4	61,1	65	66,7	57,1	61,6	64	15,2	-	19	43
Mg	%	0,0005	0,4	0,41	0,43	0,42	0,53	0,55	0,62	0,68	-	0,5	6,5
Mn	mg/kg	0,5	1740	1840	1480	1400	1090	938	842	139	-	790	2700
Mo	mg/kg	0,4	1,63	1,69	1,99	2,04	1,28	1,07	1,52	0,5	40 / 200	0,7	6,8
Na	%	0,0015	0,01	0,01	0,01	0,02	0,09	0,01	0,01	0,02	-	0	0,02
Nb	mg/kg	0,5	1,02	0,88	1,36	1,36	1,06	0,8	1,04	<LOQ	-	0,6	2,3
Ni	mg/kg	1	58,1	64,2	**75,8**	**77,1**	49,6	46,9	66	17,8	70 / 210	29	94
P	mg/kg	5	793	683	646	629	854	675	1160	673	-	1000	1800
Pb	mg/kg	1	40,1	40,5	**122**	38,4	33,2	30,4	34,9	6,6	100 / 530	34	110
S	mg/kg	30	612	566	718	586	604	345	947	586	-	300	1700
Sn	mg/kg	1	2,5	2,7	2,4	2,5	1,3	1,3	1,8	<LOQ	-	1,1	3
Sr	mg/kg	0,1	19,8	21,7	19,1	20,8	35,8	37,3	52,7	498	-	14	180
Ti	%	0,0002	0,02	0,02	0,02	0,02	0,02	0,03	0,02	0,003	-	0,006	0,07
V	mg/kg	0,1	90,8	99,5	118	123	69,3	69,8	77,6	14,7	-	40	150
Zn	mg/kg	3	87,3	89,9	95,1	82,7	83,2	81,8	111	28	300 / 720	72	170

[1]Meja kvantifikacije / Limit of Quantification; [2]Zakonodajna vrednost za tla / soil legislation value (Ur. L. RS. št. 68/96, 41/04 – ZVO-1 in 44/22 – ZVO-2); [3]Mediana za tla Slovenije / Median for Slovenian soil (Gosar et al., 2019); [4]Zgornja meja naravne variabilnosti za Slovenijo (P97,5, percentil) / Geochemical threshold (97,5th percentile) (Gosar et al., 2019); **s krepkim slogom** pisave so predstavljene vrednosti, ki presegajo zakonodajne vsebnosti / **in bold** values, which exceed legislation values are shown; s podčrtanim slogom pisave so predstavljene vrednosti, ki presegajo zgornje meje naravne variabilnosti / in underlined values, which exceed geochemical thresholds, are shown.

podlage, temveč tudi materiala, ki se pojavlja med karbonatnimi plastmi, ravno tako je verjeten tudi eolski doprinos (Zupančič et al., 2018). Pri tem velja dejstvo, da primerjava netopnega ostanka matične kamnine s tlemi vključuje domnevo, da so tla v osnovi nastala z raztapljanjem stratigrafsko višjih plasti kamnin, ki so enake vzorčeni matični podlagi, kar pa lahko drži ali ne drži; v slednjem primeru bi tudi to lahko vplivalo na razlike v geokemični porazdelitvi (Šušteršič et al., 2009). Preiskave pedoloških parametrov in porazdelitve elementov ter mineralne sestave v talnih horizontih (A, E in Bt), ki so se razvili na karbonatnih podlagah, so pokazale, da na razporeditev elementov v talnem profilu pomembno vplivajo pedološki procesi (eluvialno-iluvialno procesi) (Turniški et al., 2023). Z uporabo statističnih metod je bil preučen tudi morebiten vpliv klimatskih faktorjev

Tabela 3. Vsebnosti elementov v potočnih sedimentih in obogatitveno razmerje (ER).
Table 3. Element contents in stream sediments and enrichment ratio (ER).

Element	Enota /Unit	LOQ[1]	Suhi potok			Kolovratščica		
			LS1	LS2	ER[2]	LS3	LS4	ER
Al	%	0,0001	0,148	0,176	1,2	0,336	0,105	0,3
As	mg/kg	0,50	0,94	1,3	1,4	1,93	0,98	0,5
B	mg/kg	1,0	2,2	3,4	1,5	4,8	2,1	0,4
Ba	mg/kg	0,20	4,24	7,88	1,9	7,54	3,96	0,5
Be	mg/kg	0,010	0,116	0,141	1,2	0,193	0,073	0,4
Ca	%	50	0,812	4,46	**5,5**	8,97	12,8	1,4
Ce	mg/kg	0,500	7,11	8,59	1,2	10,6	4,38	0,4
Co	mg/kg	0,20	1,17	3,67	**3,1**	2,71	0,64	0,2
Cr	mg/kg	0,50	2,82	4,14	1,5	6,08	2,27	0,4
Cr(VI)	mg/kg	0,060	0,06	<LOQ	0,5	0,126	<LOQ	0,2
Cu	mg/kg	1,0	<LOQ	1,1	2,2	2,9	0,5	0,2
Fe	%	10	0,286	0,364	1,3	0,722	0,146	0,2
Hg	mg/kg	0,20	<LOQ	<LOQ	-	<LOQ	0,01	2,0
K	%	5,0	0,042	0,058	1,4	0,09	0,035	0,4
La	mg/kg	0,50	4,13	5,13	1,2	5,69	2,86	0,5
Li	mg/kg	1,0	1,2	2,3	1,9	6,8	2,5	0,4
Mg	%	5,0	0,058	0,392	**6,8**	3,65	6,38	1,7
Mn	mg/kg	0,50	53,1	199	**3,7**	134	48,1	0,4
Mo	mg/kg	0,40	<LOQ	<LOQ	-	0,57	<LOQ	0,4
Na	%	15	<LOQ	66	**8,8**	113	139	1,2
Ni	mg/kg	1,0	3	4,4	1,5	6	2	0,3
P	mg/kg	5,0	89	132	1,5	205	107	0,5
Pb	mg/kg	1,0	1,8	3,4	1,9	4	1,4	0,4
S	mg/kg	30	<LOQ	73	**4,9**	240	145	0,6
Sr	mg/kg	0,10	9,45	92,1	**9,7**	85,5	86,6	1,0
Ti	%	0,20	29	79,4	2,7	73,1	27,4	0,4
V	mg/kg	0,10	3,26	4,35	1,3	6,73	3,03	0,5
Zn	mg/kg	3,0	5,7	5,8	1,0	8,1	3,8	0,5

[1]Meja kvantifikacije / Limit of Quantification; [2]Obogatitveno razmerje ER = enrichment ratio; s **krepkim slogom** pisave so predstavljene vrednosti ER ≥ 3; **in bold** values of ER ≥ 3 are shown.

na porazdelitve kovin (Co, Cr, Cu, Ni, Pb in Zn) v zgornjem sloju tal (0–15 cm), ki se nahajajo na enaki karbonatni matični podlagi (zgornji triasni dolomit) na različnih koncih Slovenije (Zupančič, 2017). Avtorica ugotavlja, da so vsebnosti Co, Cr in Ni visoke (mestoma presegajo tudi mejne ali celo kritične zakonodajne vrednosti) zaradi naravnih danosti (preperevanja matične podlage), pri čemer obstaja verjetnost, da na njihovo porazdelitev vplivajo tudi pospešeno izluževanje tal zaradi padavin in vetrni transport iz bližnjih flišnih kamnin. Za vsebnosti Pb, Zn in Cd povezave s klimatskimi pogoji niso bile ugotovljene, so pa bile vsebnosti Pb in Zn na nekaterih lokacijah povišane, katerim je bil pripisan naravni izvor (bioakamulacija) zaradi odsotnosti očitnih virov onesnaževanja na obravnavanih lokacijah.

Na podlagi zgornje razprave lahko za visoke vsebnosti Pb v tleh iz območja Koprive predvidevamo, da so naravnega ali antropogenega izvora. V neposredni bližini obravnavanega območja ni aktivnih antropogenih dejavnosti. Približno 70 m SSV se nahaja odkopna površina, kjer poteka izkoriščanje naravnega kamna-apnenca. Glede na to, da se vrednost Pb z globino zniža za 3×, bi bilo možno, da so višje vrednosti posledica zračnih emisij ali bioakumulacije. Izvor B na vzorčnem mestu LT2 na območju Lipovškega vrha ni znan.

Tabela 4. Rezultati parametrov v površinskih vodah.

Table 4. Results of parameters in surface water.

Parameter	Enota / Unit	LOQ[1]	LV1	LV2	ER[2]	LV3	LV4	ER[2]	NDK-OSK[3]
Osnovni kemijski parametri / Basic chemical parameters									
Ca	mg/L	0,05	99,2	125	-	75,7	83,9	-	-
Mg	mg/L	0,0005	2,48	20,6	-	20,4	14,8	-	-
Na	mg/L	0,03	3,39	22,4	-	4,13	6,64	-	-
K	mg/L	0,05	0,526	7,6	-	1,56	1,88	-	-
Cl	mg/L	0,5	9,21	11,3	-	4,24	6,25	-	-
F	mg/L	0,02	0,062	0,182	-	0,066	0,106	-	6,8
Nitrati	mg/L	0,04	0,757	4,95	-	2,69	6,33	-	6,59,5
Sulfat	mg/L	0,5	11,2	170	-	15,5	29,4	-	-
Hidrogenkarbonat (HCO_3^-)	mg/L	0	311	341	-	314	275	-	-
Karbonati (CO_3^{2-})	mg/L	0	0	0	-	4,42	0	-	-
Prosti ogljikov dioksid kot CO_2	mg/L	0	4,88	0	-	0	0	-	-
Skupni ogljikov dioksid kot CO_2	mg/L	0	229	246	-	230	199	-	-
Agresiven CO_2	mg/L	0	0	0	-	0	0	-	-
Ortofosfat	mg/L	0,04	0,063	0,089	-	0,123	0,07	-	-
Skupni ogljik	mg/L	0,5	66,5	69,7	-	65,5	56,5	-	-
Nitriti	mg/L	0,04	<LOQ	<LOQ	-	<LOQ	0,041	-	-
Mikroelementi v raztopljeni obliki / Microelements in dissolved form									
Ba	µg/L	0,5	7,63	22,1	2,9	8,84	9,24	1,0	-
B	µg/L	10	<LOQ	24	4,8	<LOQ	<LOQ	1,0	1830
Fe	µg/L	2	11,5	<LOQ	0,1	3,9	<LOQ	0,5	-
Li	µg/L	1	<LOQ	1,2	2,4	<LOQ	<LOQ	1,0	-
Mn	µg/L	0,5	<LOQ	0,6	2,4	3,18	0,79	0,2	-
Mo	µg/L	2	<LOQ	1,9	1,9	<LOQ	<LOQ	1,0	200
Se	µg/L	10	<LOQ	1,4	0,3	<LOQ	<LOQ	1,0	72
Sr	µg/L	1	85,6	641	7,5	104	257	2,5	-
S	mg/L	30	2,75	57,7	21,0	4,69	10,5	2,2	-
U	µg/L	0,1	0,77	2,6	3,4	0,6	0,87	1,5	-
Zn	µg/L	3	<LOQ	4,6	3,1	3,6	16,8	4,7	82,2
Elementi v obliki trdnih delcev / Elements in particulate form									
Al	µg/L	10	54	<LOQ	0,1	76	59	0,8	-
Ba	µg/L	0,5	7,92	35,3	4,5	10,2	20,7	2,0	-
B	µg/L	10	<LOQ	22	4,4	<LOQ	<LOQ	1,0	1830
Fe	µg/L	5	8,8	15,1	1,7	49,5	23,4	0,5	-
Mn	µg/L	0,5	0,65	1,13	1,7	6,33	1,53	0,2	-
S	mg/L	0,1	2,61	47,3	18,1	4,32	8,36	1,9	-
Ti	µg/L	1	1	<LOQ	0,5	1,2	1,1	0,9	-
Zn	µg/L	3	<3	7,5	5,0	<LOQ	<LOQ	1,0	82,2

[1]Meja kvantifikacije / Limit of Quantification; [2]Obogatitveno razmerje / Enrichment ratio; [3]Največja dovoljena koncentracija okoljskega standarda kakovosti za kemijsko in ekološko stanje površinske vode / the maximum permissible concentration of the environmental quality standard for the chemical and ecological state of surface water.

Tabela 5. Rezultati vsebnosti elementov v izlužku.
Table 5. Results of element contents in leachates.

			Kamnina / Rock				Tla / Soil								Potočni sediment / Stream sediment			
Parameter	**Unit / Enota**	**LOQ[1]**	**KK1**	**KK2**	**LK1**	**LK2**	**KT1G1**	**KT1G2**	**KT2G1**	**KT2G2**	**LT1G1**	**LT1G2**	**LT2G1**	**LT3G1**	**LS1**	**LS2**	**LS3**	**LS4**
Al	mg/kg	0,1	2,92	3,36	1,88	2,2	1,81	2,26	0,588	0,718	3,24	0,259	5,4	<LOQ	5,94	6,06	3,37	2,39
B	mg/kg	0,1	<LOQ	<LOQ	<LOQ	<LOQ	<LOQ	<LOQ	<LOQ	<LOQ	<LOQ	<LOQ	<LOQ	<LOQ	0,14	<LOQ	<LOQ	<LOQ
Ba	mg/kg	0,005	0,13	0,17	0,13	0,16	0,186	0,194	0,152	0,637	0,278	0,0845	0,234	0,22	0,13	0,08	0,18	1,02
Ca	mg/kg	0,5	54,6	58,2	90,9	89,8	166	102	114	151	396	252	483	424	94,8	111	135	124
Cu	mg/kg	0,01	<LOQ	<LOQ	<LOQ	<LOQ	0,132	<LOQ	<LOQ	<LOQ	0,202	<LOQ	<LOQ	0,133	0,02	<LOQ	0,05	<LOQ
Fe	mg/kg	0,02	<LOQ	<LOQ	<LOQ	<LOQ	0,92	1,15	0,267	0,352	1,93	<LOQ	2,79	<LOQ	2	0,65	3,01	1,4
Hg	mg/kg	0,1	<LOQ	<LOQ	<LOQ	<LOQ	0,16	0,16	0,19	0,22	0,12	<LOQ	0,12	0,12	<LOQ	<LOQ	<LOQ	<LOQ
K	mg/kg	0,5	<LOQ	<LOQ	<LOQ	10	<LOQ	<LOQ	<LOQ	<LOQ	22,4	<LOQ	11,6	56,4	3,99	13,3	9,31	7,65
Mg	mg/kg	0,03	10,3	8,84	11,0	7,18	12	2,98	6,91	5,62	25,9	5,76	20,7	49,2	3,71	11,8	29,6	25,2
Mn	mg/kg	0,005	<LOQ	<LOQ	<LOQ	<LOQ	0,0616	0,0277	0,0394	0,0428	0,0282	<LOQ	0,0309	0,0141	0,09	0,03	0,06	0,08
Na	mg/kg	0,3	6,72	10,5	<LOQ	<LOQ	5,66	4,17	10,6	7,32	5,3	<LOQ	4,94	5,66	7,17	22	6,15	17,5
P	mg/kg	0,5	<LOQ	<LOQ	<LOQ	<LOQ	<LOQ	<LOQ	<LOQ	<LOQ	<LOQ	<LOQ	<LOQ	<LOQ	0,8	<LOQ	<LOQ	<LOQ
Sr	mg/kg	0,01	0,61	0,72	1,04	1	0,224	0,142	0,151	0,222	0,994	0,572	1,25	1,73	0,17	0,44	0,22	0,32
S	mg/kg	0,3	<LOQ	<LOQ	<LOQ	<LOQ	<LOQ	<LOQ	<LOQ	<LOQ	<LOQ	<LOQ	<LOQ	<LOQ	<LOQ	19,6	<LOQ	<LOQ
V	mg/kg	0,01	0,01	0,02	0,02	0,02	<LOQ	<LOQ	<LOQ	0,016	<LOQ	<LOQ	0,03	<LOQ	0,02	0,02	0,02	0,03
Zn	mg/kg	0,02	0,44	0,47	0,54	0,46	<LOQ	<LOQ	0,388	2,43	0,414	<LOQ	<LOQ	<LOQ	0,02	<LOQ	0,06	0,63

[1]Meja kvantifikacije / Limit of quantification

Vzorčno mesto se nahaja na kmetijski površini (pašnik, v bližini so njive). Na obravnavanem območju Lipovškega vrha so v ožji okolici možni antropogeni viri kmetijstvo, promet in izkoriščanje mineralnih surovin (apnenec za industrijske namene in tehnični kamen, ki ima veljavno koncesijo od leta 2000 (ZRP, 2024)). Dejstvo pa je, da so tla na vzorčnem mestu LT2 antropogena, od kod so bila tla pripeljana pa ni znano.

Ob upoštevanju zakonodajnih smernic za tla (Ur. l. RS št. 68/96, 41/04-ZVO-1 in 44/22 – ZVO-2), so vsebnosti za As, Cd, Cr, Cr(VI), Co, Cu, Hg, Mo, Ni, Pb in Zn pod opozorilnimi oz. kritičnimi vrednostmi (tabela 2), z izjemo Pb (122 mg/kg) v zgornjem sloju vzorčnega mesta KT2, ki presega opozorilno vrednost za tla (100 mg/kg), in Ni v zgornjem (75,8 mg/kg) ter spodnjem sloju (77,1 mg/kg) tal vzorčnega mesta KT2, ki na obeh globinah presega opozorilno vrednost (70 mg/kg). Na podlagi zgornje meje naravne variabilnosti za Ni (94 mg/kg) (Gosar et al., 2019) in dejstva, da se v tleh nastalih na karbonatni podlagi lahko pojavljajo višje vsebnosti Ni (Gosar, 2007; Zupančič, 2017; Zupančič et al., 2018; Pučko et al., 2024; Turniški et al., 2024) smatramo, da so višje vsebnosti Ni naravnega izvora. Za višje vsebnosti Pb smatramo, da so lahko antropogenega (emisije iz zraka) ali naravnega izvora (bioakumulacija). Glede na rezultate v izlužkih sta tako Ni kot Pb slabo vodotopna (slabo mobilna) v obeh slojih, izmerjeni vrednosti sta bili < LOQ oz. < 0,02 mg/kg za Ni in < 0,05 mg/kg za Pb.

Vsebnosti elementov v gorvodnih in dolvodnih potočnih sedimentih ter površinskih vodah iz območja Lipovškega vrha so podane v tabelah 3 in 4.

V Suhem potoku so v dolvodnem sedimentu višje vsebnosti Sr (9,7×), Na (8,8×), Mg (6,8×), Ca (5,5×), S (4,9×), Mn (3,7×) in Co (3,1×). Ostali elementi so bili višji za manj kot trikrat, kar smatramo za zanemarljivo. Višje vsebnosti (>3×) elementov kažejo na povečan doprinos karbonatnega materiala vzdolž Suhega potoka na vzhodni strani pridobivalnega prostora. Glede na to, da se geološka sestava v zaledju in vzdolž potoka bistveno ne spremeni, višje vsebnosti pripisujemo antropogenim vplivom (izpiranje materiala iz pridobivalnega prostora in cest). V površinski vodi Suhega potoka so bili na dolvodni lokaciji (LV2) v raztopljeni obliki višji naslednji elementi: S (21×), Sr (7,5×), B (4,8×), U (3,4×) in Zn (3,1×). V obliki trdnih delcev so bili povišani S (18,1×), Ba (4,5×) in B (4,4×). Elementa B (vzorčno mesto LT2) in Sr (vzorčno mesto LT3) sta višja tudi v tleh drenažnega zaledja Suhega potoka. Elementa Sr in S sta višja tudi v dolvodnem sedimentu Suhega potoka.

V potoku Kolovratščica je v sedimentu večina vsebnosti elementov na dolvodni lokaciji (LS4) nižja. V površinski vodi Kolovratščice (LV3, LV4) je bil na dolvodni lokaciji (LV4) višji samo Zn (4,7×) v raztopljeni obliki.

Vrednosti raztopljenih elementov v površinski vodi so v obeh obravnavanih vodotokih pod mejnimi vrednostmi za ekološko stanje površinskih voda (Ur. l. RS, št. 14/09, 98/10, 96/13, 24/16 in 44/22 – ZVO-2).

Analiza vodnih izlužkov je pokazala, da se v obeh vodotokih iz gorvodnega in dolvodnega sedimenta v vodo izlužujejo Al, Ba, Ca, Fe, K, Mg, Mn, Na, Sr, V in Zn. Iz gorvodnih sedimentov se izlužuje še Cu v obeh vodotokih in B ter P v Suhem potoku (LS1). V dolvodnem sedimentu Suhega potoka se izlužuje S.

Rezultati osnovnih fizikalno-kemijskih parametrov površinske vode (tabela 6) so pokazali, da je bila temperatura površinske vode v času vzorčenja na obeh vodotokih med 10,8 in 12,5 °C. Voda je imela pH vrednost med 7,6 in 8,5. Izmerjene vrednosti so v okviru sprejemljivih vrednosti za vode naravnega okolja. Prav tako so pri izmerjeni temperaturi vode razmere s kisikom oksidativne. Izmerjene vsebnosti raztopljenega kisika so bile med 9,69 (LV1) in 10,53 (LV2) mg/L O_2.

Tabela 6. Rezultati terenskih meritev v površinski vodi.
Table 6. Results of field measurements in surface water.

Parameter	Enota / Unit	LV1	LV2	LV3	LV4
Temperatura vode	°C	10,8	11,9	12,5	10,8
Električna prevodnost	mS/m	50,7	83,0	49,9	49,0
pH vrednost	-	7,58	8,06	8,48	7,85
Oksidacijsko-redukcijski potencial	mV	-46	-38	-55	-37
Raztopljen kisik	mg/L	9,69	10,53	9,93	10,14
Nasičenost s kisikom	%	91,3	101,1	96,6	95
Motnost	NTU	0,2	0,38	1,5	1,07

Električna prevodnost, kot merilo raztopljenih ionsko aktivnih snovi, je bila na obeh vzorčnih mestih na vodotoku Kolovratščica ter na gorvodnem vzorčnem mestu L1 na občasnem vodotoku na vzhodni strani kamnoloma podobna in je znašala okoli 50,0 mS/cm. Izjema je dolvodno vzorčno mesto LV2 na občasnem vodotoku na vzhodni strani, kjer je bila izmerjena električna prevodnost nekoliko višja, 83,0 mS/cm. Povišana vrednost električne prevodnosti na vzorčnem mestu LV2 je posledica višjih koncentracij karbonatnih komponent (Ca, Mg, HCO_3^-) ter Na, K in SO_4 v površinski vodi. Razlog za višje vrednosti ionov je lahko geogen (karbonatno zaledje), možni so tudi površinski dotoki iz dovoznih površin (ceste), njiv in travnikov v zaledju.

Zaključek

Na območju Koprive porazdelitev elementov v vzorcih kamnin kaže, da podlago, kjer bo vzpostavljeno testno območje, sestavlja jalovina iz pridobivalnega prostora. V vzorcih kamnin iz obeh območij prevladuje vsebnost Ca. Vsebnosti večine elementov v tleh so na obeh območjih višje od mediane za slovenska tla. Glede na primerjavo z zgornjimi mejami naravne variabilnosti, so v tleh na območju Koprive povišani Al, Be, Fe, Li in K, na območju Lipovškega vrha pa Li, La, Sr in B. Slednje je posledica naravnih danosti (razvoj tal na karbonatni matični podlagi). Glede na zakonodajne smernice (opozorilne vrednosti) so bile na območju Koprive v travniških tleh zaznane povišane vsebnosti Pb v zgornjem sloju, ter Ni v zgornjem in spodnjem sloju. Za povišane vsebnosti Pb smatramo, da so lahko antropogenega ali naravnega izvora. Višje vsebnosti Ni pripisujemo naravnemu izvoru. V potoku Kolovratščica je bila porazdelitev elementov v sedimentih in površinski vodi na dolvodni in gorvodni lokaciji podobna. V Suhem potoku smo v dolvodnem sedimentu ugotovili višje vsebnosti za elemente (Mg, Na, Sr, Ca, Mn in S), kar kaže na povečan antropogen doprinos karbonatnega materiala vzdolž potoka (izpiranje karbonatnega materiala iz bližnjega kamnoloma in cest). V površinski vodi Suhega potoka smo ugotovili višje vsebnosti elementov S, Sr, B, U in Zn, ki pa niso presegle zakonodajnih smernic.

Zahvala

Raziskave smo izvedli s finančno podporo evropskega projekta LIFE20 IPE/SI/000021 - LIFE IP RESTART “Boosting waste recycling into valuable products by setting the environment for a circular economy in Slovenia” in Javne agencije za znanstvenoraziskovalno in inovacijsko dejavnost Republike Slovenije (ARIS) preko raziskovalnega programa »Podzemne vode in geokemija (P1-0020)«.

Literatura

Artiola, H.F. & Brusseau, M.L. 2006: Environmental & pollution science. In: Pepper, I.D., Gerba, C.P. & Brusseau, M.L. (eds.): The Role of Environmental Monitoring in Pollution Science, second edition Chapter 12: 170–182.

Bavec, Š., Gosar, M., Biester, H. & Grčman, H. 2015. Geochemical investigation of mercury and other elements in urban soil of Idrija (Slovenia), Journal of Geochemical Exploration, 154: 213–223. https://doi.org/10.1016/j.gexplo.2014.10.011

Bavec, Š. & Gosar, M. 2016: Speciation, mobility and bioaccessibility of Hg in the polluted urban soil of Idrija (Slovenia), Geoderma, 273: 115–130. https://doi.org/10.1016/j.geoderma.2016.03.015.

Cerar, S. & Bavec, Š. 2019: Analiza vpliva vgrajenega sanacijskega materiala na rekultivacijo opuščenega peskokopa. Acta agriculturae Slovenica, 114/2: 293–311. http://www.dlib.si/?URN=URN:NBN:SI:DOC-MY5QDWC2

Darnley, A.G., Björklund, A., Bølviken, B., Gustavsson, N., Koval, P.V., Plant, J.A., Steenfelt, A., Tauchid, M., Xuejing, Xie., Garrett, R.G. & Hall, G.E.M. 1995: A Global Geochemical Database for Environmental and Resource Management. Recommendations for International Geochemical Mapping – Final Report of IGCP Project 259. Earth Science Report 19. UNESCO Publishing, Paris: 122 p. https://www.globalgeochemicalbaselines.eu/datafiles/file/Blue_Book_GGD_IGCP259.pdf

Đurić, M., Zalar Serjun, V. Mladenovič, A., Mauko Pranjić, A., Milačič, R., Ščančar, J., Urbanc, J., Mali, N., Pavlin, A., Turk, J. & Oprčkal, P. 2023: Environmental Acceptability of Geotechnical Composites from Recycled Materials: Comparative Study of Laboratory and Field Investigations. Int. J. Environ. Res. Public Health, 20/3: 2014. https://doi.org/10.3390/ijerph20032014

EN 12457-4:2002: Characterisation of waste - Leaching - Compliance test for leaching of granular waste materials and sludges - Part 4: One stage batch test at a liquid to solid ratio of 10 l/kg for materials with particle size below 10 mm (without or with size reduction).

Gałuszka A. & Migaszewski, Z. 2011: Geochemical background - an environmental perspective.

Mineralogia, 42/1: 7–17. https://doi.org/10.2478/v10002-011-0002-y

Gassama, N., Curie, F., Vanhooydonck, P., Bourrain, X. & Widory, D. 2021: Determining the Regional Geochemical Background for Dissolved Trace Metals and Metalloids in Stream Waters: Protocol, Results and Limitations—The Upper Loire River Basin (France). Water, 13/13: 1845. https://doi.org/10.3390/w13131845

Gosar, M. 2007: Porazdelitev slednih prvin v treh kraških talnih profilih v Sloveniji = Trace element distribution in three karst soil profiles from Slovenia. Geologija 50/1: 147–156. https://doi.org/10.5474/geologija.2007.012

Gosar, M., Šajn, R., Bavec, Š., Gaberšek, M., Pezdir, V. & Miler, M. 2019: Geochemical background and threshold for 47 chemical elements in Slovenian topsoil. Geologija, 62/1: 7–59. https://doi.org/10.5474/geologija.2019.001

Gosar, M., Šajn, R., Miler, M., Burger, A. & Bavec, Š. 2020: Overview of existing information on important closed (or in closing phase) and abandoned mining waste sites and related mines in Slovenia. Geologija, 63/2: 221–250. https://doi.org/10.5474/geologija.2020.018

Hawkes, 1957: Principles of geochemical prospecting. Bulletin 1000-F: 225-355. https://doi.org/10.3133/b1000F

Jurkovšek, B. 2013: Geološka karta Krasa = Geological map of Kras (Slovenia). Ljubljana, Geološki zavod Slovenije.

Koščová, M., Hellmer M., Anyona, S. & Gvozdkova, T. 2018: Geo-Environmental Problems of Open Pit Mining: Classification and Solutions. E3S Web of Conferences, 41: 01034. https://doi.org/10.1051/e3sconf/20184101034

Križnar, M. & Mikuž, V. 2014: Kamnolom Lipovica in njegove paleontološke zanimivosti. Scopolia, 82: 1–120. http://www.dlib.si/?URN=URN:NBN:SI:doc-A2JZF7YE

Kumar Das, A. & Purkait, A. 2020: Boron dynamics in soil: classification, sources, factors, fractions, and kinetics. Communications in Soil Science and Plant Analysis, 51/22: 2778–2790. https://doi.org/10.1080/00103624.2020.1849261

Mali, N., Urbanc, J., Serianz, L., Lapanje, A., Pepelnik, T., Meglič, P., Levičnik, L., Pestotnik, S., Peternel Rikanovič, R., Koren, K., Novak, M., Milanič, B., Mencin Gale, E., Jež, J., Pucihar, B. & Šolar, J.T. 2023: Hidrogeološka karta Slovenije 1: 25.000. Območje Brestovica: tolmač. Geološki zavod Slovenije, Ljubljana: 120 p.

Miler, M. & Gosar, M. 2019: Assessment of contribution of metal pollution sources to attic and household dust in Pb-polluted area. Indoor Air, 29/3: 487–498. https://doi.org/10.1111/ina.12548

Miler, M., Bavec, Š. & Gosar, M. 2022. The environmental impact of historical Pb-Zn mining waste deposits in Slovenia. Journal of Environmental Management, 308: 114580. https://doi.org/10.1016/j.jenv-man.2022.114580

MKGP, 2022: Grafični podatki RABA za celo Slovenijo (Enotna državna evidenca o dejanski rabi zemljišč). Ministrstvo za kmetijstvo, gozdarstvo in prehrano; Služba za register kmetijskih gospodarstev, Ljubljana. https://rkg.gov.si/vstop/

Pogačnik, Ž. 2022: Opis geoloških razmer v okolici površinskega kopa Lipovški vrh. Dopis GeoRudEko d.o.o. št. 778-1140/2022-GRE: 10 p.

Premru, U. 1980: Osnovna geološka karta SFRJ 1:100.000. Tolmač za list Ljubljana. Zvezni geološki zavod Beograd: 75 p.

Pučko, E., Žibret, G. & Teran, K. 2024: Comparison of elemental composition of surface and subsurface soils on national level and identification of potential natural and anthropogenic processes influencing its composition, Journal of Geochemical Exploration, 258: 107422. https://doi.org/10.1016/j.gexplo.2024.107422

Reimann, C., Fabian, K., Birke, M., Filzmoser, P., Demetriades, A., Négrel, P., Oorts, K., Matschullat, J., de Caritat, P., Albanese, S., Anderson, M., Baritz, R., Batista, M.J., Bel-Ian, A., Cicchella, D., De Vivo, B., De Vos, W., Dinelli, E., Ďuriš, M., Dusza-Dobek, A., Eggen, O.A., Eklund, M., Ernsten, V., Flight, D.M.A., Forrester, S. et al. 2018: GEMAS: Establishing geochemical background and threshold for 53 chemical elements in European agricultural soil, Applied Geochemistry, 88/B: 302–318. https://doi.org/10.1016/j.apgeochem.2017.01.021.

Salminen R. (Chief Editor), Batista M.J., Bidovec M., Demetriades A., De Vivo B., De Vos W., Duris M., Gilucis A., Gregorauskiene V., Halamic J., Heitzmann P., Lima A., Jordan G., Klaver G., Klein P., Lis J., Locutura J., Marsina K., Mazreku A., O'Connor P.J., Olsson S.Å., Ottesen R.T., Petersell V., Plant J.A., Reeder S., Salpeteur I., Sandström H., Siewers U., Steenfelt A. & Tarvainen T. 2005: FOREGS Geochemical Atlas of Europe, Part 1: Background Information, Methodology and Maps. Geological Survey of Finland, Espoo: 526 p. http://www.gtk.fi/publ/foregsatlas/

Senegačnik, A., Burger, A. & Karničnik, B. 2023: Stanje na področju mineralnih surovin v Sloveniji v letu 2022. Mineralne surovine v letu 2022, 19/1: 12–22. https://www.geo-zs.si/PDF/PeriodicnePublikacije/Bilten_2022.pdf

SIST ISO 5667-10:1996: Water quality - Sampling - Part 10: Guidance on sampling of waste waters.

SIST EN ISO 5667-6:2015: Water quality - Sampling - Part 6: Guidance on sampling of rivers and streams.

SIST ISO 18400-205:2019: Soil quality - Sampling - Part 205: Guidance on the procedure for investigation of natural, near-natural and cultivated sites.

SIST ISO 18400-104/2019: Soil quality - Sampling - Part 104: Strategies.

Šajn, R. & Gosar, M. 2004: An overview of some localities in Slovenia that became polluted due to past mining and metallurgic activities. Geologija, 47/2: 249–258. https://doi.org/10.5474/geologija.2004.020

Šušteršič, F., Rejšek, K., Mišič, M. & Eichler, F. 2009: The role of loamy sediment (terra rossa) in the context of steady karst surface lowering. Geomorphology 106: 35–45. https://doi.org/10.1016/j.geomorph.2008.09.024

TIS/ICPVO, 1999–2010. Pedološka karta 1:25 000. Infrastrukturni center za pedologijo in varstvo okolja, Biotehniška fakulteta, Univerza v Ljubljani.

Turekian, K.K. & Wedepohl, K.H. 1961: Distribution of the Elements in Some Major Units of the Earth's Crust. Geological Society of America Bulletin, 72/2: 175–192. https://doi.org/10.1130/0016-7606(1961)72[175:DOTEIS]2.0.CO;2

Turk, J., Urbanc, J., Mladenovič, A., Pavlin, A., Oprčkal, P., Fifer Bizjak, K., Likar B., Brodnik M. & Mali, N. 2020: Izgradnja lizimetrov za preučevanje izpiranja potencialno nevarnih snovi iz gradbenih proizvodov. Geologija, 63/2: 271–280. https://doi.org/10.5474/geologija.2020.020

Turniški, R., Zupančič, N. & Grčman, H. 2023: Geochemical evidence of illuvial processes in clay-rich soils on limestones in a humid temperate climate. Geoderma 429: 116266. https://doi.org/10.1016/j.geoderma.2022.116266

Uradni list RS, št. 68/96, 41/04-ZVO-1 in 44/22 – ZVO-2. Uredba o mejnih, opozorilnih in kritičnih imisijskih vrednostih nevarnih snovi v tleh. https://pisrs.si/pregledPredpisa?id=URED114

Uradni list RS, št. 14/09, 98/10, 96/13, 24/16 in 44/22 – ZVO-2. Uredba o stanju površinskih voda. https://pisrs.si/pregledPredpisa?id=URED5010

Uradni list SRS, št. 5/88 in Uradni list RS, št. 3/22 – ZDeb. Zakon o zagotavljanju dela sredstev, potrebnih za postopno zapiranje Rudnika svinca in cinka v Mežici (ZZDSP) https://pisrs.si/pregledPredpisa?id=ZAKO1741

Uradni list RS, št. 26/05 – uradno prečiščeno besedilo, 43/10, 49/10 – popr., 40/12 – ZUJF, 25/14, 46/14, 82/15, 84/18 in 204/21. Zakon o postopnem zapiranju Rudnika Trbovlje–Hrastnik in razvojnem prestrukturiranju regije (ZPZRTH). https://pisrs.si/pregledPredpisa?id=ZAKO2053

Uradni list RS, št. 26/05 – uradno prečiščeno besedilo. Zakon o preprečevanju posledic rudarjenja v rudniku živega srebra Idrija (ZPPPR). https://pisrs.si/pregledPredpisa?id=ZAKO157

Uradni list RS, št. 22/06 – uradno prečiščeno besedilo. Zakon o trajnem prenehanju izkoriščanja uranove rude in preprečevanju posledic rudarjenja v Rudniku urana Žirovski Vrh. https://pisrs.si/pregledPredpisa?id=ZAKO227

Uradni list RS, št. 14/14 – uradno prečiščeno besedilo, 61/17 – GZ, 54/22 in 78/23 – ZUNPEOVE in 81/24: Zakon o rudarstvu (ZRud-1). https://pisrs.si/pregledPredpisa?id=ZAKO5706ZRP

ZRP (Zbirka rudarskih podatkov), 2024: Zbirka podatkov s področja rudarstva. Ministrstvo za naravne vire in prostor. Izdelal geološki zavod Slovenije. https://ms.geo-zs.si/

Zupančič, N. 2017: Influence of climate factors on soil heavy metal content in Slovenia. Journal of soils and sediments, 17: 1073–1083. https://doi.org/10.1007/s11368-016-1614-z

Zupančič, N., Turniški, R., Miler, M. & Grčman, H. 2018. Geochemical fingerprint of insoluble material in soil on different limestione formations. Catena 170: 10–24. https://doi.org/10.1016/j.catena.2018.05.040

Electronic sources:

Internet 1: https://life-restart.si/(26.11.2024)

GEOLOGIJA 67/2, 333-347, Ljubljana 2024

https://doi.org/10.5474/geologija.2024.017

Izobraževalno-ustvarjalne delavnice: vključevanje ustvarjalnega izraza v geološke učne vsebine

Educational-creative workshops: integrating creative expression into geological learning content

Teja ČERU

Geološki zavod Slovenije, Dimičeva ulica 14, SI–1000 Ljubljana; e-mail: teja.ceru@geo-zs.si

Prejeto / Received 19. 11. 2024; Sprejeto / Accepted 12. 12. 2024; Objavljeno na spletu / Published online 16. 12. 2024

Ključne besede: geologija, izobraževanje, aktivno učenje, integracija umetnosti, ustvarjalnost, naravni pigmenti, akvarel
Key words: geology, education, active learning, arts-integration, creativity, natural pigments, watercolour painting

Izvleček

Kako ohranjati otroško radovednost tudi v odrasli dobi, kako se stalno preizpraševati o naravi in okolju v katerem živimo in nenazadnje, kako ozaveščati javnost o geoloških vsebinah na razumljiv in zanimiv način? Vsa ta vprašanja so pripeljala do ideje in zasnove delavnice, ki združuje različne poglede na naravo, tako z znanstvenega, uporabnega in umetniškega vidika. V prispevku je predstavljena delavnica slikanja z naravnimi pigmenti, preko katere udeleženci spoznavajo različne geološke vsebine. V prvem delu delavnice udeleženci spoznavajo celoten proces izdelave pigmentov, ki vključuje določitev primernega minerala/kamnine za izdelavo pigmenta, proces izdelave pigmentov (drobljenje, mletje in sejanje) ter mešanje pigmentov z vezivom v dokončno barvo, ki se lahko uporabi in shrani. Ta del delavnice predstavlja pristope, ki so primerljivi znanstvenim. Udeleženci na praktičen način spoznavajo nekatere lastnosti kamnin in mineralov (barva, barva črte minerala, trdota, itd.) in metode priprave vzorcev. Drugi del delavnice je bolj umetniški oz. ustvarjalen, kjer udeleženci barvajo pobarvanke z geološkimi vsebinami ali prosto slikajo ter raziskujejo značilnosti pigmentov izdelanih iz različnih materialov ter nova učenja povezujejo še na izkustveni ravni. Eden izmed glavnih ciljev zastavljene delavnice je, da se izobraževalne in ustvarjalne vsebine medsebojno prepletajo in povezujejo s poudarkom na metodah aktivnega in eksperimentalnega učenja. V prispevku so orisane tudi prilagoditve delavnice glede na starost udeležencev in značaj dogodka (npr. javni dogodki).

Abstract

How can we nurture a childlike curiosity even in adulthood, how can we constantly question ourselves about nature and the environment we live in, and last but not least, how to raise public awareness of geology in an understandable and interesting way? All these questions led to the idea and design of a workshop that includes different views of looking at nature from a scientific, practical and artistic perspective. The article presents a workshop on painting with natural pigments through which participants learn about various geological contents. In the first part of the workshop, participants learn about the entire process of making natural pigments, which includes determining a suitable mineral/rock for pigment, the pigment preparation process (crushing, grinding, and sieving), and mixing pigments with a binder into a final colour that can be used and stored. This part of the workshop introduces approaches that are comparable to scientific one. In a very practical way, participants will learn about some of the properties of rocks and minerals (colour, color of the mineral's streak, hardness, etc.) and sample preparation methods. The second part of the workshop is more creative, where participants use colouring books with geological motifs or paint freely. They explore the characteristics of pigments made from various materials, and connect new knowledge on an experiential level. One of the main aims of the workshop is to interweave and combine educational and creative content, focussing on active and experimental learning methods. The paper also shows the adaptations of the workshop to the age of the participants and the type of event (e.g. public events).

Uvod

Povod za idejo in razmišljanja o različnih pristopih poučevanju

Naravoslovne vsebine so bile v formalnem izobraževanju velikokrat potisnjene v ozadje oz. se ni posvečalo pozornosti metodam poučevanja le-teh. Poučevanje naravoslovnih predmetov je dolgo temeljilo na tradicionalnih metodah podajanja znanja, kar je vodilo v vse manjši interes otrok za naravoslovne predmete. Izsledki različnih raziskav doma in v tujini kažejo, da raven notranje motivacije za učenje naravoslovnih vsebin pri učencih skozi osnovno in srednjo šolo postopno upada (Devetak et al., 2009; Potvin et al., 2009; Juriševič et al., 2012: več v Devetak & Metljak, 2014). Strokovnjaki Evropske komisije ugotavljajo, da je eden izmed vzrokov za pomanjkanje zanimanja mladih za naravoslovje v načinu poučevanja teh vsebin (Devetak & Metljak, 2014). Raziskave so pokazale, da so učencem vsebine naravoslovja dolgočasne in ne najdejo povezave vsebin z vsakdanjim življenjem, poleg tega je podajanje vsebin preveč abstraktno s pomanjkanjem eksperimentalnega učenja (Devetak & Metljak, 2014). Vse večje zavedanje omenjenih dejstev je vodilo v premike pri poučevanju naravoslovnih vsebin, najprej na nivoju usposabljanja učiteljev in priprave učnih gradiv (npr. projekt PROFILES). Glavni namen omenjenega projekta je bil, da različni pristopi poučevanja temeljijo na osnovi smiselnega in motiviranega poučevanja in da učenci razvijejo pozitivnejši odnos do naravoslovja in med svoje karierne cilje začnejo uvrščati različna naravoslovna področja. Poleg zavedanja po potrebah uvajanja inovativnih metod je tudi razvoj različnih tehnologij povzročil velike spremembe v načinu poučevanja, ki naj bi bile usmerjene k zagotavljanju različnih spretnostih prilagojenim današnjim potrebam družbe (Delgado-Rodríguez et al., 2023). Zaradi razvoja družbeno-ekonomskih odnosov, znanosti in tehnike se tudi način preživljanja prostega časa in interes otrok v sodobnem času spreminja (Tori, 2012). Če hočemo mladim približati naravoslovne vsebine, moramo poznati njihove potrebe ter vsebine in metodološke pristope prilagoditi njim in tudi potrebam hitro se spreminjajoče današnje družbe.

Pri sodobnih pristopih učenja, še posebej pri naravoslovju, je vse več poudarka na sami predstavitvi vsebine in na vključevanju dejavnosti, ki otroku omogočajo aktivno sodelovanje in raziskovanje (Petek, 2012). Ti pristopi pa niso pomembni samo v osnovnošolskih in srednješolskih učnih programih, ampak tudi na nivoju visokošolskega izobraževanja. Poleg uvajanja različnih učnih pristopov pa so pomembne tudi kompetence učitelja. Ena izmed osnovnejših, a hkrati zelo zapostavljenih kompetenc, je učiteljeva zmožnost vodenja dialoškega pouka, ki med drugim obsega možnost odprtih vprašanj, čas za razmislek, pozorno poslušanje in pristen odziv na odgovore učencev, spodbujanje k spraševanju, diskusiji in refleksiji (Marentič Požarnik, 2008; Marentič Požarnik & Plut Pregelj, 2009 v Polak et al., 2024).

Poleg novih pristopov učenja, se dogajajo premiki tudi na povezovanju znanosti, tehnologije in umetnosti. Ameriški izobraževalni sistem že nekaj časa uspešno vpeljuje umetnost v učne sisteme znanosti, tehnologije in matematike, tako imenovano STEAM izobraževanje (Science, Technology, Engineering, Arts and Mathematics), ki spodbuja integriranje umetnosti v znanstveno učenje ter celostni pristop procesov učenja (Green et al., 2019). Čeprav je definicij tovrstnega izobraževanja veliko, pa je glavni namen le-tega, da se področja med seboj ne obravnavajo ločeno, ampak kot celota in se dopolnjujejo tam, kjer so njihove stične točke. Tudi v Evropi se pojavljajo te vsebine, predvsem na nivoju izobraževanj v okviru različnih projektov za učitelje in tudi učence. STEAM pristop učencem omogoča, da povežejo svoje učenje na različnih področjih skupaj z umetniškimi praksami, ki so ključne pri spodbujanju ustvarjalnega reševanja problemov. Učenci se učijo, da se vse stvari povezujejo, tako v šoli kot tudi v vsakdanjem življenju, pri čemer se spodbuja njihovo raziskovanje, dialog in kritično razmišljanje. STEAM izobraževanje poleg tehničnega znanja poudarja tudi t.i. mehke veščine, kot so komunikacija, timsko delo, vodstvene sposobnosti in prilagodljivost. Poleg tega je kar nekaj metodoloških pristopov vezanih na učenje naravoslovja v naravnem okolju s povezovanjem umetnosti (Cone, 2014). In prav narava je tista, kjer lahko pri njenem proučevanju ključno povezujemo njen znanstveni in tudi estetski vidik. Pri obojem je pomembno natančno opazovanje in preizpraševanje, kjer gre za kreativno reševanje problemov, raziskovanje in opisovanje narave (Nichols & Stephens, 2013), integracija obojega pa učencem omogoča videti naravo skozi oči znanstvenika in umetnika (Green et al., 2019). Nekatere raziskave so pokazale, da lahko vključevanje umetnosti izboljša kreativnost, kritično razmišljanje, inovativnost ter tako vpliva na kognitivne sposobnosti, boljšo prostorsko predstavo, večjo sposobnost abstraktnega in divergentnega razmišljanja, večjo odprtost za nove izkušnje in spodbujanje radovednosti (Liao, 2016; Swaminathan & Schellenberg, 2015). Kljub jasnim ciljem STEAM izobraževanja, pa ostaja veliko izzivov implementacije povezovanja različnih področij v praksi, predvsem vključevanje umetnosti oz. ustvarjalnosti v ostala področja (Perignat & Katz-Buonincontro, 2019). Empirične raziskave kažejo, da gre predvsem za pomanjkanje metod, ki bi bile primerne za pedagoge, ki se z umetnostjo ne ukvarjajo in nimajo tovrstnih izkušenj (Lajevic, 2013; Liao, 2016). Empiričnih raziskav o učinkih in posledicah STEAM izobraževanja je še vedno premalo, da bi lahko podrobno analizirali in vrednotili spremembe tovrstnega izobraževanja (Haesen & Van De Put, 2018). Dejstvo je, da so učenja, ki vključujejo raznolike pristope in metode, uspešnejše, saj dosežejo veliko večino učencev, ki jim ustrezajo različni pristopi poučevanja. Kakorkoli, iz prakse vemo, da je dandanes težko pritegniti pozornost mladih in je zato uporaba različnih metod učenja, pri katerih opazimo boljši učni učinek, vedno dobrodošla.

Ker je geologija pomemben del narave, na tem mestu sledi premislek, kako lahko predstavimo geološke vsebine na način, da bomo udeležence motivirali k razmišljanju o naravoslovnih vsebinah in da bodo pridobljena znanja povezovali z vsakdanjim življenjem. Glavno vprašanje, ki si ga zastavljam tudi sama je, kako ohranjati otroško radovednost in kako spodbujati otrokov interes za geološko znanje, kako sooblikovati njihove sposobnosti, potrebne za kritičen, razmišljujoč in odgovoren odnos do narave in okolja. Koncepti niso preprosti in vključujejo vrsto različnih spretnosti in izzivov, s katerimi se moramo soočiti že pred začetkom snovanja delavnice. Tovrstno poučevanje zahteva celosten pristop, pri čemer je zelo pomembno, da pri udeležencih vzbudimo motivacijo in zagotovimo, da nova učenja reflektirajo in jih povežejo s predhodnim znanjem in izkušnjami (Devetak & Metljak, 2014). Glavni izzivi so, kako skozi odraščanje ohranjati prostor za kreativno razmišljanje, čudenje naravnim pojavov, preverjanje idej v praksi, raziskovanje za novim, čemur v odrasli dobi nemalokrat pravimo tudi strast do dela. To je tista iskrica, ki nas žene v raziskovanje, ne glede na to, ali smo otroci ali odrasli. In prav tu je pomembno, da spodbujamo otrokovo individualnost razmišljanja, ki jo bo lahko ohranjal tudi v odrasli dobi in z njo ustvarjal nekaj novega. Strokovno takšnemu pristopu pravimo konstruktivizem, ki poudarja aktivno vlogo učenca pri izgradnji razumevanja in osmišljanja informacij (Petek, 2012). Veje konstruktivizma kot je didaktični konstruktivizem in raziskovalni didaktični sistem pouka so v osnovi zelo podobne znanstveno-raziskovalnemu mišljenju (Plut Pregelj, 2008). Ne glede na različna poimenovanja in pristope, ki se uveljavljajo v zadnjih 20 letih, pa je skoraj vsem skupno zavedanje, da je za otroka pomemben neposreden stik z naravo, jo doživljati z vsemi čutili, se ji čuditi in opazovati njeno raznolikost. Dejstvo je, da je motivacija eden od glavnih faktorjev pri učenju naravoslovja (Ryan & Deci, 2000), ne glede na to, kateri inovativni poučevalni pristop izberemo. To pomeni, da učenje naravoslovja postane učenčeva želja in pride iz notranje motivacije. Holbrook & Rannikmae (2007) sta s tem namenom razvila takoimenovani alternativni poučevalni pristop »izobraževanje z naravoslovjem«, ki ima poudarek na motivacijski spodbudi, za katero se uporabi različna navezovanja na socio-naravoslovni, individualno naravoslovni ali okoljsko-naravoslovni kontekst (Devetak & Metljak, 2014).

Na področju popularizacije geoloških vsebin v Sloveniji se je v zadnjem času naredilo veliko v okviru različnih tematskih geoloških delavnic tudi v naravi, informativnih tabel, vsebin v muzejih in geoparkih, izobraževanj, učil in učnih pripomočkov (učnih listov, aplikacij, učnih modelov, itd.) (nekaj primerov: Rman, 2010; 2013; Novak, 2017; Žvab Rožič, 2017; Popit et al., 2019; Brajkovič & Žvab Rožič, 2019). Geologi se vse bolj zavedamo in trudimo, da vsebine javnosti približamo na enostaven in zanimiv način v skladu s potrebami današnje družbe.

Glavni namen predstavljene delavnice je preizkusiti nov način spoznavanja geoloških vsebin s poudarkom aktivne vključenosti udeležencev delavnice preko ustvarjalnega izraza. Delavnica je bila v prvotni obliki zastavljena za predšolske in šolske otroke prve triade z namenom bolj kreativnega pristopa pri spoznavanju različnih vej geologije. V okviru delavnice smo poleg raziskovalnega pristopa, ki je značilen za znanstveno delo, želeli otrokom odpreti tudi prostor za ustvarjalen in bolj intuitiven izraz, s čimer bi znanje in izkušnjo delavnice otroci lahko bolj ponotranjili in znanje lažje integrirali. Na osnovi prvotno zastavljene delavnice, smo le-to prilagodili za različne starostne skupine in za način izvajanja v okviru manjših skupin oz. večjih dogodkov.

Vsebina osnovne delavnice

Delavnica je v osnovi zasnovana iz dveh delov, ki pa med seboj nista strogo ločena in se medsebojno prepletata. Oba dela sta zasnovana na podlagi metod aktivnega in eksperimentalnega učenja. Uvodni del delavnice je namenjen razmišljanju o glavni tematiki delavnice in udeležence motiviramo z vprašanji kot so: iz česa so lahko narejene barve, ki jih uporabljamo v vsakdanjem življenju, iz česa so jih pridobivali nekoč in kakšen je proces izdelave pigmenta in barve? Uvodu nato sledi predstavitev vseh teh vsebin, kjer udeležence spodbujamo z vprašanji, sami pa opazujejo, preizkušajo in se seznanijo z nekaterimi raziskovalnimi metodami priprave vzorcev, ki jih uporabljamo pri laboratorijskih pripravah v geologiji, kot so drobljenje v terilnici, sejanje in mletje različnih vzorcev kamnin in tal. Prvi del delavnice temelji na spoznavanju znanstvenih pristopov, kjer udeleženci aktivno sodelujejo pri določevanju različnih lastnosti kamnin/mineralov (barva, oblika, trdnost, barva črte, itd.), ki vplivajo na to, ali je material primeren za izdelavo pigmenta in kako vpliva na samo pripravo in lastnosti pigmenta. Udeleženci spoznajo celoten proces izdelave barv, vse od priprave pigmenta iz različnih geoloških materialov do izdelave barv, ki se jih lahko shrani (sl. 1). Drugi del delavnice je namenjen ustvarjanju, kjer udeleženci barvajo pripravljene geološke motive ali pa prosto slikajo. V tem delu udeleženci povezujejo pridobljeno znanje s prvega dela delavnice še preko ustvarjanja, ko barve preizkušajo, a hkrati spoznavajo njihove lastnosti in pri barvanju vnaprej določenih motivov raziskujejo še različne geološke vsebine. Na tak način prepletamo strokovne in kreativne vsebine skozi celoten drugi del delavnice, kjer udeleženci razvijajo tudi psihomotorične spretnosti. S prostim slikanjem udeleženci razvijajo domišljijo in raziskujejo lasten ustvarjalen izraz.

Zasnova delavnice poleg omenjenih učnih vsebin omogoča dodajanje različnih geoloških vsebin glede na osrednjo tematiko delavnice oziroma glede na interes in starost ciljne skupine (več o prilagoditvah delavnice v nadaljevanju). Tako lahko vzporedno prepletamo geološke vsebine o lastnostih in nastanku mineralov in kamnin, ki so primerni za pigmente, nahajališč le-teh v Sloveniji in svetu, in kako njihove kemijske in fizikalne lastnosti vplivajo na proces izdelave pigmenta in v končni fazi na lastnosti pigmenta. Tako se tekom delavnice spoznajo z različnimi vejami geologije (mineralogija, petrologija, rudna geologija, mineralne surovine, itd.).

Nekaj primerov vprašanj, s katerimi lahko vzpodbujamo aktivno vključenost in motivacijo udeležencev tekom delavnice.

- *Iz česa so izdelane barve, ki jih uporabljajo doma ali v vrtcu/šoli?*

Pri tem vprašanju spodbudimo otroka k razmisleku, iz česa pravzaprav so barve in kje vse jih uporabljamo.

- *Ali kamen riše?*

Pri tem vprašanju otroci spoznavajo različne minerale in kamnine, njihovo barvo in preverijo, kakšno barvo sledi pušča mineral/kamen. Otroci spoznavajo, tipajo, raziskujejo različne geološke materiale in opazujejo ter opisujejo njihove podobnosti in razlike.

- *Kako pridobimo pigmente iz kamnin/mineralov?*

Otroke preko izkustvenega učenja popeljemo skozi proces izdelave pigmentov (drobljenje, sejanje) od surove kamnine ali minerala do pigmenta, ki je primeren za izdelavo barve.

- *Katera barva je najbolj intenzivna/prekrivna?*

Preko ustvarjalnosti otroci preizkušajo različne barve in s tem odkrivajo različne lastnosti pigmentov kot so, intenzivnost, prekrivnost, obstojnost in teksturo, mešanje pigmentov, zrnavost, itd. Skozi lastno ustvarjalnost raziskujejo in povezujejo lastnosti geoloških materialov in barv iz njih.

Preko postavljenih vprašanj skozi delavnico otroci iščejo odgovore in raziskujejo ter preverjajo svoje domneve, teorije in zamisli. Vprašanja so seveda prilagojena tudi osrednji tematiki, ki jo lahko spreminjamo. Delavnica je lahko usmerjena v spoznavanje mineralov in otroci se na zelo neposreden način in skozi ustvarjanje seznanijo z različnimi oblikami mineralov, ki jih najprej vidijo v živo, nato pa njihove oblike še barvajo in rišejo. Spoznavajo različne geometrijske oblike preko barvanja kristalov, lahko celo s pigmentom tega minerala, če je to možno (malahit, kalcit, azurit, itd.). Na tak način otrokom abstraktne vsebine na subtilen način približamo in jih navdušimo nad raznolikimi oblikami različnih mineralov.

Materiali za izvedbo delavnice

V nadaljevanju so našteti osnovni materiali za izvedbo delavnice. Glede na prilagoditve delavnice se le-ti lahko ustrezno poenostavijo oz. dopolnijo.

- Nabor različnih mineralov, kamnin, tal in premoga (limonit, hematit, malahit, azurit, apnenec, tuf, premog, grafit, itd.)
- Pripadajoči zmleti pigmenti presejani pod velikost 0,063 mm
- Poleg naravnih pigmentov imamo lahko za primerjavo tudi nekaj umetnih pigmentov in barv
- Terilnica in sito za prikaz procesa drobljenja in sejanja materialov
- Sestavine in veziva za pripravo akvarelnih barv (gumiarabika, glicerin, med)
- Barvne palete s pripravljenimi akvarelnimi barvami, čopiči
- Akvarelne pobarvanke z geološkimi motivi, prazni akvarelni listi
- Plakati z opisanimi vsebinami glede na osrednjo tematiko delavnice: npr: naravni pigmenti skozi zgodovino slikarstva, toksični pigmenti v zgodovini, itd.
- Knjige o naravnih pigmentih (primerno za odrasle)

Sl. 1. Cikel izdelave naravnih pigmentov od kamna do barve.
Fig. 1. The process of making natural pigment from stone to paint.

Prilagoditve delavnice

V nadaljevanju so opisane prilagoditve delavnice glede na starost ciljne skupine in značaj dogodka (manjše oz. večje skupine na javnih dogodkih).

Delavnica za predšolske otroke

Pristop k spoznavanju geologije za predšolske otroke se razlikuje od prenosa znanj otrokom v osnovni in srednji šoli. Vsebine morajo biti predstavljene

Sl. 2. Delavnica v vrtcu Litija. (Fotografije: Mateja Jemec Auflič, Ivanka Mlakar).
Fig. 2. Workshop at the kindergarten in Litija. (Photos: Mateja Jemec Auflič, Ivanka Mlakar).

na preprost in nazoren način, pri čemer je pomembno, da nova znanja zaznavajo in odkrivajo tudi z uporabo vseh čutil. Predšolski otroci imajo močan domišljijski svet, a ga že začnejo razlikovati od realnega. Prav zato je pomembno, da tekom delavnice z aktivnimi vprašanji otrokom omogočimo prostor, da so pri odgovorih kreativni in dopuščamo, da uporabljajo svojo domišljijo. Nekatere vsebine osnovne delavnice so za predšolske otroke prezahtevne in preveč poglobljene, zato smo jih prilagodili. Eden izmed načinov je ta, da barvanje in ustvarjanje prepletemo znotraj izbrane geološke tematike brez podrobnih vsebin o izdelavi pigmentov in barv (sl. 2).

Glavne prilagoditve

- več slikovnega gradiva in učnih pripomočkov
- vodenje delavnice mora vključevati več aktivacijskih vprašanj, s katerimi pritegnemo pozornost in držimo motivacijo skupine otrok
- delavnica mora biti vsebinsko dinamična in vključevati mora vsebine, pri katerih bodo otro ci aktivno in skupinsko sodelovali
- prevladujejo metode eksperimentalnega učenja pri spoznavanju strokovnih vsebin
- zaradi zahtevnosti akvarelne tehnike so enostavne pobarvanke primernejše od prostega slikanja
- trajanje delavnice: max. do 1 ure

Primer izvajanja delavnice

V sklopu delavnice za predšolske otroke, kjer so bili osrednja tema dinozavri, so bili geološki koncepti predstavljeni na enostaven in eksperimentalen način. Otroci so dinozavre spoznavali preko igrač, jih vzeli v roke in opisovali njihova opažanja glede na aktivacijska vprašanja tekom delavnice. Spoznavali so različne vrste dinozavrov, njihovo velikost, kako se lahko skozi čas ohranijo njihovi fosilni ostanki, itd. Velikost zob nekaterih dinozavrov smo ponazorili npr. z velikostjo banane. Njihove velikosti stopinj pa s prikazom realne stopinje, na katero so nalepili odtise svojih nog, ki so jih pobarvali z naravnimi pigmenti. Spoznavali smo tudi, kako se ohranijo stopinje dinozavrov in to ponazorili z odtisi rok v mivki, pri čemer so otroci opazovali, kako se njihove dlani odtiskujejo v mivki (sl. 3). Delavnico spoznavanja dinozavrov smo na koncu dopolnili z barvanjem dinozavrov z naravnimi pigmenti. Zelo poenostavljeno smo si pogledali tudi nekaj različnih kamnov in pripadajoče pigmente. Otroci so imeli na voljo 4 različne vrste dinozavrov s pripadajočimi izrezanimi stopinjami, ki smo jih spoznavali v začetku delavnice. Za izbranega dinozavra so morali najti ustrezno stopinjo in nato dinozavra še pobarvati. Kot je razvidno iz opisanega, smo ustvarjalni del delavnice prepletali z raziskovanjem strokovnih vsebin, kar pripomore k večji motivaciji, večji vključenosti in boljši pozornosti otrok pri usvajanju novih vsebin.

Delavnica za osnovnošolske otroke

Izvedba delavnice in vsebine za osnovnošolske otroke so primerne na način kot je zapisano pri osnovnem opisu delavnice. Glede na starost skupine se vsebine ustrezno prilagaja in glede na interes otrok poglablja in razširja. Pri podajanju vsebin se še vedno poslužujemo metod aktivnega in eksperimentalnega učenja, pri čemer lahko dodajamo tudi nekaj več teoretičnih vsebin in kompleksnejših strokovnih vsebin. Poleg predstavitve eksperimentalnega dela delavnice, lahko delavnico pripravimo tako, da otroci pridobijo znanja, s katerimi lahko sami izdelajo pigmente s pripomočki, ki jih najdejo doma. Uporabijo lahko tla iz svoje okolice, jih zdrobijo s kladivom, presejejo skozi kuhinjsko cedilo in za vezivo uporabijo jajce.

Glavne prilagoditve

- uporaba metod aktivnega in eksperimentalnega učenja
- otroci so aktivno vključeni v sam proces izdelave pigmentov in barv z ustreznim vodenjem
- poleg pripravljenih pobarvank, lahko otroke spodbudimo, da prosto slikajo v akvarelni tehniki
- za ustvarjanje namenimo vsaj polovico časa celotne delavnice
- vodenje delavnice vključuje aktivacijska vprašanja, s katerimi mentor odpira prostor, da otroci izrazijo lasten interes za vsebine ter na podlagi tega delavnico prilagaja
- dodajanje strokovnih vsebin za višje razrede: kako nastajajo minerali, kamnine, kje jih najdemo pri nas in v svetu, kakšna je njihova pogostost, kako so se barve skozi čas spreminjale v povezavi s slikarstvom
- trajanje delavnice: 2-3 ure

Primer izvajanja delavnice

Delavnica v Knjižnici Medvode je obsegala manjšo skupino otrok starosti med 5 in 12 let. Zaradi različne starosti in različnega predhodnega znanja je bil prvi del delavnice prilagojen vsakemu posamezniku. Starejši otroci so veliko več spraševali sami, medtem ko je bilo mlajše otroke potrebno vzpodbujati z aktivacijskimi vprašanji. Prednost dogodkov v manjših skupinah je ta, da

Sl. 3. Delavnica v manjši skupini otrok v Knjižnici Medvode (22. 11. 2023).
Fig. 3. Workshop in a small group of children at the Medvode Library (November 22, 2023).

otroci lahko ustvarjajo dlje časa, saj se je izkazalo, da se med barvanjem/slikanjem sprostijo in umirijo. Ob ustvarjanju so imeli otroci čas za dodatna vprašanja in refleksijo.

Delavnica za odrasle

Delavnica za odrasle je bila vsebinsko strukturirana drugače. Uvodni del je bil namenjen obsežni, poglobljeni in sistematični predstavitvi naravnih pigmentov iz različnih materialov skozi zgodovino slikarstva. Predstavljeni so bili materiali, lastnosti njihovih pigmentov in obdobja, ko so bili ti najbolj v uporabi. Udeleženci so tako spoznali naravne materiale, ki so se uporabljali vse od prazgodovinskih poslikav, preko antike, srednjega veka, renesanse, baroka in vse do danes, ko nad naravnimi pigmenti začnejo prevladovati sintetično izdelani pigmenti. Na primerih umetnin največjih slikarskih mojstrov so spoznavali, katere pigmente in kombinacije le-teh so uporabljali za želen učinek in odtenek končne slike. Enourni teoretični predstavitvi in diskusiji je sledila enourna delavnica prostega slikanja (sl. 4). Delavnico lahko zastavimo tudi tako, da prvemu teoretičnemu delu namesto slikanja, sledi delavnica izdelave pigmentov in barv, ki zahteva več časa za samo pripravo in tudi izvedbo.

S. 4. Utrinki s predavanja o naravnih pigmentih v zgodovini slikarstva in ustvarjalna delavnica (Knjižnica Medvode, 19. 3. 2024, fotografije: Mirjam Slanovec, Anja Torkar, Teja Čeru).

Fig. 4. A glimpse from the lecture and workshop on natural pigments in the history of painting (Medvode Library, 19 March, 2024., photos: Mirjam Slanovec, Anja Torkar, Teja Čeru).

Glavne prilagoditve

- več teoretičnih vsebin
- večji poudarek na povezavi vsebin naravnih pigmentov in slikarstva
- poudarek na prostem slikanju
- za ustvarjanje namenimo vsaj polovico časa celotne delavnice
- trajanje delavnice: 2-3 ure

Splošna javnost
(naključni obiskovalci na javnih dogodkih)

Priprava delavnice na večjih dogodkih, kjer so obiskovalci naključni in vseh starosti, zahteva svojevrstno pripravo. Ker udeleženci na tovrstne dogodke večinoma ne pridejo namensko, smo pri takšnih dogodkih dali poudarek tudi na vizualen vidik delavnice. Ta je pomemben, da pritegnemo pozornost udeleženca tudi na samo vsebino delavnice. S tem namenom smo uporabili nekatere pripomočke, kot na primer slikarska stojala z nekaterimi najbolj znanimi slikami, pobarvanke geoloških motivov, itd. Za odrasle smo pripravili plakate s podrobnejšimi opisi o barvah in pigmentih za odrasle. Za otroke pa smo imeli različne pobarvanke in demonstracijo izdelave pigmentov iz različnih kamnin in mineralov. Dinamika predajanja strokovnih vsebin je zelo raznolika, saj gre za konstantno prilagajanje različnim izkušnjam in interesom mimoidočih, zato je na tovrstnih dogodkih dobrodošlo tudi večje število strokovnega osebja.

Glavne prilagoditve

- priprava vsebin za vse starosti
- večji poudarek na estetskem vidiku delavnice
- številna aktivacijska vprašanja, da pritegnemo pozornost mimoidočih
- večje število mentorjev, ki delavnico vodijo
- strnjene in krajše strokovne vsebine, saj je čas mimoidočih na prizorišču delavnice relativno kratek

Primeri izvedbe delavnic

Delavnica je bila prvič predstavljena v okviru projekta NočMoč, kjer je bila na dogodku Evropska noč raziskovalk in raziskovalcev jeseni 2023 (sl. 5) tudi prvič predstavljena javnosti (Čeru et al., 2023).

Prav tako je bila delavnica izvedena v okviru sejma mineralov in fosilov Slovenije (MINFOS 2024) z vsebinskimi prilagoditvami v skladu s strokovnim fokusom, ki je bil letos namenjen fosilni flori in sulfidnim mineralom. S tem namenom smo izdelali pobarvanke s kristali sulfidnih mineralov in fosilne rastline *Lepidodendron*. Izobraževalna vsebina delavnice je bila predstavljena z dvema plakatoma in vitrino, kjer smo predstavili sulfidne minerale in pigmente iz njih ter predstavili njihovo uporabo skozi zgodovino. Ta del delavnice je bil namenjen starejšemu delu obiskovalcev. Za odrasle in otroke so bili na mizi predstavljeni različni geološki materiali, pigmenti iz njih in predstavljen celoten cikel priprave barv (sl. 6). Nad veliko ustvarjalno mizo, kjer so udeleženci slikali, so bili plakati, ki so predstavljali nekdanja okolja z bogato floro, z namenom prikazati vzdušje velikih rastlin, ki so nekoč rastle tudi na našem območju. Poleg tega smo imeli na slikarskih stojalih predstavljene tri slike nekdanjih slavnih umetnikov s pripadajočimi informacijami o pigmentih, ki so jih uporabili na slikah.

Narava dogodka in velika površina za ustvarjanje je omogočala, da je lahko več udeležencev hkrati ustvarjalo (sl. 7). Prednost tovrstnih dogodkov z večjim prostorom za izvajanje delavnic je, da si udeleženci lahko vzamejo več časa za ustvarjanje. Večje število mentorjev na delavnici omogoča, da se vsakemu posamezniku poglobljeno posvetimo glede na njihov interes.

Sl. 5. Pripravljena delavnica na dogodku Evropska noč raziskovalk in raziskovalcev 2023 (Fotografija: Aleksandra Trenchovska).

Fig. 5. Prepared workshop for the event European Researchers‘ Night 2023 (Photo: Aleksandra Trenchovska).

Sl. 6. Pripravljena delavnica v skladu s strokovnim fokusom 50. MINFOS-a: Sulfidni minerali in fosilna flora (Fotografije: Staša Čertalič, Aleksandra Trenchovska, Zala Zarkovič).

Fig. 6. A workshop prepared in accordance with the expert focus of the 50th MINFOS: Sulfide minerals and fossil flora (Photos: Staša Čertalič, Aleksandra Trenchovska, Zala Zarkovič).

Sl. 7. Utrinki z izobraževalno-ustvarjalne delavnice na 50. MINFOS (Fotografije: Zala Zarkovič).
Fig. 7. Snapshots from the educational and creative workshop at the 50th MINFOS (Photos: Zala Zarkovič).

Zaključki in razmišljanja za delo v prihodnje

Predstavljeni primeri izvajanja delavnice so eden izmed načinov popularizacije oz. ozaveščanja geoloških vsebin javnosti na malce drugačen način. Vsak dogodek posebej od nas zahteva tako strokovne prilagoditve kot tudi prilagoditve v metodah poučevanja le-teh. Za učinkovito poučevanje smo soočeni s številnimi izzivi, ki pa jih lahko uspešno rešujemo le na podlagi stalnega izobraževanja ne samo strokovnih, ampak tudi pedagoških vsebin. Poleg tega pa največ štejejo različne izkušnje, ki jih imamo na področju popularizacije stroke ter naša odprtost za enakovreden dialog s splošno javnostjo in prilagodljivost glede na različne potrebe in znanja ciljne skupine. Gre za izmeničen proces, kjer se ne učijo le učenci, ampak tudi mi ter na podlagi odzivov ljudi znanja nadgrajujemo in izboljšujemo.

Na podlagi odziva udeležencev na različnih dogodkih, lahko zaključim, da so delavnice doživele veliko zanimanja in da je podajanje vsebin z metodami aktivnega in eksperimentalnega učenja veliko bolj uspešno od tradicionalnih metod učenja. Prav tako se je izkazalo, da je ustvarjalen del delavnice zelo zanimiv za otroke in nemalokrat tudi za odrasle in da doprinese k celi izkušnji spoznavanja novih vsebin. Z nekaj truda se da uspešno povezovati različna področja in udeleženci so imeli možnost geološke vsebine integrirati še preko ustvarjalnega izraza. Delavnica ima poleg opisanih prilagoditev še veliko prostora za navezave na različne geološke vsebine, ki tu niso bile predstavljene. Poleg tega bi bila zanimiva tudi izvedba delavnice v naravi, kjer bi bili udeleženci vključeni v celoten proces izdelave pigmentov, od iskanja tal in kamnin, do postopkov mletja, sejanja in izdelave barv. Tako bi na neposreden način spoznali delo geologa na zabaven in raziskovalen način. Namen raziskovalnega poučevanja je namreč v odkrivanju novega in v uvajanju otrok v metode in tehnike znanstvenoraziskovalnega mišljenja.

Ker sama naravo dojemam tako z znanstvenega kot tudi umetniškega vidika, bom zaključila z mislijo Alberta Einsteina, ki je dejal: *"Najlepše, kar lahko doživimo, je skrivnostno. Je vir prave umetnosti in znanosti"*. Na stičišču znanosti in umetnosti je narava. Tu imamo geologi srečo, saj imamo veliko prostora, kako lahko geološke vsebine predstavimo na zanimiv in igriv način, ki je posamezniku blizu v vsakdanjem življenju. V marsikaterih pogledih se znanost in umetnost res razhajata, a skupno obema je čudenje, raziskovanje ter skrivnostnost neznanega. Znanost pri tem temelji na znanstvenih metodah, preverljivosti, dokazljivosti, medtem ko pri umetnosti ni meja, temveč svobodni izraz. In prav ta brezmejni prostor v umetnosti daje prostor za razmišljanja izven okvirjev v znanosti, kjer se porodijo nove ideje. Tudi v novih pristopih učenja različnih področij, gre vse v to smer, da se področja povezujejo in obravnavajo celostno. Seveda je v teoriji vse bolj enostavno kot v praksi, lahko pa v tej smeri razmišljamo in delamo majhne korake in se prepustimo kreativnosti pri ustvarjanju vsebin za namen popularizacije geologije.

Zahvala

Začetna ideja se je realizirala v okviru projekta NočMoč 2022–2023, prva izvedba delavnice na dogodku Noč raziskovalk in raziskovalcev. Ideja je bila nato realizirana na dogodku MINFOS in v okviru drugih manjših delavnic, tako da gre zahvala vsem, ki so ideji dali prosto pot in omogočili njeno izvedbo. Posebno bi se zahvalila Barbari Čeplak za pomoč pri mletju vzorcev in pripravi barv in Staši Čertalič za vso izvedbo kreiranja pobarvank, plakatov in idej postavitve delavnic v sklopu različnih dogodkov. Zahvala tudi vsem, ki so prispevali kakšen kos kamnine, kakorkoli pomagali na dogodkih in avtorjem fotografij, ki so ujeli trenutke iz različnih delavnic.

Literatura

Brajkovič, R. & Žvab Rožič, P. 2019: KamenCheck - učna aplikacija za prepoznavanje kamnin. Konkrecija: revija Društva prijateljev mineralov in fosilov Slovenije, 8: 100–101.

Cone, C.S. 2014: Using Art to Teach Students Science Outdoors: How Creative Science Instruction Influences Observation, Question Formation, and Involvement. Thesis, Science Teaching, Portland State University: 71 p. https://doi.org/10.15760/etd.2096

Čeru, T., Čeplak, B. & Čertalič, S. 2023: Didaktični pristop pri spoznavanju geoloških vsebin za otroke: primer barvanja geoloških motivov z naravnimi pigmenti. In: Rožič, B. (ed.): Razprave, poročila = Treatises, reports: 26. posvetovanje slovenskih geologov = 26th Meeting of Slovenian Geologists, Oktober 2023. Univerza v Ljubljani, Naravoslovnotehniška fakulteta, Oddelek za geologijo, Geološki zbornik, 26/1: 12–15.

Delgado-Rodríguez, S., Domínguez, S.C. & Garcia-Fandino, R. 2023: Design, Development and Validation of an Educational Methodology Using Immersive Augmented Reality for STEAM Education. J. New Approaches Educ. Res., 12: 19–39. https://doi.org/10.7821/naer.2023.1.1250

Devetak, I. & Metljak, M. (eds.) 2014: Inovativno poučevanje naravoslovja in spodbujanje naravoslovne pismenosti v osnovni in srednji šoli (na spletu), Pedagoška fakulteta, Ljubljana: 109 p. http://pefprints.pef.uni-lj.si/2603/ (12. 11. 2024).
Devetak, I., Drofenik Lorber, E., Juriševič, M. & Glažar, S.A. 2009: Comparing Slovenian year 8 and year 9 elementary school pupils' knowledge of electrolyte chemistry and their intrinsic motivation. Chemistry Education Research and Practice, 10/4; 281–290. https://doi.org/10.1039/B920833J
Green, K., Trundle, K. C. & Shaheen, M. 2019: Integrating the arts into science teaching and learning: A literature review. Journal for Learning through the Arts, 14/1: unpaginated. https://doi.org/10.21977/D914140829
Haesen, S. & Van De Put, E. 2018: STEAM Education in Europe: A Comparative Analysis Report, EuroSTEAM, 82 p. http://www.eurosteamproject.eu http://www.eurosteamproject.eu (13. 11. 2024).
Holbrook, J. & Rannikmae, M. 2007: The Nature of Science Education for Enhancing Scientific Literacy. International Journal of Science Education, 29/11: 1347–1362. https://doi.org/10.1080/09500690601007549
Juriševič, M., Vrtačnik, M., Kwiatkowski, M. & Gros, N. 2012: The interplay of students' motivational orientations, their chemistry achievements and their perception of learning within the hands-on approach to visible spectrometry. Chemistry Education Research and Practice, 13/3: 237–247. https://doi.org/10.1039/C2RP20004J
Lajevic, L. 2013: Arts Integration: What Is Really Happening in the Elementary Classroom? Journal for Learning through the Arts, 9/1: unpaginated. http://escholarship.org/uc/item/9qt3n8xt
Liao, C. 2016: From Interdisciplinary to Transdisciplinary: An Arts-Integrated Approach to STEAM Education. Art Education, 69/6: 44–49. https://doi.org/10.1080/00043125.2016.1224873
Nichols, A.J. & Stephens, A.H. 2013: The scientific method and the creative process: Implications for the K-6 classroom. Journal for Learning through the Arts, 9/1: 1–14. https://doi.org/10.21977/D99112599
Marentič Požarnik, B. 2008: Konstruktivizem na poti od teorije spoznavanja do vplivanja na pedagoško razmišljanje, raziskovanje in učno prakso. Sodobna pedagogika, 59/4: 28-51. https://www.dlib.si/stream/URN:NBN:SI:doc-TQ-JF0VFP/979159d1-921e-423b-b0e7-db7b-b48454e8/PDF
Marentič Požarnik, B. & Plut Pregelj, L. 2009: Moč učnega pogovora. Ljubljana: DZS
Novak, M. 2017: Geološki sprehod po Ljubljani kot primer izobraževanja na prostem. In: Rožič, B. (ed.): Razprave, poročila = Treatises, reports. 23. posvetovanje slovenskih geologov = 23rd Meeting of Slovenian Geologists, Ljubljana, marec 2017. Univerza v Ljubljani, Naravoslovnotehniška fakulteta, Oddelek za geologijo, Geološki zbornik, 24: 121–125.
Petek, D. 2012: Zgodnje učenje in poučevanje naravoslovja z raziskovalnim pristopom. Revija za elementarno Izobraževanje, Pedagoška fakulteta, 5/4: 101–114.
Perignat, E. & Katz-Buonincontro, J. 2019: STEAM in practice and research: An integrative literature review. Thinking Skills and Creativity, 31: 31–43. https://doi.org/10.1016/j.tsc.2018.10.002
Plut Pregelj, L. 2008: Ali so konstruktivistične teorije učenja in znanja lahko osnova za sodoben pouk? Sodobna pedagogika, 59/4: 14–27.
Polak, A., Gradišek, P. & Marentič-Požarnik, B. 2024: Kakšen naj bo učitelj prihodnosti? Prispevek h kritičnemu premisleku ob prenovi slovenskega izobraževanja. Sodobna pedagogika, 75/1: 49–68. http://www.dlib.si/?URN=URN:NBN:SI:DOC-1LFXGS83
Popit, T., Žvab Rožič, P., Verbovšek, T., Pušnik, N., Petek, T., Tomažič, M., Mušič, M., Rome, T., Vodušek, J., Ostruh, P., Gajšek, M., Kos, U., Šantl, L. & Kokalj, M. 2019: Podajanje geoloških vsebin v osnovnih in srednjih šolah preko interaktivnih učnih listov (EDUGEO, PKP). In: Rožič, B. (ed.): Razprave, poročila = Treatises, reports. 24. posvetovanje slovenskih geologov Ljubljana: Univerza v Ljubljani, Naravoslovnotehniška fakulteta, Oddelek za geologijo. Geološki zbornik, 25: 95–99.
Potvin, G., Hazari, Z., Tai, R. H. & Sadler, P.M. 2009: Unraveling bias from student evaluations of their high school science teachers. Science Education, 93/5: 827–845. https://doi.org/10.1002/sce.20332
Rman, N. 2010: Geological workshop for primary schools. Geologija, 53/1: 93–96. https://doi.org/10.5474/geologija.2010.007
Rman, N. 2013: How to use an educational sand-box model to enhance the knowledge groundwater dynamics. Geologija, 56/2: 257–264. https://doi.org/10.5474/geologija.2013.017

Ryan, R.M. & Deci, E.L. 2000: Intrinsic and Extrinsic Motivations: Classic Definitions and New Directions. Contemporary Educational Psychology, 25/1: 54–67. https://doi.org/10.1006/ceps.1999.1020

Swaminathan, S. & Schellenberg, E.G. 2015: Arts education, academic achievement and cognitive ability. In: Tinio, P.P.L. & Smith J.K. (eds.): The Cambridge Handbook of the Psychology of Aesthetics and the Arts, Cambridge University Press: 364–384. https://doi.org/10.1017/CBO9781139207058.018

Tori, M. 2012: Prosti čas mladih. Diplomsko delo. Univerza v Ljubljani, Fakulteta za družbene vede, Ljubljana: 99 p. http://dk.fdv.uni-lj.si/diplomska/pdfs/tori-martina.pdf (15. 11. 2024)

Žvab Rožič, P. 2017: Šolske učne geološke zbirke. In: Rožič, B. (ed.): Razprave, poročila = Treatises, reports. 23. posvetovanje slovenskih geologov. Univerza v Ljubljani, Naravoslovnotehniška fakulteta, Oddelek za geologijo, Geološki zbornik, 24: 214–217.

GEOLOGIJA 66/2, 349-351, Ljubljana 2024

Poročila in ostalo - Reports and More

Poročilo o mednarodnem neogenskem srečanju NCSEE (Neogene of Central and South-Eastern Europe)

Kristina IVANČIČ

Geološki zavod Slovenije, Dimičeva ulica 14, SI–1000 Ljubljana, Slovenija; e-mail: kristina.ivancic@geo-zs.si

Letošnje leto je od 27. do 31. maja v Podčetrtku, v kongresnem centru term Olimje potekalo jubilejno 10. neogensko srečanje NCSEE (Workshop of the Neogene of Central and South-Eastern Europe) (sl. 1). Srečanje je organiziral Geološki zavod Slovenije (GeoZS) v sodelovanju s Paleontološkim inštitutom Ivana Rakovca ZRC SAZU. Tovrstno srečanje poteka vsaki dve leti in se ga udeležijo raziskovalci s področja sedimentologije, paleontologije, stratigrafije in strukturne geologije, ki se ukvarjajo z razvojem Panonskega bazena, Centralne in Vzhodne Paratetide ter tudi Mediterana.

Dogodka se je udeležilo 58 registriranih udeležencev iz enajstih držav. Vse skupaj je bilo 49 predstavitev, od tega 27 predavanj in 22 posterjev. Struktura udeležencev je bila zelo raznolika, od študentov in mladih raziskovalcev na začetku svoje kariere do uveljavljenih raziskovalcev in starejših, že upokojenih udeležencev, ki še vedno z veseljem delijo svoje znanje z mlajšimi generacijami. Dogodek je vključeval predavanja, predstavitve plakatov, paleontološko delavnico ter dve ekskurziji.

Sl. 1. Vhod v kongresno dvorano Kongresnega centra v Olimjah.

V ponedeljek je potekala registracija udeležencev, ki ji je sledila torkova uradna otvoritev srečanja. Po otvoritvenem dogodku so se pričela plenarna predavanja. Najprej je dr. Jure Atanackov z Geološkega zavoda Slovenije predstavil strukturni pregled vzhodne Slovenije, nato pa je dr. Michal Kováč z Oddelka za geologijo in paleontologijo Univerze Comenius v Bratislavi predstavil stare in nove koncepte stratigrafije, geodinamike in paleogeografije v Dunajskem bazenu, ki so temeljile na

Sl. 2. Predavanje dr. Michala Kováča v polni predavalnici.

Sl. 3. Debate pri posterski sekciji.

Sl. 4. Skupinska fotografija udeležencev kongresa pred znamenito antiklinalo v Mestinjah.

re-evaluaciji obstoječih podatkov (sl. 2). Srečanje se je nadaljevalo s kratkimi predavanji, predvsem na temo sedimentologije, stratigrafije in paleontologije. Dan se je zaključil s predstavitvijo posterjev (sl. 3).

V sredo smo izvedli medkonferenčno ekskurzijo. Ta je potekala v okolici Rogaške Slatine in Podčetrtka, obiskali smo štiri točke. Pri prvi točki smo si ogledali profil egerijskih in eggenburgijskih plasti v Dreveniku. Zaporedje je sestavljeno iz bazalnih konglomeratov in breč, peščenjakov ter meljastega laporja. Druga točka je bila v Mestinjah, kjer v markantni antiklinali izdanjajo biokalkareniti, ter peščena, meljasta in laporanata badenijska zaporedja (sl. 4). Pot nas je nato vodila v okolico Podčetrtka, kjer smo si na Plohovem bregu ogledali debelo skladovnico egerijskih peskov z vmesnimi peščenjaki ter meljastimi laporovci, ter v stratigrafsko višjem delu tudi badenijski kalkarenit. Profil se zaključi s sarmatijskimi meljastimi laporji. Zadnji postanek je bil v Imenski gorci, kjer izdanjajo plasti drobnozrnatih panonijskih sedimentov bogatih z ostrakodi.

Naslednji dan smo nadaljevali s predstavitvami. Plenarna predavanja je otvoril dr. Dan V. Palcu z Nacionalnega inštituta za morsko geologijo in geoekologijo v Bukarešti, ki je predstavil predavanje z naslovom Dediščina Tetide. Sledilo je plenarno predavanje dr. Valentine Hajek-Tadesse (Hrvaški Geološki inštitut), ki je predstavila srednjemio-

Sl. 5. Kongresna delavnica: predstavitev neogenskih makrofosilov z območja SV Slovenije

Sl. 6. Paleontološka delavnica.

censke endemične mehkužce Dinarskega jezerskega sistema z območja Bosne in Hercegovine. Srečanje se je nadaljevalo s kratkimi predavanji, ki so bila precej paleontološko obarvana. Nato je sledila paleontološka delavnica, ki se je na takem srečanju odvijala prvič. Na njej so si udeleženci lahko ogledali zbirko makrofosilov neogenske starosti, značilnih za območje Slovenije, ki jih je predstavil Matija Križnar (Prirodoslovni muzej Slovenije) (sl. 5). Poleg tega, so bili na ogled postavljeni tudi ostrakodi, najdenih na območju zahodne Centralne Paratetide, ki jo je vodila dr. Valentina Hajek Tadesse (HGI) skupaj z Mihom Marinškom (GeoZS). Ogledali smo si lahko tudi kenozojske foraminifere, ki jih je predstavila dr. Katica Drobne (sl. 6) in nanoplanktonske fosile iz okolice Podčetrtka, ki sta jih pripravila dr. Miloš Bartol (GeoZS) in dr. Stjepan Ćorić (Geosphere). Dan se je zaključil s postersko sekcijo.

Zadnji dan je potekala pokonferenčna ekskurzija. Tokrat je bila zaradi obilnega deževja turistično obarvana, saj smo bili zaradi vremena primorani spremeniti prvotni plan. Tako smo se namesto ogleda geološke učne poti Paškega Kozjaka odpravili na okušanje magnezijeve vode v Rogaški Slatini, kjer je bil kljub vsemu najbolj zanimiv kamnit tlak (sl. 7 in 8). Nato smo odšli na ogled razgibane neogenske pokrajine z višine, in sicer s stolpa Kristal v Rogaški Slatini. Ekskurzijo smo zaključili z ogledom slikovitega Minoritskega samostana v Olimju in obiskom Čokoladnice Olimje.

Informacije o desetem neogenskem srečanju NCSEE so dostopne na spletni strani https://www.geo-zs.si/ncsee/#, kjer je na voljo tudi knjiga povzetkov, okrožnice ter celoten program.

Sl. 7 in 8. Po-konferenčna ekskurzija. Okušanje Mg vode :).

Nacionalna delavnica o izotopih: Izboljšanje zmogljivosti upravljanja z vodnimi viri

Klara ŽAGAR[1], Katja KOREN PEPELNIK[2], Nina RMAN[2] & Polona VREČA[1]

[1]Institut "Jožef Stefan", Odsek za znanosti o okolju, Jamova cesta 39, SI–1000, Ljubljana, Slovenija;
e-mail: klara.zagar@ijs.si; polona.vreca@ijs.si;
[2]Geološki zavod Slovenije, Dimičeva ulica 14, SI–1000 Ljubljana, Slovenija;
e-mail: katja.koren@geo-zs.si; nina.rman@geo-zs.si

V okviru nacionalnega IAEA projekta NC SLO7001 - Izboljšanje zmogljivosti upravljanja z vodnimi viri je bila 2. oktobra 2024 na Geološkem zavodu Slovenije (GeoZS) v sodelovanju z Institutom "Jožef Stefan" (IJS) organizirana delavnica na področju upravljanja z vodnimi viri v Sloveniji. Udeležilo se je je 39 upravljavcev vodnih virov, raziskovalcev, strokovnjakov in študentov, ki uporabljajo podatke o izotopski sestavi kisika in vodika v raziskavah vodnega kroga, v naravnih in urbanih okoljih Slovenije. Cilj nacionalne delavnice je bila izmenjava izkušenj in dobrih praks, dolgoročni cilj projekta pa je vzpostavitev mreže sistematičnih opazovanj izotopske sestave vodnega kroga v Sloveniji in javne baze tovrstnih podatkov.

Dogodek se je pričel z uvodnimi nagovori in pozdravi predstavnikov GeoZS (dr. Miloš Bavec), Uprave Republike Slovenije za jedrsko varnost (g. Igor Sirc), Direktorata za vode Ministrstva za naravne vire in prostor (dr. Stanka Koren), Stalnega predstavništva Republike Slovenije pri OZN, OVSE in drugih mednarodnih organizacijah na Dunaju (mag. Melita Župevc), Ministrstva za zunanje in evropske zadeve (ga. Tanja Miškova) ter IJS in Mednarodne podiplomske šole Jožefa Stefana (prof. dr. Milena Horvat). V nagovorih so poudarili pomen naše vodne diplomacije, saj je Slovenija zelo aktivna pri zaščiti vodnih virov in zagotavljanju dostopa do vode kot temeljne človekove pravice ter promociji takšnega pristopa v mednarodnem okolju. Zaradi odvisnosti od globalnih vodnih virov je voda prepoznana kot ključno vprašanje miru in varnosti, pri čemer naše aktivno mednarodno povezovanje prispeva k stabilnosti v svetu. Izpostavljena je bila dolga tradicija miroljubne uporabe jedrskih tehnik ter sodelovanje z IAEA, kjer Slovenija prispeva k razvoju mednarodnih standardov, usposabljanju strokovnjakov in izboljšanju upravljanja vodnih virov. Poseben poudarek je bil na izkušnjah z uporabo stabilnih izotopov kisika in vodika, ki omogočajo napredne raziskave za trajnostno upravljanje z vodnimi viri.

Sl. 1. Predstavitve na nacionalni delavnici.

IAEA (International Atomic Energy Agency – Mednarodna agencija za jedrsko energijo) je ena od agencij Združenih narodov, ki deluje na področju jedrske varnosti, uporabe jedrske energije v miroljubne namene in tehnološkega razvoja. Njeno poslanstvo zajema podporo državam pri reševanju okoljskih izzivov, med katere sodi tudi upravljanje vodnih virov. IAEA zagotavlja tehnično pomoč, financiranje opreme in izgradnjo kompetenc, kar državam omogoča dostop do naprednih raziskovalnih tehnik, kot je uporaba stabilnih izotopov vodika in kisika v vodi. Te metode so ključne za razumevanje dinamike in sestave vode v različnih komponentah vodnega kroga in njegovih sprememb tako v naravnih kot v urbanih okoljih.

V prvem delu delavnice so bile izpostavljene možnosti in obstoječe prakse mednarodnega sodelovanja. Tako je predsedujoči v biroju Vodne konvencije, dr. Aleš Bizjak iz Direktorata za vode Ministrstva za naravne vire in prostor predstavil Cilj 6 Agende ZN 2030 Vodne konvencije in priložnosti za posredovanje slovenskega znanja v svet. Širše ozadje, pomen in možnosti za prijave in sodelovanje v IAEA projektih so predstavili Mayumi Yamamoto (regionalna koordinatorka NC SLO7001 projekta, IAEA), dr. Oliver Kracht (tehnični koordinator NC SLO7001 projekta, IAEA) in doc. dr. Nina Rman (vodja NC SLO7001 projekta, GeoZS).

Drugi del delavnice je vseboval predstavitve domačih in tujih strokovnjakov na temo rabe, izkušenj in potreb po podatkih o izotopski sestavi kisika in vodika v vodi. Svoje izkušnje so predstavili dr. Peter Frantar in dr. Urša Pavlič - Agencija RS za okolje, dr. Sonja Cerar - GeoZS, dr. Polona Vreča in dr. Sonja Lojen – IJS, dr. Petra Žvab Rožič - Naravoslovnotehniška fakulteta, mag. Branka Bračič Železnik - JP VOKA-SNAGA d.o.o., dr. Jože Ratej - IRGO Consulting, mag. Miha Pavšek - Geografski inštitut Antona Melika ZRC SAZU, dr. Tom Levanič - Gozdarski inštitut, doc. dr. Vesna Zupanc - Biotehniška fakulteta Univerze v Ljubljani in Žiga Begelj - Fakulteta za gradbeništvo in geodezijo v Ljubljani. Mednarodni pridih so dali gostje iz Madžarske in Malte, dr. István G. Hatvani in dr. Zoltán Kern - Institute for Geological and Geochemical Research in HUN-REN Research Centre for Astronomy and Earth Sciences, Budimpešta, ter Ella Busuttil - Maltese Energy & Water Agency, Qormi.

Prijavni obrazec na nacionalno delavnico je vključeval vprašalnik s sedmimi vprašanji, da bi laže ocenili stanje izkušenj, izzivov in potreb v Sloveniji (sl. 2).

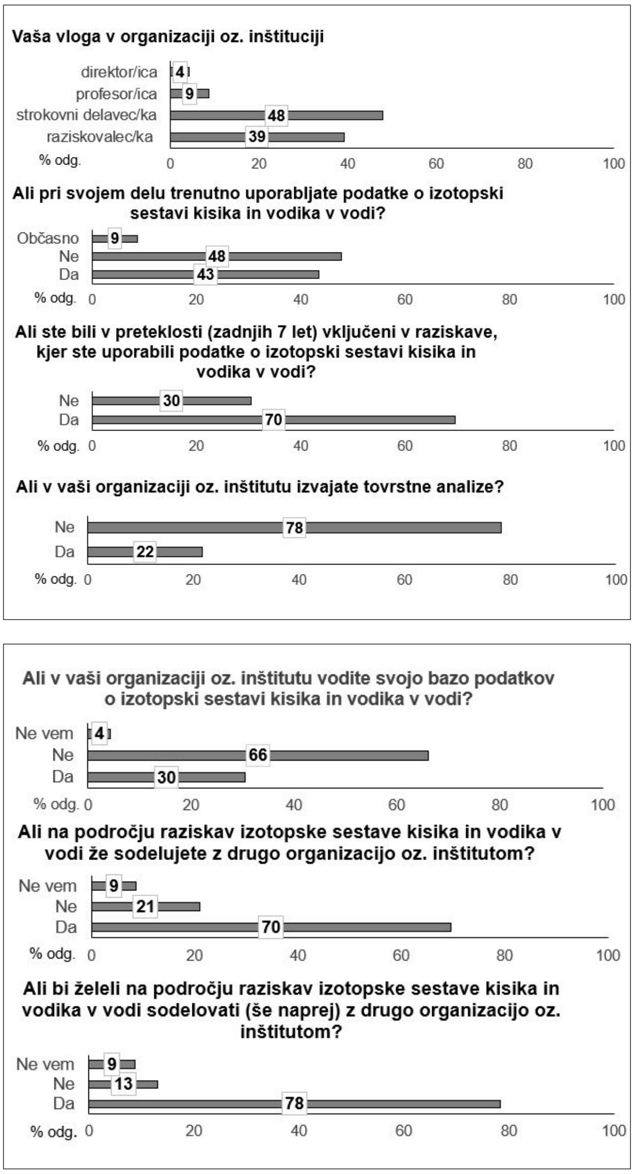

Sl. 2. Grafični prikaz odgovorov na sedem vprašanj. Na vprašalnik je odgovorilo 23 udeležencev (59 % vseh udeleženih).

Skupno število izpolnjenih vprašalnikov je bilo 23, kar pomeni 59 % udeležencev z delavnice. Večina udeležencev, ki so odgovorili na vprašalnik, je bila v preteklih sedmih letih vključena v raziskave, kjer so bili uporabljeni podatki o izotopski sestavi kisika in vodika v vodi. Približno polovica takšne podatke tudi trenutno vključuje v raziskave, večina pa jih že sodeluje z drugo organizacijo oz. inštitutom na tem področju oziroma bi si želeli sodelovati tudi v prihodnje. Zbirke podatkov o izotopski sestavi kisika in vodika v vodi v Sloveniji so trenutno razpršene in individualne, zato je do arhivskih podatkov razmeroma težko priti. Analize izotopske sestave kisika in vodika v vodi se trenutno izvajajo na dveh institucijah v Sloveniji, in sicer na IJS in GeoZS. Še vedno se veliko analiz izvede v drugih laboratorijih po svetu, tudi zato ker v Sloveniji ni akreditiranega laboratorija za tovrstne analize, zato je nujna nadgradnja nacionalnih laboratorijskih kapacitet. Ob izboljšanju infrastrukture je pomembno tudi praktično izobraževanje, ki temelji na rezultatih raziskav in omogoča izmenjavo mnenj in razvoj za reševanje zapletenih izzivov.

Z izvedbo delavnice smo dobili vpogled v trenutno stanje področja v Sloveniji, kar predstavlja izhodišče za načrtovanje bolj sistematičnega razvoja izotopske hidrologije. Ugotovili smo, da že imamo izkušnje z opazovanjem izotopske sestave v skoraj celotnem vodnem krogu, ne le v padavinah (vseh oblik), ampak tudi v talni, površinski in podzemni vodi, v antropogenih vodah (odpadne vode in podobno) in vodo v biosferi (drevesa, ekosistemi), potrebno pa je še nekaj truda za ureditev dostopa do številnih že zbranih podatkov in sčasoma uvedba enotne javne podatkovne baze. Dvoletni nacionalni projekt NC SLO7001 predstavlja dobro osnovo, saj krepi sodelovanje institucij na področju pridobivanja in rabe podatkov o izotopski sestavi vode, s posebnim poudarkom na pripravi osnov za dolgoročno vključitev teh informacij v nacionalno opazovalno mrežo Agencije RS za okolje. Za boljši prenos znanja v prakso ter k upravljanju vodnih virov in področij trajnostnega razvoja pa krepimo tudi sodelovanje strokovnjakov in odločevalcev, ki, kot je bilo poudarjeno na delavnici, prepoznavajo potrebe po izboljšanju informacij.

Zahvala

Projekt se izvaja na podlagi protokola o sodelovanju Geološkega zavoda Slovenije v programu tehnične pomoči in sodelovanja z Mednarodno agencijo za atomsko energijo. Kot slovenski projektni partner sodeluje tudi Institut "Jožef Stefan". Sofinanciranje projekta NC SLO7001 zagotavljata raziskovalna programa št. P1-0020 Podzemne vode in geokemija in P1-0143 Kroženje snovi v okolju, snovna bilanca in modeliranje okoljskih procesov ter ocena tveganja, ki ju financira Javna agencija za znanstvenoraziskovalno in inovacijsko dejavnost Republike Slovenije iz državnega proračuna. Urnik delavnice in informacije o projektu so na voljo na https://www.geo-zs.si/?option=com_content&view=article&id=1506.

From a Birthday Conference to an Apricot Plantation - An unusual business trip to Kyrgyzstan and Tajikistan (with a lot of food)

October 6th to 19th, 2024

Gisela DOMEJ

Geološki zavod Slovenije, Dimičeva ul. 14, SI-1000 Ljubljana, Slovenija
e-mail: gisela.domej@geo-zs.si

In this report, we find out how the most unusual setup for a business trip comes to the most satisfying results. Why? Because Central Asia is the place where "everything possible and impossible comes out of the oil lamp" – even in the countries that don't have oil. They replace it with cooking oil because after all, the essential aspect of Central Asian culture is hospitality.

In short, the trip was planned long before I joined GeoZS in September 2024, and – happy with my new employment – we decided to add a bit of GeoZS flavor to it: a MASPREM poster and openness for new cooperation. It paid off!

Kyrgyzstan: Always a reason to celebrate

The saying goes, if Central Asia was an apartment, then Kyrgyzstan was the courtyard: there is always something going on, people meet, and thereby new ideas, strategies, opportunities, and institutions are created.

Some of them were new already decades ago, and so it happened that the Central Asian Institute of Applied Geosciences (CAIAG) celebrated its 20th anniversary in 2024 by holding a birthday conference on the occasion. The institute was founded by the Government of Kyrgyzstan and the German Research Centre for Geosciences (GFZ) to conduct research in the fields of geodynamics, geohazards, climate change, hydrology, geoecology, resource protection, and many more. Most of those disciplines were represented on the 8th and 9th of October in various sessions by presentations and posters at the International University of Kyrgyzstan (IUK) with the overall topic "Past achievements and future challenges of applied geosciences in Central Asia" and "Five Years of Action for Sustainable Development of Mountain Regions (2023-2027)" (CAIAG, 2024; GFZ, 2024). Researchers, experts, governmental officials, and students from over 15 countries participated in the event; amongst them were colleagues from Kyrgyzstan, Uzbekistan, Kazakhstan, Tajikistan, Russia, Switzerland, Italy, Germany, Japan, and me representing Slovenia with two contributions (Fig. 1a-b):

- CataEx: How to quickly start the Google Earth Engine with JavaScript? (Domej & Pluta, 2024)
- MASPREM – the Slovenian Landslide Forecasting and Warning System (Peternel et al., 2024)

Originally, the content of my presentation drew from another project at my previous place of work as a post-doctoral researcher at Adam Mickiewicz University (AMU) in Poznan, Poland, where we looked for ways to map landslide debris falling on glaciers (Domej et al., 2023). One outcome was,

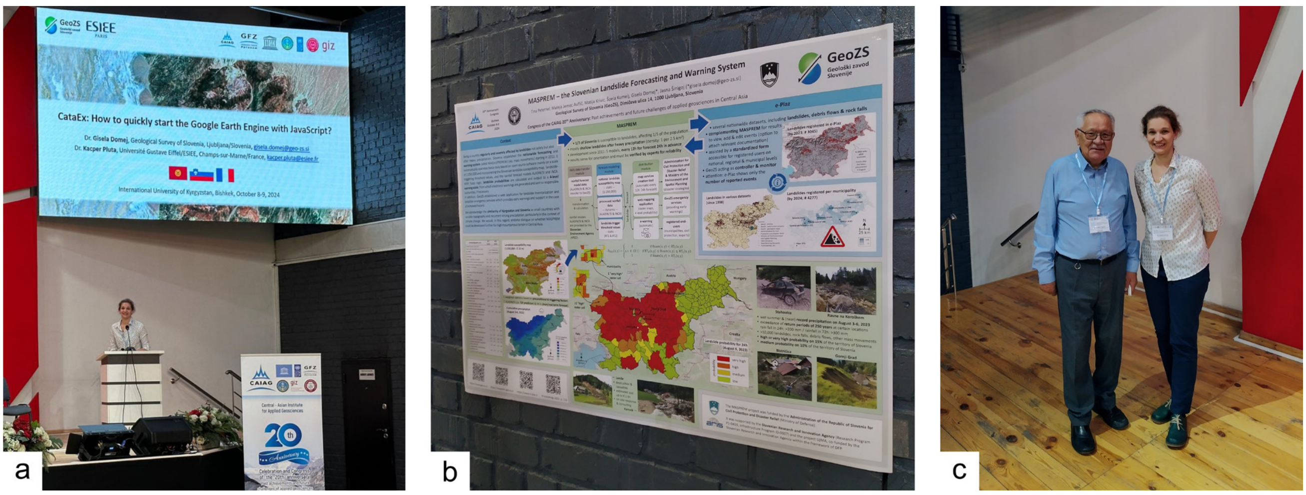

Fig. 1. Conference hall at the International University of Kyrgyzstan (IUK) where I presented my Google Earth Engine code (a) and our MASPREM poster (b); I also met Dr. Isakbek Torgoev (c).

more broadly, a routine coded in JavaScript that performs a variety of useful computations in the Google Earth Engine such as retrieving satellite imagery from the Google Earth Engine Catalog, masking clouds on the images, pixel statistics, index computation, export to other GIS software, and several different tasks. Although initially designed to serve for specific purpose in the Polish project, we found that applications can be much broader, which was reflected by vivid questions from colleagues working in fields ranging from climatology via resource prospection to environmental protection. As I found out the day after my presentation, my session had been filmed by the Kyrgyz broadcaster ELTR (2024) and besides Dr. Bolot Moldobekov, the director of CAIAG, I had the chance to appear with some birthday wishes living up to the Slovenian motto "yes, we can!".

The same day, the poster session took place, and against our expectations, the poster on the Slovenian landslide early-warning system MASPREM (GeoZS, 2024) attracted even more attention than my presentation. How smart that we decided to bring along some GeoZS spice to the trip!

Visitors at our poster were numerous, I brought back a stack of new visit cards, and the stock of GeoZS booklets had disappeared rather quickly. By chance, I also met Dr. Isakbek Torgoev (Fig. 1c), one of the best landslide scientists in Central Asia. He promptly offered me his new book on the topic as a gift.

Later that day, the actual birthday party was held on the premises of CAIAG, and like the conference itself, the organization was impressive – the food and music alike (Fig. 2).

Fig. 2. Traditional Kyrgyz orchestra in the gardens of the Central Asian Institute of Applied Geosciences (CAIAG).

While visiting the fast-changing city center of Bishkek with its fancy high-rise buildings between the typical monumental structures that link history back to the Soviet Union (Fig. 3a-b), I got a call from my colleague Dr. Ruslan Umaraliev (author of an article in this issue of Geologija) a disaster risk specialist working at Osh State University (OshGU) and the unit of Disaster Risk Reduction and Management of the World Food Program (WFP). He told me he would be coming to Bishkek, and that we should meet for a project dinner. No sooner said than done, and over some delicious Kyrgyz shashlik we concluded that we could set up a project as landslide early-warning stands at the very top of the governmental agenda of Kyrgyzstan for the next years. He would connect to the Ministry of Emergency Situations (MES) of the Kyrgyz Republic. Handshake, "Yes we can!".

Fig. 3. Historic timeline of Kyrgyzstan on Ala-Too Square in central Bishkek – prehistoric times documented in the State History Museum (a-b), the national hero Manas on his horse, Lenin as a representative for the communist past of the country, the flag of the independent Kyrgyz Republic since 1991.

Uzbekistan: Tovarna bovdenov in plastike

Saturday 12th was the day to travel to Tajikistan, where I would carry out a mapping job for the NGO Hilfswerk International (HWI). More precisely: in the very north of Tajikistan, to where no connection by plane exists from Bishkek. Therefore, the solution was to fly to Tashkent, the capital of Uzbekistan, travel by car southwards to the

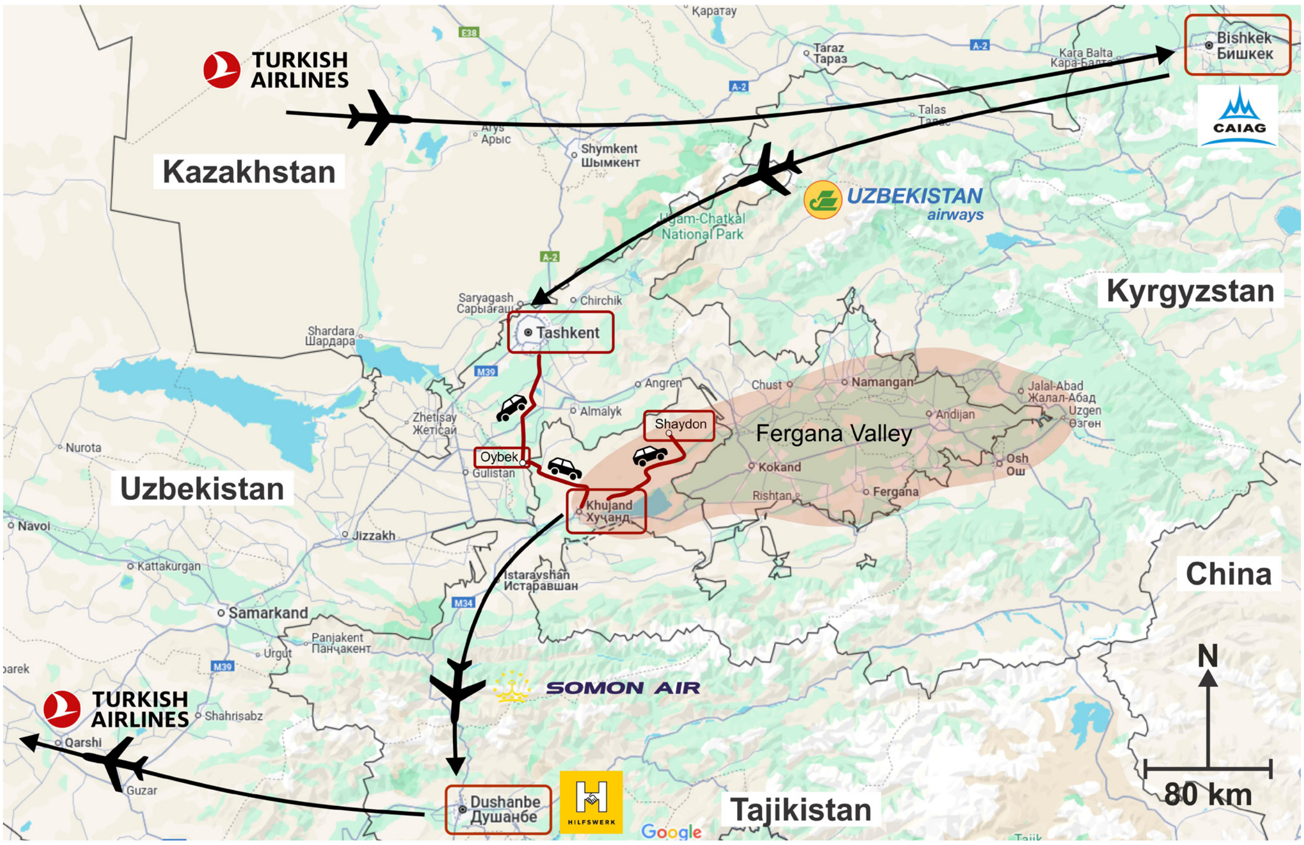

Fig. 4. Travel route from October 6th to 19th, 2024, from Kyrgyzstan via Uzbekistan to Tajikistan.

border crossing at Oybek and then onwards to Khujand, the capital of the Tajik Viloyat Sughd (Fig. 4). As such, this plan seemed very feasible, not too long, and quite comfortable, as HWI booked all segments of transportation and accommodation – had there not been a day-long confusion about my origin.

While at Bishkek Airport, everybody was relaxed, passport controls in Tashkent took it already to a different level:

- Passport! Look camera!
- (So, I looked into the camera.)
- You first time in Uzbekistan?
- No, it's the third time.
- What you do?
- I'm a geologist.
- Where you from?
- I'm from Austria.
- No, where you from today?
- I came from Bishkek.
- You not have return ticket. Where you go?
- Tonight, I travel to Oybek and exit to Tajikistan.

Maybe the precise location convinced him, and very energetically I got my passport stamped. Outside the terminal, my driver was waiting and we set off south on the sparsely illuminated motorway, which interestingly has bus stops and zebra crossings. Around 10:30 pm, we reached a slightly more lit-up parking lot in front of an iron gate, the location the furthest the driver could go. Behind the gate started the border zone, where – to my surprise – had accumulated hundreds of people with their belongings all waiting in a queue to be admitted in groups to the Uzbek exit checkpoint. And the crowd even grew larger, as a yellow bus with a post horn arrived on whose front screen it showed "*Der Deutsche Postbus fährt für Sie*". Just behind it parked his cousin, a truck from *Tovarna bovdenov in plastike* (Fig. 5), a Slovenian cable producer.

Fig. 5. A Slovenian second-hand truck at the Uzbek border post in Oybek (secretly photographed out of the queue; therefore blurred).

While I was reflecting on globalization, the selling of discarded vehicles from Europe to Central Asia, I eventually arrived at the passport control after one long hour with a few stains of motor oil on my pants:

- Passport! Camera!
- (I looked at the camera again.)
- Where you from?
- From Bishkek. (Hoping that this time I gave the proper answer.)
- No, not possible. Where you live?
- In Slovenia.
- But you have passport from Austria?
- Yes, I'm Austrian.
- You enter Uzbekistan when?
- About four hours ago by plane.
- And now you go out Tajikistan?
- Yes.
- Do what there?
- It's for a food project.
- You not like here? Our food also good.

Unsure if border officers are supposed to joke, I just confirmed that, yes, if Central Asia was an apartment, Uzbekistan would definitely be the kitchen, and he gave me the next stamp and sent me further. As there was nothing to be seen except for a pavement leading in the complete dark, I asked where to find the Tajik entry checkpoint just to receive the simple answer: *"dalshe, dalshe, podalshe"*. With that prospect, I remembered well my first Slovenian word that I learned on day one of my employment – *podaljšek* (Slo. extension cable) – thinking that maybe the truck of *Tovarna bovdenov in plastike* could have brought some of them to install a bit of light in that section of no-man's-land. Another thought was that a four-wheel-drive car would be comfortable, but as car crossing is a hassle there, at least a suitcase should have a four-wheel-drive function. At the next streetlight the Tajik border post came in sight, and I prepared for the interview with all my previous knowledge:

- *Ba kamera nigared!*
- Sorry, do you speak Russian too?
- You are not Tajik? Where are you from?
- I'm Austrian, I live in Slovenia, and I traveled from Bishkek through Uzbekistan in one day.
- Alone? At night? As a woman!?
- Yes, a driver is waiting outside for me.
- What will you do here in the north?
- I'm a tourist.
- But what would you visit here?
- A fruit plantation.
- Plantation?
- Yes, *zardolu* (Taj. apricot). I like fruit.

The officer threw me a skeptical glance and hit the fourth stamp of the day into my passport. Outside I met the second driver who would take me to Khujand, where the local colleagues of HWI proceeded to the official beginning of my stay – to a dinner at 1 am because hospitality cannot be food-less.

Lessons learned from the day:

1. We Europeans have the luxury of extremely powerful passports. We are so pampered and used to crossing borders with minimal effort, that we have forgotten that for most people crossing borders is an experience worse than mine that day.
2. Even though the experience was lengthy, I could still see it with humor because, with my privileged passport, I was sure to be able to cross, whereas for others a long wait with several hurdles does not automatically result in the allowance to enter another country.

Being a geologist, and traveling the world for work, sometimes teaches aspects of life, and although the trip was overall a very happy time with celebrations every few days, it was this 1 km in the no-man's-land between two countries that exemplified the fact that some travel for leisure, and some others it is an uncomfortable necessity.

Tajikistan: How to transport 7 kg of fruit as a hand luggage

"We need our geologist because we are not scientific enough." Sometimes I feel that reasoning amongst the HWI Team, although I don't agree with its justification. All our team members have an academic background. The question is just how to combine tasks properly to achieve good results.

Initially, I came to know the Austrian NGO in 2011 during my Master's project at the University of Natural Resources and Life Sciences (BOKU) in Vienna, Austria. Back then, the representative office in Central Asia in Dushanbe, the capital of Tajikistan, assisted us in implementing the EU-funded natural-hazard project PAMIR (HWI, 2024a) in the Gorno-Badakhshan Autonomous Region in Eastern Tajikistan, which eventually allowed me to successfully write my diploma thesis (Domej et al., 2019) and finish my degree. Since then, we have always been in close contact, and over time I grew into the activities of HWI on a voluntary basis, having a hand in web administration, data management, and a variety of other tasks that need a little scientific input such as the current efforts to map production areas of different sorts of fresh and dried agricultural products.

What is here then geologic? Not so much, admittedly. But the ambitions of HWI deserve support and acknowledgment. Over the last decade, it engaged in a series of EU projects in the field of farming, food production and processing, food safety standards, export of goods, and the support of small and medium-sized enterprises in the four countries of Tajikistan, Kyrgyzstan, Uzbekistan and Kazakhstan (HWI, 2024b). With dedication and constant endeavor, new strategies find their consideration nowadays in government agendas and a specifically created working group – the Central Asian Working Group (CAWG) – is recognized by the United Nations Economic Commission for Europe (UNECE) in Geneva, Switzerland.

One of the newest undertakings driven by HWI and the CAWG is the branding of local food products with registered geographical indications (GI), that link a product to a specific origin – similar to Styrian Pumpkin Seed Oil from Austria. And where an area of production is strictly defined, an accurate map is needed. That's where someone would like to borrow a geologist!

While last year, we mapped the area of production of the Khorezm Melon in the Xorazm Region and the Autonomous Republic of Karakalpakstan in Uzbekistan, this year, we targeted the Ashtak Dried Apricot in Tajikistan's northernmost district Asht in the Tajik Fergana Valley. As the area of production is located on a single slope and, therefore, considerably smaller than the one of the melons, our task consisted of visiting the plantations and drawing a clear distinction between Ashtak Apricots and other sorts.

With a bunch of modified satellite imagery created with the Google Earth Engine Code I had presented a few days earlier at the CAIAG's birthday conference in Bishkek, we hit the road up north from Khujand to a plateau resembling the Planet Mars not only due to its reddish gravel but also due to the complete emptiness in terms of infrastructure. The expression "hitting the road" turned out to be taken very seriously, although, for most of the time, it remained unclear whether we hit the road or the other way around (Fig. 6). The herd of goats, that appeared out of nowhere during a heavy rainstorm, was – however – handled with the best care possible.

Once having passed the plateau, plantations started to emerge throughout the rough terrain. Ravshan Hasanov, an irrigation specialist, and I took action for the day: he driving, I mapping – or more precisely, stopping at farmers' plantations, visiting processing units including a giant fridge (Fig. 7a), conducting interviews (Fig. 7b), snacking here and there dried apricots and other fruit, counting irrigation canals and roads which serve as addresses in the area, refusing more snack invitations but accepting more dried apricots in various formats of packaging as take-home-gifts, crossing through gardens (Fig. 7c) and carefully navigating over canal embankments to the maximum extents of the Ashtak plantations (Fig. 7d).

The day had two highlights: the topographic one at the top end of the plantation slope with a breathtaking view into the valley above (Fig. 8a), and the other – how could it be different – a culinary one in the form of an extended lunch in the town of Shaydon, the capital of the Asht District, which seemed not to have changed much since Soviet times: decorated citizens are displayed beneath an impressive mosaic (Fig. 8b), and even the entire irrigation system is a result of industrialized agriculture from decades ago. Here, having Ravshan as a guide turned out to be perfect. During the hours of driving through barren but fascinating landscapes (Fig. 9), I learned a lot about recent local history and agricultural practices. He also made an extra detour before returning to Khujand to show me the Kayrakkum Reservoir on the Syr Darya which partly forms the border between Tajikistan and Uzbekistan a little further up north (cf. border in Fig. 4). While driving over the dam crest, we met another cousin of the German Postbus: a FlixBus from Poland.

Fig. 6. Welcome monument to the Asht District on the road from Khujand to Shaydon.

Fig. 7. Fieldwork to map the Ashtak plantations in the Asht District – fresh apricots (a), interviews with producers (b), comparing satellite images with plantation lots (c), irrigation canal embankments used as connection roads between lots (d).

Fig. 8. Valley above Shaydon (a) with different fruit plantations; mosaic remaining from Soviet times advertising farming activities and a wall of honor for decorated citizens (b).

Fig. 9. Return trip to Khujand with a mountain ridge resembling a colorful puff pastry; in these countries, not even the landscape can escape culinary art.

For once, the following day was not about oil, but about a derivative of it: kerosene. The previous day, the HWI office called us in Asht asking whether I preferred to fly to Dushanbe instead of going by car – as it turned out later with a Tajik Boeing 737.

At the check-in, the ground staff insisted on taking my 7 kg of apricot gifts with me into the *salon* rather than sending it into the hold luggage. Although I tried my best to explain, that I had already two pieces of hand luggage, the final answer was: "Better take it, the apricots might get wet, it's raining today."

I pushed away the idea that rain could penetrate the plane and strolled into a waiting area, where it became immediately clear that a total of 15 kg of hand luggage was still quite modest. – Conclusion of the flight: the most children on all my flights, one of the shortest flights ever (i.e., only about 40 minutes), not a single turbulence, but the luggage was indeed delivered wet. Everything is possible, also with kerosene in the oil lamp.

Arriving in Dushanbe was a real time travel. Not only is the contrast between Khujand (Fig. 10a-c) and Dushanbe quite striking, but the city had also changed enormously since my last visit in 2011. High-rise buildings flank the streets, sparkle at night like in the Gulf States, and many old Soviet-style panel houses gave way to gigantic new buildings and monuments that difficultly find lookalikes in Europe (Fig. 11a-d). If Central Asia was an apartment, Tajikistan could cover even two elements: the balcony with its high Pamir Mountains as well as the reception hall to impress guests.

As a geologist, I just wondered whether those fascinating constructions could resist strong earthquakes. In October 1948, an earthquake of magnitude 7.3 heavily destroyed Ashgabat (Marshall et al., 2024), the capital of Turkmenistan, and so did another one of magnitude 5.2 in April 1966 in Tashkent (Kulahmatovich & Bohodirovich, 2021). Several decades later, after a rapid increase in population and infrastructure in big cities, such high magnitudes could cause tremendous damage. Unfortunately, this seems to be a real threat for Dushanbe, as the city is located in close vicinity to two active fault systems with which magnitudes as high as 7.5 (Bindi et al., 2012) are associated.

The head of HWI in Tajikistan picked me up from the airport, just to announce to me that they had organized a brand-new apartment of 60 m² in such a high-rise block: € 40 per night, and a supermarket in the basement, where a liter of milk

Fig. 10. City center of Khujand – mausoleum of Sheikh Muslihiddin next to the central mosque on Panjshanbe Square (a), cable car over the Syr Darya to the northern part of the city (b), public display of statistics on cotton farming (c).

Fig. 11. Sparkling Dushanbe – the newly constructed parliament (a) and the high-rise triplets displaying news about the president (b) on Rudaki Avenue, the independence monument displaying Tajikistan's history (c), the tea house Rohat (d).

imported from Kazakhstan costs about € 2.20. Quite a price in a country where the average salary amounts to roughly 2300 Somoni (i.e., roughly € 200; CEIC, 2024)! It made me think.

The rest of the week was quite enjoyable. Usually, I spent the day with the HWI colleagues in the office, post-processing the data of the field mission and drawing the map for the GI registration process for the Ashtak Dried Apricot (Fig. 12). Curiously, the Ashtak plantation area is limited to the gently inclined slope above the main road and to the shape of a fan approximately corresponding to the channel of Shaydon. Farmers reported in our interviews that not only the drying time was shorter compared to apricot sorts growing further downslope between the road towards the Syr Darya and the salt pan (cf. Solonchak Aksikon in Fig. 12), but also the taste is considerably different. One suspicion for my part could be an influx of specific minerals through the channel into the plantation fan. As it happens, the channel catchment includes a geologic unit of conspicuous red rock (cf. northwestern corner in Fig. 12), presumably containing iron as its stone fragments are surprisingly heavy. The stream passes right through this unit at the catchment outlet, before discharging with seasonal intensities onto the fan below. Perhaps another field mission including geologic sampling could solve the mystery!

In the early evenings, I had time to visit the city, which definitely can compete with any other capital; I found a Kärcher Shop, the Segafredo Zanetti Café, and fortunately, the Rohat Choikhona dating from 1958 (Fig. 11d), one of Tajikistan's oldest and most famous tea houses for which petitions were held to prevent its destruction (eurasianet, 2022).

And finally, how could it be different? The last office day we had a little cooking party. The head of HWI himself took action and prepared a feast: tender meat with ¼ kg of butter (instead of oil) – and a toast on our mission of this year. Apricots for dessert! Hopefully, next year we will map apples in Kazakhstan or honey in Kyrgyzstan.

The aftermath

With certainty, the trip was one of the most unusual business trips in my career, but also one of the most exciting, impressive, and instructive. Maybe even one that led to new dynamics faster than after other trips.

On the 22nd of November, we held a kick-off meeting for cooperation on landslide susceptibility and early-warning between GeoZS, the MES of the Kyrgyz Republic, and WFP as agreed during the business dinner with the handshake with Ruslan. As if mutual interest and six dedicated presentations were not yet enough, GeoZS was asked if members of the Kyrgyz Ministry could visit in the

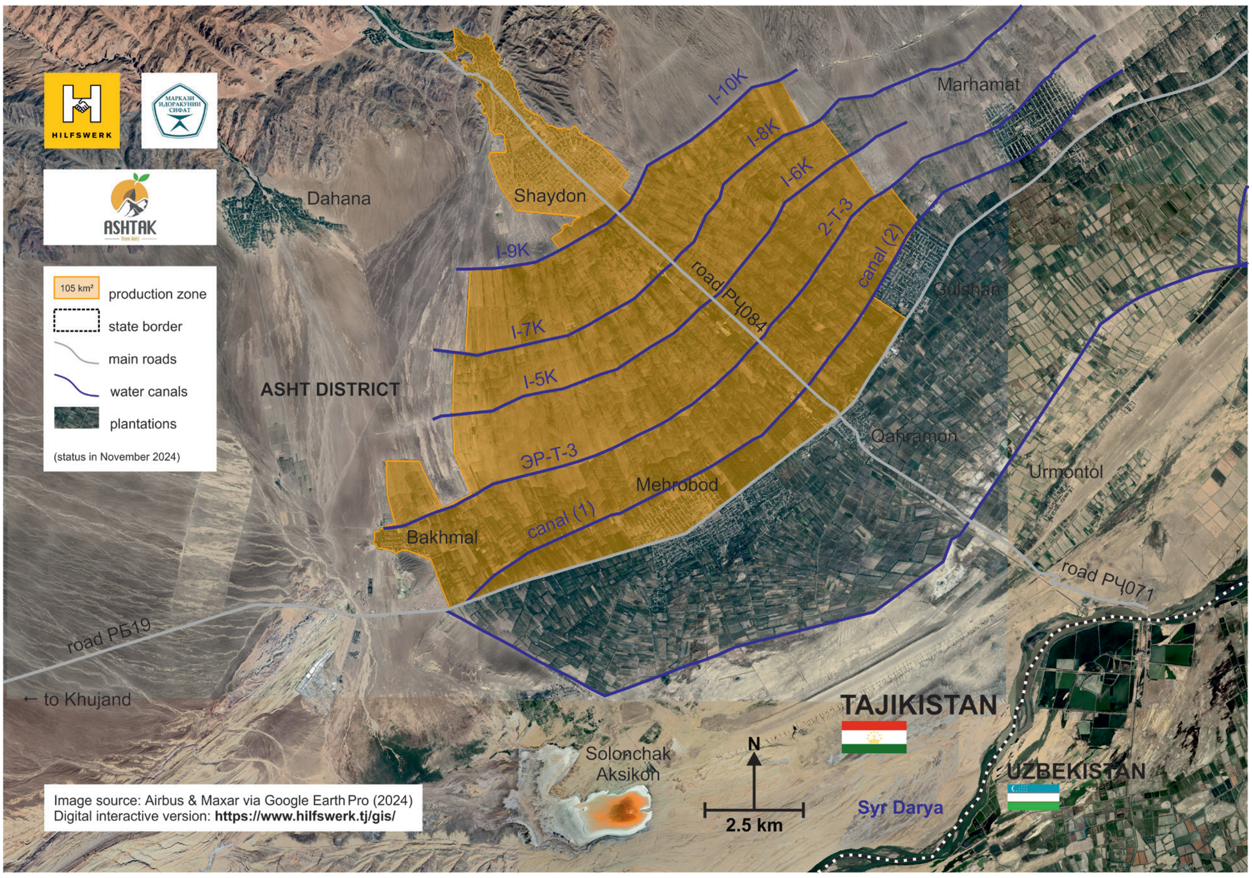

Fig. 12. Plantations of Ashtak (by courtesy of Hilfswerk International (HWI)).

framework of a study tour and members of the GeoZS were invited to join a conference on landslide monitoring in February 2025 in Bishkek.

Myself, I held a seminar on JavaScript coding in the Google Earth Engine on the 28th of November in a hybrid format for GeoZS and Vilnius University in Lithuania. After discovering the interest of the audience during the conference in Bishkek, I decided to design a 4-hour seminar including practical exercises, that can help colleagues not specialized in GIS and remote sensing to acquire satellite data in a relatively simple way. The seminar could later be held for other audiences in Slovenia or abroad.

Likewise, HWI (i.e., the headquarters in Austria and the representative office in Tajikistan) emphasized their interest in future cooperation with GeoZS. Playing the role of project implementors and facilitators without thematic limitations, it is open to topics such as environment and climate change, livelihood preservation, and safety against natural hazards. In this context, HWI positively commented on the proposition of GeoZS to cooperate with the Kyrgyz Government on landslide susceptibility and early-warning, mentioning that the subject could be likewise applicable to Tajikistan with its mountainous areas covering more than 90 % of the country (FAO, 2012).

Acknowledgments

First, I would like to thank GeoZS for having closed an eye on me going on a mission only one month after having accepted my position, the flexibility of handling this exception, and the positivity towards future cooperation with Central Asia.

Fig. 13. A little lunch (a) and the last selfie before returning to Slovenia (b).

I also would like to mention the company and support of GFZ, particularly by Dr. Oliver Bens and Dr. Sigrid Roessner, and the fact that I could join the GFZ Team in all activities during the first week in Bishkek almost as if I belonged to GFZ myself.

Particularly, I thank the HWI Team (Fig. 13a-b): Umed Aslanov for the organization of the Uzbek-Tajik part of my trip, Shuhrat Qodirov for the excellent accommodation in Dushanbe and being my late-night taxi to the airport, Gulbarg Lalbekova for her kind support with administration, and Ravshan Hasanov for the field mission to Asht.

References

Bindi, D., Abdrakhmatov, K., Parolai, S., Mucciarelli, M., Grünthal, G., Ischuk, A., Mikhailova, N. & Zschau, J. 2012: Seismic hazard assessment in Central Asia: Outcomes from a site approach. Soil Dynamics and Earthquake Engineering, 37: 84–91. (https://doi.org/10.1016/j.soildyn.2012.01.016)

CAIAG, 2024: Conference dedicated to the 20th anniversary of CAIAG. Online at: https://www.caiag.kg/en/news/888-conference-dedicated-to-the-20th-anniversary-of-caiag (last accessed in November 2024)

CEIC, 2024: Tajikistan Average Monthly Salary. Online at: https://www.ceicdata.com/en/tajikistan/average-monthly-salary/average-monthly-salary (last accessed in November 2024)

Domej, G., Aslanov, U. & Ischuk, A. 2019: Geophysical investigations on the contribution of irrigation channels to landslide activity in Tusion, Tajikistan. Journal of Himalayan Earth Sciences, 52/2: 161–177. (https://www.researchgate.net/publication/341608914_Geophysical_investigations_on_the_contribution_of_irrigation_channels_to_landslide_activity_in_Tusion_Tajikistan)

Domej, G., Ewertowski, M., Tomczyk, A. & Małecki, J. 2023: Landslide-covered glaciers: towards a new global geodatabase. Poster & Research Abstract, EGU23-11262, EGU General Assembly 2023, Vienna. (http://dx.doi.org/10.13140/RG.2.2.19902.36169)

Domej, G. & Pluta, K., 2024: CataEx: How to quickly start the Google Earth Engine with JavaScript? Talk & Abstract, Congress of the CAIAG 20th anniversary – Past achievements and future challenges of applied geosciences in Central Asia, Central Asian Institute for Applied Geosciences, Bishkek. (http://dx.doi.org/10.13140/RG.2.2.36624.62728)

ELTR, 2024: Climate Week, 20th Birthday of CAIAG (YouTube Video). Online at: https://www.youtube.com/watch?v=NnBHog-zl-0&t=93s (last accessed in November 2024)

Eurasianet, 2022: Tajikistan: Dushanbe's Rohat teahouse saved from wrecking ball. Online at: https://eurasianet.org/tajikistan-dushanbes-rohat-teahouse-saved-from-wrecking-ball (last accessed in November 2024)

FAO, 2012: Country profile – Tajikistan. Food and Agriculture Organization of the United Nations, AQUASTAT Report, 21 p. (https://openknowledge.fao.org/server/api/core/bitstreams/c04b5ebe-7df5-4235-a261-b52304ed2d63/content)

GeoZS, 2024: Masprem Pregledna plošča. Online at: https://masprem.geo-zs.si/ (last accessed in November 2024)

GFZ, 2024: 20 years of CAIAG: GFZ co-operation with Central Asia. Online at: https://www.gfz-potsdam.de/en/press/news/details/20-jahre-zaiag-gfz-kooperation-mit-zentralasien (last accessed in November 2024)

HWI, 2024a: Poverty Alleviation by Mitigation of Integrated High-mountain Risk. Online at: https://www.hilfswerk.tj/en/pamir-en/ (last accessed in November 2024)

HWI, 2024b: Hilfswerk International in Tajikistan (and subpages for CANDY I-V, AgroDev, and HECAFS). Online at: https://www.hilfswerk.tj/en/ (last accessed in November 2024)

Kulahmatovich, K.K. & Bohodirovich, I.M. 2021: The 1966 Tashkent earthquake and the people of Tashkent. Linguistics and Culture Review, 5(S2): 1439–1450. (https://doi.org/10.21744/lingcure.v5nS2.1959)

Marshall, N., Ou, Q., Begenjev, G., Bergman, E., Bezmenov, Y., Dodds, N., Gruetzner, C., Hudson, T., Pierce, I., Mirzin, R., Rhodes, E., Walker, R.T. & Wordsworth P. 2024: Seismotectonic aspects of the Ms 7.3 1948 October 5 Aşgabat (Ashgabat) earthquake, Türkmenistan: right-lateral rupture across multiple fault segments, and continuing urban hazard. Geophysical Journal International, 237/1: 315–338. (https://doi.org/10.1093/gji/ggad488)

Peternel, T., Jemec Auflič, M., Krivic, M., Kumelj, Š., Domej, G. & Šinigoj, J. 2024: MASPREM – the Slovenian landslide forecasting and warning system. Poster & Abstract, Congress of the CAIAG 20th anniversary – Past achievements and future challenges of applied geosciences in Central Asia, Central Asian Institute for Applied Geosciences, Bishkek. (http://dx.doi.org/10.13140/RG.2.2.27187.44328)

Tea Kolar-Jurkovšek elected as Honorary Fellow of the Geological Society of America

John E. Repetski (Research Geologist-Emeritus, U.S. Geological Survey)

The Geological Society of America (GSA), founded in 1888, is a nonprofit organization dedicated to the advancement of geosciences. It is headquartered in Boulder, Colorado, USA, and its membership has up to today grown to some ten thousand members. The main mission of GSA is to advance geoscience research and service to society by improving the professional growth of geoscientists thorough programs at all career levels. Publishing of scientific literature among others includes peer-reviewed journals Geological Society of America Bulletin, and Geology, as well as science magazine GSA Today.

GSA key activities are linked with sponsoring scientific meetings, of which organizing the annual meetings are of utmost importance. At the occasion of the Annual meeting Connects 2024 in Anaheim, California, in September several honors and awards have been presented, among them four new recipients of the GSA Honorary Fellowship. This award is intended for non-North American geoscientists with distinguished original scientific research and internationally recognized contributions to science.

Below is Citation for GSA International Honorary Fellow – Dr. Tea Kolar-Jurkovšek.

It is a privilege and honor to award to Dr. Tea Kolar-Jurkovšek an Honorary Fellowship of the Geological Society of America, for her very substantial scientific contributions over four decades.

Tea Kolar-Jurkovšek is a scientific advisor at the Geological Survey of Slovenia, a geologist/biostratigrapher, and a leader in the study of Paleozoic and Triassic conodonts (biostratigraphically important microfossils) and geology of the European Dinarides. Her extensive field studies have resulted in many works on biostratigraphy, paleontology, and paleogeography.

After graduate study at Ljubljana University and the University of Belgrade, she has been employed as a researcher and program leader at the Geological Survey of Slovenia. Tea actively collaborates in other scientific institutions, as member of the editorial board of a journal and as member of the IUGS International Commission on Triassic Stratigraphy, actively participating in several working groups.

Her work has focused on paleontology and biostratigraphy of Devonian, Carboniferous, Permian, but mainly Triassic, geology and conodonts of Slovenia and the wider Dinarides region. Her studies include the definition of boundary stratotypes, stratigraphic correlations, geological mapping, mineral resource prospecting and tectonic studies of the region. Her achievements include work on the Permian/Triassic boundary, faunal zonation *and paleogeographic studies within the Triassic, and significant taxonomic advances. During the last forty years, her professional contributions include over 400 published works; she is among the most productive researchers at the Geological Survey of Slovenia, and in Europe.*

She collaborates with numerous leading international experts and has taken part in international projects to solve biostratigraphic and paleogeographic issues in, for example, Romania, Oman, Kurdistan, China-Tibet, and she has trained master and doctoral students.

Together with her geologist/husband Bogdan, she recently authored the monographs: "Conodonts of Slovenia" (bilingual Slovene and English; 259 pp., 44 plates), "Fossils of Slovenia" (bilingual, 264 pp., 33 plates) and the comprehensive, well-illustrated book on the classic Slovenian Karst region: "Geology of Kras" (also bilingual; 205 pp. 48 plates). These books, issued by Geological Survey of Slovenia and supplemented by original art illustrations, some by daughter Barbara, show her commitment to transfer her work to the general public. She also has organized exhibitions to highlight the value of fossils as part of the natural heritage.

Using conodonts as the leading fossil group Dr. Kolar-Jurkovšek has solved geologic problems and revised the ages of certain formations. She documented conodont faunas from the Alps in Slovenia and in the Dinarides. She has assisted many geological surveys of the region, providing stratigraphic age assignments based on conodonts and solving important stratigraphical questions. Her notable achievements during her career include the recognition of several late Paleozoic conodont faunas and the introduction of Triassic conodont zonation of the area with documented difference with the standard zonation, distinguishing 34 conodont zones and two subzones. The Early Triassic zonation was recognized only more recently, of which some zones (late Griesbachian, Dienerian and Smithian) are based on euryhaline taxa, and their use is confirmed to be an important regional biostratigraphic tool for the shallow shelf environments of the western Tethys (Kolar-Jurkovšek and Jurkovšek, 2015, 2019). The Middle and Late Triassic conodont zonation mainly corresponds to the standard zonation with the exception of two faunas that usually appear as monospecific fauna, i.e. the Ladinian Pseudofurnishius murcianus Zone designating the Sephardic province, and the Nicoraella? budaensis Zone that is an important regional marker indicating the stressful conditions of the Carnian Pluvial Event. Moreover, she introduced the concept of multielement apparatus taxonomy in the region and made comprehensive taxonomic revisions to some Triassic conodont genera. More recently, her ongoing study, together with colleagues, is focused on a remarkable fossil record of Pseudofurnishius murcianus clusters in the Triassic of Slovenia and Bosnia that is largely based on the application of novel tomographic techniques.

Her work on the Permian-Triassic Boundary (PTB) is also remarkable. During the last two decades, in the areas of former Yugoslavia, she conducted extensive research of the PTB and Lower Triassic strata, enhanced with detailed sampling that revealed the recovery of Hindeodus parvus, the marker of basal Triassic. The Lukač section in Slovenia with an excellent successive conodont record is the standard section to define the PTB in the entire Dinarides according to international standards and the site has been added to a list of new natural value of national significance. Likewise, the Teočak section in Bosnia and Herzegovina that includes the PTB as well as the Induan-Olenekian Boundary strata with relatively large set of paleontological data represents an important contribution due to its relevance to the paleogeography of Western Tethys.

In summary, Tea Kolar-Jurkovšek has been one of the most productive and influential geologist researchers in her country, establishing a network of researchers, international scientific exchanges and student supervisions. For those reasons, and close to her retirement, we honestly consider that Tea Kolar-Jurkovšek deserves the recognition for a lifetime of achievements in diverse studies of regional geology and palaeontology, and applying their relevance to society, and to be recognized as an Honorary Fellow of the GSA.

V spomin zaslužnemu profesorju dr. Simonu Pircu

V novembru 2024 nas je za vedno zapustil naš dragi kolega, zaslužni profesor doktor znanosti Simon Pirc. Za njim bo ostala praznina, tako na strokovnem področju kot tudi v naših osebnih življenjih.

Zaslužni profesor dr. Simon Pirc se je rodil 2. marca 1932, v Lipnici pri Kropi. Po končani realni gimnaziji v Ljubljani, se je vpisal na Fakulteto za gradbeništvo, a je po letu dni postala in ostala njegova življenjska izbira geologija. Po diplomi leta 1961 se je kot ekonomski geolog zaposlil na Geološkem zavodu Ljubljana. Sodeloval je pri raziskavah svinčevo-cinkovih rudišč ter urana v Sloveniji, in urana v Makedoniji. Verjetno so njegov nemirni duh, želja po novih izzivih in obvladovanje več svetovnih jezikov, prispevali k odločitvi, da se je priključil skupini Geološkega zavoda, ki je raziskovala rudišča v Alžiriji. Tam je prvič postavil temelje geokemičnemu kartiranju, metodi, ki se je takrat komaj začela uveljavljati v svetu. A žal se je delo v Alžiriji tragično končalo. Prometna nesreča mu je pustila tako hude posledice pri hoji, da je moral poiskati drugačno poklicno pot. Leta 1970 se je tako kot asistent zaposlil na Odseku za geologijo na Fakulteti za naravoslovje in tehnologijo, Univerze v Ljubljani. Kot asistent je sodeloval pri predmetih Mikroskopija rud in premogov ter Ocena in metode raziskav nahajališč mineralnih surovin. Pod mentorstvom prof. Matije Drovenika se je v magistrski nalogi, ki jo je zaključil 1975, posvetil Geokemičnim raziskavam v zahodnem delu posavskih gub. Zavedal se je, da je napredek v stroki mogoč le, če smo v stiku s svetovnimi dosežki. Za nadaljevanje na doktorski stopnji študija se je zato odločil za odhod v ZDA, na Pennsylvanijsko državno univerzo, kjer je pridobil nova znanja predvsem s področja geokemije pri prof. Rosu in statistike pri prof. Griffitsu. Leta 1979 je doktoriral s tezo o Porazdelitvi urana in drugih kemičnih prvin v devonski Catskillski formaciji v osrednji Pensilvaniji.

Pridobljeno znanje je prenesel v Slovenijo predvsem z modernizacijo študijskega programa. Leta 1980 je bil izvoljen v naziv docenta, 1985 v izrednega in 1991 v rednega profesorja za področje geologije. Bogate izkušnje terenskega geologa in poznavalca rudišč je s študenti delil pri predmetu Ekonomska geologija. Vedno je poudarjal, da se geologija ne konča znotraj državnih meja in je zato pogosto organiziral ekskurzije v tujino. Študente je popeljal v Albanijo, Avstrijo, Češko, Italijo, Madžarko, Nemčijo in Poljsko. Imel je izreden smisel za tuje jezike in jih več tudi odlično obvladal. Poleg tega je bil vedoželjen iskalec drugačnih pogledov in novega znanja. Predmet Uporaba tuje strokovne literature mu je bil zato pisan na kožo. Že na prvi uri nas je presenetil s kratkimi stavki, zapisanimi v različnih svetovnih jezikih, med drugimi tudi v japonščini in arabščini, in nam pokazal, da lahko strokovno besedilo smiselno razberemo že z zelo omejenim poznavanjem besedišča. Marsikomu od nas je tako premagani strah, odprl vrata v svet branja, in kasneje pisanja, mednarodnih objav. Študentom geotehnologije in rudarstva je predaval Tehnično geologijo in študentom krajinarstva Uvod v geologijo. Najpomembnejši doprinos prof. Pirca pa je zagotovo uvedba dveh novih predmetov – Geokemije in Statistike v geologiji. Kljub izredni razgledanosti in obvladovanju zelo različnih tematik tudi izven geologije, ali pa morda prav zato, njegova predavanja niso sledila klasičnim vzorcem. S hitrimi miselnimi preskoki in nepričakovanimi vprašanji, nas je spodbujal k razmišljanju, kritičnim dvomom in k samostojnemu iskanju odgovorov. Njegov odnos s študenti in sodelavci je bil pristen, odkrit, strpen in spoštljiv. V vsakem od nas je videl potencial in nam želel pomagati na naši poklicni pa tudi osebni poti. S svojo odprtostjo in človeškim odnosom je pritegnil številne študente. Tako je bil mentor pri 37 diplomah, 14 znanstvenih magisterijih in 6 doktoratih. Kot mentor je bil zahteven. A prav to nam je omogočilo, da so naša dela postala ne le strokovno, ampak tudi jezikovno in slogovno boljša. Prof. dr. Simon Pirc je bil vedno odprt za sodelovanje in videl možnosti za razvoj novih področij. Tako je bil tudi eden izmed pobudnikov in ustanoviteljev interdisciplinarnega doktorskega študija Varstva okolja na Univerzi v Ljubljani.

Na raziskovalnem področju se je prof. dr. Simon Pirc usmeril predvsem v geokemično kartiranje in statistične tehnike reprezentativnega vzorčenja. Uspešno je rešil probleme geokemičnega kartiranja na kraških področjih. Kot vzorčna sredstva je uvajal potočni in poplavni sediment, potočni mah in hišni prah. Možnost ugotavljanja in ločevanja geogenega in antropogenega vpliva je odprlo vrata še trem novim področjem – Okoljski geologiji, Geomedicini in Vojaški geologiji. Sodeloval je pri nastanku Geokemičnega atlasa Evrope. Pod njegovim mentorstvom so nastale tudi prve geokemične karte različnih delov Slovenije. Bil je avtor ali soavtor pri 17 znanstvenih člankih, treh monografijah in 18 kongresnih objavah. Prof. dr. Simona Pirca so visoko cenili tudi v mednarodni znanstveni skupnosti. Njegovi kolegi iz skupine evropskih geokemikov FORGES so v njem prepoznali ne le odličnega strokovnjaka, ki je znal preprosto razložiti zapletene probleme, ampak predvsem velikega človeka in dobrega prijatelja, ki je vedno pripomogel k pozitivnemu vzdušju.

Prof. dr. Simon Pirc je bil med prvimi slovenskimi geologi, ki je začel uvajati mednarodno sodelovanje in projektno delo. Bil je vodja skupnih projektov z ZDA, projektov Alpe – Jadran in IGCP projektov. Vodil je raziskovalni projekt Geokemija supergenih procesov v Sloveniji ter bil vodja programske skupine Geologija in geotehnologija, ki je poleg geologov, združila tudi sodelavce iz oddelka za Geotehnologijo in rudarstvo. Dvakrat je bil predstojnik Oddelka za geologijo in od 1998 predsednik in potem častni član slovenskega odbora IGCP za UNESCO. Bil je član uredniškega odbora in recenzent revij Geologija, RMZ Materiali in geookolje, Geologia Croatica in Journal of Geochemical Exploration. Zagovarjal je načelo, da recenzent ne sme biti uničujoč kritik, ampak tisti, ki avtorju pomaga, da jasneje predstavi svoje misli in omogoči bralcu lažje razumevanje.
Tudi po upokojitvi leta 2002 ni opustil stika s stroko. S svojim bogatim znanjem in duhovitostjo je občasno popestril redna predavanja študentom. Prevajal je strokovna in znanstvena besedila ter sodeloval pri Slovenskem terminološkem slovarju. Za svoje delo je leta 2005 prejel Lipoldovo medaljo, leta 2006 pa je postal zaslužni profesor ljubljanske univerze.
Zaslužni profesor dr. Simon Pirc v življenju ni bil le pronicljiv raziskovalec in razumevajoč pedagog temveč vedno in na prvem mestu človek. Kljub resnim zdravstvenim težavam, je ostal neizmeren optimist neutruden iskalec vedno novih znanj iz zelo različnih področij. Neizbrisno bo ostal zapisan v slovenski geologiji, njegovi učenci pa ga bomo s hvaležnostjo ohranili v trajnem spominu.

Nina Zupančič

GEOLOGIJA

št.: 67/2, 2024

www.geologija-revija.si

GeoZS
Geološki zavod Slovenije

ISSN 0016-7789

9 770016 778002